ISSN 0169-6548

Communications on hydraulic and geotechnical engineering

Hydraulic rams - a comparative investigation

March 1988

J.H.P.M. Tacke

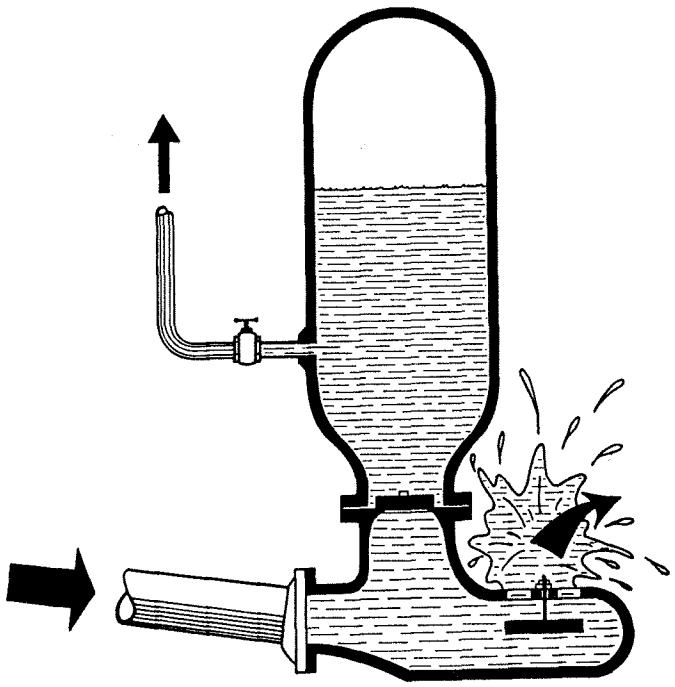

TU Delft
Delft University of Technology

Faculty of Civil Engineering

HYDRAULIC RAMS
A COMPARATIVE INVESTIGATION

J.H.P.M. Tacke

Report no. 88 - 1
Delft University of Technology
Department of Civil Engineering
Delft, The Netherlands

ABSTRACT

A mathematical model describing the essential features of hydraulic ram operation is developed in order to clarify the possibilities and limitations of the ram relative to its site and its adjustments. The model distinguishes three different periods in the pumping cycle of the hydraulic ram: acceleration - retardation - recoil. Making use of the theory of unsteady flow in pipelines, for each period the relation between velocity and time is derived for the water in the drive pipe of the hydraulic ram installation. Ultimately, from these relationships mathematical expressions are obtained for the time rate of pumping of the ram and for the supply flow required to operate the ram. It is shown that the model is sufficiently accurate to yield at the least a qualitative explanation of the effect of the various parameters governing the performance of the hydraulic ram. For calculation purposes the mathematical model is modified to some extent in order to improve the description of the phenomenon governing the motion of the water during the period of retardation.

Laboratory tests were taken on twelve commercially-available hydraulic rams in order to determine their specific performance characteristics. To enable mutual comparison the results are partly presented in a non-dimensional form.

PREFACE

Hydraulic rams are special water pumping devices that utilize the energy available in a flow of water to lift a small portion of that water to a higher level. In the past quite a number of hydraulic rams have been installed and many have given long and reliable service. With the advent of steam-power, fossil fuel driven engines and electrification, the interest in using hydraulic rams has declined. Recently, though, it has revived as a potentially useful component in rural water supply programs in developing countries.
In order to arrive at sound decisions on a wide-scale application of hydraulic rams in developing countries, preliminary knowledge on limitations, cost implication, acceptability, adaptability, reliability and maintainability is necessary[21]*. As a contribution to this knowledge an investigation on hydraulic rams has been carried out at the Delft University of Technology (Faculty of Civil Engineering). Part of the investigation consisted of extensive tests on several commercial hydraulic rams in order to determine their operating and performance characteristics. These tests were executed in the period 1982 - 1984 at the Laboratory of Fluid Mechanics of the Delft University of Technology.
In the same program field-tests have been conducted by the Foundation of Dutch Volunteers in Rwanda. In this part of the investigation emphasis was layed upon technical performance and durability under operating conditions in a community setting, social acceptance and community participation in installing, operating and maintaining the hydraulic ram system.

This report reflects the results of the above-mentioned laboratory investigation.

*[numerals] refer to the bibliography at the end of this report.

ACKNOWLEDGEMENTS

The writer wishes to thank the members of the Laboratory of Fluid Mechanics of the Delft University of Technology for their assistance and kind cooperation and for creating such a pleasant working environment. In particular he is greatly indebted to Mr J. Tas and Mr J.F. van der Brugge for building the test installation and adapting it time and again, ir. R.E. Slot for the preparation of the electronical equipment and the development of the 'data logging program' for the micro-computer and ir. H.L. Fontijn for his support, keen interest and helpful suggestions during the experiments.
The advice and encouragement given by prof.dr.ir. M. de Vries, professor of Fluid Mechanics of the Delft University of Technology, are highly appreciated. Special thanks are due to ir. C. Verspuy (Hydraulic and Geotechnical Engineering Group - section Fluid Mechanics) for his contributions to the investigation and for his critical reading of the manuscript and valuable comments.
Finally, the accurate word processing of part 1 performed by Mr P. de Jong is greatly acknowledged.

DISCLAIMER

This report was prepared by the Delft University of Technology - Faculty of Civil Engineering, as part of a project sponsored by the Netherlands' Ministry of Foreign Affairs - Directorate General for Development Cooperation.
The views expressed in this report do not necessarily reflect those of the Netherlands' Ministry of Foreign Affairs or of the Delft University of Technology. Neither the Ministry nor the University makes any warranty, expressed or implied, or assumes any legal liability for the completeness of the information presented. The mention of specific companies or certain manufacturers' products does not imply that these are endorsed or recommended in preference to others of a similar nature that are not mentioned.

CONTENTS

ABSTRACT		i
PREFACE		iii
ACKNOWLEDGEMENTS		iv
DISCLAIMER		iv
CONTENTS		v
I	INTRODUCTION	1
II	OPERATION OF THE HYDRAULIC RAM	3
II-1	Principle of action	3
II-2	Performance characteristics	7
II-3	Practical use	18
III	HYDRAULIC RAM ANALYSIS	25
III-1	Division of the cycle into periods	25
III-2	Period of acceleration	38
III-3	Period of retardation	44
III-4	Period of recoil	53
III-5	Review of the complete analysis	55
III-6	Calculation example	72
IV	LABORATORY INVESTIGATION	79
IV-1	Selection of hydraulic rams	79
IV-2	Experimental set-up	83
IV-3	Test results	94
V	SUMMARY AND CONCLUSIONS	105
LIST OF SYMBOLS		107
BIBLIOGRAPHY		109

	page
Appendix A: TEST RESULTS	A.1
A.1 Blake Hydram	A.3
A.2 Bélier Alto	A.19
A.3 Vulcan	A.33
A.4 Sano	A.47
A.5 Davey/Rife	A.63
A.6 Schlumpf	A.79
Appendix B: UNSTEADY FLOW IN A PIPELINE	B.1
B-1 Introduction	B.1
B-1.1 Classification of flow	B.1
B-1.2 Pressure waves	B.1
-Transient flow equations	B.2
-Effect of gas in liquids	B.12
-Wave propagation and reflections	B.14
B-1.3 Rigid water-column theory	B.18
B-2 Basic differential equations of unsteady pipe flow	B.20
B-2.1 Equation of continuity	B.20
B-2.2 Equation of motion	B.24
B-3 Methods of solution	B.28
B-3.1 Method of characteristics	B.29
-Characteristic equations	B.29
-Graphical solution	B.36
B-3.2 Rigid water-column solution	B.44
Appendix C: HYDRAULIC RAM MANUFACTURERS	C.1

I INTRODUCTION

The hydraulic ram is a self-operating water raising machine. Instead of an external power source (oil, electricity etc.) the ram utilizes the energy contained in a flow of water running through it, to lift a small volume of this water to a higher level. The phenomenon involved is that of a pressure surge which develops when a moving mass of water is suddenly stopped (waterhammer).
Hydraulic rams can be used for pumping drinking-water from a spring or stream to a tank or reservoir (cistern) at a higher level. A steady and reliable supply of water is required with a fall sufficient to operate the ram. Favourable conditions are mostly found in hilly and mountainous areas with fairly plentiful supplies of water. A well-made ram will pump an appropriate amount of water to a height from about 20 to 30 times the supply head, with an efficiency of about 60 to 70 per cent. Alternatively, hydraulic rams can be used for pumping water to low heads over large distances (up to 10 km or more), i.e. vertical lift can be traded off for horizontal distance.
The hydraulic ram can fill a number of needs providing water for either domestic or non-domestic purposes. Its application varies from individual installations supplying families or livestock, to larger systems supplying water to small rural communities or irrigation schemes. As so it can provide a cost-effective, energy-saving alternative to fuel driven pumps.

The discovery of the underlying principle of the hydraulic ram and its first practical application are due to John Whitehurst. However, his machine was not working automatically, but the operation was controlled manually by opening and closing a stop-cock (Fig. I-1a). In 1775 Whitehurst called public attention to his invention through a communication to the Royal Society of Engineers in London [27].
In 1776 Joseph M. de Montgolfier [14, 15], the French co-inventor of the hot-air balloon, invented a machine based on the same fundamental principle, but acting automatically (Fig. I-1b). He named his machine 'le bélier hydraulique' from which the term 'hydraulic ram' is derived. A patent was granted to Montgolfier in 1797.

Hydraulic rams have been (commercially) available for many years. Though not applied to a widespread scale, in some parts of the Western world they were common 100 - 150 years ago. But in modern times the availability of piped water systems using engine-driven pumps has relegated the hydraulic ram to a comparatively unimportant position.

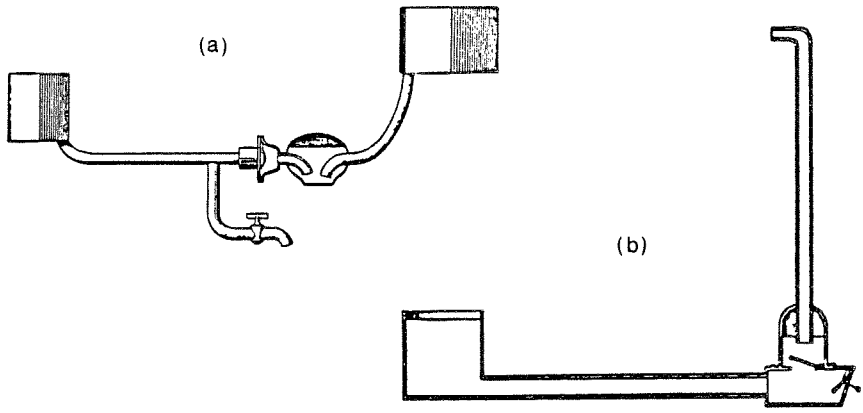

Fig. I-1 (a) Whitehurst's hydraulic machine (England - 1772)
(b) Montgolfier's automatic hydraulic ram (France - 1776)

There has been increasing interest, however, in the use of hydraulic rams to provide a potable water supply for scattered rural populations in developing countries. Yet, up to now the use of the hydraulic ram in developing countries has not become as widespread as its simplicity, ease of operation and maintenance, dependability and economy would seem to warrant. This has been due largely to the lack of reliable information concerning the limiting conditions under which the ram is applicable and the phenomena governing its action.

It was the purpose of this investigation to make a study of the hydraulic ram and to carry out tests on commercially-available hydraulic rams in order to determine their performance characteristics and to compare these results with the information provided by the manufacturers.
In **chapter II** a description of a typical hydraulic ram installation is given; the mode of action of the ram is explained by means of a description of a complete cycle of operation. Performance characteristics and practical aspects of use of the hydraulic ram are being discussed. **Chapter III** deals with a (simplified) mathematical analysis of the operation of the hydraulic ram. The cycle is divided into seperate parts (periods) and each part is analysed individually. Laboratory tests were taken on twelve commercially-available hydraulic rams (six different manufactures). In **chapter IV** a summary of all test results is presented (detailed results are included in Appendix A). Finally, a summary and conclusions are included in **chapter V**.

II OPERATION OF THE HYDRAULIC RAM

II-1 Principle of action

Hydraulic ram installation. Fig. II-1 shows the various components from which a typical hydraulic ram installation is constructed: supply reservoir - drive pipe - hydraulic ram - delivery pipe - storage tank. The hydraulic ram itself is structurally simple, consisting of a pump chamber fitted with only two moving parts: an impulse valve through which the driving water is wasted (waste valve) and a check valve through which the pumped water is delivered (delivery valve).

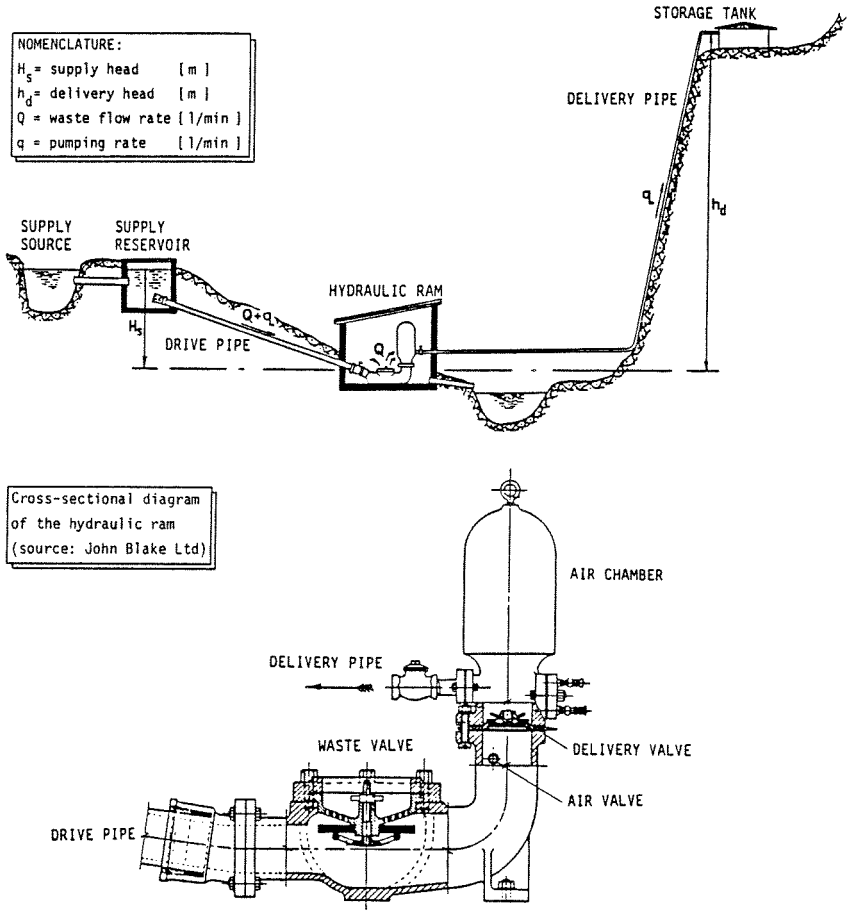

Fig. II-1 Typical hydraulic ram installation.

The waste valve normally falls open by gravity. Some designs of hydraulic ram use a spring-activated waste valve (see e.g. Fig. II-2a); such a valve may open either with or against the action of its own weight. The delivery valve usually is a simple rubber disc covering a grid-shaped seat. Surmounting the delivery valve is the air chamber or surge tank. When the ram operates this tank is partly filled with water and partly with air. Connected to the air chamber is the delivery pipe, so that the pressure in the air chamber is the delivery pressure. An inclined conduit, the so-called drive pipe, connects the ram body with the water supply. This drive pipe is the essential part of the installation in which the potential energy of the supply water is first converted into kinetic energy and subsequently into the potential energy of water delivered.

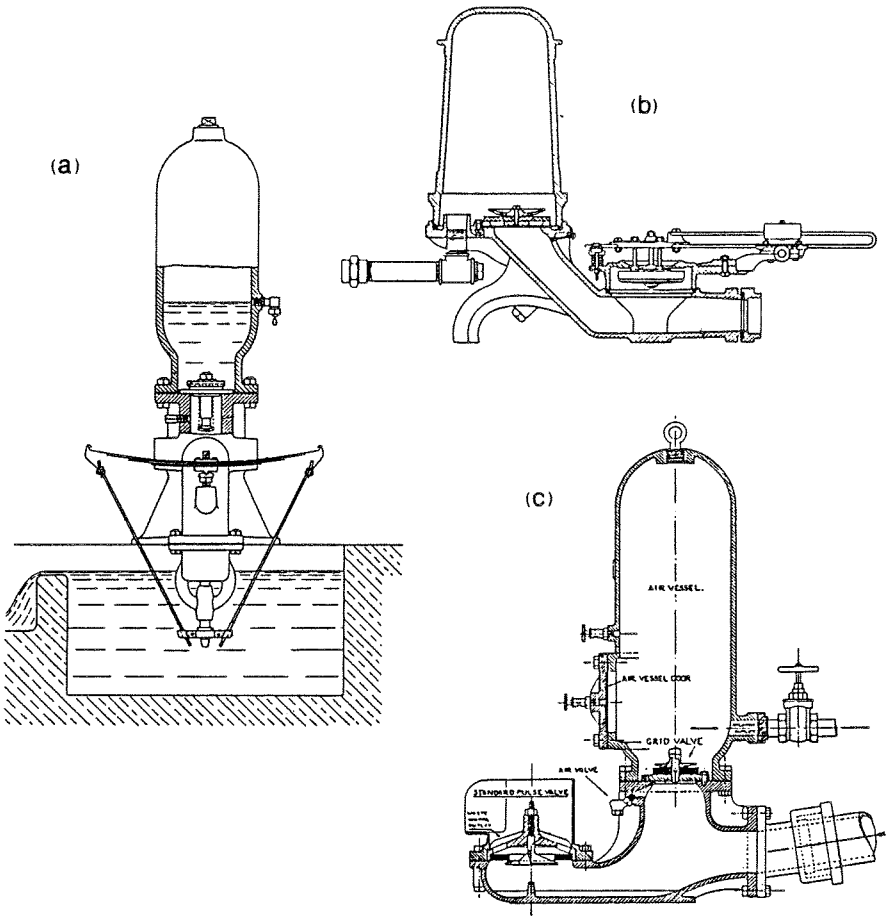

Fig. II-2 Various designs of hydraulic ram
(a) SANO, (b) RIFE, (c) VULCAN

Mode of action. The ram operates on a flow of water falling under a head H_s from the supply reservoir down through the drive pipe into the pump chamber. The water escapes through the opened waste valve into the surrounding area (Fig. II-3a). With the acceleration of the water the hydrodynamic drag and pressure on the waste valve will increase. When the flow of water through the waste valve attains sufficient velocity, the upward force on the valve will exceed its weight and the valve will slam shut. (In a good ram design the valve closure is rapid, almost instantaneous.)
Thus the flow through the waste valve is abruptly stopped, but since the column of water in the drive pipe still has a considerable velocity a high pressure develops in the ram, locally retarding the flow of water. If the pressure rise is large enough to overcome the pressure in the air chamber the delivery valve will be forced open (Fig. II-3b), which in turn limits the pressure rise in the ram body to slightly above the delivery pressure. The front of this pressure rise expands upstream, partly reducing the flow velocity in successive cross-sections of the drive pipe as it passes. In the meantime the remainder of the flow passes through the opened delivery valve into the air chamber. The air cushion permits water to be stored temporarily in the air chamber with only a comparatively low rise in local pressure, thus preventing the occurrence of waterhammer (shock waves) in the delivery pipe.

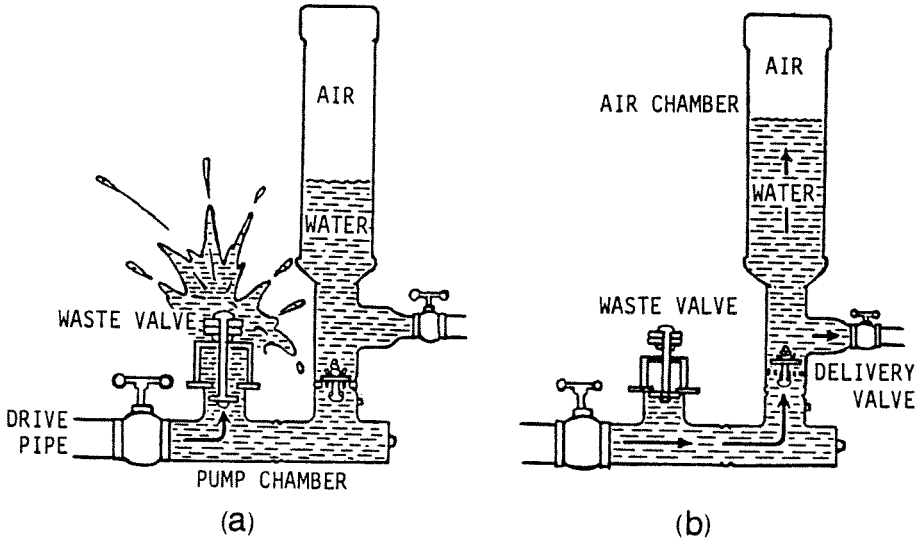

Fig. II-3 Operation of the hydraulic ram (source: [23])
(continued on next page)

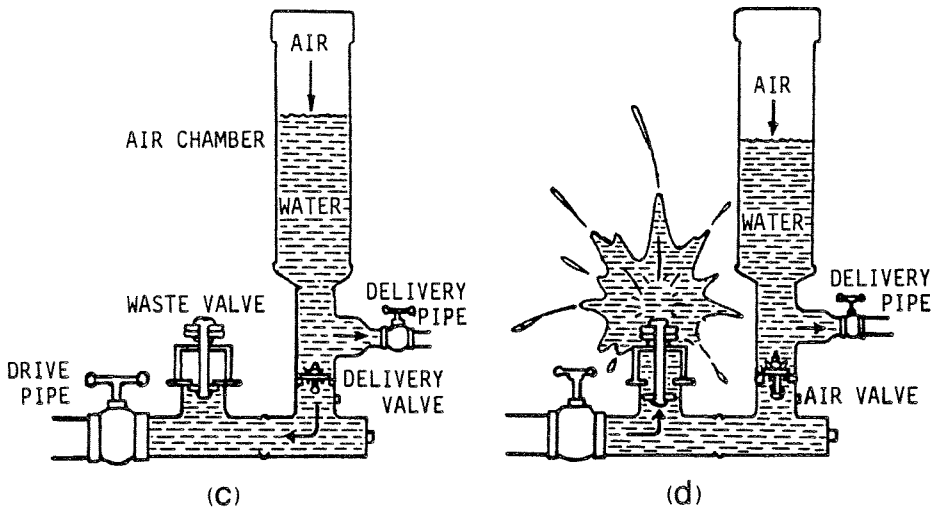

Fig. II-3 Operation of the hydraulic ram (cont.)

With the propagation of successive pressure surges up and down the drive pipe water continues to flow into the air chamber with step-wise decreasing velocity until the momentum of the water column in the drive pipe is exhausted. The higher pressure which now exists in the air chamber causes the delivery valve to close, thus preventing the pumped water from flowing back into the ram body, while the water in the drive pipe is flowing away from the ram in the direction of the supply reservoir (Fig. II-3c). The 'recoil' of water in the drive pipe produces a slight suction in the ram body, thus creating an underpressure near the waste valve. The underpressure makes it possible for the waste valve to reopen, water begins to flow out again, and a new operating cycle is started (Fig. II-3d). Meanwhile the water forced into the air chamber, is driven into the delivery pipe to the storage tank at the high level, from which it can be distributed by gravitation as required.
An air valve or snifter valve is mounted into the ram body to allow a small amount of air to be sucked in during the suction part of the ram cycle. This air is carried along with the next surge of water into the air chamber. The air in this chamber is always compressed and needs to be constantly replaced as it becomes mixed with the water and lost to the storage tank. Without a suitable air valve the air chamber would soon be full of water; the hydraulic ram would then cease to function.

Depending on supply head, waste valve adjustment and in a less degree on drive pipe length and delivery head the cycle is repeated with a frequency of about 30 to 150 times a minute (period time T = 0.40 - 2.00 s). Once the

adjustment of the waste valve has been set (valve stroke and - if present - tension of the return spring), the hydraulic ram needs almost no attention provided the water flow from the supply source is continuous and at an adequate rate and no foreign matters get into the pump blocking the valves.

II-2 Performance characteristics

Delivery flow. For the end-users of the hydraulic ram installation the pumping rate q (output capacity) is the first consideration, since this amount should meet their demand. Given an available source supply the pumping rate q of a hydraulic ram is primarily determined by the supply head H_s and the delivery head h_d. As an example Fig. II-4 shows performance characteristics compiled from measurements taken on a 2 1/2"- hydraulic ram operating under a supply head H_s = 2.00 m. It can be seen from the figure that the hydraulic ram can pump much water for low delivery heads, but as the delivery head increases the pumping rate decreases as might be expected. Fig. II-4 also pictures efficiency versus delivery head; the efficiency curve shows that this specific ram can pump water with an efficiency of about 60 % over a broad range of delivery heads. Efficiency requires special attention and is therefore discussed separately, later in this section.

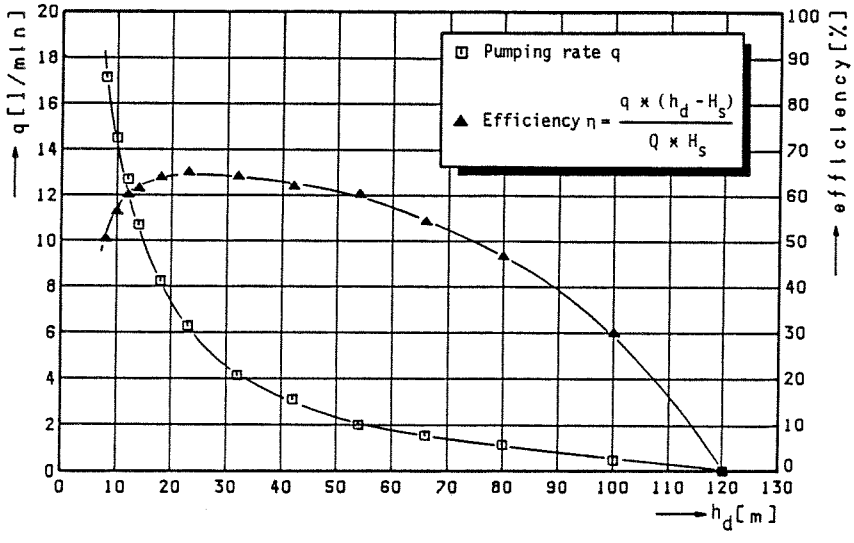

Fig. II-4 Performance characteristics - Blake Hydram No. 3 1/2 (2 1/2") H_s = 2 m; Q ≈ 100 l/min; T ≈ 1 s.

An increase of supply head H_s increases the pumping frequency (more beats per minute) and by that the pumping rate q increases. This may be noted from Fig. II-5 showing q, h_d-curves resulting from experiments carried out on the same 2 1/2"- hydraulic ram, for H_s = 1.35 m, 2.00 m and 3.00 m respectively.

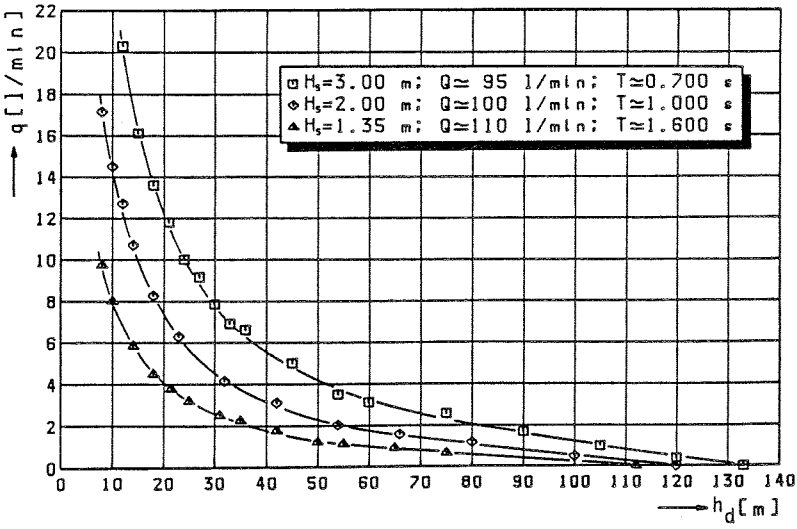

Fig. II-5 Effect of supply head on ram performance (Blake Hydram No. 3 1/2)

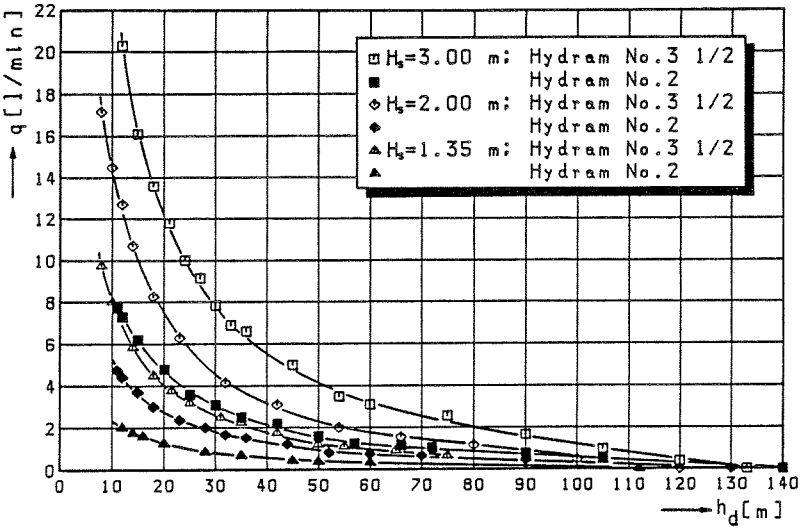

Fig. II-6 Effect of ram size on ram performance; Hydram No. 3 1/2: Q≈100 l/min, Hydram No. 2: Q ≈ 40 l/min.

Commercially-made hydraulic rams are available in various sizes, covering a wide range of source supplies. The size of the ram (traditionally given in inches) usually denotes the nominal diameter of the drive pipe. The larger the size of the ram the more water is required to operate the ram and the more water can be delivered to a higher level. For example, Fig. II-6 compares ram performances (obtained from experiments) for various arrangements of supply and delivery heads for two rams of the same manufacture but of different size: Blake Hydram No. 2 (1 1/2") and Blake Hydram No. 3 1/2 (2 1/2"). It may also be observed from the figure that a small amount of water with 'plenty' of fall (e.g. $Q = 40$ l/min; $H_s = 3$ m) will deliver as much water as an arrangement using plenty of water having only a small fall ($Q = 100$ l/min; $H_s = 1.50$ m).

Trying to eliminate the effect of ram size by plotting flow ratio (q/Q) versus delivery head results in curves such as those of Fig. II-7. The figure illustrates that for this specific type of ram the output (q) is proportional to the input (Q) regardless the size of the ram; for different supply heads different curves are obtained.

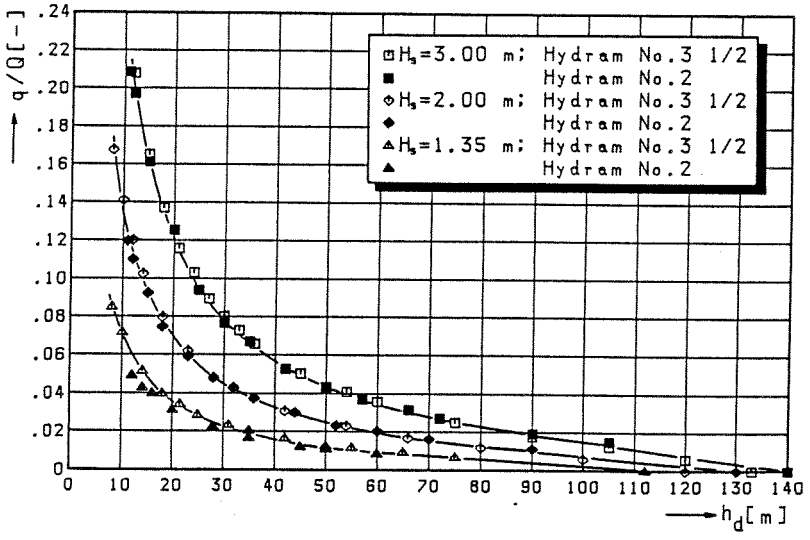

Fig. II-7 Flow ratio versus delivery head - Blake Hydram No.2 : Q = 40 l/min, Blake Hydram No.3 1/2 : Q = 100 l/min.

Finally, eliminating the effect of supply head H_s leads to a dimensionless curve depicting flow ratio (q/Q) versus head ratio (h_d/H_s).

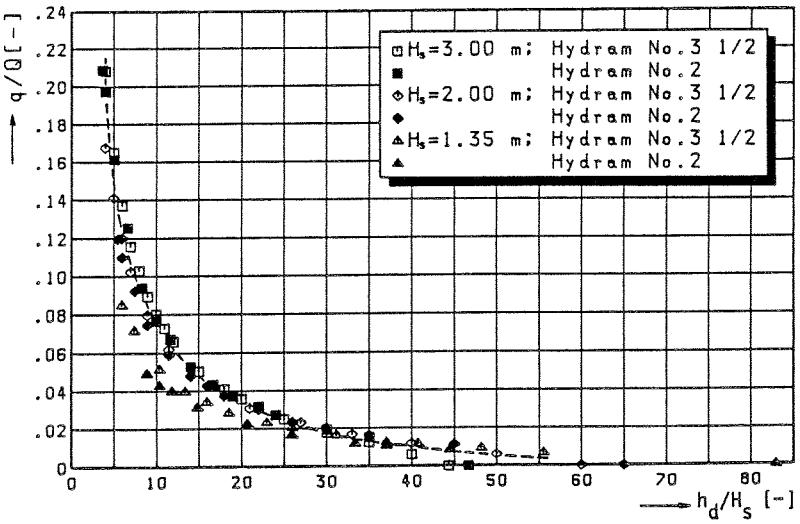

Fig. II-8 Flow ratio versus head ratio - Blake Hydram No. 2 and No. 3 1/2

The object of Fig. II-8 is to determine trends rather than absolute values. The figure illustrates that for the higher supply heads the dimensionless ram performances tend to be similar. Some divergence is observed for the lower supply head, partly owing to the length of drive pipe used in the test installation (approx. 12 m), which is somewhat on the large side for a supply head H_s = 1.35 m (see also Appendix A).

It must be noted at this point that the performance characteristics presented so far, are obtained from experiments taken on two commercial hydraulic rams and in a way are restricted to these specific rams. However, general conclusions on ram performance as portrayed in the figures may be found to be true for any well-designed ram, but the exact shape of the curves and the magnitude of the numerical values will vary according to the particular design. Detailed information on performance characteristics of the commercial rams tested in this investigation are included in Appendix A.

Efficiency. As previously mentioned, definition of efficiency requires special attention since two different expressions can be obtained. One expression is attributed to D'Aubuisson [2], the other to Rankine [19] but both are in fact proposed by Eytelwein [6] (see also Calvert [4a]).
The Rankine concept considers the installation as a whole and takes the

head water level (a) as datum (see Fig. II-9). The useful work done in unit time, i.e the net amount of potential energy of the water delivered, is given by $\rho g q(h_d - H_s)$. The net amount of energy used by the ram, i.e. the change in potential energy of the driving water is given by $\rho g Q H_s$.

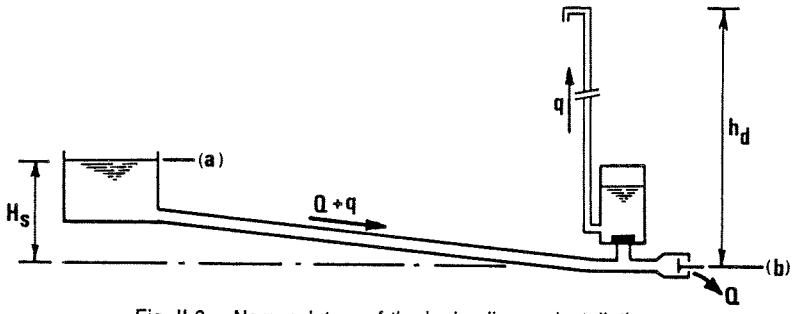

Fig. II-9 Nomenclature of the hydraulic ram installation.

Hence the Rankine efficiency is

$$\eta_{rnk} = \frac{\Delta E_{pot} \text{ water delivered}}{\Delta E_{pot} \text{ driving water}} = \frac{q * (h_d - H_s)}{Q * H_s} \qquad \text{(II-1)}$$

D'Aubuisson considers the ram alone and takes the tail water level (b) as datum. The useful work done in unit time is then given by $\rho g q h_d$, while the energy supplied to the ram per unit time is $\rho g(Q + q)H_s$.
Hence the D'Aubuisson efficiency is

$$\eta_{aub} = \frac{q * h_d}{(Q + q) * H_s} \qquad \text{(II-2)}$$

In product information of hydraulic ram manufacturers, as well as in some other publications on hydraulic rams, efficiency is often simply defined as

$$\eta_{trd} = \frac{q * h_d}{Q * H_s} \qquad \text{(II-3)}$$

The Rankine figure is always the lowest, while the 'trade expression' yields somewhat higher values; especially at low delivery heads the difference is significant. This is illustrated in Fig. II-10, showing efficiency curves compiled from measurements taken on a Blake Hydram No. 3 1/2.

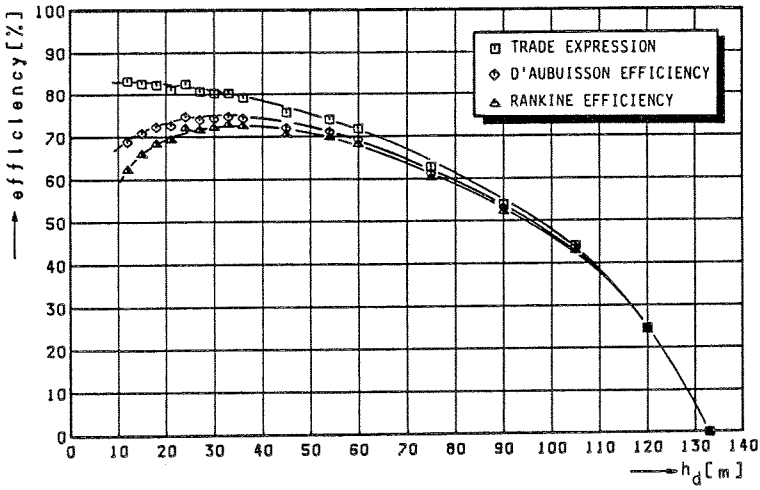

Fig. II-10 Efficiency curves - Blake Hydram No. 3 1/2 (2 1/2") (H_s = 3 m; Q ≈ 95 l/min).

Of the expressions (II-1), (II-2) and (II-3) the Rankine efficiency is to be preferred, since both the D'Aubuisson expression and the trade expression admit of efficiencies when there is no net output above the surface elevation of the supply source (level a).
Alternatively, efficiency can be plotted as a function of pumping rate q (see Fig. II-11).

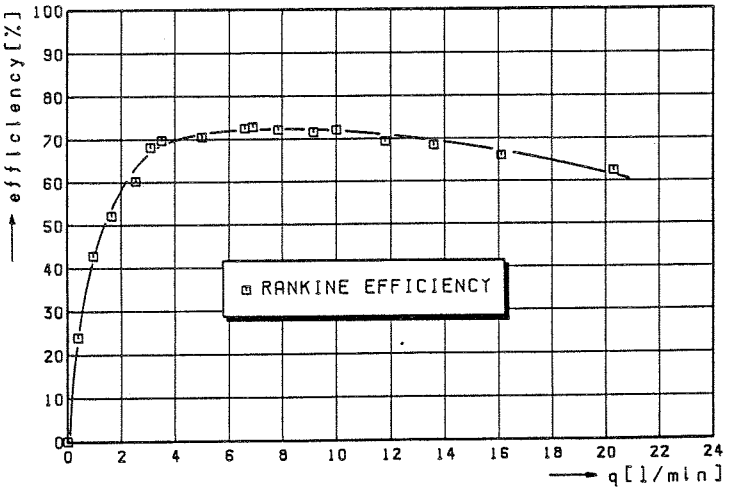

Fig II-11 Rankine efficiency versus pumping rate
Blake Hydram No. 3 1/2 (H_s=3 m; Q ≈ 95 l/min).

The efficiency curve is most important when the supply source is limited and waste water must be kept to a minimum. In situations where there is an abundance of supply water the efficiency is a secondary matter. However, efficiency figures give a good indication of the hydraulic performance of the ram. High efficiency machines are hydraulically well-designed, i.e. have fair and smooth waterways and consequently have low energy losses.

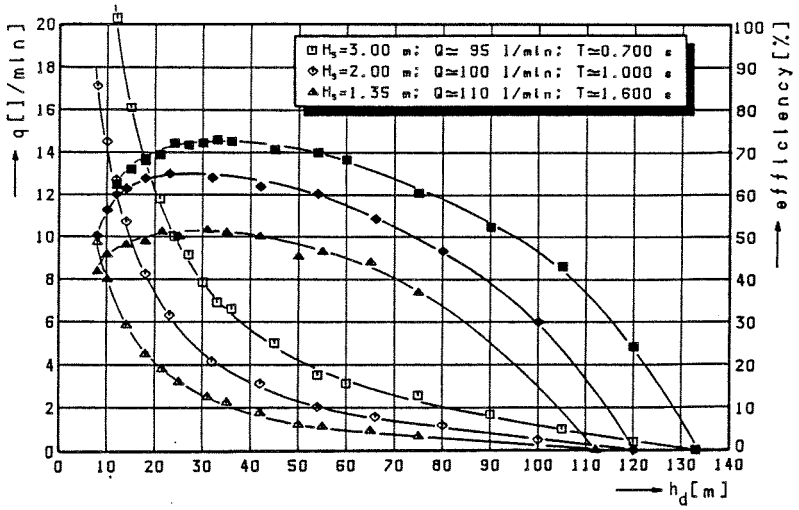

Fig. II-12 Effect of supply head on efficiency - Blake Hydram No. 3 1/2
■ , ◆ , ▲ : Efficiency versus delivery head
□ , ◇ , △ : Pumping rate versus delivery head.

Given a hydraulic ram installation working under a supply head H_s, peak efficiencies generally occur in the range of delivery heads at which the q,h_d-curve changes slope (Fig. II-12). Lansford and Dugan [12] found this to be true for the rams they tested as well. In terms of dimensionless parameters the maxima of the efficiency curves are usually found for head ratios of between 10 and 20.

Data from manufacturers. It should be standard commercial practice that manufacturers of hydraulic rams provide comprehensive and reliable information on the performance characteristics of their rams. Unfortunately this is not always the case.
For example, some ram manufacturers state that the 'output' of their rams can be calculated using the simple formula

$$q = \frac{Q * H_s}{h_d} * 0.6$$

where q, Q, H_s and h_d are as defined earlier (see e.g. Fig. II-1). The formula

is based merely on the rule of thumb that a typical efficiency of a hydraulic ram is around 60 %. Apart from the fact whether the specific ram is capable of attaining this efficiency, it is unlikely that the use of the formula is correct for all arrangements of supply and delivery heads, since it has been found from experiments that efficiency eventually diminishes as head ratio h_d/H_s increases (see also Appendix A). A more realistic approach is followed by manufacturers recommending the formula

$$q = \frac{Q * H_s}{h_d} * \eta$$

where numerical values of η are given in relation to head ratio h_d/H_s.
To our knowledge only a few manufacturers provide empirically obtained operating tables. The use of such tables is best demonstrated with some examples.

Size of Hydram			1	2	3	3½	4	5	6	7	8	10
Volume of driving water available	Litres per minute	From	7	12	27	45	68	136	180	750	1136	1545
		To	16	25	55	96	137	270	410	364	545	770
	Gallons per minute	From	1.5	2.5	6	10	15	30	40	165	250	340
		To	3.5	5.5	12	21	30	60	90	80	120	170
Maximum height to which Hydram will pump water	Metres		150	150	120	120	120	105	105	105	105	105
	Feet		500	500	400	400	400	350	350	350	350	350
Nominal diameter of Drive Pipe	m.m. bore		32	40	50	65	80	100	125	150	175	200
	ins. bore		1¼	1½	2	2½	3	4	5	6	7	8

Table II-1 Hydram input capacity (source: John Blake Ltd)

Working Fall (Metres)	Vertical height to which water is raised above the Hydram (Metres)											
	5	7.5	10	15	20	30	40	50	60	80	100	125
1.0	144	77	65	33	29	19.5	12.5					
1.5		135	96.5	70	54	36	19	15				
2.0		220	156	105	79	53	33	25	19.5	12.5		
2.5		280	200	125	100	66	40.5	32.5	24	15.5	12	
3.0			260	180	130	87	65	51	40	27	17.5	12
3.5				215	150	100	75	60	46	31.5	20	14
4.0				255	173	115	86	69	53	36	23	16
5.0				310	236	155	118	94	71.5	50	36	23
6.0					282	185	140	112	93.5	64.5	47.5	34.5
7.0						216	163	130	109	82	60	48
8.0							187	149	125	94	69	55
9.0							212	168	140	105	84	62
10.0	LITRES PUMPED IN 24 HOURS PER LITRE/MIN OF DRIVE WATER						245	187	156	117	93	69
12.0							295	225	187	140	113	83
14.0								265	218	167	132	97
16.0									250	187	150	110
18.0									280	210	169	124
20.0										237	188	140

Table II-2 Hydram output capacity (source: John Blake Ltd)

For instance Tables II-1 and II-2 show the performance data for the Blake Hydram as provided by its manufacturer (John Blake Ltd). In Table II-1 are listed the various sizes of Hydrams together with the volume of water per minute which each can accept. The lower limits indicate the minimum flow rate which should be available to operate the ram. The upper limits are the approximate volumes of water used by the Hydrams at full power. Table II-2 gives the quantity, in litres, of water raised per 24 hours for each litre of driving water used per minute, under the chosen conditions of delivery head and supply head (working fall).
Thus, to calculate the total amount of water raised per 24 hours multiply the figure obtained from Table II-2 by the litres of driving water used by the Hydram per minute. The distance over which the pumped water travels can be taken into account by adding the equivalent friction head loss to the vertical height.

Example II-1: Given a source supply of 100 l/min. The height to which the water must be raised is 50 metres measured from the source level (see Fig. II-13). The length of the delivery pipe is known to be approximately 1250 m.

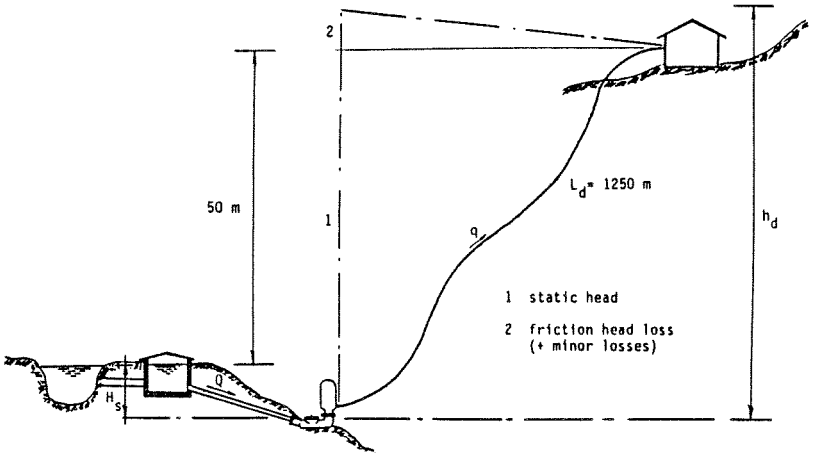

Fig. II-13 Calculation example

First the delivery head should be established:
Delivery head = static head (i.e. vertical lift above the ram) + friction head loss (+ minor losses).
Suppose the imposed friction head for 1000 m length of delivery pipe is

approximately 4 m. Then, for 1250 m of pipe, the friction head loss is

$$\frac{1250}{1000} * 4 = 5 \text{ m.}$$

If the supply head H_s, which can be obtained from the source, is 5 m then the delivery head $h_d = 5 + 50 + 5 = 60$ m. With 5 m supply head and 60 m delivery head the Hydram will pass 71.5 litres of water per 24 hours for every litre per minute which flows into the Hydram (see Table II-2). Thus for a supply flow of 100 l/min the quantity of water pumped will be 71.5 * 100 = 7150 l/day.

By increasing the vertical fall the output will be proportionally increased. For instance, take $H_s = 7$ m then $h_d = 7 + 50 + 5 = 62$ m.
By interpolation Table II-2 indicates that 106 l/day per l/min of driving water will be delivered. Thus: total daily delivery is 100 * 106 = 10600 l/day.

Alternatively, it may be necessary to increase the supply head in order to deliver the same amount of water with less water available to drive the ram. For example, it follows from the previous calculations that for $H_s = 7$ m and $h_d = 62$ m, a daily demand of 7150 l/day requires a supply flow of

$$\frac{7150}{106} = 68 \text{ l/min}$$

to power the ram (instead of the original 100 l/min for $H_s = 5$ m). This will allow of applying a Hydram No. 3 1/2 instead of No. 4 (see Table II-1).

Table II-2 also shows that the amount of water delivered becomes smaller as the hydraulic ram must pump against a greater delivery head. Take $H_s = 5$ m and $h_d = 80$ m (friction head loss included) then for 100 l/min of drive water the total delivery will be 100 * 50 = 5000 litres/day.

Example II-2: Given the following data: supply head $H_s = 4$ m and delivery head $h_d = 50$ m. What source supply should be available to accomplish a pumping rate of 5500 l/day.
Under the given conditions of supply head and delivery head a Blake Hydram will pump 69 litres/day for every litre/minute of driving water (see Table II-2). Thus, to meet a daily demand of 5500 litres, the available source supply should be at least

$$\frac{5500}{69} = 80 \text{ litres/min.}$$

Table II-1 indicates that either size No. 3 1/2 or size No. 4 can handle this volume. Sensibly the choise favours the Hydram No. 3 1/2 to allow for any flow reduction caused by say drought conditions (seasonal variation).

SANO-ram performance data for different sizes of pump and for various arrangements of head ratio are given in Table II-3. The use of this table is explained in the next example.

Example II-3: Given the following data: source supply Q = 150 l/min, supply head H_s = 5 m and delivery head h_d = 70 m.
The top part of Table II-3 indicates the ram size to be applied according to the available source supply. In this case (Q = 150 l/min) size No. 6 will do.
Introducing the head ratio h_d / H_s the bottom part of the table yields the daily delivery per l/min of drive water for the various ram sizes.

SANO No.		0	1	2	3	4	5	6	7	8	9
drive pipe	mm. bore	20	25	32	40	50	65	80	100	125	150
	ins.bore	3/4	1	1¼	1½	2	2½	3	4	5	6
driving water [l/min]	from	3	6	12	18	30	50	80	120	180	280
	to	6	16	30	45	65	110	180	250	400	700
	4:1	245	252	262	272	282	288	294	300	305	312
h	6:1	167	171	177	183	189	194	200	206	212	215
e	8:1	124	128	131	135	141	145	148	153	156	160
a	10:1	94	96	99	104	108	111	114	115	118	122
d	12:1	72	73	76	79	84	86	89	91	92	95
h_d/H_s	14:1	55	58	60	63	66	69	72	73	75	76
r	16:1		45	48	52	55	58	59	60	62	63
a	18:1			40	43	46	48	49	50	52	53
t	20:1				36	37	40	42	43	45	46
i	22:1					33	35	36	37	38	39
o	24:1	litres pumped in 24 hours per l/min of drive water.					30	32	33	34	36
	25:1							29	30	32	33

Table II-3 SANO-ram performance - source: Pfister + Langhanss

Thus: head ratio h_d / H_s = 14 :1, then ram No. 6 will pump 72 l/day per l/min of drive water. So, for Q = 150 l/min the total delivery is 150*72 = 10800 litres/day.

II-3 Practical use

Quite a number of publications on the practical use of hydraulic rams have been written (see e.g. [8,10,21,23,25,26]). Most of the commercial ram manufacturers provide information on the subject as related to their rams;

some of these manuals give a good set of instructions on the necessary field survey and the design and construction of the hydraulic ram installation at a given site. There is little to add to this, but to summarize some of the main features. Much of the information here presented is adopted from references [21,23,26] as well as from trade brochures (Blake, Rife).

Basic Requirements. The use of a hydraulic ram requires the availability of a suitable and reliable supply of water, with a fall sufficient to operate the ram. The supply can be any source of flowing or stagnant water such as a spring, stream, river, lake, dam or even a pond fed by an artesian well. It may be remembered from the previous section (Tables II-1 and II-3) that small size rams require a supply flow of at least 5 to 25 litres per minute, whereas very large rams may need as much as 750 to 1500 l/min. For most hydraulic rams the fall in driving water from the source to the ram must be at least 1 m.

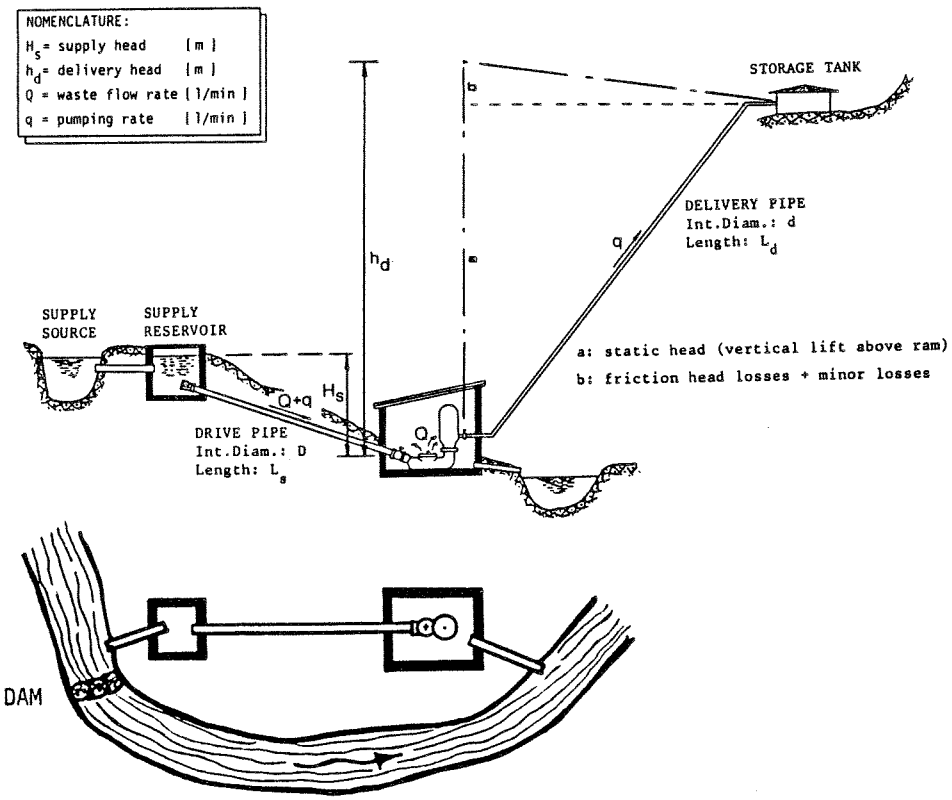

Fig.II-14 Hydraulic ram installation.

Site Selection. When selecting a potential site for the hydraulic ram installation it is essential that provisions can be made both for water input to the ram and for proper drainage of the waste water away from the ram (see Fig. II-14). Under no circumstances, flood conditions included, should the hydraulic ram be submerged to a level higher than the top of the waste valve, since this will seriously affect its operation.

Before any possible lay-out of the installation can be designed a preliminary survey must reveal the following items:

1) Amount of water available to power the ram (source flow) [l/min]
2) Minimum daily quantity of water to be pumped (delivery flow) [l/day]
3) Working fall (supply head) which can be obtained from the source [m]
4) Distance in which the working fall can be obtained [m]
5) Vertical lift from potential ram site to delivery site [m]
6) Approx. length of delivery pipe from ram to delivery site. [m]

Unless the supply water is obviously more than adequate, the source flow must be measured with reasonable accuracy. The possible change of flow at different times of the year should be established in order to determine the minimum guaranteed flow available. Techniques for measuring flows may be found in the appropriate literature; e.g. reference [26] partly deals with the subject as well as with levelling methods for measuring differences in height (working fall, vertical lift).

The total daily volume of water required to be pumped to the delivery site can be calculated according to the purpose of use. For example, if the water is to be used for domestic consumption in a rural setting, the daily demand may be approximated by:

$$\text{Water Demand} = \text{Population} * \text{Per Capita Consumption} \qquad \text{(II-4)}$$

A typical per capita consumption is 40 to 50 litres/person/day. If live-stock is present, its water use should be included also.
Given the fact that the hydraulic ram is capable of operating continuously twenty-four hours per day, the required pumping rate (q) is obtained by dividing the daily water demand by 24 * 60 = 1440 minutes; in formula:

$$\text{Pumping Rate } q\ [\text{l/min}] = \frac{\text{Water Demand } [\text{l/day}]}{1440\ [\text{min/day}]} \qquad \text{(II-5)}$$

The working fall (supply head H_s) is measured vertically from the supply

source level to the output level at the waste valve of the ram. Remembering the previous section (Fig. II-5), the pumping capacity of the hydraulic ram varies directly with increased supply head.
The supply head can be increased by increasing the input level (e.g. by selecting the water input further upstream) and/or by lowering the position of the ram itself (as long as it can be placed on a spot from which the waste water can be easily drained away, e.g. to a suitable discharge point further downstream). When the desired working fall is not obtainable in the distance which is specified for the drive pipe (L_s should be approx. 4 to 7 times H_s), reference to Fig. II-15 will show various methods of obtaining it under different site conditions.

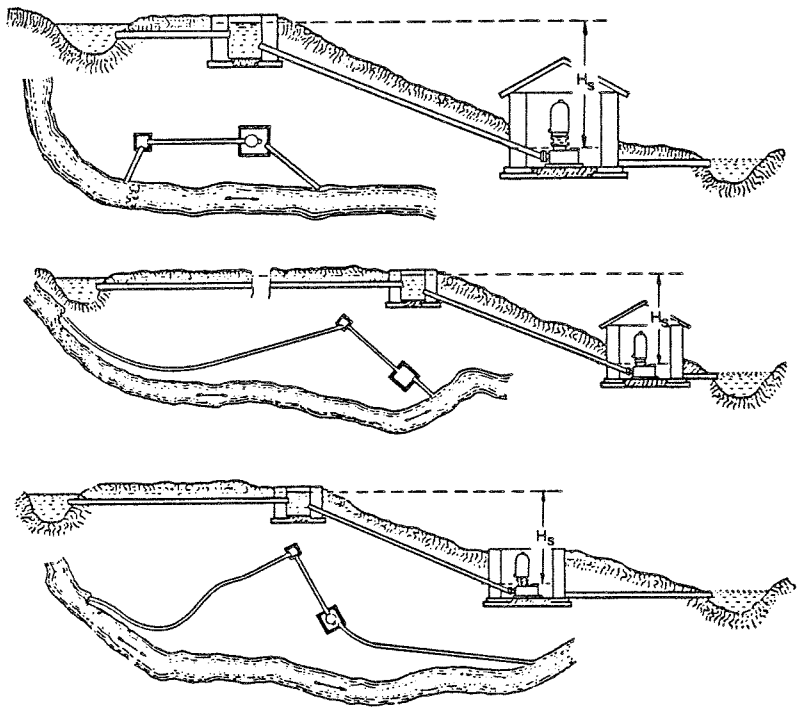

Fig. II-15 Possible lay-outs of a hydraulic ram installation (source: John Blake Ltd)

The next question to be adressed is what pressure head the hydraulic ram will need to supply to lift the water to the storage tank and to overcome all energy losses in the delivery pipe. In general this will be equal to (see Fig. II-14):

$$\text{Delivery Head } (h_d) = \text{Vertical Lift above Ram} + \left[\frac{f\,L_d}{d} + \xi_d\right]\frac{v^2}{2g} \qquad \text{(II-6)}$$

where	f	= pipe friction factor	[-]
	L_d	= length of delivery pipe	[m]
	d	= internal diameter of delivery pipe	[m]
	ξ_d	= sum of minor loss factors	[-]
	v	= average velocity in delivery pipe	[ms^{-1}]
	g	= acceleration due to gravity	[ms^{-2}]

Vertical lift must be measured from the location of the ram to the highest possible water surface level (overflow level) in the storage tank. Minor losses may usually be neglected (or roughly estimated) as compared with vertical lift and friction head loss.
As an example, Table II-4 lists the imposed friction head loss for various delivery flows using different sizes of pipe bore.

f = 0.04; L_d = 1000 m			
delivery flow [l/day]	del. pipe bore [inch]	[mm]	imposed friction head ΔH_{fr} [m/1000 m pipe]
5000	3/4	20	3.40
9000	1	25	3.60
16000	1 1/4	32	3.30
28000	1 1/2	40	3.35
50000	2	50	3.50
95000	2 1/2	65	3.40
135000	3	75	3.35

Table II-4 Friction head losses

Knowing the available source supply (Q_{source}), the required pumping rate (q), the supply head (H_s) and the delivery head (h_d) the size of the hydraulic ram can be selected with the aid of the appropriate performance tables or, when available, with use of empirically obtained q/Q versus h_d/H_s-curves (see also examples II-1, II-2 and II-3 in the previous section):

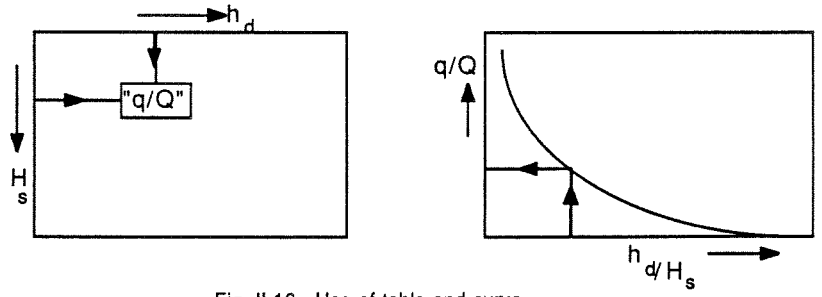

Fig. II-16 Use of table and curve

The sum of the waste flow (Q) used by the ram and the pumping rate (q) must be less than the minimum guaranteed source flow, i.e.

$$Q + q < Q_{source} \qquad \text{(II-7)}$$

Since supply head (H_s) and delivery head (h_d) are more or less fixed by the terrain conditions (topography), the size of the hydraulic ram is mainly determined by the desired pumping rate, or limited by the source supply available to drive the ram.
In cases where the installation has not enough (or no longer enough) capacity to meet the daily water demand (and/or no larger ram is available), a battery of several rams may be used (Fig II-17). Of course, this requires a source which can supply water at a sufficient high rate. Each ram must have its own individual drive pipe, but they may use the same delivery pipe unless they are meant to deliver to different places.

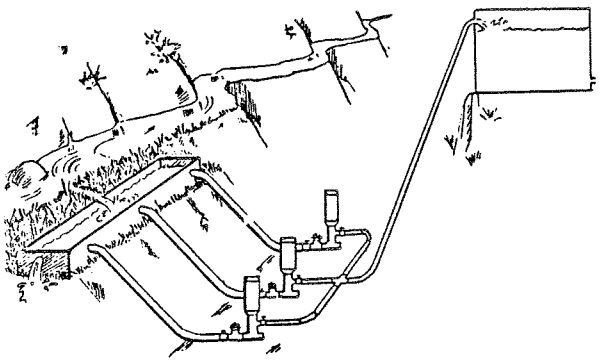

Fig II-17 Hydraulic rams placed parallel (source: [23])

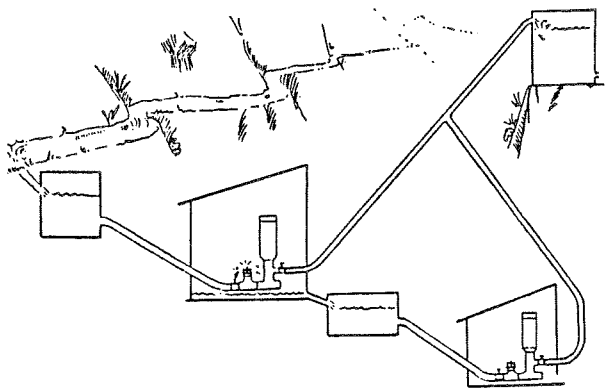

Fig II-18 Hydraulic rams placed in series (source: [23])

A battery of hydraulic rams is also very useful in a situation where the minimum flow during periods of drought is enough to power only one or two rams and the maximum flow is sufficient to drive three or more rams.
On the other hand, in a case where the supply water is sufficient to power only one hydraulic ram, but the delivery flow does not quite meet the requirements, the waste water from the initial ram may be used to drive another ram (Fig. II-18).

Installation and maintenance. Since the hydraulic ram may experience savage pounding under operation, it should be firmly bolted to a concrete base.
The drive pipe is by far the most important part of the installation; it carries the water from the supply reservoir to the ram and contains the high pressure surges (waterhammer) during the pumping stage of the operating cycle of the ram (see chapter III). The drive pipe should therefore be made of strong, rigid material, preferably galvanized iron. It should be watertight and rigidly anchored. The length (L_s) should be approximately 4 to 7 times the supply head H_s. The inlet to the drive pipe must always be submerged to prevent air from entering the pipe; air bubbles in the drive pipe will dramatically affect the operation of the ram or even lead to complete failure. For this reason the drive pipe should be laid as straight as possible throughout its entire length without any elevated sections which could trap air. A dip to allow the drive pipe to follow the contour of the ground is permissible.
The delivery pipe may be made of any material (e.g. P.V.C. - polyvinyl chloride or HDP - high density polyethylene) provided that it is able to withstand the delivery pressure. If the delivery head exceeds the pipe's pressure specification, than the lower portion of the delivery pipe must be galvanized iron pipe. In fact it may be advisable always to use an initial length of galvanized iron pipe to ensure a sturdy connection to the ram.
To facilitate operation and maintenance of the hydraulic ram the drive pipe and the delivery pipe should each be connected to the ram with union joints and stop-valves. The stop-valve in the drive pipe should be incorporated in such a manner as to prevent the formation of air pockets; a rotary type of valve (globe valve) is preferable to an ordinary gate valve since the latter may not be proof against the severe loads of the waterhammer pressures.
In general, hydraulic rams are not self-starting. Normally, the waste valve must be operated by hand for a couple of strokes until the ram has built up enough air chamber pressure to start its automatic impulse action.

The maintenance required for a hydraulic ram is very little and infrequent. It

includes:
- replacement of the valve rubbers when they wear out
- adjustment of the tuning of the waste valve
- thightening bolts which work loose.

The most suitable adjustment of the waste valve is that in which the hydraulic ram raises a maximum volume of water without lowering the water level in the supply tank.

Occasionally the hydraulic ram may need dismanteling for cleaning. It is essential that as little debris as possible enters the drive pipe. It is therefore necessary to provide a grate at the intake from the supply source as well as a strainer at the inlet side of the drive pipe to keep back floating leaves and debris. The grate and strainer must be checked every now and then and cleaned if necessary to ensure that the water supply is flowing at the maximum rate.

It must be stated once again that the foregoing section on the practical use of the hydraulic ram only highlights some of the main features of the installation. Every situation may vary in detail and specific design and techniques suited to the particular site may be necessary to create the most appropriate hydraulic ram installation. More detailed information on how to construct, operate and maintain the hydraulic ram installation can be found in the cited literature as well as in the appropriate product information.

III HYDRAULIC RAM ANALYSIS

In this chapter the operation of the hydraulic ram is analysed more in detail. It should be noticed that for the proper understanding of the phenomena governing the action of the hydraulic ram some basic knowledge of 'Pressure Wave Theory' is required. For this purpose and for the sake of completeness Appendix B deals with the subject of 'Unsteady Flow in a Pipeline'. The main results of the theory will be summarized in the appropriate parts of this chapter.

III-1 Division of the cycle into periods

Fig. III-1 (1 through to 6) presents a review of the sequence of events that can be distinguished in a complete cycle of operation of the hydraulic ram. In addition to the hydraulic ram installation the figures show a diagram of the assumed velocity-time relation for the water at the lower end of the drive pipe (i.e. near to the ram). A clock roughly indicates the length of time taken by the various events; the corresponding parts of the u(t)-diagram are drawn as thick solid lines.

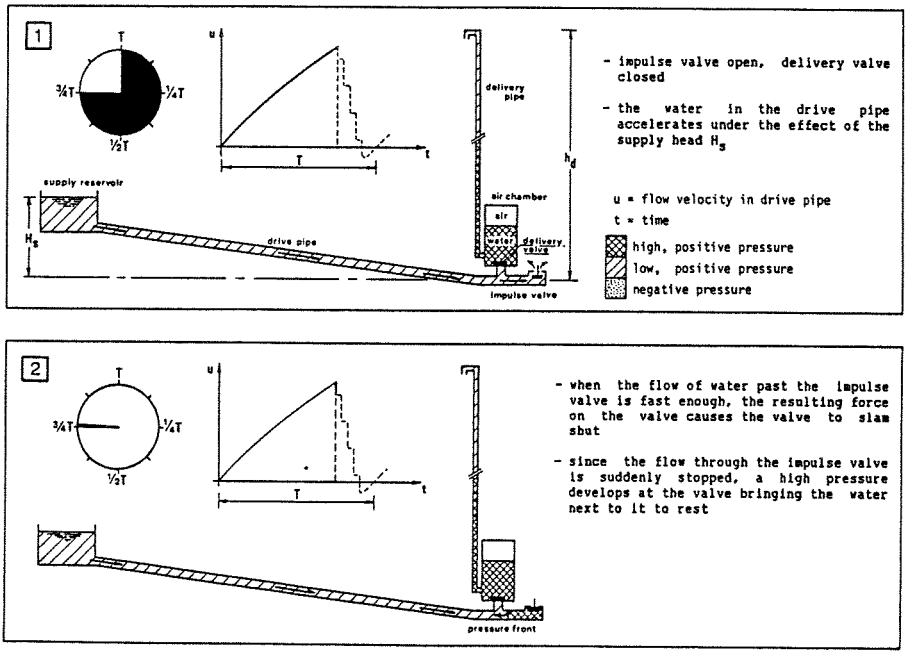

Fig. III-1 Hydraulic ram cycle - sequence of events
(continued on next page)

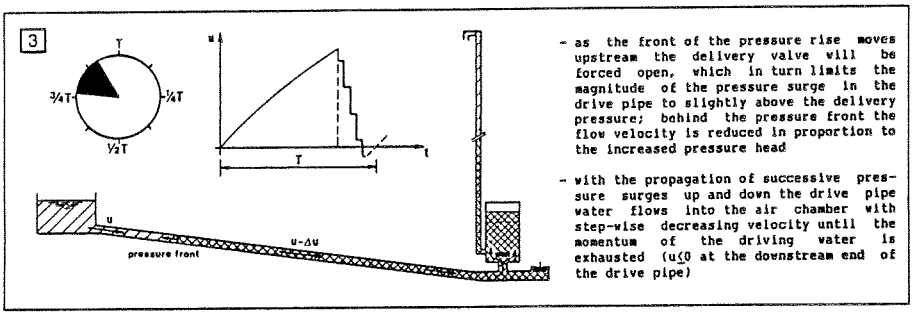

- as the front of the pressure rise moves upstream the delivery valve will be forced open, which in turn limits the magnitude of the pressure surge in the drive pipe to slightly above the delivery pressure; behind the pressure front the flow velocity is reduced in proportion to the increased pressure head

- with the propagation of successive pressure surges up and down the drive pipe water flows into the air chamber with step-wise decreasing velocity until the momentum of the driving water is exhausted ($u \leq 0$ at the downstream end of the drive pipe)

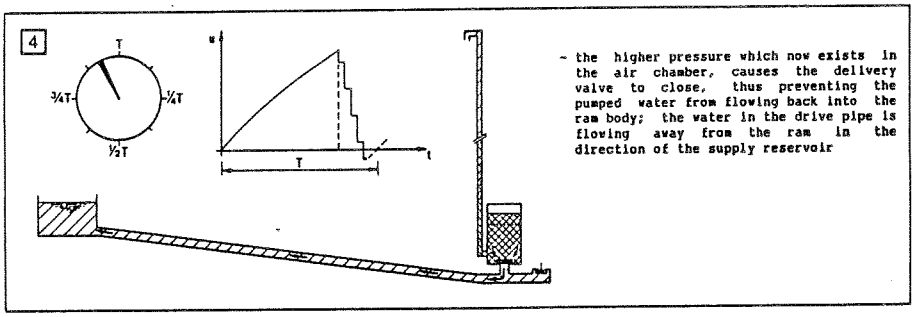

- the higher pressure which now exists in the air chamber, causes the delivery valve to close, thus preventing the pumped water from flowing back into the ram body; the water in the drive pipe is flowing away from the ram in the direction of the supply reservoir

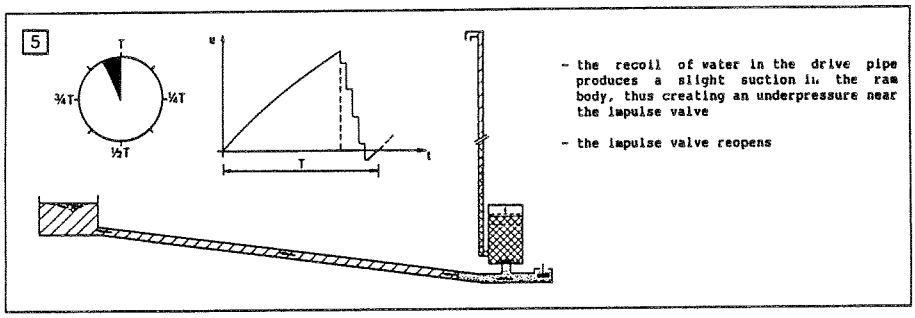

- the recoil of water in the drive pipe produces a slight suction in the ram body, thus creating an underpressure near the impulse valve

- the impulse valve reopens

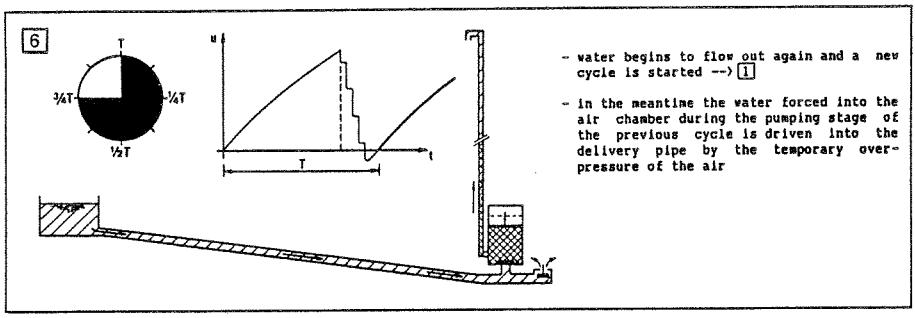

- water begins to flow out again and a new cycle is started --> 1

- in the meantime the water forced into the air chamber during the pumping stage of the previous cycle is driven into the delivery pipe by the temporary overpressure of the air

Fig. III-1 Hydraulic ram cycle - sequence of events

The analysis of the hydraulic ram operation is attacked by dividing the operating cycle into seperate parts (periods) and by attempting to obtain the relation between velocity (u) and time (t) for the water column in the drive pipe during each part of the cycle. From these relationships the quantity of water wasted and the quantity pumped per cycle may be found (Fig. III-2); the period time T of a complete cycle of operation may also be determined. From these values the time rate of pumping (q) and of wasting (Q) can be easily obtained.

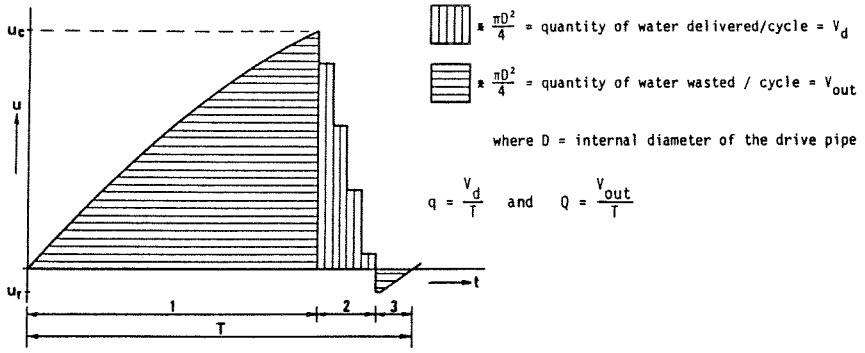

Fig. III-2 Method of approach

With the 'sequence of events' (Fig. III-1) in mind, it may be clear that the division of the cycle into (sub-)periods should be based on the positions (open - closing - closed) of impulse valve and delivery valve; any change in valve setting implies a change in the downstream boundary condition for the motion of the water in the drive pipe. A logical point to start the cycle seems to be the moment of zero velocity in the drive pipe with the impulse valve in open position. Initially this leads to a division into six periods as shown in Fig. III-3.

The division of the cycle into periods (a) through to (f), Fig. III-3, may be briefly outlined as follows:

Period a: includes the time from the instant of zero velocity (u = 0) to the beginning of impulse valve closure.

Period b: includes the time from the instant the valve begins to close until the instant at which it is completely closed.

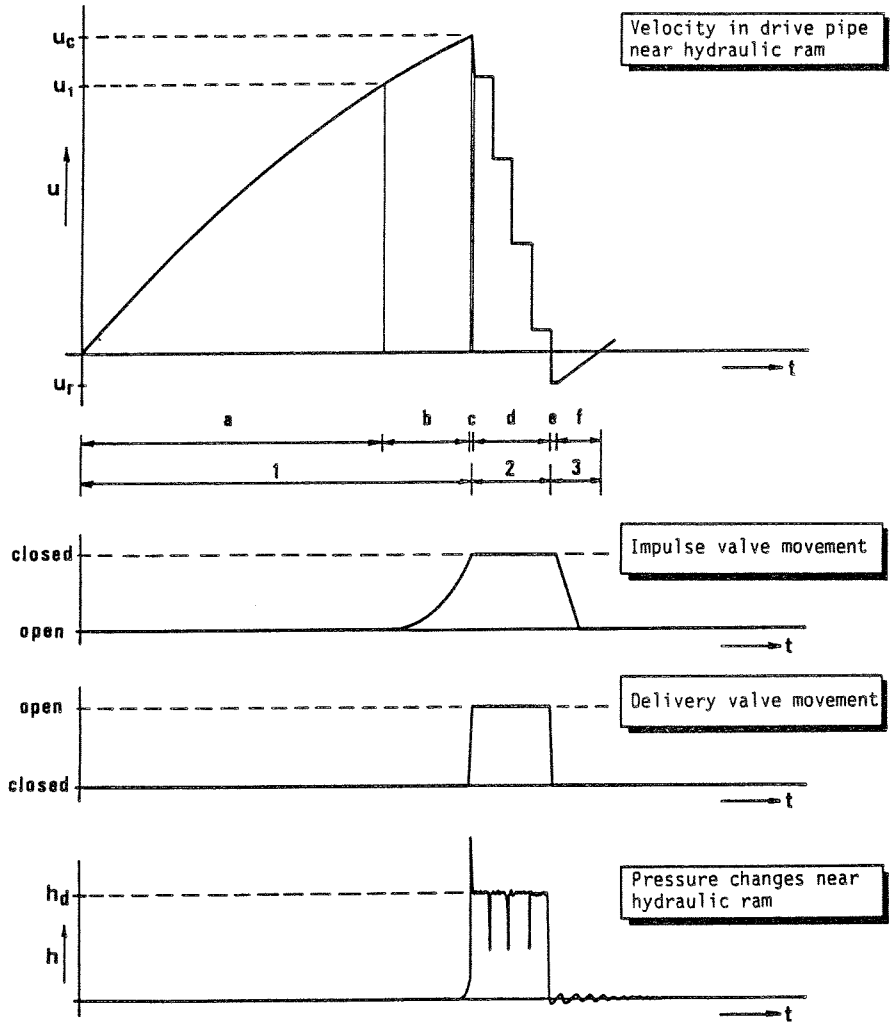

Fig. III-3 Division of the cycle into periods

Period c: includes the time between the instant of complete closure of the impulse valve and the instant of opening of the delivery valve.

Period d: includes the time during which the delivery valve is open.

Period e: includes the time between the closing of the delivery valve and the moment the impulse valve reopens.

Period f: includes the time between the instant the impulse valve reopens and the instant of zero velocity.

The following assumptions may now be made:

1. Periods (a) and (b) may be combined to one period:
During period (a) the water in the drive pipe accelerates towards the ram and is wasted through the impulse valve. For a given valve design with known length of valve stroke the head loss at the valve varies only with the magnitude of the velocity (u). When the velocity reaches beyond a certain value ($u = u_1$; Fig. III-3) the drag and pressure forces on the valve exceed the weight of the valve, which then begins to close. During the period of closing of the impulse valve the head loss at the valve depends both on the value of (u) and on the actual position of the valve: as the valve opening becomes smaller the resistance at the valve will increase and the consequent force will cause the valve to close increasingly more rapid.
Indeed, it follows from observations that the major part of the closure takes place at the end of period (b), while there is no significant pressure rise in the ram body until the valve is almost completely closed. This is illustrated in Fig. III-4, showing time recordings of respectively

(I) pressure variation at the lower end of the drive pipe,
(II) pressure variation in the air chamber,
(III) actual motion of the impulse valve and
(IV) actual motion of the delivery valve.

The most interesting parts of the recordings are shown in detail in Fig. III-5. A study of the recordings (I) and (III) will justify the combination of periods (a) and (b) to one period at the end of which the impulse valve is assumed to close instantaneously.

2. Duration of period (c) is neglible:
The delivery valve is forced open by the sudden pressure rise created in the ram body at the moment the impulse valve is completely closed. In addition, visual observation of the delivery valve movement of one of the tested rams showed that the distance through which the valve moves is comparatively small (3 - 5 mm at the most). It may therefore be assumed that the delivery valve opens instantaneously at the moment of complete closure of the impulse valve.
The rightness of this assumption is confirmed by the simultaneous time recordings of impulse valve movement and delivery valve movement (see Figs. III-4 and III-5).

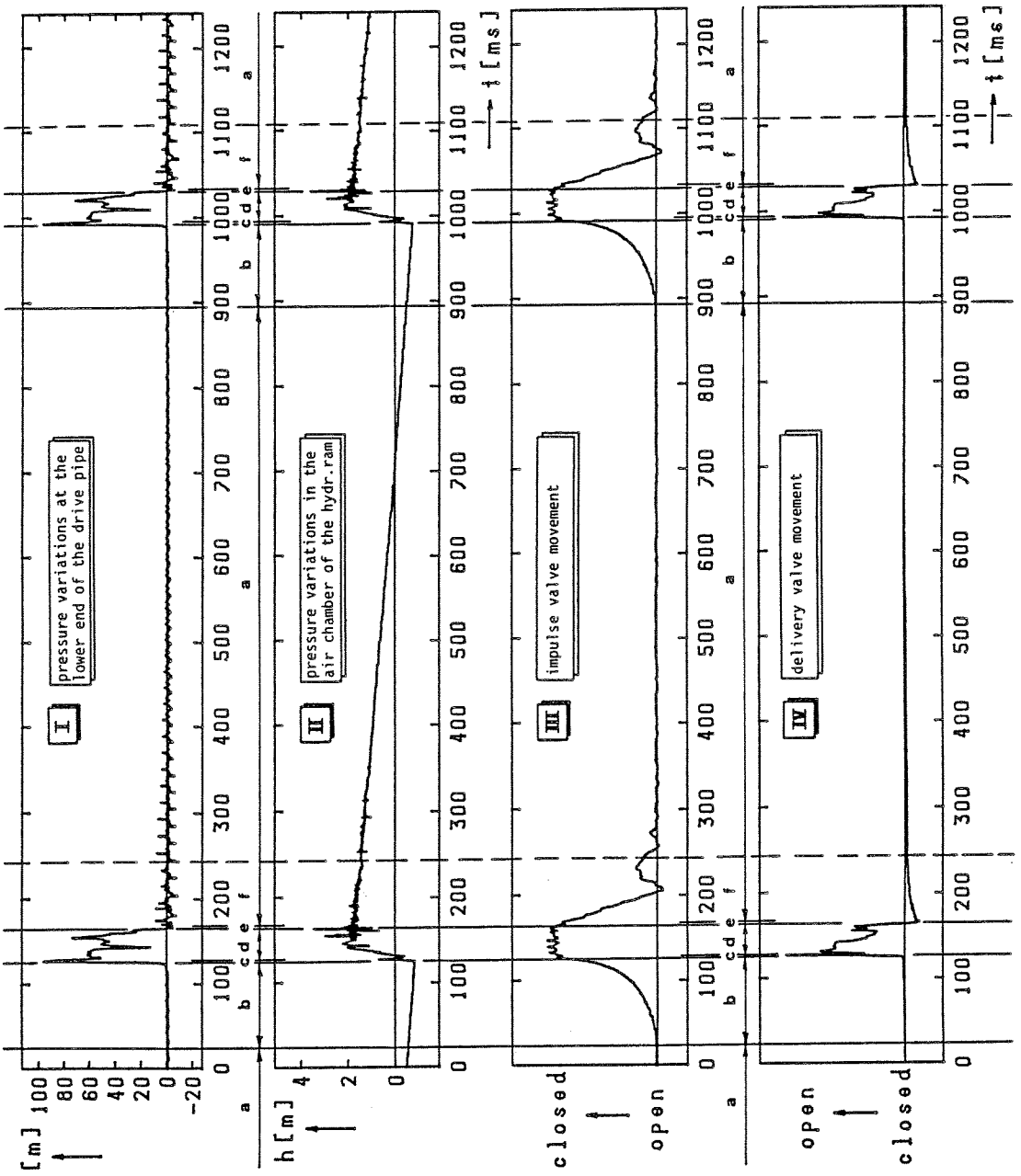

Fig. III-4 Time recordings of pressure variations and valve movements

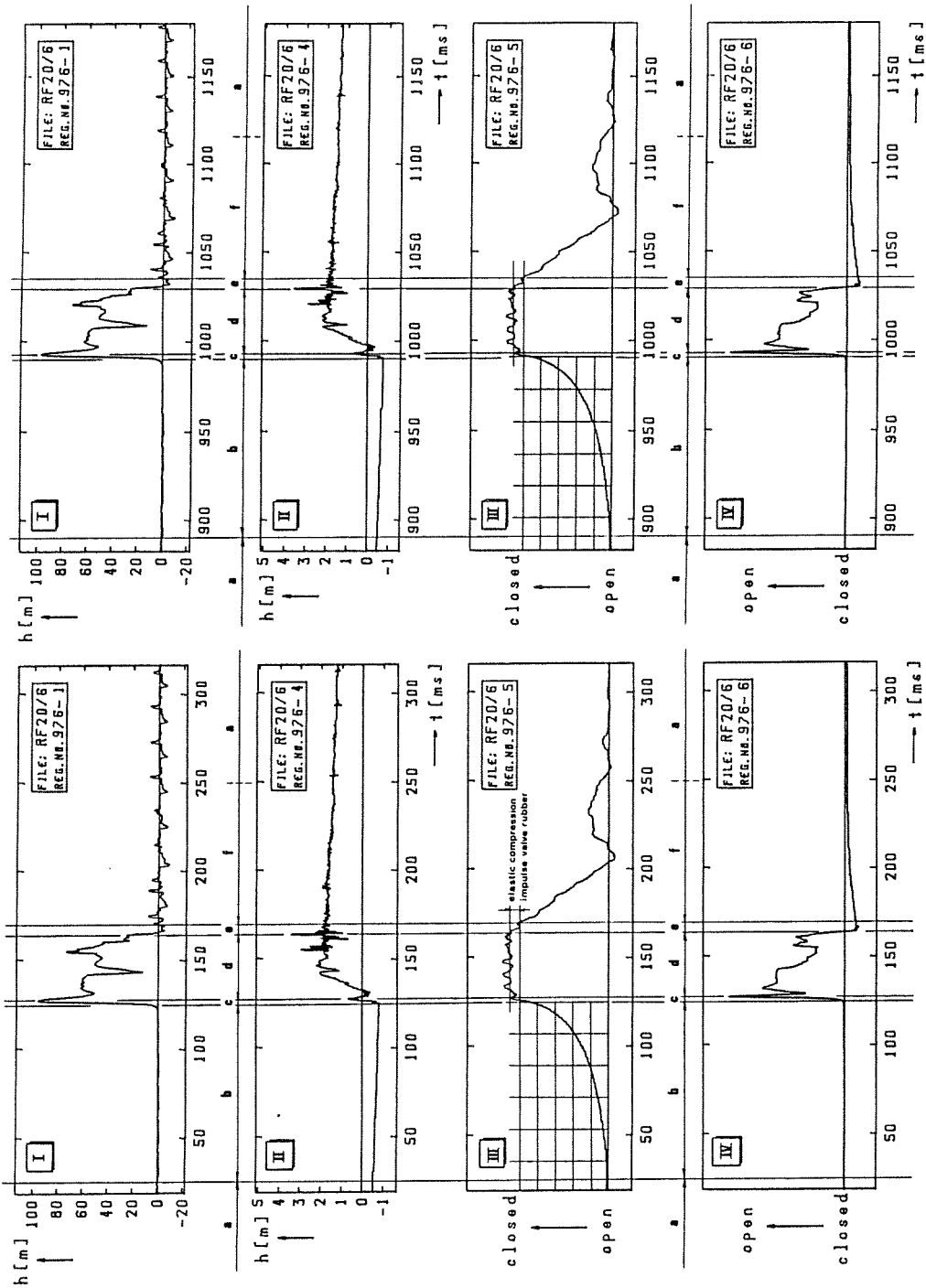

Fig. III-5 Time recordings of pressure variations and valve movements

Note: it may also be observed from Figs. III-4 and III-5 that at the end of period (d), when the momentum of the water column in the drive pipe is exhausted and water tends to flow out of the air chamber in the direction of the supply tank, the delivery valve closes instantaneously, thus preventing the pumped water from flowing back into the ram body.

3. Periods (e) and (f) may be combined to one period:
There is no other basis for this assumption than convenience. As will become clear later, there are two possibilities with respect to period (e):

- either the duration of period (e) is negligible, that is to say the impulse valve reopens shortly after the moment the delivery valve is closed (see Figs. III-4 and III-5),
- or the impulse valve reopens 2 L_s/c second after delivery valve closure (2 L_s/c = time required for a pressure wave to move up and down the drive pipe; see for instance section III-3).

With use of the foregoing simplifications, the hydraulic ram analysis may be based on a division of the operating cycle into three main periods (Fig.III-6):

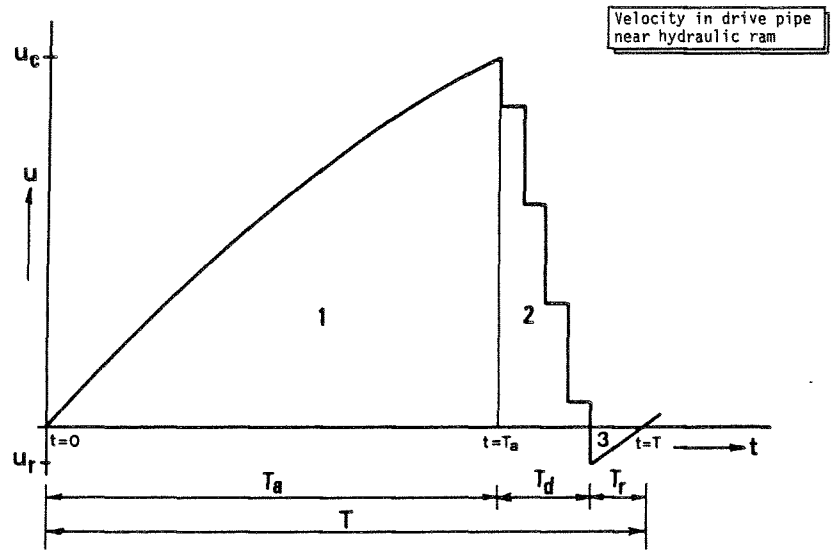

Fig. III-6 Division of cycle into three periods

1. Period of Acceleration (Wasting):
   impulse valve open, delivery valve closed;
   positive velocity (towards the ram);
   $0 \leq t \leq T_a$ and $0 \leq u \leq u_c$.

2. Period of Retardation (Pumping):
   impulse valve closed; delivery valve open;
   decelerating flow into the air chamber;
   $T_a < t \leq T_a + T_d$ and $u_r \leq u \leq u_c$.

3. Period of Recoil (Reverse Flow):
   delivery valve closed; impulse valve reopens;
   negative flow (in the direction of the supply tank);
   $T_a + T_d < t \leq T$ and $u_r \leq u \leq 0$.

When once the relationship u(t) for the water column in the drive pipe has been found the time rate of pumping (q) and of wasting (Q) may be obtained from (see also Fig. III-2):

$$q = \frac{1}{T} * \frac{\pi D^2}{4} * \int_{T_a}^{T_a + T_d} u(t)\, dt \qquad \text{(III-1)}$$

and

$$Q = \frac{1}{T} * \frac{\pi D^2}{4} * \left[\int_{0}^{T_a} u(t)\, dt + \int_{T_a + T_d}^{T} u(t)\, dt \right] \qquad \text{(III-2)}$$

where

D	= internal diameter of the drive pipe	[m]
T_a	= duration of the period of acceleration	[s]
T_d	= duration of the period of retardation	[s]
T	= duration of the complete cycle $= T_a + T_d + T_r$	[s]
T_r	= duration of the period of recoil	[s]
u	= velocity of the water column in the drive pipe	$[ms^{-1}]$
t	= time	[s]
q	= time rate of pumping	$[m^3s^{-1}]$
Q	= time rate of wasting	$[m^3s^{-1}]$

Before the three periods (Acceleration - Retardation - Recoil) are analysed

individually, it seems logical to reveal some of the main features of 'Unsteady Flow', the details of which are being discussed in Appendix B.

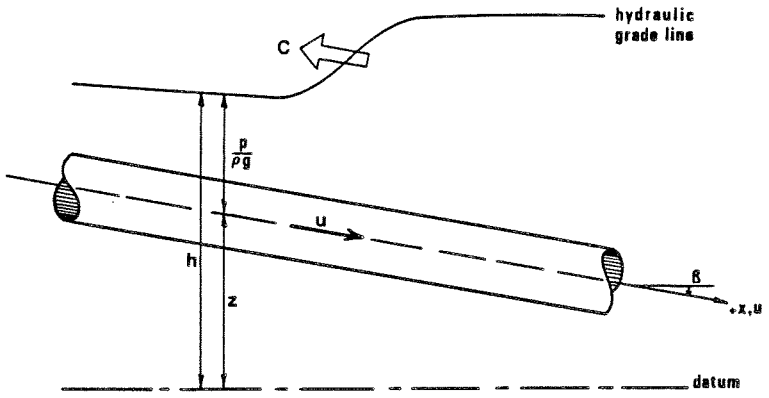

Fig. III-7 Nomenclature for unsteady flow equations

Unsteady flow of liquids through a cylindrical pipe of circular cross-section is governed by (see also nomenclature of Fig. III-7):

the equation of continuity:

$$\frac{1}{c^2}\frac{\partial h}{\partial t} + \frac{u}{c^2}\frac{\partial h}{\partial x} + \frac{u}{c^2}\sin\beta + \frac{1}{g}\frac{\partial u}{\partial x} = 0 \qquad \text{(III-3)}$$

where

$$c^2 = \left[\frac{\rho}{K} + \frac{\rho D}{E e}\phi_1\right]^{-1} \qquad \text{(III-4)}$$

and the equation of motion:

$$\frac{\partial u}{\partial t} + u\frac{\partial u}{\partial x} + g\frac{\partial h}{\partial x} + f\frac{u|u|}{2D} = 0 \qquad \text{(III-5)}$$

in which

h	=	piezometric head	[m]
u	=	cross-sectional average of the liquid velocity	[ms^{-1}]
x	=	distance along the pipe	[m]
t	=	time	[s]
g	=	acceleration due to gravity (g = 9.81 ms^{-2})	[ms^{-2}]
β	=	angle of declination	[-]

c	=	wavespeed	[ms^{-1}]
ρ	=	mass density of the liquid	[kgm^{-3}]
K	=	bulk modulus of elasticity of the liquid	[Nm^{-2}]
D	=	internal diameter of the pipe	[m]
e	=	thickness of the pipe wall	[m]
E	=	Young's modulus of the pipe wall material	[Nm^{-2}]
ϕ_1	=	coefficient introducing pipe constraint condition	[-]
f	=	Darcy-Weisbach friction factor	[-]

Wavespeed c is the acoustic speed with which pressure waves propagate through the liquid. Eq.(III-4) shows that the wavespeed is modified by the compressibility of the liquid and the elasticity of the pipe wall; for simplicity it may normally be assumed that the pipe constraint factor $\phi_1 = 1$.

Since the dependant variables h and u are functions of the independant variables x and t, it follows from differential calculus that

$$\frac{\partial u}{\partial t} dt + \frac{\partial u}{\partial x} dx = du \qquad \text{(III-6)}$$

and

$$\frac{\partial h}{\partial t} dt + \frac{\partial h}{\partial x} dx = dh \qquad \text{(III-7)}$$

After some mathematical elaborations (see Appendix B), Eqs. (III-3), (III-5), (III-6) and (III-7) can be transformed into two particular total differential equations, the so-called characteristic equations:

$$\frac{dx}{dt} = u \pm c \qquad \text{(III-8)}$$

and

$$\frac{dh}{dt} = \mp \frac{c}{g} \frac{du}{dt} \mp \frac{c}{g} f \frac{u|u|}{2D} - u \sin \beta \qquad \text{(III-9)}$$

In general, the characteristic equations are the starting point for either graphical or numerical solution of unsteady flow problems. They may also be used to estimate the relative importance of the various terms.
For example, for water in a metal pipe typical values for u and c are

$$u \sim 1 \text{ ms}^{-1} \text{ and } c \sim 1400 \text{ ms}^{-1}$$

so that

$$u << c$$

and Eq. (III-8) simplifies to

$$\frac{dx}{dt} = \pm c \qquad \text{(III-10)}$$

Furthermore, for a typical hydraulic ram installation the following values may apply:

$D \sim 0.05$ m
$f \sim 0.03$ [-]
$0.10 < \sin \beta < 0.25$

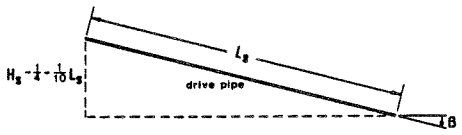

Substitution into Eq. (III-9) yields:

$$\frac{dh}{dt} \simeq \mp 140 \frac{du}{dt} \mp 42 \cdot 0.25$$

Hence, the numerical value of $u \sin \beta$ may surely be neglected as compared with 'friction', and

$$\frac{dh}{dt} \simeq \mp 140 \frac{du}{dt} \mp 42 \qquad \text{(III-11)}$$

Now, in order to estimate a value for the factor du/dt distinction must be drawn between 'acceleration' and 'retardation' (see also Fig. III-6):

Acceleration: The velocity in the drive pipe at the moment of complete impulse valve closure, u_c, is more or less fixed by the adjustment of the impulse valve (valve stroke, weight/spring-tension), while the duration T_a depends mainly on supply head H_s and the fore-mentioned velocity u_c.

From the experiments typical values have found to be:

$$u_c \sim 1 \text{ ms}^{-1} \text{ and } T_a \sim 1 \text{ s}$$

So,

$$\frac{du}{dt} \sim + 1 \text{ ms}^{-2} \qquad \text{(gradually changing flow)}$$

and

$$\frac{dh}{dt} \simeq \mp 140 \mp 42$$

from which it may be concluded that during the period of acceleration pipe friction must be taken into account. The characteristic equations then take the form

$$\frac{dx}{dt} = \pm c \qquad \text{(III-12a)}$$

and

$$\frac{dh}{dt} = \mp \frac{c}{g}\frac{du}{dt} \mp \frac{c}{g} f \frac{u|u|}{2D} \qquad \text{(III-12b)}$$

Retardation: As will become clear later (section III-3) the duration of the period of retardation, T_d, depends on the delivery head (that is to say on the number of pressure surges, each requiring $2L_s/c$ second to move up and down the drive pipe). Typical values for T_d may range from 0.01 s to 0.1 s. Hence,

$$\left.\begin{array}{l} u_c \sim 1 \text{ ms}^{-1} \\ T_d \sim 0.05 \text{ s} \end{array}\right. \quad \Rightarrow \quad \frac{du}{dt} \sim -20 \text{ ms}^{-2} \text{ (rapidly changing flow)}$$

and from Eq. (III-11) it follows that

$$\frac{dh}{dt} \approx \pm 2800 \mp 42$$

So, during the period of retardation the effect of friction may be neglected (friction head losses are small as compared with waterhammer pressures) and the characteristic equations simplify to

$$\frac{dx}{dt} = \pm c \qquad \text{(III-13a)}$$

and

$$\frac{dh}{dt} = \mp \frac{c}{g}\frac{du}{dt} \qquad \text{(III-13b)}$$

Eq. (III-13b) is the infinitesimal representation of the basic equation of waterhammer (see Appendix B):

$$\Delta h = \mp \frac{c}{g} \Delta u \qquad \text{(III-14)}$$

The equation describes the sudden change in flow related to a sudden change in head (pressure wave), vice versa, where the minus sign must be used for changes at the downstream end of the pipe (wave front moving in upstream direction) and the plus sign for changes at the upstream end (wave front moving in downstream direction). The equation holds for sudden changes, that is to say for any alteration taking place within 2L/c second, i.e. the time required for a complete reflection of the pressure wave travelling along the pipe.

For example, when the flow at the lower end of the drive pipe is suddenly stopped by the instantaneous closure of the impulse valve, then

$$\Delta u = - u_c$$

and

$$\Delta h = - \frac{c}{g} * (-u_c) = + \frac{c}{g} u_c$$

Given the velocity u_c, this is the greatest possible rise in pressure head which can be developed in the hydraulic ram:

$$h_{max} = + \frac{c}{g} u_c \qquad \text{(III-15)}$$

In practice, the delivery head h_d must be below this value,

$$h_d < h_{max}$$

otherwise no water will be actually pumped (q = 0).

III-2 Period of acceleration

The relation u(t) during the period of acceleration may be determined (graphically or numerically) using the characteristic equations (III-12a) and (III-12b). However, for the gradually varying flow observed during the period of acceleration an analytical solution can be obtained using the Rigid-Water-Column-Theory. The theory is based on the fact that the time scale of velocity changes is large as compared with the time scale of pressure wave propagation; in formula:

$$T_a >> \frac{2 L_s}{c} \qquad \text{(III-16)}$$

In practice this means that the wavespeed c is assumed to be infinitely large,

$$c \dashrightarrow \infty \qquad \text{(III-17)}$$

which implies that the actual propagation of the pressure waves may be left out of consideration.

With use of Eq. (III-17), the continuity equation (III-3) reduces to

$$\frac{\partial u}{\partial x} = 0 \qquad \text{(III-18)}$$

and the equation of motion (III-5) then simplifies to

$$\frac{\partial u}{\partial t} + g\frac{\partial h}{\partial x} + f\frac{u|u|}{2D} = 0$$

or

$$\frac{\partial h}{\partial x} = -\frac{1}{g}\frac{\partial u}{\partial t} - \frac{f}{D}\frac{u|u|}{2g} \qquad \text{(III-19)}$$

From Eq. (III-18) it follows that

$$\frac{\partial u}{\partial t} \equiv \frac{du}{dt}$$

and that both u and du/dt are constant throughout the pipelength (the entire water column in the drive pipe accelerates at the same value throughout its length).

Hence, the right-hand side of Eq. (III-19) is no longer a function of x and the equation can be integrated with respect to x to give

$$\int_{x=0}^{Ls} \frac{\partial h}{\partial x}\,dx = -\int_{x=0}^{Ls} \frac{1}{g}\frac{du}{dt}\,dx - \int_{x=0}^{Ls} \frac{f}{D}\frac{u|u|}{2g}\,dx$$

or

$$h(L_s,t) - h(0,t) = -\frac{L_s}{g}\frac{du}{dt} - \frac{f L_s}{D}\frac{u|u|}{2g} \qquad \text{(III-20)}$$

where $h(L_s,t)$ and $h(0,t)$ are the boundary conditions at the downstream end and the upstream end of the pipe respectively (see Fig. III-8).

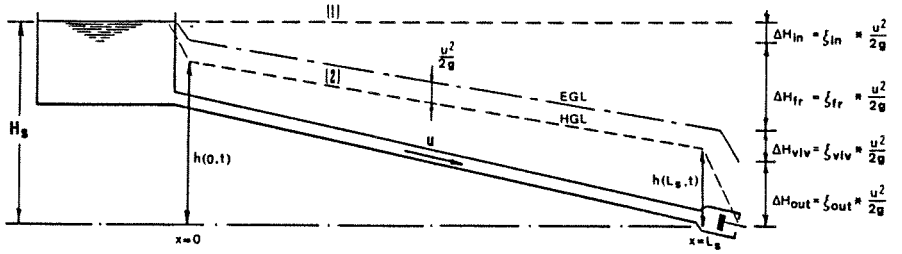

Fig. III-8 Acceleration: (1) Initial steady state (t=0; u=0)
(2) Final steady state ($t\to\infty$; $u=u_o$)

Boundary conditions:

upstream (x = 0): $h(0,t) = H_s - \Delta H_{in} - \frac{u^2}{2g}$

$$= H_s - (\xi_{in} + 1) * \frac{u^2}{2g} \qquad \text{(III-21)}$$

downstream ($x = L_s$): $h(L_s, t) = \Delta H_{out} + \Delta H_{vlv} - \frac{u^2}{2g}$

$$= (\xi_{out} + \xi_{vlv} - 1) * \frac{u^2}{2g} \qquad \text{(III-22)}$$

Initial condition (t=0): $u=0$ (III-23)

Substituting Eqs. (III-21) and (III-22) into (III-20) yields:

$$(\xi_{out} + \xi_{vlv} - 1) * \frac{u^2}{2g} - H_s + (\xi_{in} + 1) * \frac{u^2}{2g} = -\frac{L_s}{g}\frac{du}{dt} - \frac{f L_s}{D}\frac{u|u|}{2g} \qquad \text{(III-24)}$$

During the period of acceleration $u \geq 0$, so that $u|u| = +u^2$ and Eq. (III-24) may be rearranged to yield:

$$\left(\xi_{out} + \xi_{vlv} + \xi_{in} + \frac{f L_s}{D}\right) * \frac{u^2}{2g} - H_s = -\frac{L_s}{g}\frac{du}{dt}$$

or

$$H_s - \xi * \frac{u^2}{2g} = \frac{L_s}{g}\frac{du}{dt} \qquad \text{(III-25)}$$

where

ξ = sum of head loss coefficients

$$\xi = \xi_{out} + \xi_{vlv} + \xi_{in} + \xi_{fr} \quad ; \quad \xi_{fr} = \frac{f L_s}{D} \qquad \text{(III-26)}$$

Eq. (III-25) can be written as

$$\frac{du}{dt} = \frac{g}{L_s}\left[H_s - \xi\frac{u^2}{2g}\right]$$

or

$$\frac{du}{dt} = \frac{\xi}{2L_s}\left[\frac{2gH_s}{\xi} - u^2\right] \qquad \text{(III-27)}$$

In Eq. (III-27)

$$\frac{2gH_s}{\xi} \equiv u_0^2 \qquad \text{or} \qquad u_0 = \sqrt{\frac{2gH_s}{\xi}} \qquad \text{(III-28)}$$

where u_0 is the asymptotic value of u when t tends to infinity.

Note: with the increase of the velocity (u) an increasing part of H_s is lost to friction and minor losses (see Eq. III-25); theoretically the water continues to accelerate until the total head losses equal the supply head H_s (steady-state condition; du/dt = 0):

$$H_s = \xi * \frac{u_0^2}{2\,g} \quad \Rightarrow \quad u_0^2 = \frac{2\,g\,H_s}{\xi}$$

Indeed, it follows from Eq. (III-27) that du/dt = 0 when $u = u_0$.

Substituting Eq. (III-28) into Eq. (III-27):

$$\frac{du}{dt} = \frac{\xi}{2\,L_s}\left[u_0^2 - u^2\right]$$

If it is assumed that the total loss coefficient ξ may be approximated by the parameters determined under steady flow condition, and with use of Eq. (III-23) the above expression may be integrated with respect to u and t to yield:

$$\int_0^u \frac{du}{u_0^2 - u^2} = \int_0^t \frac{\xi}{2\,L_s}\,dt$$

Solving by partial fractions:

$$\frac{1}{2\,u_0}\left[\int_0^u \frac{du}{u_0 + u} + \int_0^u \frac{du}{u_0 - u}\right] = \frac{\xi}{2\,L_s}\int_0^t dt$$

or

$$\frac{1}{2\,u_0}\left[\ln(u_0 + u) - \ln(u_0 - u)\right] = \frac{\xi}{2\,L_s}t$$

$$\therefore \quad \ln\frac{u_0 + u}{u_0 - u} = \frac{\xi\,u_0}{L_s}\,t \qquad \text{(III-29)}$$

Eq. (III-29) may also be written as:

$$\frac{u_0 + u}{u_0 - u} = \exp\left(\frac{\xi\,u_0}{L_s}t\right)$$

which can be rearranged to yield:

$$u = u_0 * \frac{\exp\left(\frac{\xi u_0}{L_s} t\right) - 1}{\exp\left(\frac{\xi u_0}{L_s} t\right) + 1} \qquad \text{(III-30)}$$

Using the definition of the hyperbolic tangent

$$\tanh \theta = \frac{e^{2\theta} - 1}{e^{2\theta} + 1}$$

Eq. (III-30) can be conveniently expressed as

$$u = u_0 \tanh \frac{u_0 \xi}{2 L_s} t \qquad \text{(III-31)}$$

where

$$u_0 = \sqrt{\frac{2 g H_s}{\xi}} \qquad \text{(III-28)}$$

with the various parameters as defined earlier.

A graph of the relation u(t) is plotted in Fig. III-9. From Eq. (III-27) it follows that

$$\left[\frac{du}{dt}\right]_{u=o} = \frac{g H_s}{L_s} \qquad \text{(III-32a)}$$

while for small values of u

$$\left[\frac{du}{dt}\right]_{u \ll u_0} \approx \frac{g H_s}{L_s} \qquad \text{(III-32 b)}$$

Hence, near the origin the slope of the graph is independent of the total loss coefficient ξ (which might be expected since head losses become insignificant for small velocities and therefore may usually be omitted then).

The period of acceleration of the hydraulic ram cycle ends with the instantaneous closure of the impulse valve when $u = u_c$ at $t = T_a$ (see Fig. III-9).

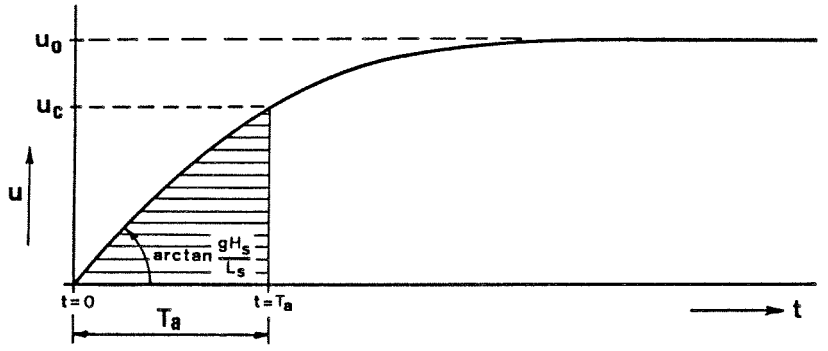

Fig. III-9 Period of acceleration; $u = u_0 \tanh \frac{u_0 \xi}{2 L_s} t$; $u_0 = \sqrt{\frac{2 g H_s}{\xi}}$

From Eq.(III-31) it follows that

$$u_c = u_0 \tanh \frac{u_0 \xi}{2 L_s} T_a \qquad \text{(III-33)}$$

or (see Eq. (III-29))

$$T_a = \frac{L_s}{u_0 \xi} \ln \frac{u_0 + u_c}{u_0 - u_c} \qquad \text{(III-34)}$$

The amount of water flowing through the ram during the period of acceleration (V_a) can be calculated from:

$$V_a = \frac{\pi D^2}{4} * \int_0^{T_a} u(t)\, dt$$

where $\int_0^{T_a} u(t)\, dt$ is equal to the shaded area of Fig. III-9.

So,

$$V_a = \frac{\pi D^2}{4} * \int_0^{T_a} u_0 \tanh \left(\frac{u_0 \xi}{2 L_s} t \right) dt$$

$$= \frac{\pi D^2}{4} * \frac{2 L_s}{\xi} * \int_0^{T_a} \tanh \left(\frac{u_0 \xi}{2 L_s} t \right) d \left(\frac{u_0 \xi}{2 L_s} t \right)$$

or

$$V_a = \frac{\pi D^2}{4} * \frac{2 L_s}{\xi} \ln \cosh \frac{u_0 \xi}{2 L_s} T_a \qquad \text{(III-35)}$$

III-3 Period of retardation

The flow observed during the period of retardation may be classified as 'rapidly changing' (see section III-1). The propagation of pressure waves must be considered (Pressure Wave Theory). Friction and minor losses are neglected as they usually are small compared with waterhammer pressures.

Note: Since the waterhammer pressures experienced in the hydraulic ram are limited by the delivery head (see hereafter), the assumption of negligible head losses holds better as the delivery head is larger.

As discussed in section III-1, sudden changes in flow and pressure head are related to each other by

$$\Delta h = -\frac{c}{g} \Delta u \qquad \text{(III-36)}$$

at the downstream end of the drive pipe (wave front moving in upstream direction), and

$$\Delta h = +\frac{c}{g} \Delta u \qquad \text{(III-37)}$$

at the upstream end of the drive pipe (wave front moving in downstream direction).

At time $t = T_a$ the velocity $u = u_c$ everywhere in the drive pipe; as the impulse valve is instantaneously and completely closed the flow through the valve is suddenly stopped ($u = 0$ at the valve) and a high pressure develops at the valve bringing the water near to it to rest ($\Delta u = - u_c$). According to Eq. (III-36) the theoretical pressure rise in the rambody is given by

$$\Delta h = -\frac{c}{g} \Delta u = +\frac{c}{g} u_c \qquad \text{(III-38)}$$

If this pressure rise is large enough to overcome the pressure in the air chamber ($h = h_d$) the delivery valve is forced open, consequently limiting the pressure rise to (slightly above) the delivery pressure ($\Delta h \approx h_d$). The front of this pressure surge moves upstream at wavespeed c, reducing the flow velocity in successive cross-sections as it passes (Fig. III-10a).

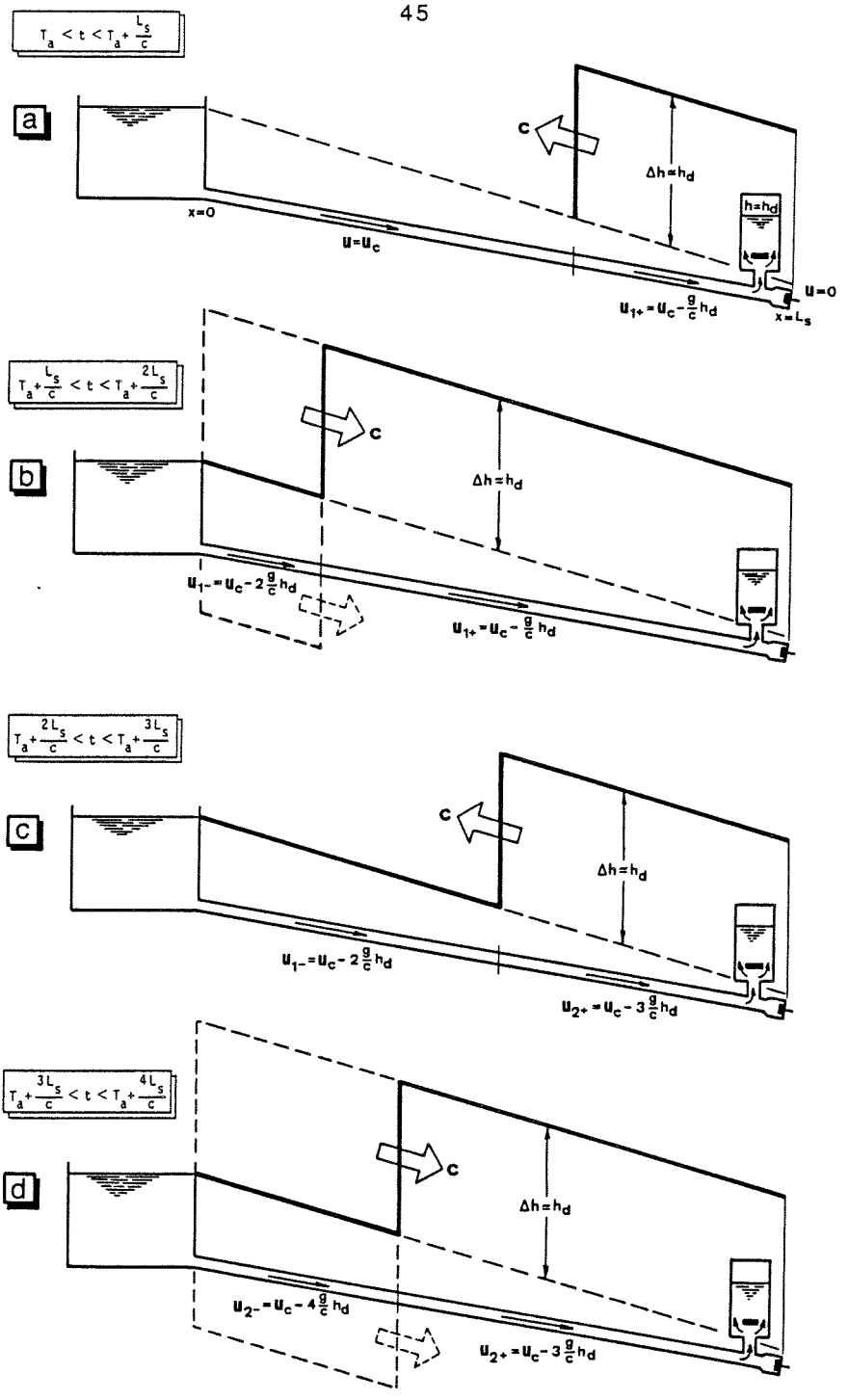

Fig. III-10 Period of retardation; propagation of successive pressure waves

Thus, the flow velocity behind the wave front is reduced in proportion to

$$\Delta h = h_d \qquad \text{(III-39)}$$

From Eq. (III-36) it follows that

$$\Delta u = -\frac{g}{c}\Delta h \quad \text{or} \quad \Delta u = -\frac{g}{c}h_d$$

and, since the delivery valve is open, water flows into the air chamber at velocity

$$u_{l^+} = u_c + \Delta u \quad \text{or} \quad u_{l^+} = u_c - \frac{g}{c}h_d \qquad \text{(III-40)}$$

At time

$$t = T_a + \frac{L_s}{c}$$

the front of the pressure wave reaches the supply reservoir. Since the supply level remains unchanged ($h = H_s$ = constant) the pressure head at the upstream end of the drive pipe must drop by

$$\Delta h = -h_d \qquad \text{(III-41)}$$

According to Eq. (III-37)

$$\Delta h = +\frac{c}{g}\Delta u \quad \text{or} \quad \Delta u = +\frac{g}{c}\Delta h$$

at the upstream end of the drive pipe and thus, with substitution of Eq. (III-41)

$$\Delta u = -\frac{g}{c}h_d$$

In other words: on the arrival of the positive pressure wave ($\Delta h = +h_d$; Eq. III-39) at the supply reservoir an equal but negative wave ($\Delta h = -h_d$; Eq. III-41) travels away from the reservoir towards the ram (see Fig. III-10b). Behind the wave front, i.e. on the upstream side, the water is flowing with velocity

$$u_{l^-} = u_{l^+} + \Delta u \quad \text{or} \quad u_{l^-} = u_{l^+} - \frac{g}{c}h_d$$

or with use of Eq. (III-40)

$$u_{l^-} = u_c - 2\frac{g}{c}h_d \qquad \text{(III-42)}$$

When, at time

$$t = T_a + \frac{2\,L_s}{c}$$

the negative wave arrives at the ram the pressure head in the entire drive pipe is reduced to, approximately, its original (low) value and the flow velocity $u = u_1$ - everywhere. But since a high pressure exists at the ram ($h = h_d$) and water is still flowing in the direction of the air chamber a new positive pressure wave is generated at the ram, again reducing the velocity by

$$\Delta u = -\frac{g}{c} h_d$$

as it travels upstream (see Fig. III-10c). Behind the wave front, i.e. on the downstream side, the flow velocity

$$u_{2^+} = u_{1^-} + \Delta u = u_{1^-} - \frac{g}{c} h_d$$

or with use of Eq. (III-42)

$$u_{2^+} = u_c - 3\,\frac{g}{c} h_d \qquad \text{(III-43)}$$

At time

$$t = T_a + \frac{3\,L_s}{c}$$

the front of the pressure wave reflects at the supply reservoir as a negative wave, travelling in the direction of the ram and reducing the flow velocity in the drive pipe to (Fig. III-10d):

$$u_{2^-} = u_{2^+} - \frac{g}{c} h_d = u_c - 4\,\frac{g}{c} h_d \qquad \text{(III-44)}$$

and so on and so forth.

The action of successive pressure surges moving up the drive pipe as a positive wave ($\Delta h = + h_d$), reflecting against the supply level and returning to the ram as a negative wave ($\Delta h = - h_d$), meanwhile water discharging into the air chamber with step-wise decreasing velocity, continues until at last the velocity which remains at the arrival of the negative wave at the ram is either

A. negative, i.e. water in the entire drive pipe is flowing away from the ram;

or B. positive, but insufficient to built up the next pressure wave to a value equal to the delivery pressure.

In both cases the delivery valve closes instantaneously at the arrival of the negative wave ($\Delta h = - h_d$), thereby ending the pumping stage of the ram cycle.
Cases A and B differ in that in case A ($u < 0$ at delivery valve closure) conditions are present for the immediate reopening of the impulse valve (Fig. III-11).

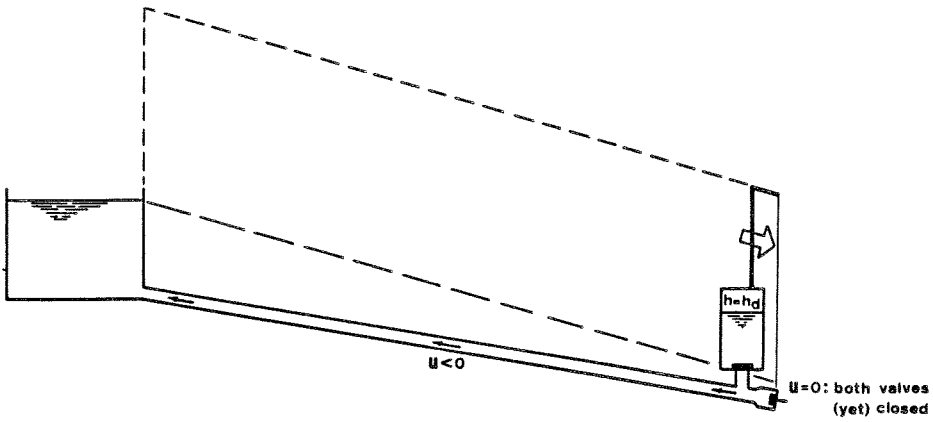

Fig.III-11 Delivery valve closure - Case A

In case B it takes another 2 L_s/c second before the impulse valve is allowed to reopen. These 2 L_s/c second is the time required for the remaining pressure wave ($\Delta h' < h_d$) to move upstream, bringing the water in the drive pipe to rest ($u = 0$) and to return to the ram as a negative wave with the water behind the wave front flowing in backward direction ($u < 0$; see Fig. III-12).

Fig. III-13 illustrates examples of the u(t)-diagram for the velocity at the downstream end of the drive pipe for case A and case B respectively.

Note: 1. It may be clear that cases A and B refer to different arrangements (i.e. different velocity u_c and/or delivery head h_d).
2. The velocity 'step' Δu used in Fig. III-13 and in the text hereafter differs is sign from the velocity change Δu used so far.

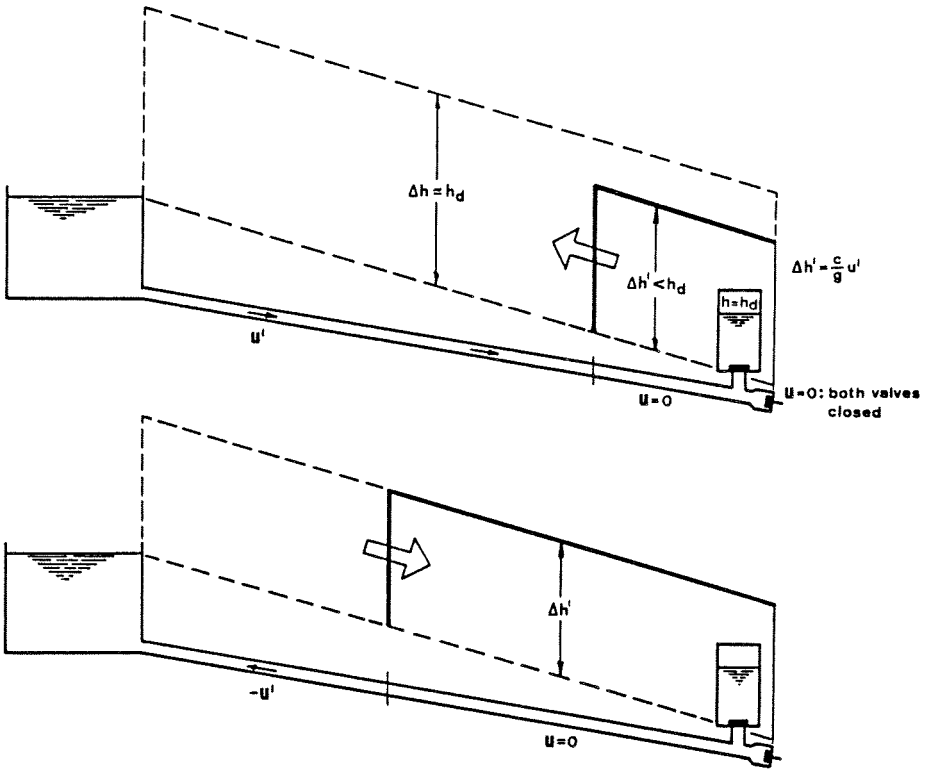

Fig.III-12 Delivery valve closure - Case B

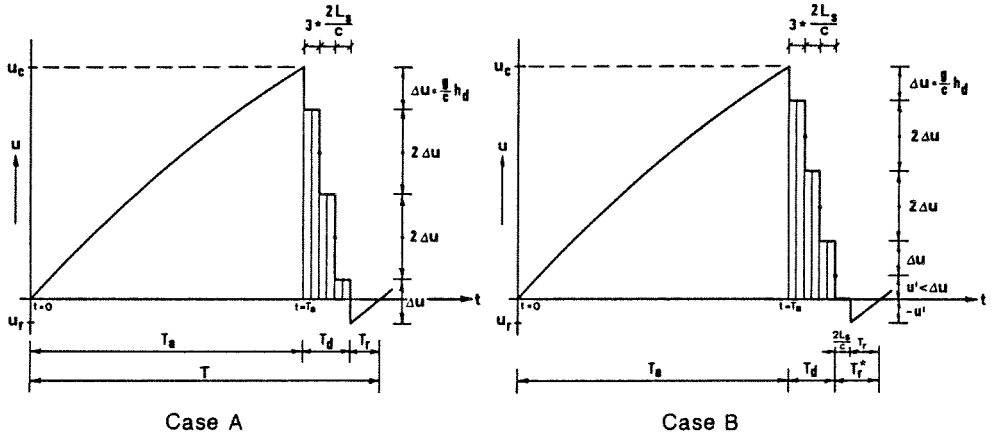

Fig.III-13 u(t)-diagram at the downstream end of the drive pipe.

Hence: during the period of retardation the following velocities are observed at the downstream end of the drive pipe (see Fig. III-13):

$$T_a \leq t < T_a + \frac{2\,L_s}{c} : \text{1st pressure surge} : u_1 = u_c - \Delta u$$

$$T_a + \frac{2\,L_s}{c} \leq t < T_a + \frac{4\,L_s}{c} : \text{2nd pressure surge} : u_2 = u_c - 3\,\Delta u$$

$$T_a + \frac{4\,L_s}{c} \leq t < T_a + \frac{6\,L_s}{c} : \text{3rd pressure surge} : u_3 = u_c - 5\,\Delta u$$

etc., until the delivery valve instantaneously closes (case A or case B). In general:

$$T_a + (i-1) * \frac{2\,L_s}{c} \leq t < T_a + i * \frac{2\,L_s}{c} :$$

$$i^{th} \text{ pressure surge} : \quad u_i = u_c - (2i-1) * \Delta u \qquad \text{(III-45)}$$

If N denotes the number of surges experienced during the period of retardation, i.e. while pumping takes place, it follows that N must be the largest integer number satisfying the condition

$$u_N > 0$$

or with use of Eq. (III-45)

$$u_c - (2N-1) * \Delta u > 0$$

or

$$u_c + \Delta u > 2N\,\Delta u$$

and so

$$N < \frac{u_c + \Delta u}{2\,\Delta u} \qquad \text{(III-46)}$$

$$\text{where } \Delta u = \frac{c}{g} h_d \qquad \text{(III-47)}$$

Hence: N is the largest integer number smaller than

$$\frac{u_c + \Delta u}{2\,\Delta u}$$

It can be seen from Eqs. (III-46) and (III-47) that, given the velocity u_c, the number of pressure surges (and thus the duration T_d) is determined by the delivery head. This is also illustrated in Fig. III-14, showing the u(t)-diagram for a high and low delivery head respectively.

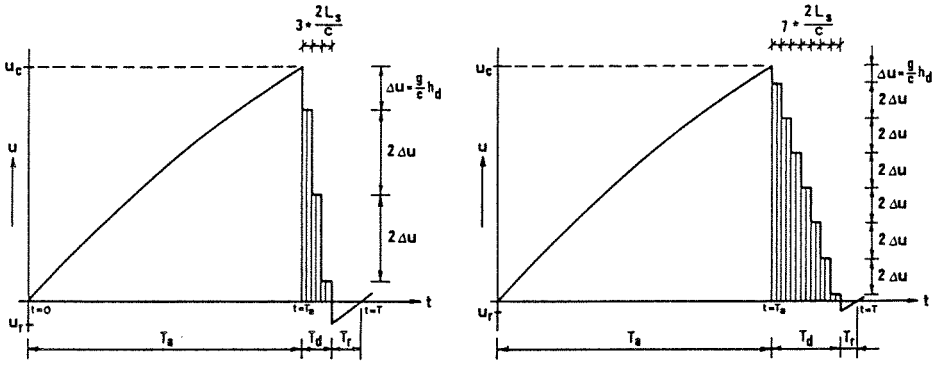

a. high delivery head h_d b. low delivery head h_d

Fig. III-14 u(t)-diagram; high and low delivery head.

Knowing the number of surges N, the duration of the period of retardation

$$T_d = N * \frac{2\,L_s}{c} \qquad \text{(III-48)}$$

while the amount of water pumped per cycle (V_d), i.e. the amount of water flowing into the air chamber during T_d, can be computed from

$$V_d = \frac{\pi\,D^2}{4} * \frac{2\,L_s}{c} * \sum_{i=1}^{N} u_i \qquad \text{(III-49)}$$

where $\frac{2\,L_s}{c} * \sum_{i=1}^{N} u_i$ equals the shaded area of Figs. III-13 and III-14 with u_i as defined in Eq. (III-45).

In view of the next section (Period of Recoil) it still remains to be established whether delivery valve closure takes place according to case A or case B. As stated before, case A occurs when the N^{th} surge returns at the ram, with the water behind the wave front flowing away from the ram ($u < 0$). Hence, (see Figs. III-11 and III-13a)

$$u_N < \Delta u \quad \text{or} \quad u_N - \Delta u < 0$$

With use of Eq. (III-45) it follows that

$$u_c - (2N - 1) * \Delta u - \Delta u < 0$$

or

$$u_c - 2N * \Delta u > 0$$

and so

$$N > \frac{u_c}{2\,\Delta u} \qquad \text{(III-50)}$$

Hence, when the (integer) number of pressure surges calculated from Eq. (III-46) satisfies Eq. (III-50) case A occurs, otherwise case B applies.

Furthermore, close observation of Fig. III-13 will clarify that

case A:

$$u_r = u_N - \Delta u = u_c - (2N - 1) * \Delta u - \Delta u$$

or

$$u_r = u_c - 2\,N * \Delta u \qquad \text{(III-51)}$$

and

case B:

$$u_r = - u' = - (u_N - \Delta u)$$

or

$$u_r = 2\,N * \Delta u - u_c \qquad \text{(III-52)}$$

III- 4 Period of recoil

At the instant the delivery valve closes, a negative velocity exists everywhere in the drive pipe (or will exist $2L_s/c$ second later - see section III-3), i.e. water flows away from the ram in the direction of the supply reservoir. But since both the delivery valve and the impulse valve are closed (u = 0 at the ram) a negative pressure develops in the ram body, allowing the impulse valve to fall open (h ≈ 0 at the valve). From this moment on the water in the drive pipe accelerates under the effect of the supply head H_s. The period of recoil ends when u = 0 at the impulse valve with the valve in open position.

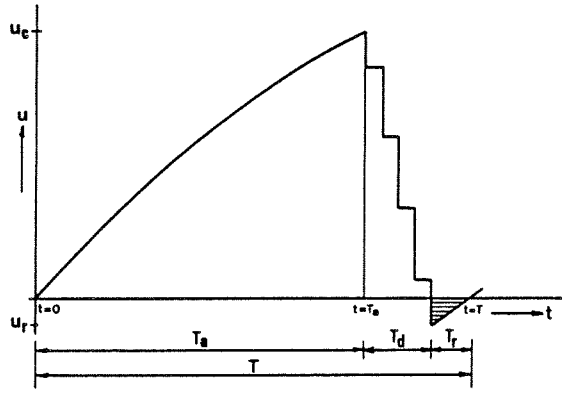

Fig. III-15 u(t)-relation at the ram (downstream end of drive pipe).

As shown in section III-2 the gradually accelerating flow is theoretically described by (see Eq. III-25):

$$H_s - \xi * \frac{u^2}{2g} = \frac{L_s}{g}\frac{du}{dt} \qquad \text{(III-25)}$$

with the exception that during the period of recoil u < 0 and thus u|u| = - u^2, so that in Eq. (III-26):

$$\xi_{fr} = - \frac{f L_s}{D}$$

However, as the values of u usually are small during the period of recoil, head losses may be neglected and Eq. (III-25) simplifies to:

$$H_s = \frac{L_s}{g}\frac{du}{dt} \qquad \text{(III-53)}$$

or

$$du = \frac{g\,H_s}{L_s}\,dt$$

Integration of the equation within the limits $u = u_r$ at $t = T_a + T_d$ and $u = u$ at $t = t$, with $T_a + T_d < t < T$ (see Fig. III-15), gives

$$\int_{u_r}^{u} du = \int_{T_a+T_d}^{t} \frac{g\,H_s}{L_s}\,dt$$

or

$$u - u_r = \frac{g\,H_s}{L_s}\left[t - (T_a + T_d)\right]$$

Hence, during the period of recoil the relation u(t) is given by

$$u = u_r + \frac{g\,H_s}{L_s}\left[t - (T_a + T_d)\right] \;;\; T_a + T_d \le t \le T \qquad \text{(III-54)}$$

With use of the condition

$$u = 0 \quad \text{at} \quad t = T\,(= T_a + T_d + T_r)$$

it follows that

$$0 = u_r + \frac{g\,H_s}{L_s} * T_r$$

or

$$T_r = -\frac{u_r * L_s}{g\,H_s} \qquad \text{(III-55)}$$

The amount of water flowing through the ram during the period of recoil (V_r) can be calculated from

$$V_r = \frac{\pi D^2}{4} * \int_{T_a+T_d}^{T} u(t)\,dt$$

where the integral represents the shaded area of Fig. III-15.

So,

$$V_r = \frac{\pi D^2}{4} * \frac{1}{2}\,u_r\,T_r$$

or with use of Eq. (III-55)

$$V_r = - \frac{\pi D^2}{4} * \frac{u_r^2 L_s}{2 g H_s} \qquad \text{(III-56)}$$

III-5 Review of the complete analysis

With reference to Fig. III-16 the results obtained in the previous sections can be summarized as follows:

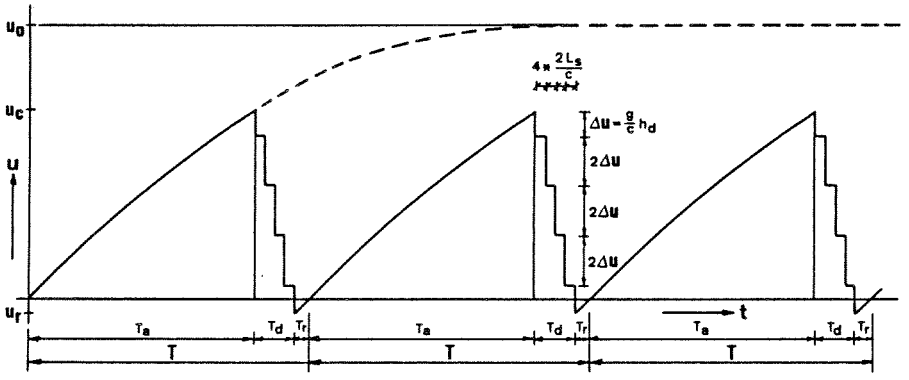

Fig.III-16 Successive ram cycles

Period of Acceleration:

$$T_a = \frac{L_s}{u_0 \xi} \ln \frac{u_0 + u_c}{u_0 - u_c} \qquad \text{(Eq. III-34)}$$

$$V_a = \frac{\pi D^2}{4} * \frac{2 L_s}{\xi} \ln \cosh \frac{u_0 \xi}{2 L_s} T_a \qquad \text{Eq. (III-35)}$$

where $u_0 = \sqrt{\frac{2 g H_s}{\xi}}$ (Eq. III-28)

ξ = sum of head loss coefficients (Eq. III-26)

Period of Retardation:

$$T_d = N * \frac{2 L_s}{c} \qquad \text{(Eq. III-48)}$$

$$V_d = \frac{\pi D^2}{4} * \frac{2 L_s}{c} * \sum_{i=1}^{N} u_i \qquad \text{(Eq. III-49)}$$

where N = number of pressure surges ; $N < \frac{u_c + \Delta u}{2 \Delta u}$ (Eq. III-46)

$$u_i = u_c - (2 i - 1) * \Delta u \qquad \text{(Eq. III-45)}$$

$$\Delta u = \frac{g}{c} h_d \qquad \text{(Eq. III-47)}$$

Period of Recoil:

$$T_r = - \frac{u_r * L_s}{g H_s} \qquad \text{(Eq. III-55)}$$

$$V_r = - \frac{\pi D^2}{4} * \frac{u_r^2 L_s}{2 g H_s} \qquad \text{(Eq. III-56)}$$

where $u_r = u_c - 2 N * \Delta u$ (case A) (Eq. III-51)

respectively

$u_r = 2 N * \Delta u - u_c$ (case B) (Eq. III-52)

Note 1. In case B (see Fig. III-13b):

$$T_r = - \frac{u_r * L_s}{g H_s} + \frac{2 L_s}{c} \qquad \text{(III-55*)}$$

2. With use of Eq. (III-45), Eq. (III-49) can be written as

$$V_d = \frac{\pi D^2}{4} * \frac{2 L_s}{c} * \sum_{i=1}^{N} \{u_c - (2 i - 1) * \Delta u\}$$

which can be elaborated to yield

$$V_d = \frac{\pi D^2}{4} * \frac{2 L_s}{c} * N (u_c - N \Delta u)$$

or with use of Eq. (III-48)

$$V_d = \frac{\pi D^2}{4} * T_d * (u_c - N \Delta u) \qquad \text{(III-57)}$$

Remembering Fig. III-2 and Eqs. (III-1) and (III-2) it follows that the time rate of pumping

$$q = \frac{1}{T} V_d = \frac{\pi D^2}{4} * \frac{T_d}{T} * (u_c - N \Delta u) \qquad \text{(III-58)}$$

and the time rate of wasting

$$Q = \frac{V_{out}}{T} = \frac{1}{T} (V_a + V_r) = \frac{1}{T} * \frac{\pi D^2}{4} * \left[\frac{2 L_s}{\xi} \ln \cosh \frac{u_0 \xi}{2 L_s} T_a - \frac{u_r^2 L_s}{2 g H_s} \right] \qquad \text{(III-59)}$$

where the duration of the complete cycle

$$T = T_a + T_d + T_r \qquad \text{(III-60)}$$

With use of the foregoing hydraulic ram analysis most of the performance characteristics presented in section II-2 can be easily explained. Successively the effect of (a) delivery head h_d, (b) supply head H_s, (c) ram size (i.e. drive pipe diameter D) and (d) impulse valve adjustment shall be considered.

(a) <u>delivery head h_d</u>: pumping rate q decreases as delivery head h_d increases, other factors (supply head, ram size, impulse valve adjustment) held constant.
From Eqs. (III-46) and (III-47) it follows that, as the delivery head h_d increases, Δu increases whereas the number of successive pressure surges, each requiring $2L_s/c$ second to move up and down the drive pipe, decreases. Fig. III-17 shows examples of the u(t)-diagram, as can be observed at the downstream end of the drive pipe, for a low and high delivery head respectively (see also Fig. III-14, section III-3).

It can be seen from the figure that

$$V_{out,I} \approx V_{out,II} \quad (V_{out} = V_a + V_r) \qquad \text{(III-61)}$$

and

$$V_{d,I} > V_{d,II} \qquad \text{(III-62)}$$

Furthermore

$$T_I \approx T_{II} \qquad \text{(III-63)}$$

so that, since $Q = \frac{1}{T} V_{out}$ and $q = \frac{1}{T} V_d$:

$$Q_I \approx Q_{II} \text{ and } q_I > q_{II} \qquad \text{(III-64)}$$

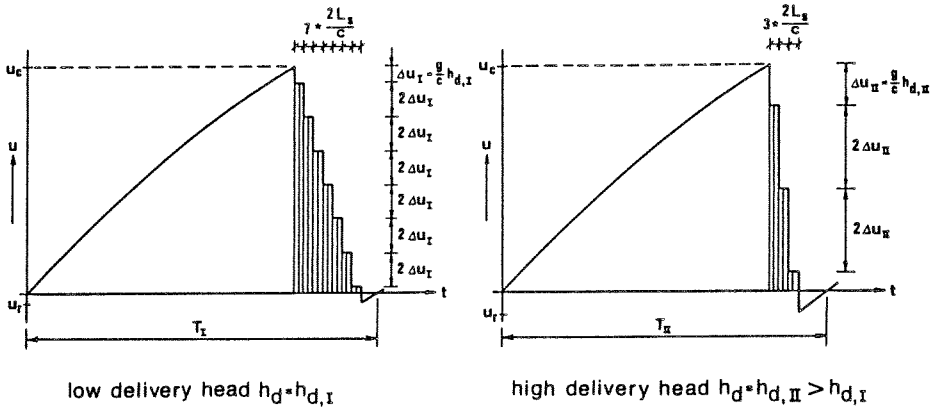

Fig. III-17 u(t)-diagram for low and high delivery head

(b) supply head H_s: an increase of supply head H_s increases the pumping frequency (more beats per minute), thereby increasing the pumping rate q, other factors (delivery head, ram size, impulse valve adjustment) kept the same.
Fig. III-18 shows examples of u(t)-diagrams for a given delivery head h_d, but for different supply heads: $H_s = H_{s,I}$ and $H_s = H_{s,II} > H_{s,I}$. From Eqs. (III-28) and (III-32) it follows that

$$u_{0,I} \left(= \sqrt{\frac{2\,g\,H_{s,I}}{\xi}} \right) < u_{0,II} \left(= \sqrt{\frac{2\,g\,H_{s,II}}{\xi}} \right) \qquad \text{(III-65)}$$

and

$$\left[\left(\frac{du}{dt}\right)_{u=0}\right]_I = \frac{g\,H_{s,I}}{L_s} < \left[\left(\frac{du}{dt}\right)_{u=0}\right]_{II} = \frac{g\,H_{s,II}}{L_s} \qquad \text{(III-60)}$$

It can be observed from Fig. III-18 that

$$V_{out,II} < V_{out,I} \quad \text{and} \quad V_{d,II} = V_{d,I} \qquad \text{(III-67)}$$

while

$$T_{II} < T_I \qquad \text{(III-68)}$$

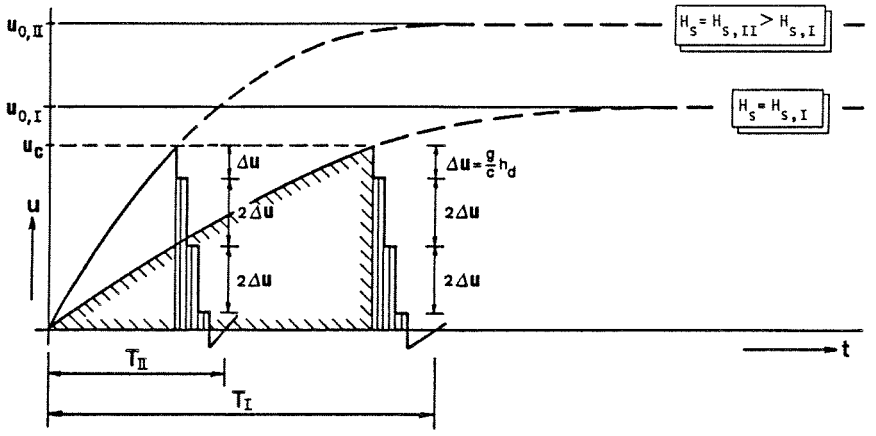

Fig. III-18 u(t)-diagrams for different supply heads

Hence,

$$q_{II} \left(= \frac{V_{d,II}}{T_{II}} \right) > q_I \left(= \frac{V_{d,I}}{T_I} \right) \qquad \text{(III-69)}$$

whereas at first sight no conclusion can be drawn relating to

$$Q = \frac{V_{out}}{T}$$

since both V_{out} and T decrease as H_s increases. However, it can be noted that by approximation

$$Q \approx \frac{V_a}{T_a} \approx \frac{\frac{\pi D^2}{4} * \frac{1}{2} u_c T_a}{T_a} = \frac{\pi D^2}{4} * \frac{1}{2} u_c \qquad \text{(III-70)}$$

so that,

$$Q_{II} \approx Q_I \qquad \text{(III-71)}$$

For example, it follows from experiments (see Appendix A):

Blake Hydram No. 2 (1 1/2")

H_s = 1.35 m	$V_{out} \approx 1000*10^{-6}$ m³/cycle	T ≈ 1.600 s	Q ≈ 40 l/min
2.00 m	$650*10^{-6}$ m³/cycle	1.000 s	39 l/min
3.00 m	$425*10^{-6}$ m³/cycle	0.700 s	38 l/min

Vulcan 2"

H_s = 1.00 m	V_{out} ≈ $700*10^{-6}$ m^3/cycle	T ≈ 1.150 s	Q ≈ 35 l/min
2.00 m	$350*10^{-6}$ m^3/cycle	0.600 s	33 l/min
3.00 m	$250*10^{-6}$ m^3/cycle	0.450 s	34 l/min

Blake Hydram No. 3 1/2 (2 1/2")

H_s = 1.35 m	V_{out} ≈ $2850*10^{-6}$ m^3/cycle	T ≈ 1.600 s	Q≈110 l/min
2.00 m	$1650*10^{-6}$ m^3/cycle	1.000 s	100 l/min
3.00 m	$1100*10^{-6}$ m^3/cycle	0.700 s	95 l/min

So far it is assumed that in both cases ($H_s = H_{s,I}$ and $H_s = H_{s,II}$) the velocity u_c at impulse valve closure is the same. However, it follows from experiments that as the supply head H_s increases the magnitude of velocity u_c slightly increases (see Fig. III-19).

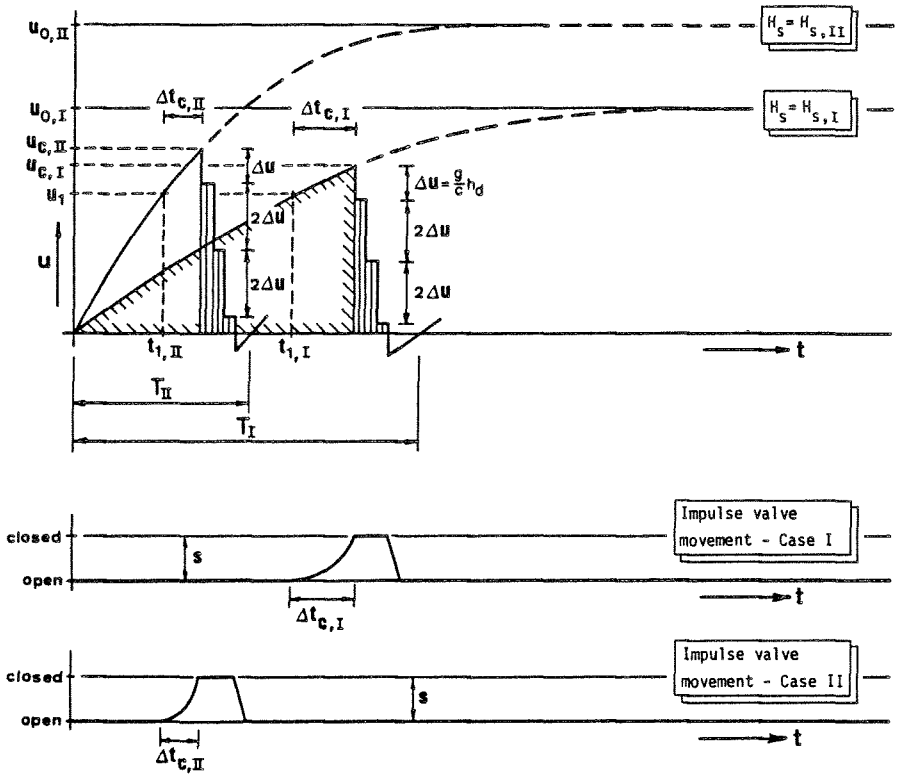

Fig. III-19 Period of acceleration and impulse valve closure for different supply heads

In Fig. III-19:

u_1 = velocity in the drive pipe at the instant the impulse valve begins to close, as determined by valve shape, valve weight and/or spring load of the impulse valve adjustment.

u_c = velocity in the drive pipe at the instant the impulse valve is completely closed, as determined by u_1, $(du/dt)_{u \geq u_1}$ and Δt_c:

$$u_c = u_1 + \int_{t_1}^{t_1 + \Delta t_c} \left(\frac{du}{dt}\right) dt \qquad \text{(III-72)}$$

and

Δt_c = time taken for the impulse valve to move from open to closed position, as determined by the length of the valve stroke (s) and the velocity of the impulse valve (v_{valve}):

$$s = \int_{t_1}^{t_1 + \Delta t_c} v_{valve}\, dt \qquad \text{(III-73)}$$

where v_{valve} , in turn, depends on the valve shape and on the motion of the surrounding water.

In both cases valve shape, weight and spring load (as well as stroke length) are the same, so that

$$u_{1,II} = u_{1,I} \qquad \text{(III-74)}$$

but since

$$\left[\left(\frac{du}{dt}\right)_{u \geq u_1}\right]_{II} > \left[\left(\frac{du}{dt}\right)_{u \geq u_1}\right]_{I} \qquad \text{(III-75)}$$

it follows that

$$\Delta t_{c,II} < \Delta t_{c,I} \qquad \text{(III-76)}$$

and

$$u_{c,II} > u_{c,I} \qquad \text{(III-77)}$$

To illustrate Eq. (III-76), Fig. III-20 shows recordings of the impulse valve movement, as obtained from experiments taken at different supply heads.

From Eq. (III-77) and Fig. III-19 it can be noted that

$$V_{d,II} > V_{d,I} \qquad \text{(III-78)}$$

Hence, given the delivery head h_d, the amount of water delivered per cycle

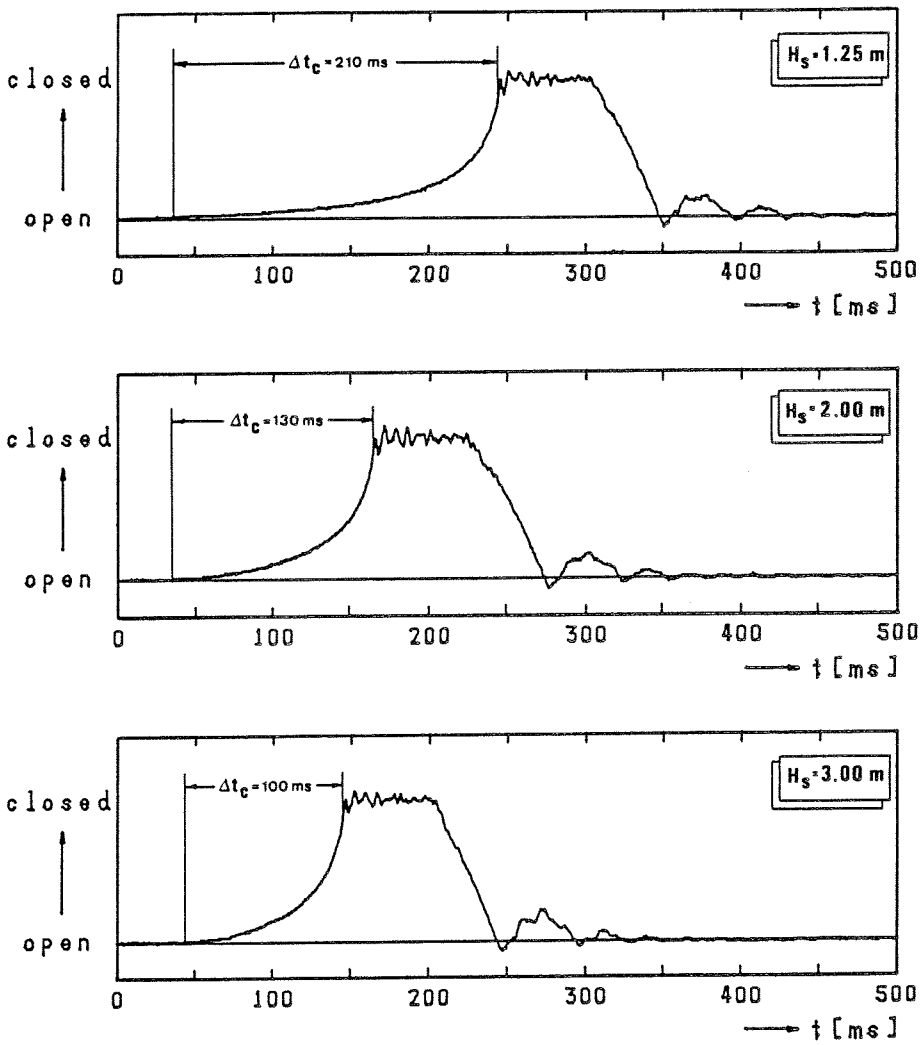

Fig.III-20 Impulse valve movement for different supply heads

(V_d) increases as H_s increases; this is also illustrated in Fig. III-21, showing V_d versus h_d curves for different supply heads, compiled from experiments taken on a Blake Hydram No. 2.

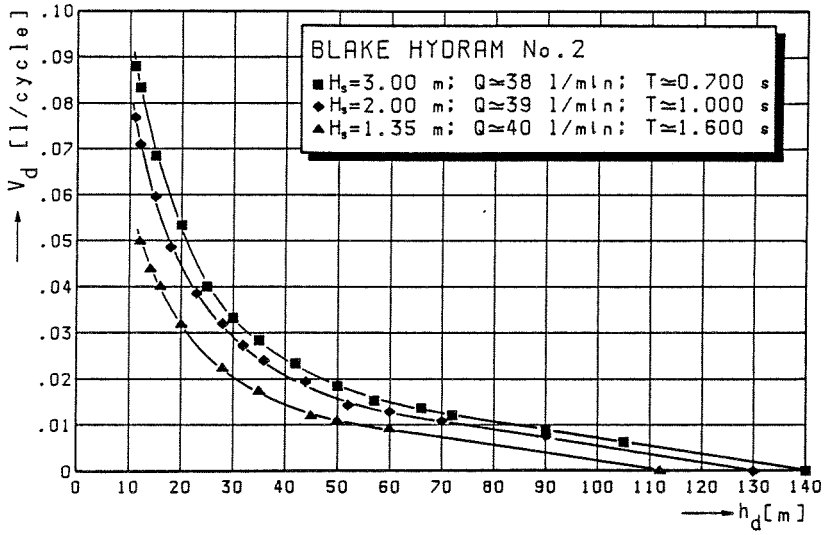

Fig. III-21 Amount delivered per cycle (V_d) versus delivery head (h_d)

Note: If $u_{c,II} = u_{c,I} + \Delta u_c$, it follows from Eq. (III-57) that

$$V_{d,II} = V_{d,I} + \frac{\pi D^2}{4} * T_d * \Delta u_c \qquad \text{(III-79)}$$

so that, given the delivery head h_d, the actual difference between $V_{d,I}$ and $V_{d,II}$ is determined by Δu_c, i.e. the difference in $(du/dt)_{u \geq u_l}$ for $H_{s,I}$ and $H_{s,II}$ respectively, whereas - given $H_{s,I}$ and $H_{s,II}$ - the differences in V_d become smaller as T_d decreases, i.e. as h_d increases (see Fig. III-21).

Finally, in accordance with Eq. (III-69), it may be concluded that as H_s increases the pumping rate

$$q = \frac{V_d}{T}$$

increases, primarily because of the decreased period time T (Eq. III-68) and second because of the slight increase of V_d (Eqs. III-78 and III-79).
The combined effect is illustrated in Fig. III-22, showing the q versus h_d curves as obtained from the 'Hydram No. 2' experiments.

(c) ram size: as stated before, the size of a hydraulic ram is usually denoted by the nominal diameter (D) of the drive pipe, which depends on the waste opening of the impulse valve.

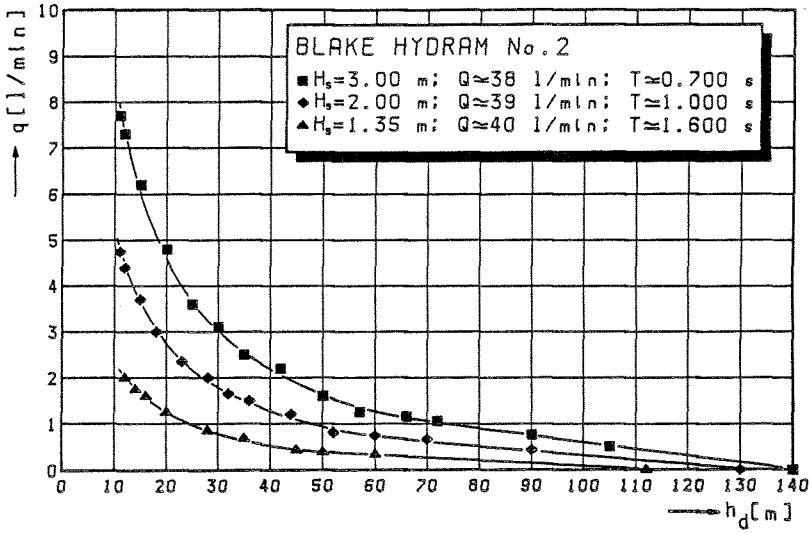

Fig.III-22 Pumping rate (q) versus delivery head (h_d)

From Eqs. (III-35), (III-49), (III-58) and (III-59) it may become clear that the larger the size of the ram, the more water (Q) is required to operate the ram and the more water (q) can be delivered to a higher level (see Fig. III-23).

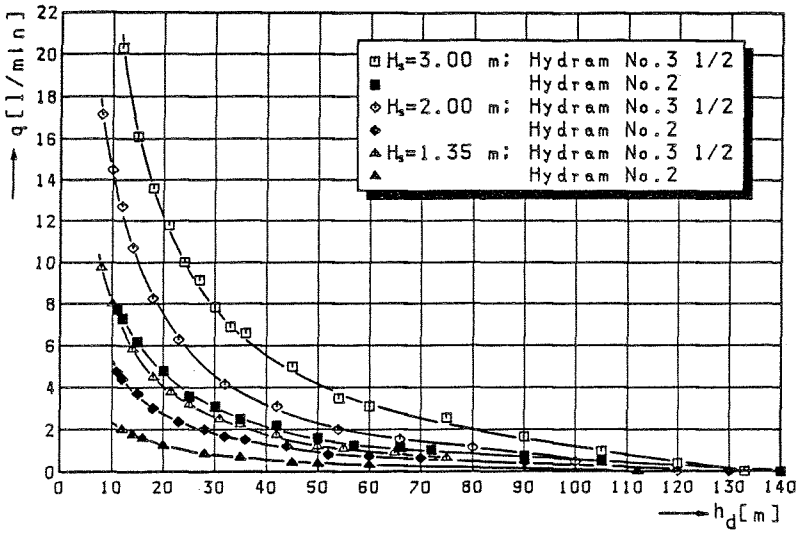

Fig. III-23 Effect of ram size on ram performance; Hydram No. 3 1/2: Q≈100 l/min, Hydram No. 2: Q ≈ 40 l/min.

(d) impulse valve adjustment: by increasing the weight and/or spring load on the impulse valve, the velocity u_1 (see Fig. III-19) increases and thereby the velocity u_c at impulse valve closure increases. In addition, the velocity u_c can be increased by lengthening the valve stroke.

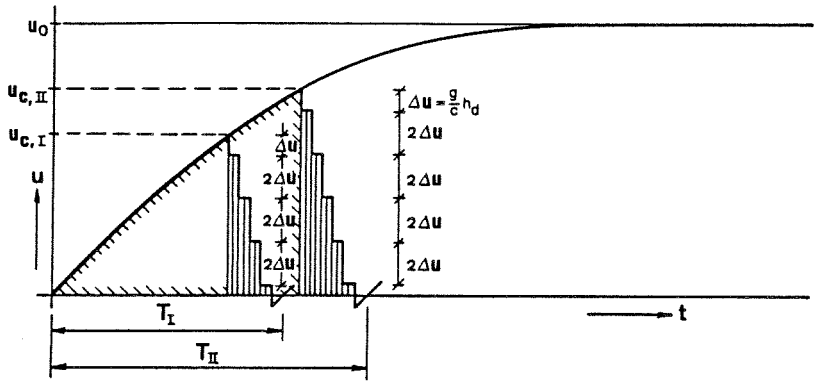

Fig. III-24 Effect of impulse valve adjustment

Fig. III-24 illustrates that as u_c increases, the amount of water wasted per cycle (V_{out}) increases, while in accordance with Eq. (III-70) the amount of water wasted per unit time

$$Q = \frac{V_{out}}{T} \approx \frac{\pi D^2}{4} * \frac{1}{2} u_c$$

increases as well ($V_{out,II} > V_{out,I}$ and $T_{II} > T_I$ and $Q_{II} > Q_I$)
It may also be observed from the figure that the amount of water delivered per cycle (Eqs. III-57 and III-46)

$$V_d = \frac{\pi D^2}{4} * T_d * (u_c - N \Delta u) \approx \frac{\pi D^2}{4} * \frac{1}{2} u_c T_d \qquad \text{(III-80)}$$

increases, whereas the pumping rate

$$q = \frac{V_d}{T}$$

normally increases likewise, provided that $u_{c,II}$ is still sufficiently lower than u_0. For examples, an increase in u_c as illustrated in Fig. III-25 is senseless since it is accompanied by a considerable increase in period time T, which may even lead to a decrease of pumping rate q while, as before, Q increases.
The best pumping results are usually obtained for $u_c \approx 0{,}6$ to $0{,}8 * u_0$, where the actual value depends on the supply head H_s, i.e. on $(du/dt)_{u=u_c}$.

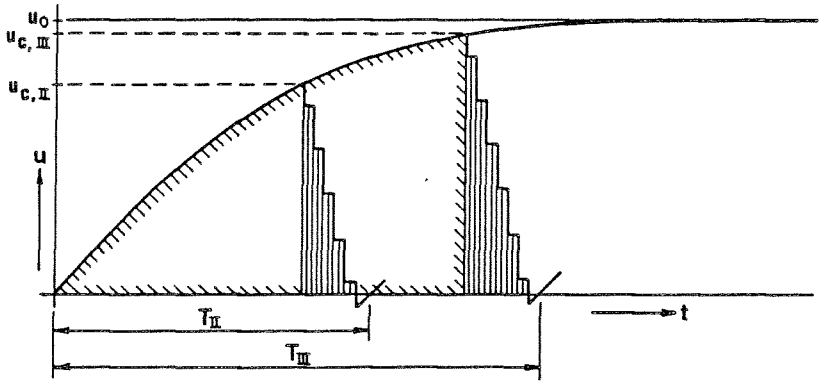

Fig.III-25 Effect of impulse valve adjustment

Hence, an increase in u_c normally increases the pumping rate q, while the number of beats per minute decreases (which may eventually reduce valve wear), but more water (Q) is needed to operate the ram. Alternatively, the increase in u_c may be used to deliver the original amount of water (q_I) to a higher level.

To illustrate the foregoing, Table III-1 includes experimental results obtained from tests carried out on a commercial hydraulic ram operated at two different values of impulse valve load.

Hydraulic ram : SANO No. 4 - 50 mm				Supply Head Hs = 3.00 m Drive pipe D = 2" (50 mm) L = 12.20 m		
Delivery Head hd [m]	Period Time T [s]	Pumping Rate q [l/min]	Waste Flow Q [l/min]	Efficiency (Rankine) [%]	Volume of Water Delivered [x 10^{-3} l/cycle]	Volume of Water Wasted Vout [x 10^{-3} l/cycle]
Spring load waste valve : 10.80 N						
12	0.741	10.75	66.65	48.4	132.8	823
21	0.720	7.05	68.90	61.4	84.6	827
30	0.743	4.45	66.60	60.1	55.1	825
45	0.720	3.15	69.80	63.2	37.8	838
60	0.776	2.00	63.60	59.7	25.9	823
90	0.729	1.30	67.70	55.7	15.8	823
120	0.863	0.65	51.85	48.9	9.3	746
Spring load waste valve : 14.40 N						
12	0.870	11.25	76.70	44.0	163.1	1112
21	0.817	7.50	80.10	56.2	102.1	1091
30	0.836	4.75	80.25	53.3	66.2	1118
45	0.811	3.50	83.15	58.9	47.3	1124
60	0.856	2.25	77.80	54.9	32.1	1110
90	0.823	1.50	81.75	53.2	20.6	1121
120	0.934	0.85	69.10	48.0	13.2	1076

Table III-1 Effect of impulse valve load on performance

Combined Alteration

The effect of combined alterations may be immediately apparent from the foregoing as well. For example, an increase in supply head H_s may be accompanied by an adjustment of the impulse valve such that u_c increases in accordance with the increased value of u_o (Fig. III-26).

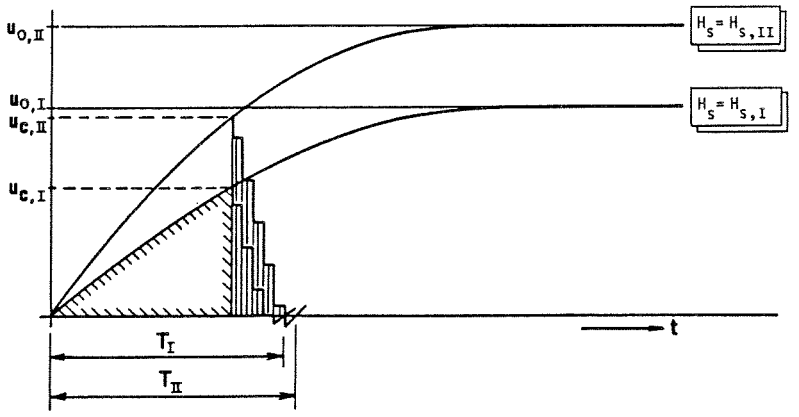

Fig. III-26 Effect of increments in H_s and u_c

As can be seen from the figure the combined alteration results in an increase in pumping rate q while the pumping frequency may remain approximately the same, but more water (Q) is required to operate the ram. Again, under the new circumstances higher delivery heads h_d come within reach.

Refinement of the formulae

In the hydraulic ram analysis presented so far it is assumed that the magnitude of all pressure surges observed during the period of retardation is the same, except for sign: $\Delta h = \pm h_d$ (i.e. the wave fronts move on top of the approximate hydraulic grade line going with the motion of the water in the drive pipe at the end of the period of acceleration - see Fig. III-10). This assumption has been made for simplicity, while the results thus obtained are sufficiently accurate to yield at the least a qualitative explanation of the operation of the hydraulic ram as well as of the effect of the various parameters governing its performance.

In reality only the first pressure surge relates to a pressure rise $\Delta h \approx h_d$ at the downstream end of the drive pipe, whereas in successive cross-sections upstreams the pressure rise equals the difference between the hydraulic grade line and the delivery pressure h_d (see Fig. III-27a). When this pressure

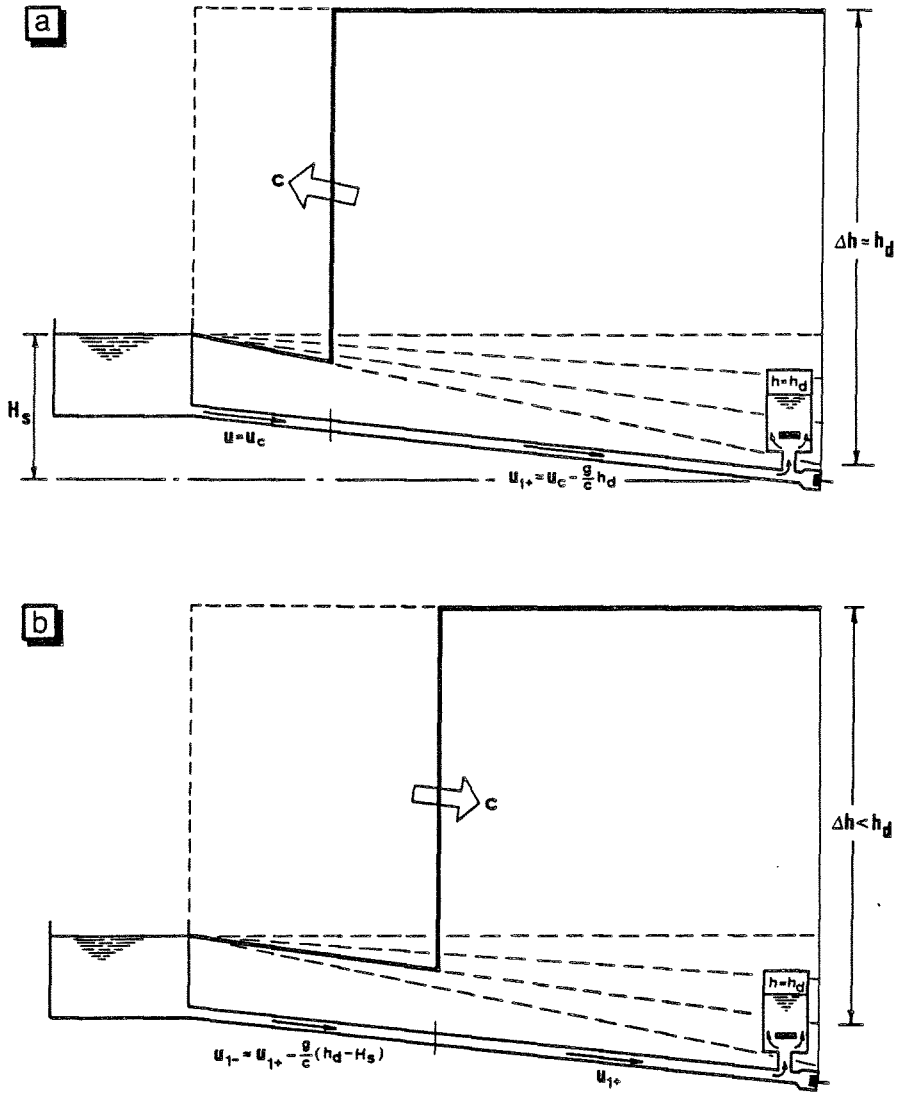

Fig. III-27 Period of retardation; propagation of successive pressure waves

surge arrives at the supply reservoir the subsequent reflected wave is accompanied by a pressure drop $\Delta h \approx -(h_d - H_s)$ at the upstream end of the drive pipe, since a constant pressure head ($h = H_s$) must remain at the supply reservoir. As the reflected wave moves downstream the hydraulic

grade line behind the wave front slightly rises in accordance with the decreased velocity ($u = u_1$-) of the water in the drive pipe (see Fig. III-27b). Consequently a smaller pressure rise ($\Delta h < h_d$) is needed to generate the second pressure surge travelling away from the ram.
In this way all successive pressure surges created at the downstream end of the drive pipe will slightly differ in magnitude: $\Delta h = h_d - \alpha H_s$; $0 \leq \alpha \leq 1$ (note that $\alpha = 1$ for all pressure waves reflected at the upstream end of the drive pipe).

Hence, for calculation purposes a more realistic approximation is obtained by modifying the equations derived in section III-3 as follows (see also the results of the graphical solution included in Appendix B).

Period of Retardation

- magnitude of pressure surges
  $\Delta h = \pm (h_d - \alpha H_s)$; + at the downstream end of the drive pipe
  - at the upstream end of the drive pipe
  where $\alpha = 0$ for the first pressure wave created at the ram
  $\alpha = 1$ for all subsequent pressure waves (both at the upstream and the downstream end of the drive pipe).

- velocities at the downstream end of the drive pipe (Fig. III-28):

$$T_a \leq t < T_a + \frac{2 L_s}{c} \quad : 1^{st} \text{ pressure surge} : u_1 \approx u_c - \frac{g}{c} h_d$$

$$T_a + \frac{2 L_s}{c} \leq t < T_a + \frac{4 L_s}{c} : 2^{nd} \text{ pressure surge} : u_2 \approx u_c - \frac{g}{c} h_d - 2 \frac{g}{c} (h_d - H_s)$$

$$T_a + \frac{4 L_s}{c} \leq t < T_a + \frac{6 L_s}{c} : 3^{rd} \text{ pressure surge} : u_3 \approx u_c - \frac{g}{c} h_d - 4 \frac{g}{c} (h_d - H_s)$$

etc.

or in general:

$$T_a + (i - 1) \frac{2 L_s}{c} \leq t < T_a + i \frac{2 L_s}{c} : i^{th} \text{ pressure surge}$$

$$u_i = u_c - \Delta u - 2 (i - 1) \Delta u^* \qquad \text{(III-81)}$$

where $\Delta u = \frac{g}{c} h_d$ (III-82)

$\Delta u^* = \frac{g}{c} (h_d - H_s)$ (III-83)

- number of surges N observed during the period of retardation, is the largest integer number satisfying the condition

$$u_N > 0$$

or

$$N < 1 + \frac{u_c - \Delta u}{2\,\Delta u^*} \qquad \text{(III-84)}$$

- amount of water pumped per cycle

$$V_d = \frac{\pi D^2}{4} * \frac{2\,L_s}{c} * \sum_{i=1}^{N} u_i$$

or

$$V_d = \frac{\pi D^2}{4} * T_d * \left[u_c - \Delta u - (N - 1)\,\Delta u^* \right] \qquad \text{(III-85)}$$

where

$$T_d = N * \frac{2\,L_s}{c} \qquad \text{(III-86)}$$

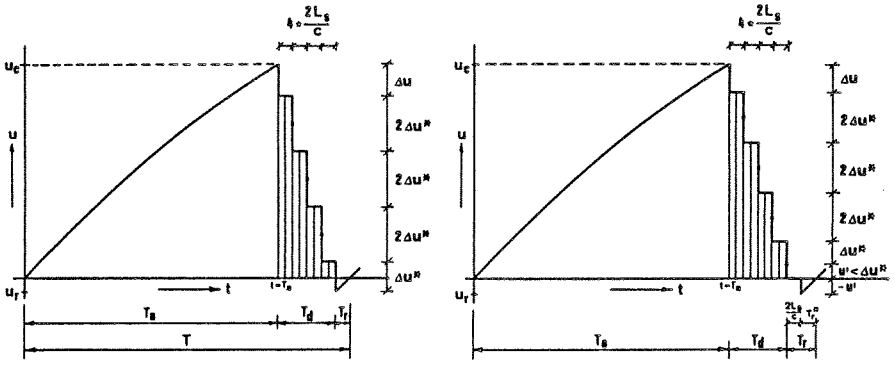

Fig. III-28 u(t)-diagram at the downstream end of the drive pipe

Period of Recoil

If

$$u_N < \Delta u^*, \text{ i.e. } N > \frac{u_c - \Delta u + \Delta u^*}{2\,\Delta u^*} \qquad \text{(III-87)}$$

then Case A :

$$u_r = u_c - \Delta u - (2\,N - 1)\,\Delta u^* \qquad \text{(III-88)}$$

$$T_r = -\frac{u_r\,L_s}{g\,H_s} \qquad \text{(III-89)}$$

$$V_r = -\frac{\pi\,D^2}{4} * \frac{u_r^2\,L_s}{2\,g\,H_s} \qquad \text{(III-90)}$$

otherwise Case B :

$$u_r = (2\,N - 1)\,\Delta u^* + \Delta u - u_c \qquad \text{(III-91)}$$

$$T_r = -\frac{u_r\,L_s}{g\,H_s} + \frac{2\,L_s}{c} \qquad \text{(III-92)}$$

$$V_r = -\frac{\pi\,D^2}{4} * \frac{u_r^2\,L_s}{2\,g\,H_s} \qquad \text{(III-93)}$$

The foregoing refinements have been given mainly for the sake of completeness and in view of the calculation examples to be presented in the next section. As stated before they do not alter any of the qualitative explanations on hydraulic ram operation given earlier in this section. In particular it can be noted from the equations that the differences with the results obtained in section III-3 may become of importance for low head ratios h_d/H_s only (i.e. for large numbers of N and/or large supply heads H_s). For example: the modified Eq. (III-85)

$$V_d = \frac{\pi\,D^2}{4} * T_d * \left[u_c - \Delta u - (N - 1)\,\Delta u^*\right]$$

can be written as (with use of Eqs. (III-82) and (III-83)):

$$V_d = \underbrace{\frac{\pi\,D^2}{4} * T_d * \left[u_c - N\,\Delta u + (N - 1)\,\frac{g}{c}\,H_s\right]}$$

unmodified Eq. (III-57)

so that the difference in the calculated amount of water pumped per cycle is given by

$$\Delta V_d = \frac{\pi\,D^2}{4} * T_d * (N - 1) * \frac{g}{c}\,H_s$$

from wich it is obvious that $\Delta V_d \neq 0$ for $N > 1$, while ΔV_d becomes more significant as either N or H_s increases (or both).

III-6 Calculation example

According to the simplified hydraulic ram analysis, presented in the previous sections, knowledge of ξ and u_c is sufficient to predict the hydraulic ram performance, provided that all other physical and geometrical properties of the particular installation are known.

A good estimate of the total loss coefficient ξ can be obtained from Eq. (III-28):

$$u_0 = \sqrt{\frac{2\,g\,H_s}{\xi}}$$

by measuring the amount of water (Q_0) flowing through the ram per unit time, with the impulse valve held in open position;

$$Q_0 = \frac{\pi D^2}{4} * u_0 \qquad \text{(fully developed, steady flow).}$$

Theoretically, the velocity u_c at impulse valve closure can be calculated from (see Eq. III-15):

$$u_c = \frac{g}{c} h_{max}$$

where h_{max} could be obtained from a gauge-reading of the pressure head in the air chamber, while the hydraulic ram is working with the stop-cock in the delivery pipe closed ($q = 0$, $h = h_{max}$).
However, it has been our experience that the value of u_c thus obtained is on the low side (approx. 10 - 20 %) due to energy losses and due to the fact that most hydraulic rams don't work properly under 'h_{max}-conditions', the latter because of the strong recoil ($h = h_{max}$: $\Delta u = u_c$ and $u_r = - u_c$; see Eq. III-51) which may lead to a large amount of air to be sucked in through the impulse valve during the period of recoil.

Alternatively, knowing the total loss coefficient ξ, a better estimate of u_c can be obtained by establishing the minimum supply head $H_{s,min}$ necessary to close the impulse valve.

With knowledge of $H_{s,min}$ it follows from Eq. (III-28) and Fig. III-29 that

$$u_c \geq \sqrt{\frac{2\,g\,H_{s,min}}{\xi}}$$

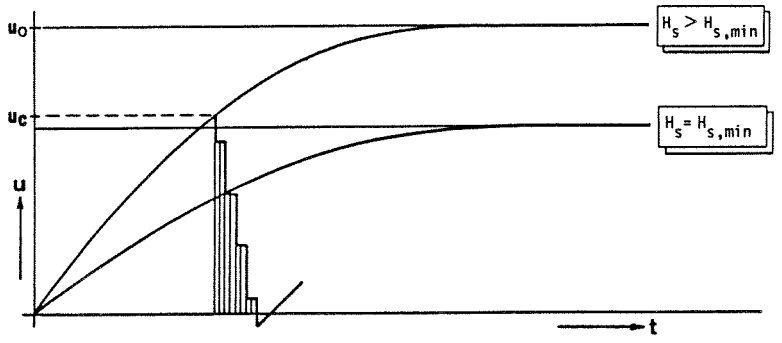

Fig.III-29 Acceleration for different supply heads

Example: the following data refer to experiments taken on a Blake Hydram No. 2 (11/2"):

H_s = 3.00 m	K = 2.15 GPa = 2.15 * 10^9 Nm^{-2}
L_s = 11.90 m	E = 210 GPa
D = 38 mm	ρ = 1000 kgm^{-3}
e = 3.5 mm	g = 9.81 ms^{-2}

Furthermore it has been estimated that:

$\xi = 20$

$u_c \approx 1.2$ ms^{-1} ($H_{s,min} \approx 1.20$ m; $u_c > 1.1$ ms^{-1})

Eq.(III-4):

$$c = \frac{1}{\sqrt{\frac{\rho}{K} + \frac{\rho D}{E e}}} = 1390 \text{ ms}^{-1}$$

Experimental result, obtained from simultaneous pressure + time recordings at two different places in the drive pipe (see chapter IV): $c = 1380$ ms^{-1}.

Note: the experimental value will be used in the calculations hereafter.

Acceleration:

Eq. (III-28) $$u_0 = \sqrt{\frac{2 g H_s}{\xi}} = 1.72 \text{ ms}^{-1}$$

Eq. (III-34) $$T_a = \frac{L_s}{u_0 \xi} \ln \frac{u_0 + u_c}{u_0 - u_c} = 0.597 \text{ s}$$

Eq. (III-35) $$V_a = \frac{\pi D^2}{4} * \frac{2 L_s}{\xi} \ln \cosh \frac{u_0 \xi}{2 L_s} T_a$$

$$= 450 * 10^{-6} \text{ m}^3/\text{cycle}$$

1. Delivery head $h_d = 57$ m

Retardation:

Eq. (III-82) $$\Delta u = \frac{g}{c} h_d = 0.405 \text{ ms}^{-1}$$

Eq. (III-83) $$\Delta u^* = \frac{g}{c} (h_d - H_s) = 0.384 \text{ ms}^{-1}$$

Eq. (III-84) $$N < 1 + \frac{u_c - \Delta u}{2 \Delta u^*} = 2.04 \qquad N = 2$$

Eq. (III-86) $$T_d = N * \frac{2 L_s}{c} = 0.034 \text{ s}$$

Eq. (III-85) $$V_d = \frac{\pi D^2}{4} * T_d * \left[u_c - \Delta u - (N - 1) \Delta u^* \right]$$
$$= 15.8 * 10^{-6} \text{ m}^3/\text{cycle}$$

Recoil:

Eq. (III-87) $$\frac{u_c - \Delta u + \Delta u^*}{2 \Delta u^*} = 1.54 < N \text{ : Case A}$$

Eq. (III-88) $$u_r = u_c - \Delta u - (2N - 1) \Delta u^* = - 0.357 \text{ ms}^{-1}$$

Eq. (III-89) $$T_r = - \frac{u_r * L_s}{g H_s} = 0.144 \text{ s}$$

Eq. (III-90) $$V_r = - \frac{\pi D^2}{4} * \frac{u_r^2 L_s}{2 g H_s} = - 29.2 * 10^{-6} \text{ m}^3/\text{cycle}$$

Hence:

Eq. (III-60) $$T = T_a + T_d + T_r = 0.775 \text{ s}$$

Eq. (III-58) $$q = \frac{1}{T} * V_d = 20.4 * 10^{-6} \text{ m}^3/\text{s} = 1.20 \text{ l/min}$$

Eq. (III-59) $$Q = \frac{1}{T} * (V_a + V_r) = 543 * 10^{-6} \text{ m}^3/\text{s} = 32.60 \text{ l/min}$$

2. Delivery head h_d = 42 m

Retardation:

Eq. (III-82) $\Delta u = 0.299\ ms^{-1}$

Eq. (III-83) $\Delta u^* = 0.277\ ms^{-1}$

Eq. (III-84) $N < 2.63 \quad : \quad N = 2$

Eq. (III-86) $T_d = 0.034\ s$

Eq. (III-85) $V_d = 24.1 * 10^{-6}\ m^3/cycle$

Recoil:

Eq. (III-87) $$\frac{u_c - \Delta u + \Delta u^*}{2\ \Delta u^*} = 2.13 > N \ : \ \text{Case B}$$

Eq. (III-91) $u_r = (2\ N - 1)\ \Delta u^* + \Delta u - u_c = -\ 0.07\ ms^{-1}$

Eq. (III-92) $$T_r = -\frac{u_r * L_s}{g\ H_s} + \frac{2\ L_s}{c} = 0.045\ s$$

Eq. (III-93) $V_r = -\ 1.1 * 10^{-6}\ m^3/cycle$

Hence:

Eq. (III-60) $T = T_a + T_d + T_r = 0.676\ s$

Eq. (III-58) $q = \frac{1}{T} V_d = 35.6 * 10^{-6}\ m^3/s = 2.15\ l/min$

Eq. (III-59) $Q = \frac{1}{T} (V_a + V_r) = 664 * 10^{-6}\ m^3/s = 39.85\ l/min$

3. Delivery head h_d = 35 m

Retardation:

Eq. (III-82) $\Delta u = 0.249\ ms^{-1}$

Eq. (III-83) $\Delta u^* = 0.227\ ms^{-1}$

Eq. (III-84) $N < 3.09 \quad : \quad N = 3$

Eq. (III-86) $T_d = 0.051\ s$

Eq. (III-85) $V_d = 28.7 * 10^{-6}\ m^3/cycle$

Recoil:

Eq. (III-87) $\frac{u_c - \Delta u + \Delta u^*}{2\,\Delta u^*} = 2.59 < N$: Case A

Eq. (III-88) $u_r = -0.184\ ms^{-1}$

Eq. (III-89) $T_r = 0.074\ s$

Eq. (III-90) $V_r = -7.7 * 10^{-6}\ m^3/cycle$

Hence:

Eq. (III-60) $T = T_a + T_d + T_r = 0.722\ s$

Eq. (III-58) $q = \frac{1}{T} V_d = 39.8 * 10^{-6}\ m^3/s = 2.40\ l/min$

Eq. (III-59) $Q = \frac{1}{T} (V_a + V_r) = 613 * 10^{-6}\ m^3/s = 36.75\ l/min$

4. Delivery head $h_d = 25$ m

Retardation:

Eq. (III-82) $\Delta u = 0.178\ ms^{-1}$

Eq. (III-83) $\Delta u^* = 0.156\ ms^{-1}$

Eq. (III-84) $N < 4.27$: $N = 4$

Eq. (III-86) $T_d = 0.068\ s$

Eq. (III-85) $V_d = 42.7 * 10^{-6}\ m^3/cycle$

Recoil:

Eq. (III-87) $\frac{u_c - \Delta u + \Delta u^*}{2\,\Delta u^*} = 3.78 < N$: Case A

Eq. (III-88) $u_r = -0.07\ ms^{-1}$

Eq. (III-89) $T_r = 0.028\ s$

Eq. (III-90) $V_r = -1.1 * 10^{-6}\ m^3/cycle$

Hence:

Eq. (III-60) $T = T_a + T_d + T_r = 0.693$ s

Eq. (III-58) $q = \frac{1}{T} * V_d = 61.6 * 10^{-6}$ m^3/s = 3.70 l/min

Eq. (III-59) $Q = \frac{1}{T} (V_a + V_r) = 648 * 10^{-6}$ m^3/s = 38.85 l/min

Fig. III-30 shows the u(t)-diagrams for the velocity at the downstream end of the drive pipe, as compiled from the previous calculation examples.
In addition, pressure + time recordings illustrating the number of pressure surges observed during the period of retardation, will be presented in

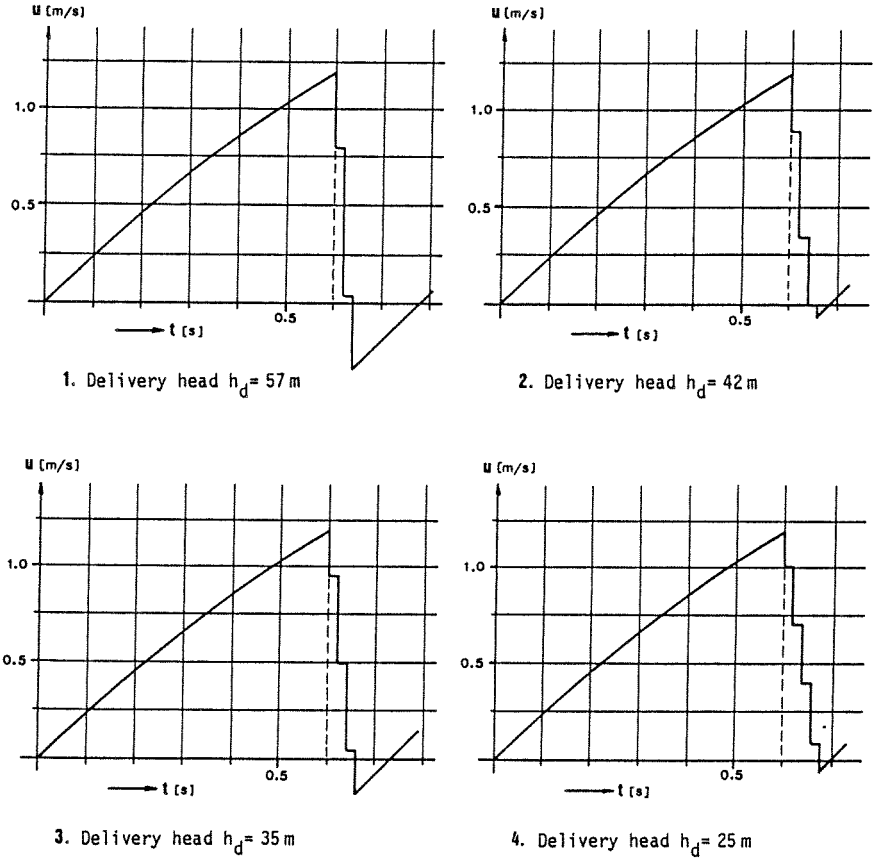

Fig.III-30 u(t)-diagrams for the flow velocity at the downstream end of the drive pipe.

chapter IV (section IV-2). Finally, Table III-2 compares calculated results (refined model) with results obtained from experiments. As can be seen from the table the agreement may be called reasonably good.

Blake Hydram No. 2 (1 1/2") - Supply Head H_s = 3.00 m											
h_d	N	V_d 10^{-6} m³/cycle		V_{out} 10^{-6} m³/cycle		per. time T [s]		pump. rate q [l/min]		waste flow Q [l/min]	
[m]	[-]	Calc.	Exp.	Calc.	Exp.	Calc.	Exp.	Calc.	Exp.	Calc.	Exp.
72	1	13.3	12.2	441	445	0.711	0.695	1.10	1.05	37.20	38.40
57	2 *	15.8	15.4	420	413	0.775	0.737	1.20	1.25	32.60	33.60
42	2	24.1	23.5	449	444	0.676	0.640	2.15	2.20	39.85	41.65
35	3 *	28.7	28.5	442	424	0.722	0.683	2.40	2.50	36.75	37.25
25	4 *	42.7	40.1	448	427	0.693	0.669	3.70	3.60	38.85	38.30
20	5 *	55.3	53.4	449	426	0.695	0.667	4.75	4.80	38.75	38.30
*) see also pressure ÷ time recordings in section IV-2											

Table III-2 Comparison of calculated and experimental results

IV LABORATORY INVESTIGATION

Recent activities in hydraulic ram investigation have been reported from research centres in, amongst others, Indonesia, Canada and Tanzania (see e.g. Schiller [21]). However, to our knowledge there has been no wide scale, fully comparative testing of hydraulic rams under controlled laboratory conditions. Therefore, one of the purposes of the present investigation was to carry out tests on commercially-available hydraulic rams in order to determine their performance characteristics and to compare these results with the information - if any - provided by the manufacturers.
The tests have been fairly extensive, each ram being performance-tested for approximately one month. Durability-tests were designed to run in the field program carried out by the Foundation of Dutch Volunteers in Rwanda (Africa).

IV-1 Selection of hydraulic rams

Before any testing could commence it was necessary to select 12 hydraulic rams (6 different manafactures) as being applicable in typical village or domestic water supply schemes. Letters were sent to the ram manufacturers known to us at the beginning of the investigation, asking for detailed information on the rams they made, such as types and sizes including prices, range of operational uses, performance data, basic requirements for the installation, specifications of spare parts plus prices, etc. An updated list of some present day ram manufacturers is included as Appendix C.
From the replies received a selection of hydraulic rams was made, based generally on the following criteria:

(1) As many different types of hydraulic rams as possible should be included in the test, i.e. rams using different types of waste valve and delivery valve, both in design (spring-operated, weight-loaded, no external load) and material used (rubber, gunmetal/brass).
(2) The tests should include some old, well-established hydraulic ram designs, as well as some of a more 'modern' construction.
(3) The hydraulic rams to be tested should, at least on paper, show a reasonable price ÷ performance ratio. For this purpose a comparison of hydraulic rams was made for an arbitrary arrangement of supply head, delivery head and available source supply (Table IV-1). The pumping rate q and the efficiency η mentioned in the table, are as claimed by the performance data provided by the ram manufacturers.

Arrangement : Source Supply $Q = 90$ l/min
Supply Head $H_s = 7.50$ m
Delivery Head $h_d = 75$ m

Type of Hydraulic Ram	Drive Pipe [inch]	[mm]	Volume of Driving Water Required [l/min]	Pumping Rate q [l/min]	Efficiency η_{trd} [%]	Approx. Price for Ram Alone [US $ - 1982]
Vulcan 21/2	21/2	65	36-114	6.10	68	1200
Blake Hydram 31/2	21/2	65	45- 96	6.00	67	1000
Sano No. 5/65 mm	21/2	65	50-110	6.95	77	1000
Rife 20 HDU	2	50	38- 95	5.40	60	1100
Schlumpf 5A23	2	50	50-100	5.50	61	2700
Alto CH 66-110-18	21/2	65	50- 90	5.40	60	2100
Briau D4	2	50	45- 90	5.40	60	3200
CeCoCo - H50	2	50	25-115	6.90	77	3500
WAMA No. 6	21/2	65	60-100	4.50	50	1500
BZH-Ram W6	21/2	65	45- 90	2.70	30	1200

Table IV-1 Comparison of hydraulic rams

A first look at Table IV-1 shows that as far as performance is concerned the choise should favour the upper eight manufactures. Taking the ram cost into consideration, this leaves the top six hydraulic rams. The final choise, including what sizes of ram were to be ordered, was made in consultation with the people responsible for the field trials. A list of the hydraulic rams selected is given in Table IV-2 together with a brief description of the essential features of each.

Notes:

1. In the initial stage of the investigation we were not familiar with commercial rams made in developing countries, otherwise some of them could have been included in preference to similar designs of Western descent.
2. Most of the rams mentioned in Table IV-2 were purchased directly from the manufacturers, with the exception of the Vulcan rams, the SANO No. 1 and the Davey No. 3. The named rams were got on loan from friendly

institutes of technology*), where they were occasionally used for demonstration purposes only. Except for the necessity to replace some of the gaskets (mainly to prefer the certain to the uncertain) the rams proved to be in good condition and in their original state.

Type of Hydraulic Ram	Manufacturer	Drive Pipe Diameter [ins]	[mm]	Intake capacity [l/min]	Description
Blake Hydram No. 2 Blake Hydram No. 3,5	John Blake Ltd, England	1,5 2,5	40 65	12 - 25 45 - 96	A well-established, standard design made of cast-iron. Both waste valve and delivery valve consist of a rubber disc covering a perforated gunmetal seat.
Alto J 26-80-8 Alto CH 50-110-18	J.M. Desclaud, France	1 2	25 50	8 - 15 30 - 60	A recently renewed pump design made of steel pipe components, but using conventional valve designs. Weight-loaded gunmetal waste valve; spring-loaded rubber clack as delivery valve.
Vulcan 1" Vulcan 2"	Green & Carter, England	1 2	25 50	4 - 18 23 - 46	A standard design made of cast-iron; like the Blake Hydram available for a long time. Both waste valve and delivery valve consist of a rubber disc covering a grid shaped, gunmetal seat.
SANO No. 1 - 25 mm SANO No. 4 - 50 mm	Pfister + Langhanss, Germany	1 2	25 50	6 - 16 30 - 65	A rather 'unconventional' design, nowadays made of fire zinc-coated steel. Both waste valve and delivery valve are spring-activated and substantially made of gunmetal.
Davey No. 3 Rife 20 HDU	Rife Hydr. Eng. Mfg. Co., U.S.A.	1 2	25 50	5 - 15 38 - 95	Rife: a fairly standard design made of cast-iron. Weight-loaded rubber waste valve, mounted on a rocker-arm; delivery valve is a rubber disc covering a grid iron seat. Davey: less efficient, less expensive low-base configuration, using a weight-loaded gunmetal waste valve and a weight-loaded leather washer as delivery valve.
Schlumpf 4A5 Schlumpf 4A23	Schlumpf AG Maschinenfabrik, Switzerland	1,5 1,5	40 40	30 - 60 30 - 60	A design available in 2 models. Model A23 uses a spring-loaded rubber waste valve mounted on a rocker and a weight-loaded rubber washer as delivery valve. The less efficient model A5 uses a weight-loaded rubber waste valve.

Table IV-2 Hydraulic rams selected

*) Eindhoven University of Technology, Eindhoven, the Netherlands;
International Institute for Hydraulic and Environmental Engineering, Delft, the Netherlands.

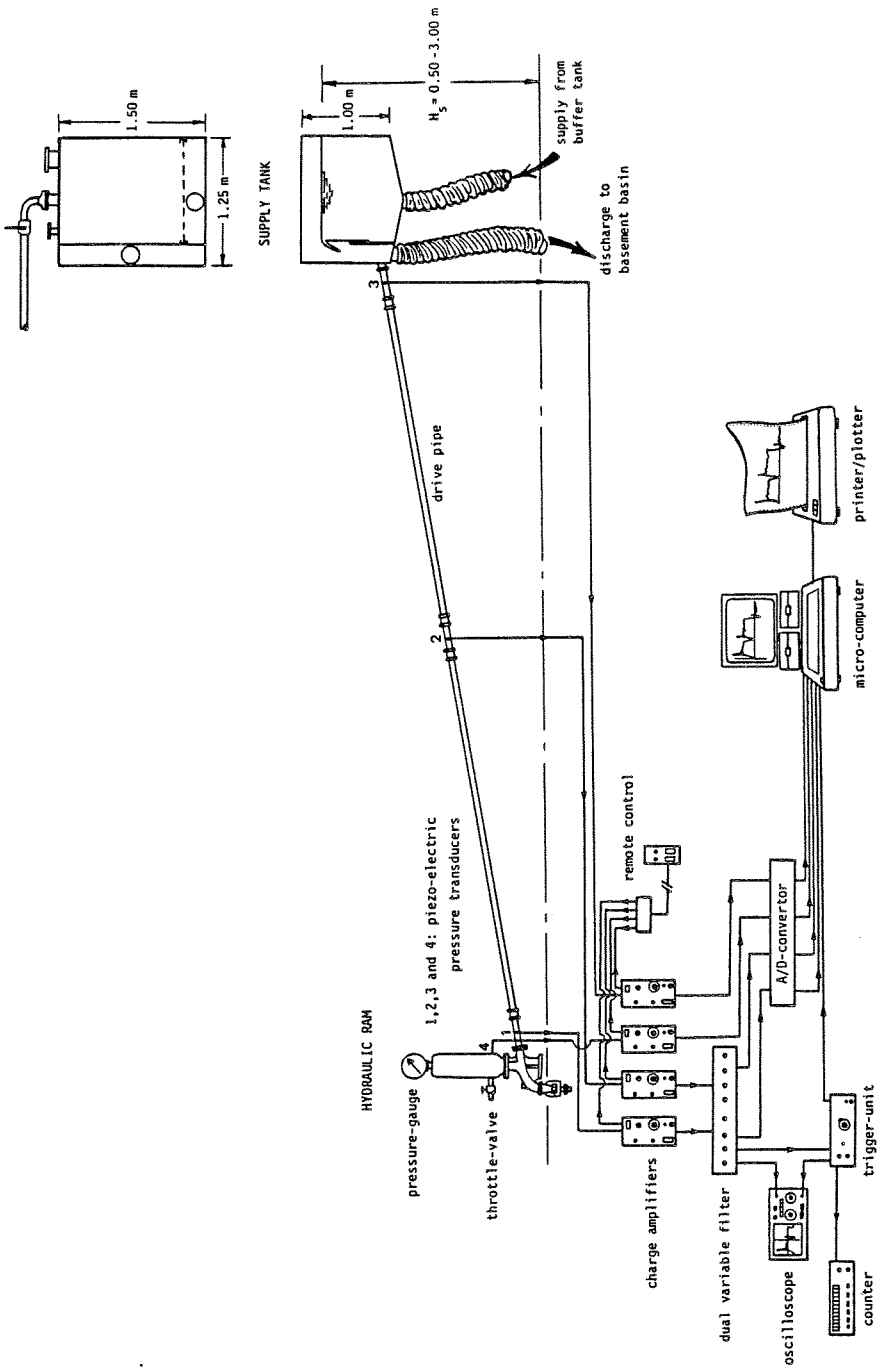

Fig. IV-1 Test installation

IV-2 Experimental set-up

For the selected hydraulic rams performance data had to be obtained by determining the pumping rate q and the waste flow Q for varying arrangements of supply head H_s and delivery head h_d.
The hydraulic rams were installed for testing as illustrated in Fig. IV-1. Four different diameters of drive pipe were used: 1", 1.5", 2" en 2.5", corresponding the various sizes of the rams to be tested. Each drive pipe consisted of about 12 m of galvanized iron pipe. Water was supplied to the rams from a supply tank, equipped with an adjustable overflow. The water surface in this tank could thus be maintained at a constant level by supplying a surplus of water to the tank. The supply head H_s, measured vertically from the output level at the waste valve of the ram to the water level in the supply tank, could be varied by lowering or raising the overflow as well as by putting the supply tank in its entirety on a lower or higher elevation. In this way supply heads ranging from approximately 0.50 m to 3.00 m were available.
All the hydraulic rams were operated at three different supply heads: H_s = 1.00 m, 2.00 m and 3.00 m. For the Blake Hydrams and the Rife 20 HDU the lowest supply head applied has been 1.35 m and 1.25 m respectively, since an unsteady functioning of these rams was observed when operation at a lower supply head was attempted (supply head insufficient to accomplish a rapid waste valve closure, i.e. $u_c/u_o \rightarrow 1$).
For each of the three values of the supply head a series of tests was made in which the delivery head (h_d) was varied from $h_d = h_{max}$ (q = 0) downwards, until it became so low that the ram ceased to function (note: a certain minimum delivery pressure is required to ensure a continuous, automatic action of the ram). Variable delivery heads were simulated by imposing an artificial head with a throttle-valve at the outlet of the air chamber of the rams. The delivery heads were measured by a pressure-gauge connected to the air chamber. For each arrangement of supply head and delivery head the waste flow Q was determined by measuring the time required for wasting a known quantity of water (caught in a small tank and measured with scales). These measurements were repeated at least 10 times to get a reliable average value. In the same way the pumping rate q was determined by measuring the time required for pumping a given quantity of water. It was normally sufficient to repeat this measurement 4 or 5 times. The period time T of the pumping cycle was determined by measuring the time required for 100, 200, 300, 400 and 500 cycles successively. In addition an electronic beat frequency counter was used, either to count the number of beats (cycles) or to get a direct reading of the period time T.

As became clear in the previous chapters, the action of both waste valve and delivery valve is of paramount importance for a successful operation of the hydraulic ram. It may be remembered that waste valve closure at the end of the period of acceleration should be rapid, almost instantaneous. That is to say: the greater part of the closure must take place in the last 2 L_s/c second, while there should be no significant pressure rise in the ram body until the waste valve is almost completely closed. It is only in this way that a sudden and effective pressure rise will be created immediately after waste valve closure. In its turn the delivery valve should respond to this pressure rise by instantaneous opening, thus allowing water to be pumped into the air chamber, whereas it should re-close instantly when the momentum of the driving water is exhausted, i.e. $u \leq 0$ at the downstream end of the drive pipe, thus preventing the pumped water from flowing back into the ram body.

The actual motion of both valves has been recorded for the Rife 20 HDU ram, using a highly sensitive, inductive displacement transducer at the waste valve and strain gauges attached to the valve rubber of the delivery valve. An example of such recordings was presented in section III-1. With reference to these recordings as well as with knowledge of the foregoing it may be clear that, alternatively, a good or in a way an even better impression of valve action can be obtained by observing the pressure variations both at the downstream end of the drive pipe, i.e. near to the ram and in the air chamber of the ram itself. These 'high-frequent' pressure variations (note that for instance for the test installation 2 L_s/c is approx. 20 milliseconds) can be recorded using piezo-electric pressure transducers.

As pictured in Fig. IV-1, altogether four piezo-electric pressure transducers were used, one mounted into the air chamber of the ram and three mounted flushed into the pipe wall of the drive pipe: one at the downstream end, one half way up and one at the upstream end of the drive pipe. The signals of the transducers were amplified by charge amplifiers before entering the recording circuit, in which an A/D-convertor and a micro-computer were used for the simultaneous sampling of the signals. Subsequently the data could be saved on diskette for processing later on, such as plotting of the signals. Examples of the results thus obtained are illustrated in Figs. IV-2, IV-3 and IV-4 and will be discussed hereafter.

Note: the recordings are tagged for identification as follows:

file : XX/YY
reg. no. NN-TT

where XX/YY = file-name of the simultaneous recordings as saved on diskette; XX = code for the hydraulic ram; for example B2 = Blake Hydram No. 2

YY = serial number of the file

NN-TT = registration number of the recording:

NN = test number (each number relates to an unique combination of hydraulic ram, supply head and delivery head)

TT = transducer code:

1 = pressure transducer downstream end of the drive pipe

2 = pressure transducer half way up the drive pipe

3 = pressure transducer upstream end of the drive pipe

4 = pressure transducer air chamber hydraulic ram

occasionally:

5 = displacement transducer waste valve

6 = strain gauges delivery valve

As mentioned, Figs. IV-2, IV-3 and IV-4 illustrate pressure ÷ time diagrams recorded simultaneously at four different places in the test installation. All three figures refer to the same hydraulic ram (Blake Hydram No. 2) operating under a supply head H_s = 3.00 m, whereas the delivery head h_d = 57 m, 35 m and 25 m respectively. The upper part of the figures represents the recordings at full length, while underneath the most interesting portions, i.e. the successive periods of retardation, are shown in detail. It should be noted that the diagrams portray the pressure variations as measured relative to the local quasi-static pressure; besides, for convenience all pressures were converted to pressure heads ($h = p/\rho g$) before being plotted. It can be seen from the figures that, indeed, after a relative long period of acceleration a sudden pressure rise is created in the ram body. Within a few milliseconds this pressure rise drops to a value approximately equal to the delivery pressure ($h = h_d$), thus indicating that the delivery valve has opened. This may also be observed from the pressure ÷ time recording for the air chamber, in which both opening and closing of the delivery valve are distinctly marked by sudden pressure fluctuations, the first because of the sudden flow of water into the air chamber, the latter due to the rebound of the water tending to flow back out of the air chamber. The propagation of successive pressure waves, moving up and down the drive pipe during the period of retardation, may be apparent from the recordings obtained from the pressure transducers mounted into the drive pipe. In particular the wavespeed c can be established from these recordings by determining the

time required for the first pressure pulse to move from the downstream end (transducer 1) to half way up the drive pipe (transducer 2). For example, for the 1,5"-drive pipe it followed from a great number of recordings that Δt_{1-2} (see Fig. IV-2) was approximately 4.5 milliseconds; with known distance from transducer 1 to transducer 2 the wavespeed has been evaluated to be $c = 1380\ ms^{-1}$. The number of surges N, occurring during the period of retardation, appears clearly from the recordings as well. In addition it can be checked that in all cases the time elapsed between delivery valve opening and delivery valve closure equals $N * 2\ L_s/c$ second, as it ought to be (note: $2\ L_s/c \approx 17$ milliseconds for the 1,5"-drive pipe).

Finally, Figs. IV-5 through to IV-8 show additional recordings for the foregoing arrangements as well as for $h_d = 20$ m. Instead of four signals, only two have been recorded (transducers 1 and 4) but for a longer period of time: approximately three times the period time T of the pumping cycle. The recordings illustrate the similarity in successive pumping cycles, giving evidence of the periodical character of the hydraulic ram operation. Again it follows from the recordings that the number of surges N = 2, 3, 4 and 5 for h_d = 57 m, 35 m, 25 m and 20 m respectively, which is in conformity with the calculated results as summarized in Table III-2.

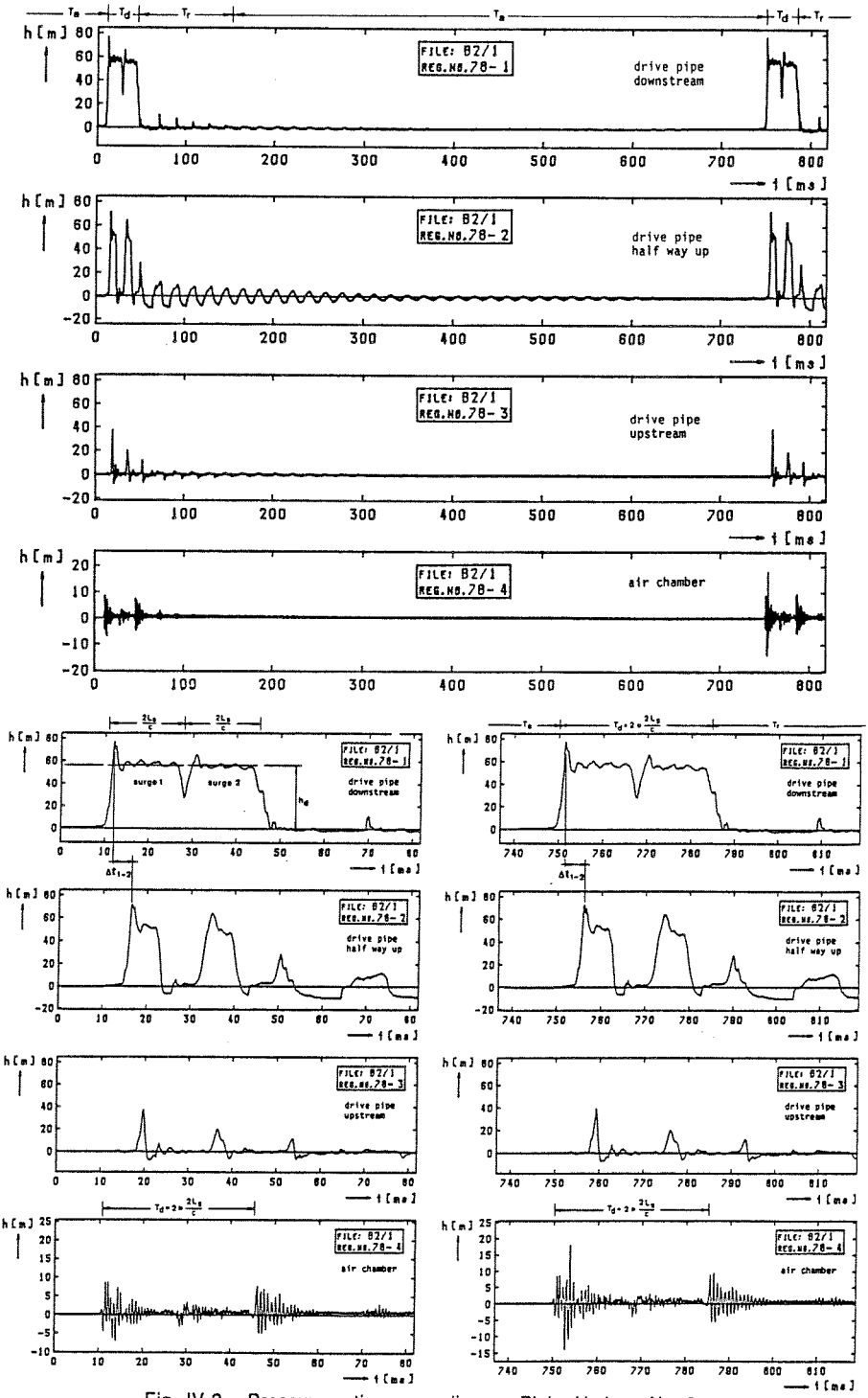

Fig. IV-2 Pressure + time recordings; Blake Hydram No. 2

H_s = 3.00 m, h_d = 57 m

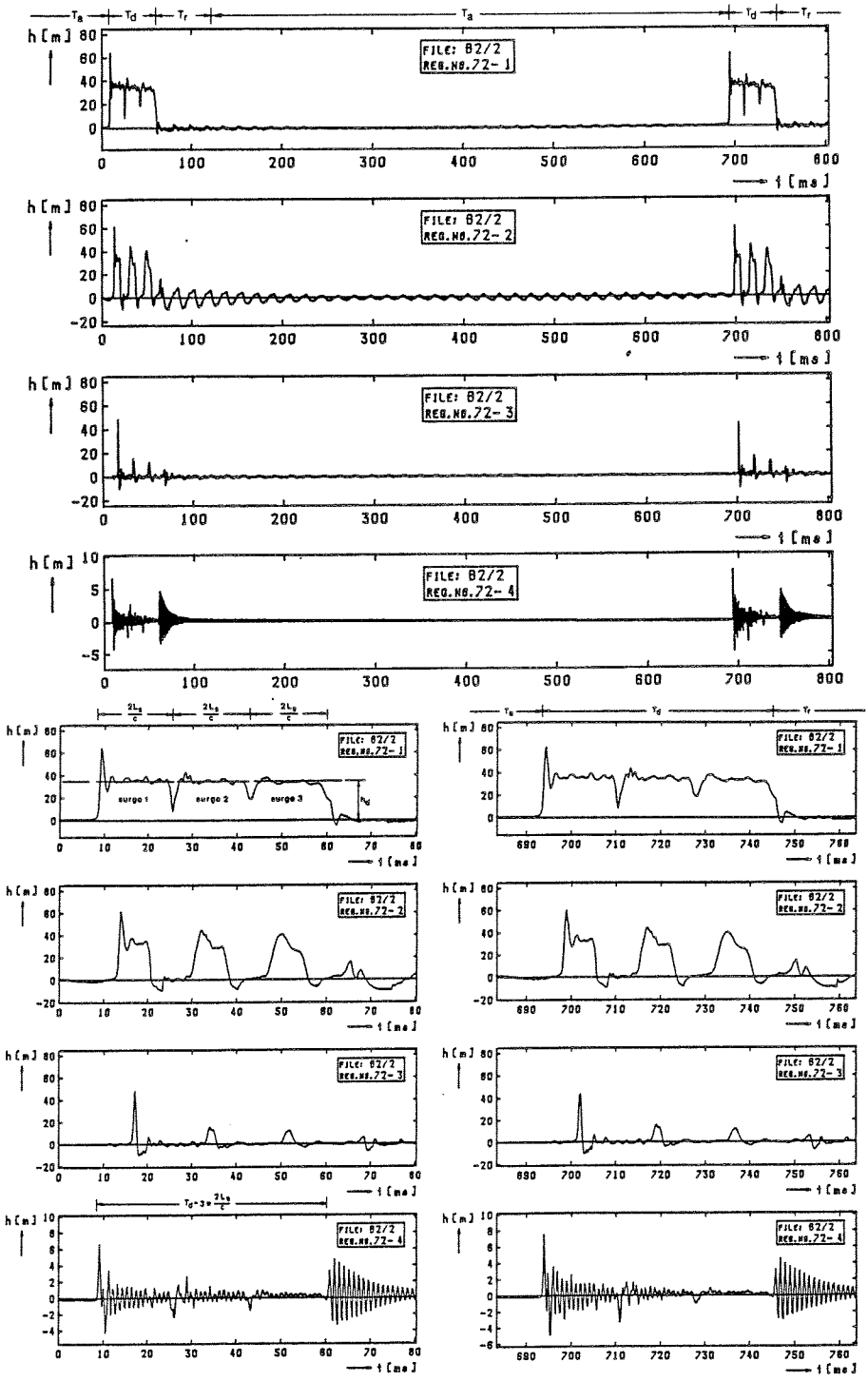

Fig. IV-3 Pressure + time recordings; Blake Hydram No. 2

H_s = 3.00 m, h_d = 35 m

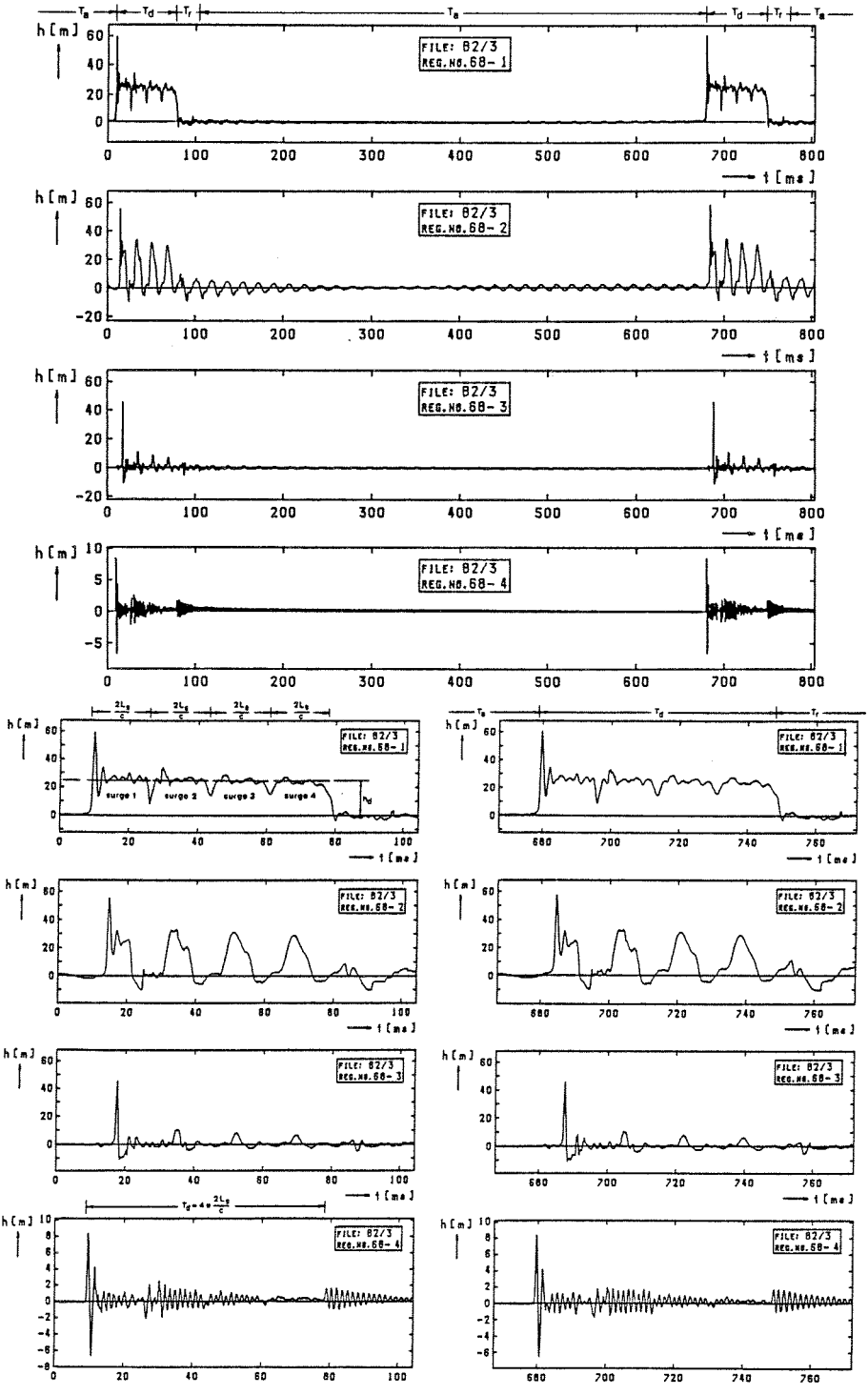

Fig. IV-4 Pressure + time recordings; Blake Hydram No. 2

H_s = 3.00 m, h_d = 25 m

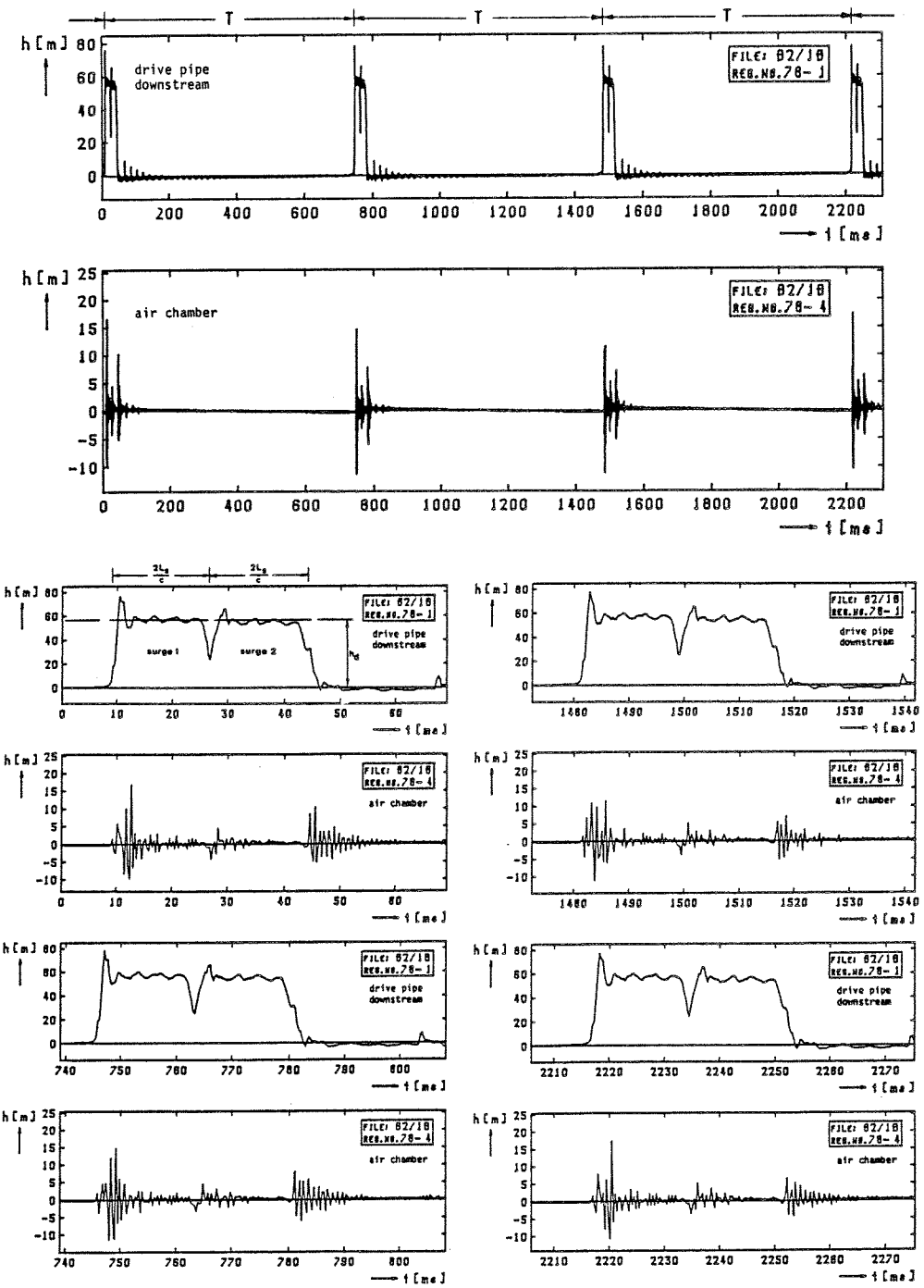

Fig IV-5 Pressure + time recordings; Blake Hydram No. 2

H_s = 3.00 m, h_d = 57 m (N = 2)

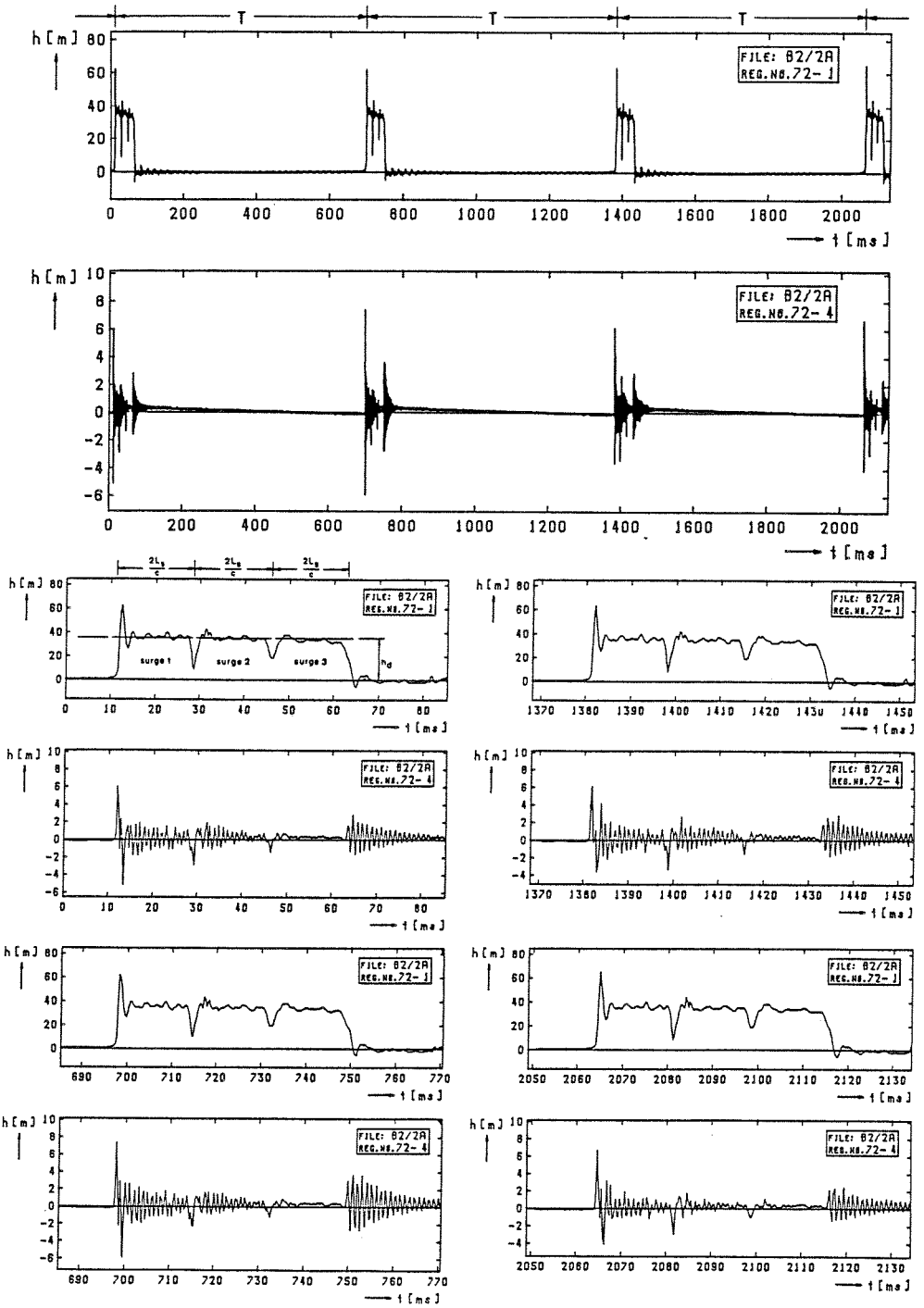

Fig IV-6 Pressure + time recordings; Blake Hydram No. 2

H_s = 3.00 m, h_d = 35 m (N = 3)

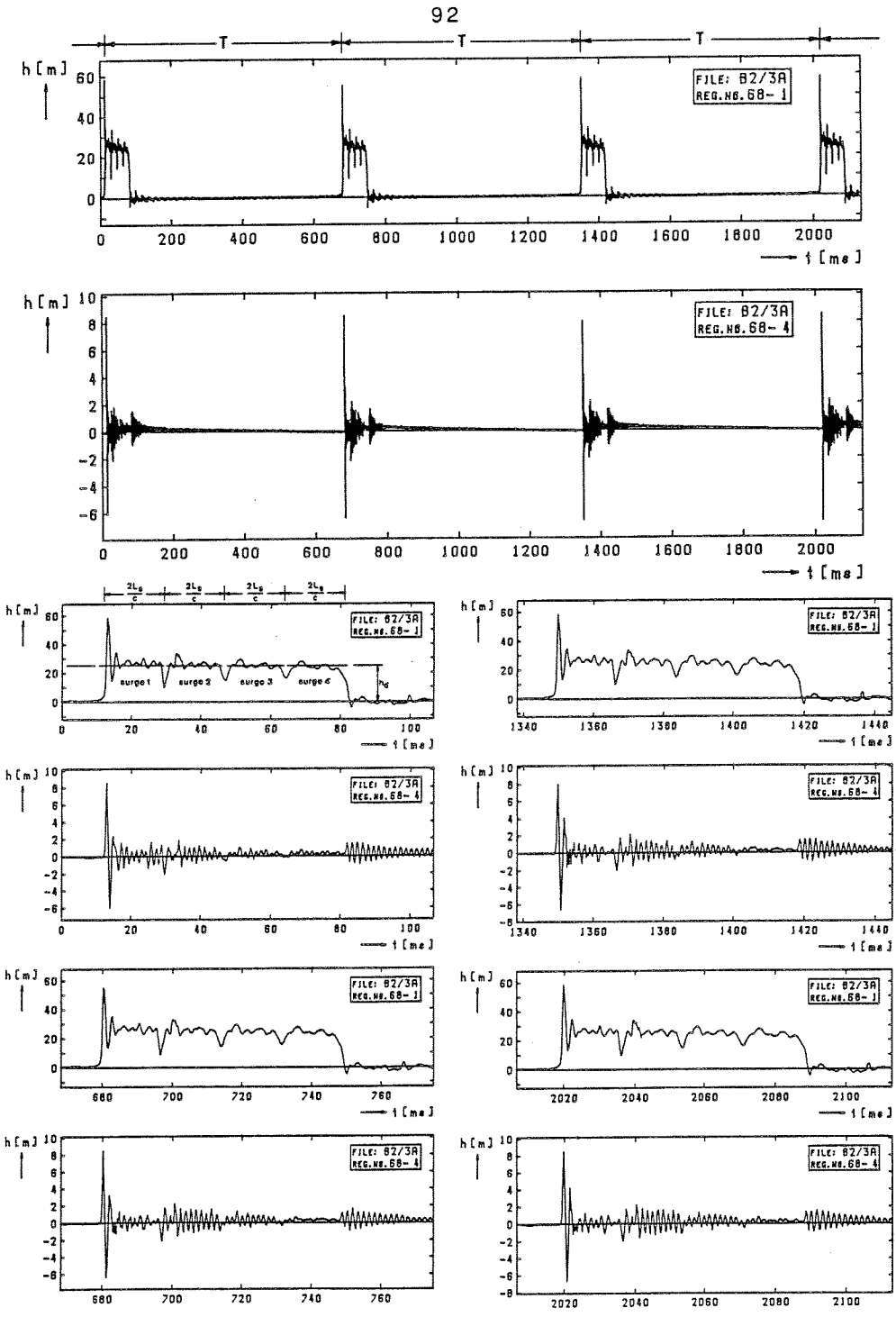

Fig IV-7 Pressure + time recordings; Blake Hydram No. 2

H_s = 3.00 m, h_d = 25 m (N = 4)

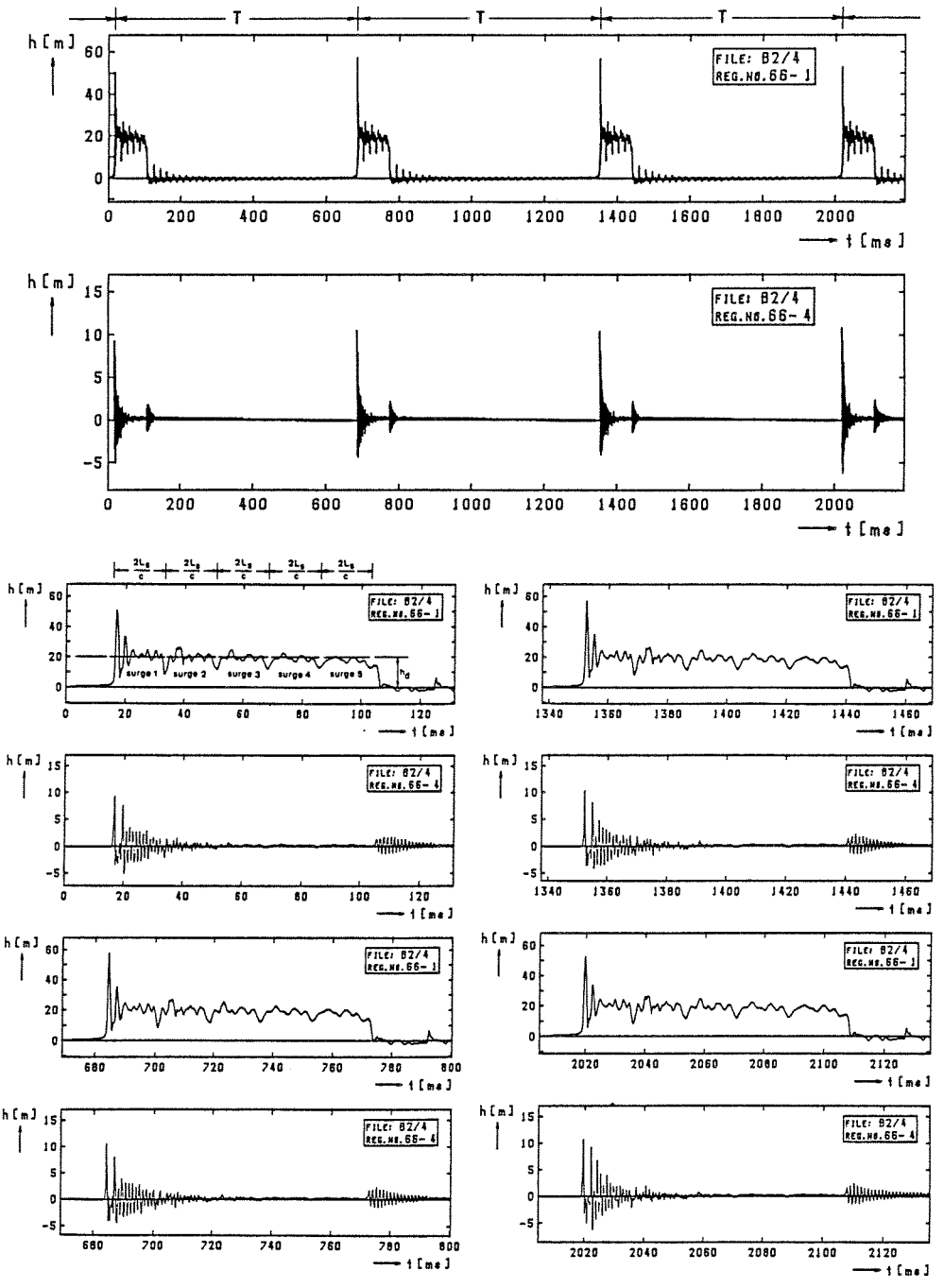

Fig IV-8 Pressure + time recordings; Blake Hydram No. 2

H_s = 3.00 m, h_d = 20 m (N = 5)

IV-3 Test results

As already mentioned in the previous section, for each hydraulic ram a series of tests was made with each of three different values of the supply head H_s. In each series the delivery head h_d was varied over the entire range of pressures under which the ram would continue to operate, all other factors such as waste valve adjustment kept constant. For each setting of the delivery head the waste flow Q, the pumping rate q and the period time T of the pumping cycle were measured. From the measurements compound variables such as head ratio h_d/H_s, flow ratio q/Q, Rankine efficiency η, amount of water pumped per cycle V_d and amount of water wasted per cycle V_{out} were established.

All test results are included in Appendix A, together with the information provided by the manufacturers. To avoid repetition only a summary of test results is given in this section (Table IV-3). In addition $q \div h_d$ and $\eta \div h_d$ curves, as compiled from the measurements obtained for the rams when operating at a supply head H_s = 3.00 m, are presented in Figs. IV-9 through to IV-20. Finally, Fig. IV-21 illustrates dimensionless performance characteristics (q/Q versus h_d/H_s) for all rams as obtained from the tests taken at H_s = 2.00 m and 3.00 m. To enable mutual comparison all curves in Fig. IV-21 are drawn to the same scale.

Hydraulic Ram	Supply Head H_s [m]	Waste Flow Q *) [l/min]	Period Time T *) [s]	Delivery Head h_d [m]		Pumping Rate q [l/min]	
				from	to	from	to
Blake Hydram No.2 (1 1/2")	1.35	40	1.600	12	112	2.00	0
	2.00	39	1.000	11	130	4.75	0
	3.00	38	0.700	11	140	7.70	0
Blake Hydram No.3 1/2 (2 1/2")	1.35	110	1.600	8	112	9.75	0
	2.00	100	1.000	8	120	17.15	0
	3.00	95	0.700	12	133	20.30	0
Alto J 26-80-8 (1")	1.00	14	1.300	6	19	1.10	0
	2.00	14	0.700	9	33	1.75	0
	3.00	15	0.550	12	42	2.20	0
Alto CH 50-110-18 (2")	1.00	33	1.000	6	40	1.25	0
	2.00	36	0.600	7	60	3.05	0
	3.00	39	0.450	10	66	4.45	0
Vulcan 1" (1")	1.00	15	1.550	4	75	1.00	0
	2.00	17	0.950	8	117	1.90	0
	3.00	16	0.650	13	134	2.25	0
Vulcan 2" (2")	1.00	35	1.150	6	68	4.25	0
	2.00	33	0.600	12	80	5.05	0
	3.00	34	0.450	18	88	5.40	0
SANO No.1-25mm (1")	1.00	10	1.100	4	67	1.05	0
	2.00	10	0.550	9	81	1.50	0
	3.00	10	0.400	11	93	2.05	0
SANO No.4-50mm (2")	1.00	60	1.900	4	102	4.70	0
	2.00	55	0.900	8	120	8.40	0
	3.00	60	0.650	12	138	10.25	0
Davey No.3 (1")	1.00	13	1.900	2	28	2.67	0
	2.00	13	1.000	4	44	3.77	0
	3.00	12	0.750	6	54	4.80	0
Rife 20HDU (2")	1.25	85	2.500	4	112	3.90	0
	2.00	80	1.300	4	133	8.90	0
	3.00	80	0.900	6	154	12.90	0
Schlumpf 4A5 (1 1/2")	1.00	25	1.500	4	32	3.85	0
	2.00	32	1.400	6	29	9.30	0
	3.00	30	1.000	9	27	10.30	0
Schlumpf 4A23 (1 1/2")	1.00	25	1.900	4	40	3.70	0
	2.00	45	1.600	8	78	7.65	0
	3.00	36	1.100	9	73	11.70	0

*) approx. average value for the whole range of operation

Table IV-3 Summary of test results

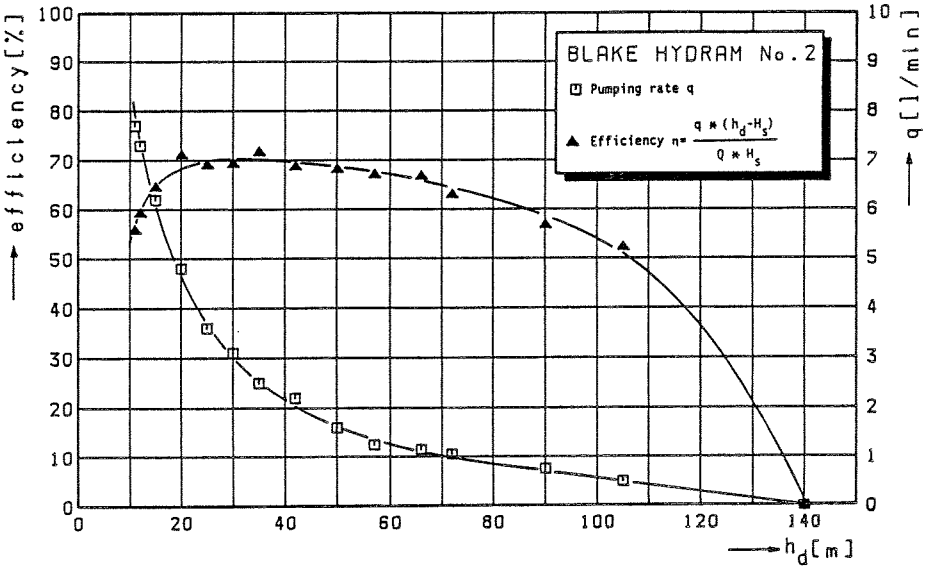

Fig. IV-9 Performance characteristics Blake Hydram No. 2; H_s = 3.00 m, Q ≈ 38 l/min

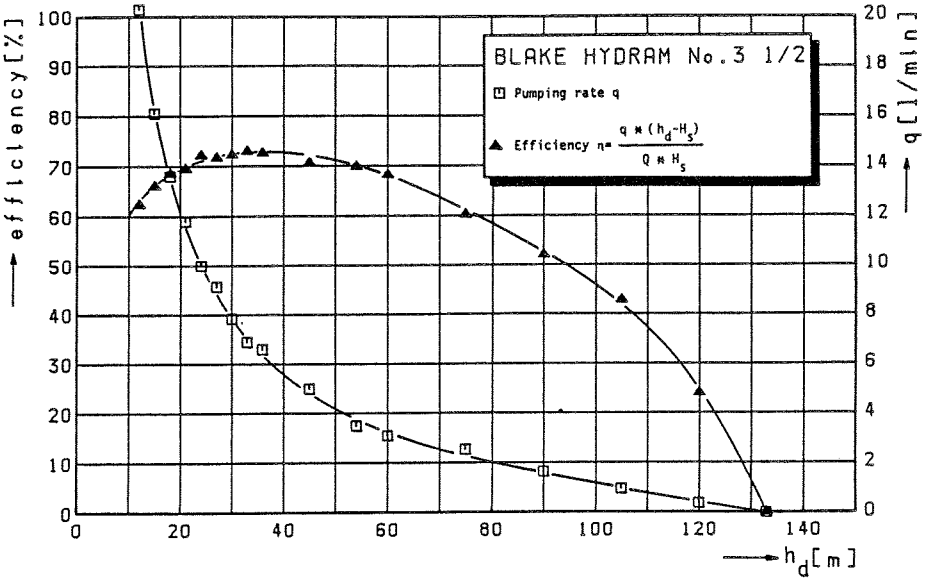

Fig. IV-10 Performance characteristics Blake Hydram No. 3 1/2; H_s = 3.00 m , Q ≈ 95 l/min

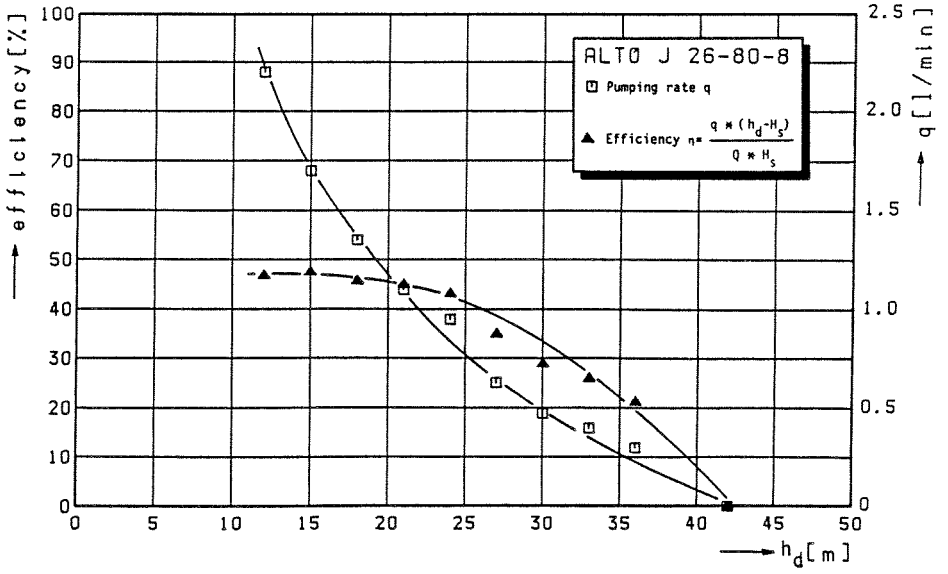

Fig. IV-11 Performance characteristics Alto J 26-80-8; H_s = 3.00 m, Q ~ 15 l/min

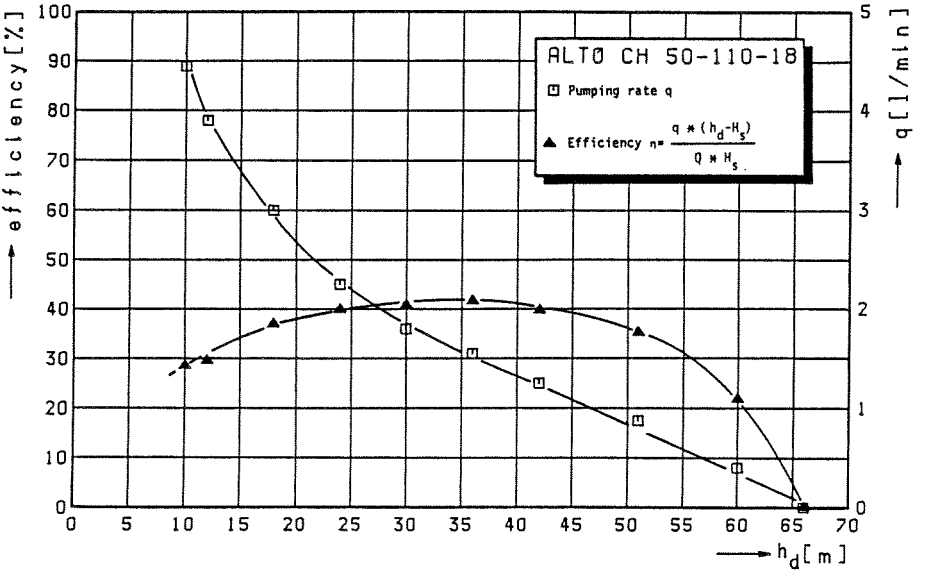

Fig. IV-12 Performance characteristics Alto CH 50-110-18; H_s = 3.00 m, Q ~ 39 l/min

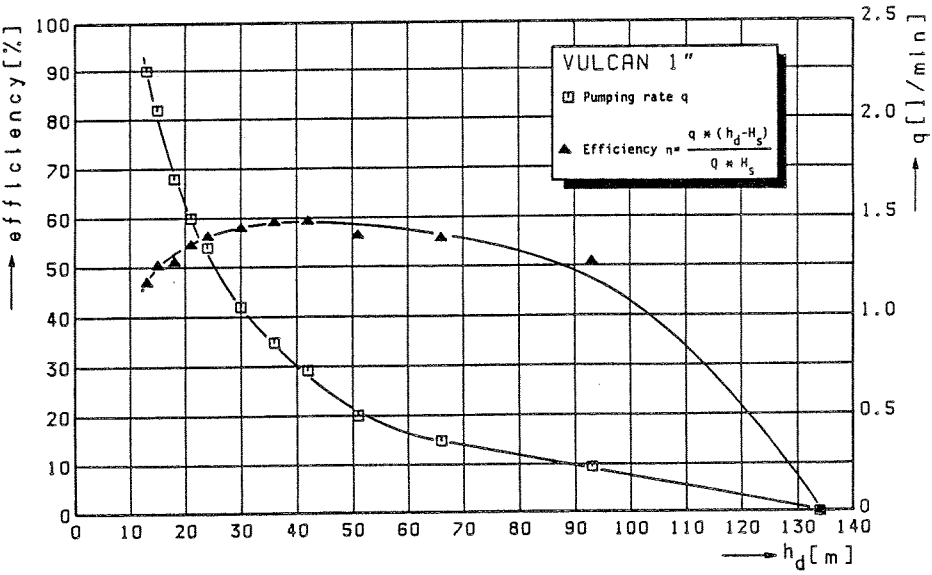

Fig. IV-13 Performance characteristics Vulcan 1"; H_s = 3.00 m, Q ≈ 16 l/min

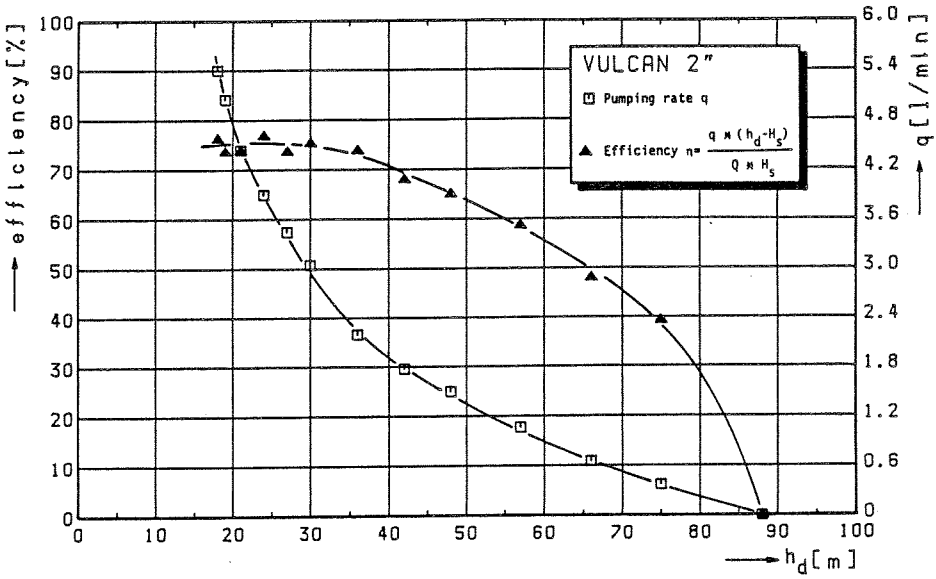

Fig. IV-14 Performance characteristics Vulcan 2"; H_s = 3.00 m, Q ≈ 34 l/min

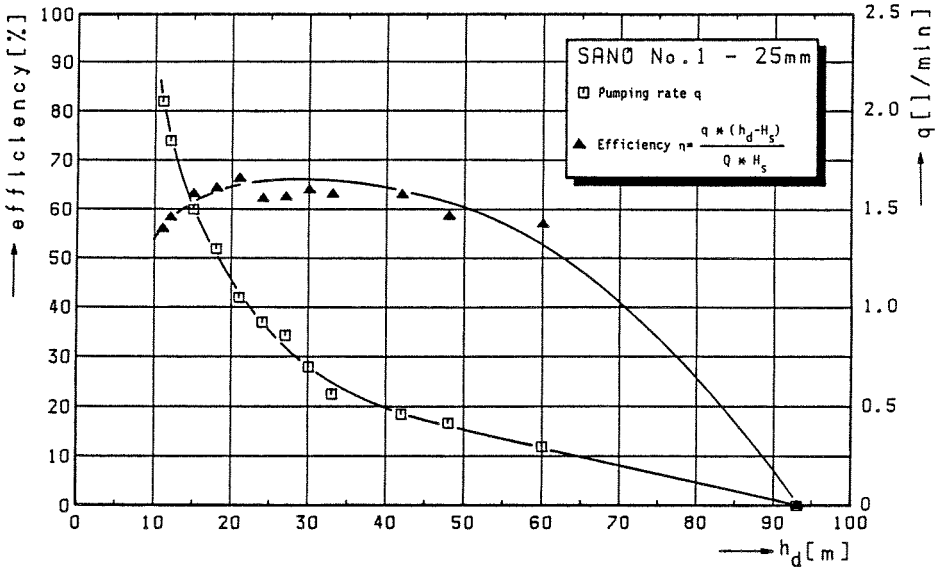

Fig. IV-15 Performance characteristics SANO No. 1 - 25 mm; H_s = 3.00 m, Q ≈ 10 l/min

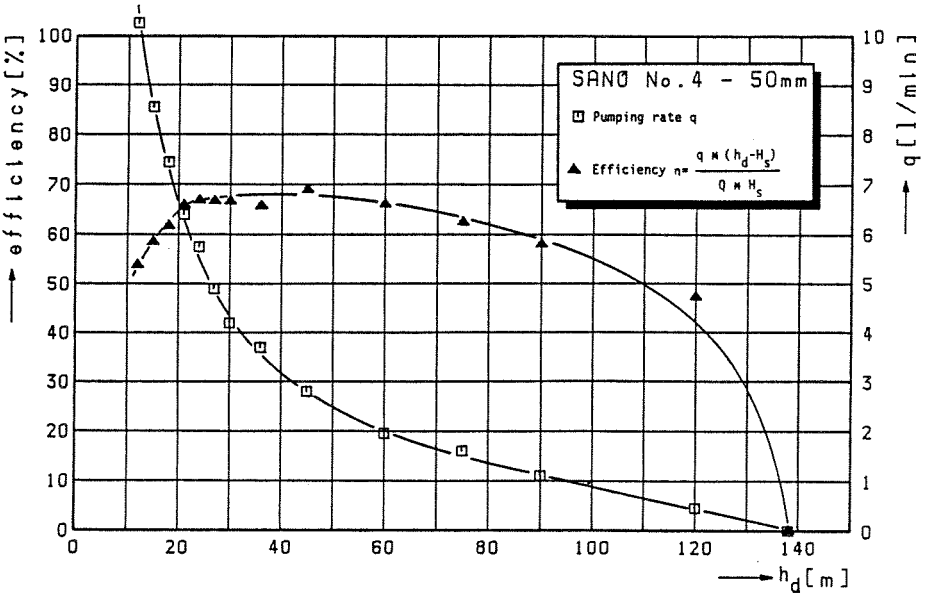

Fig. IV-16 Performance characteristics SANO No. 4 - 50 mm; H_s = 3.00 m, Q ≈ 60 l/min

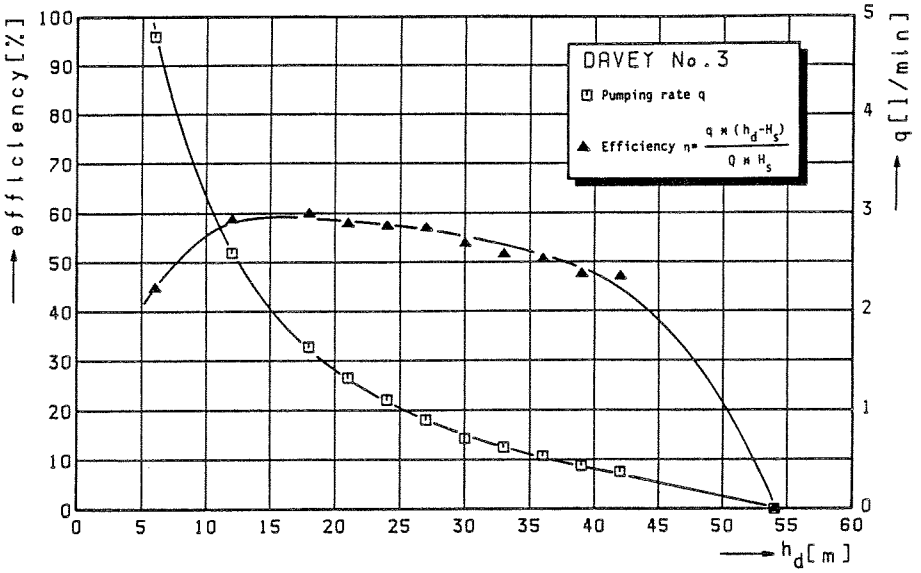

Fig. IV-17 Performance characteristics Davey No. 3; H_s = 3.00 m, Q ≈ 12 l/min

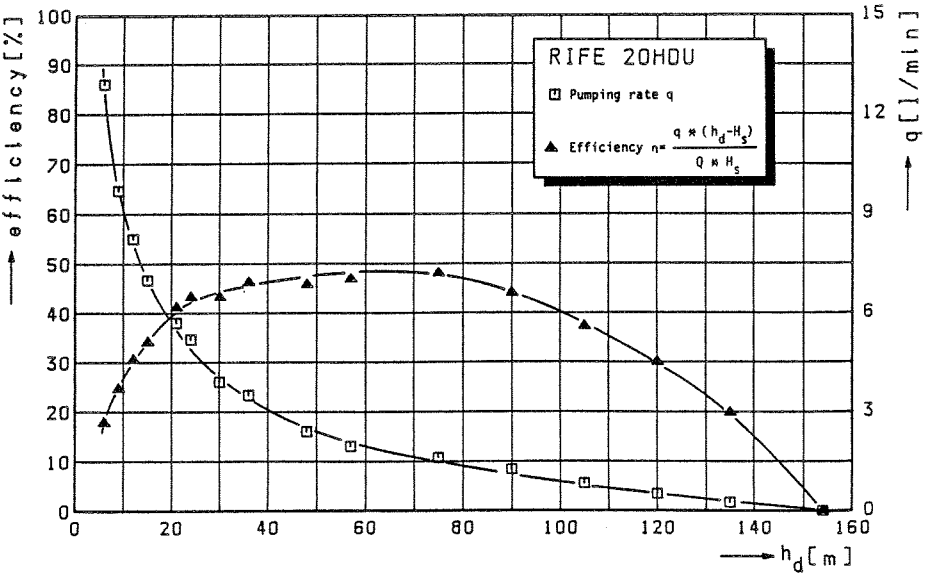

Fig. IV-18 Performance characteristics Rife 20 HDU; H_s = 3.00 m, Q ≈ 80 l/min

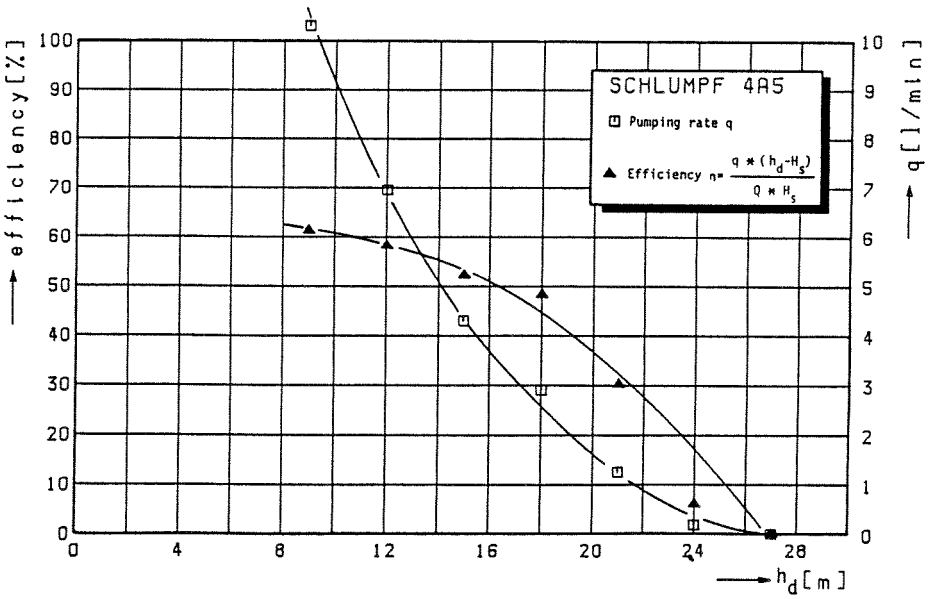

Fig. IV-19 Performance characteristics Schlumpf 4A5; H_s = 3.00 m, Q ≈ 30 l/min

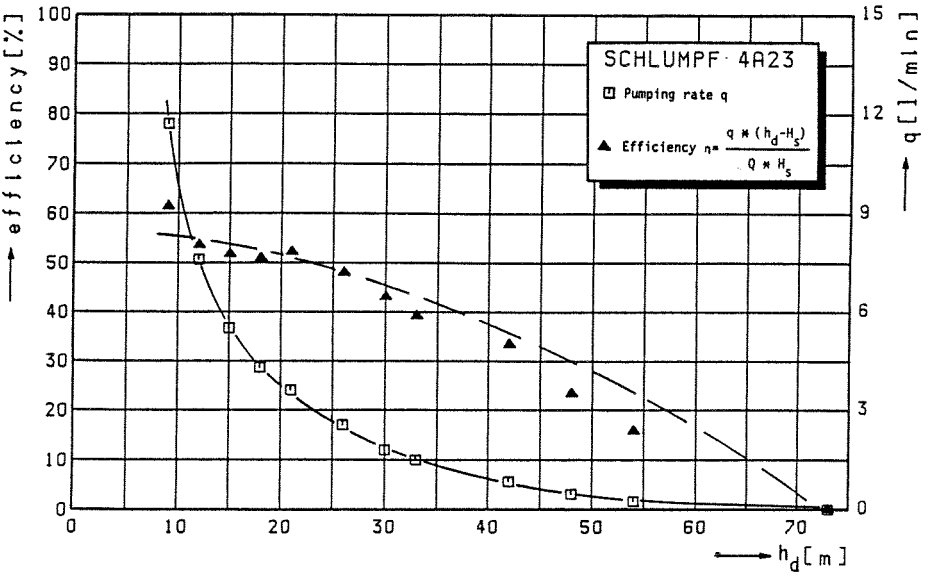

Fig. IV-20 Performance characteristics Schlumpf 4A23; H_s = 3.00 m, Q ≈ 36 l/min

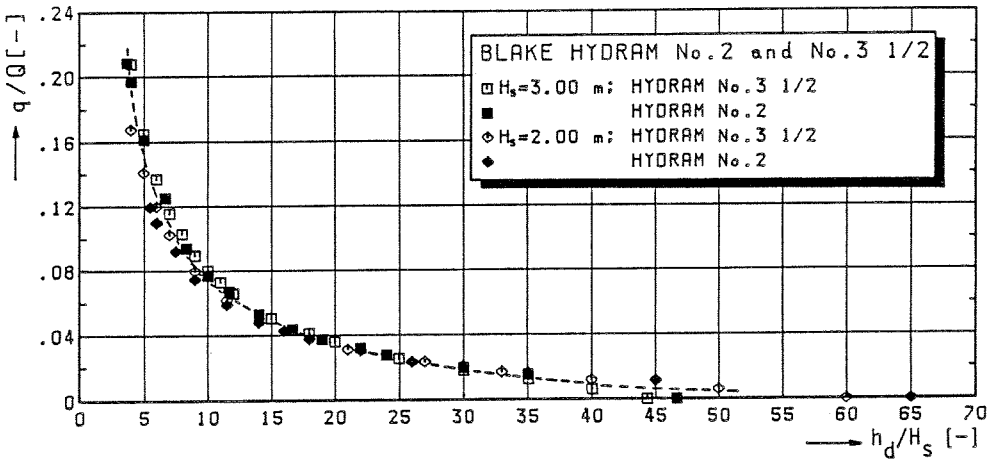

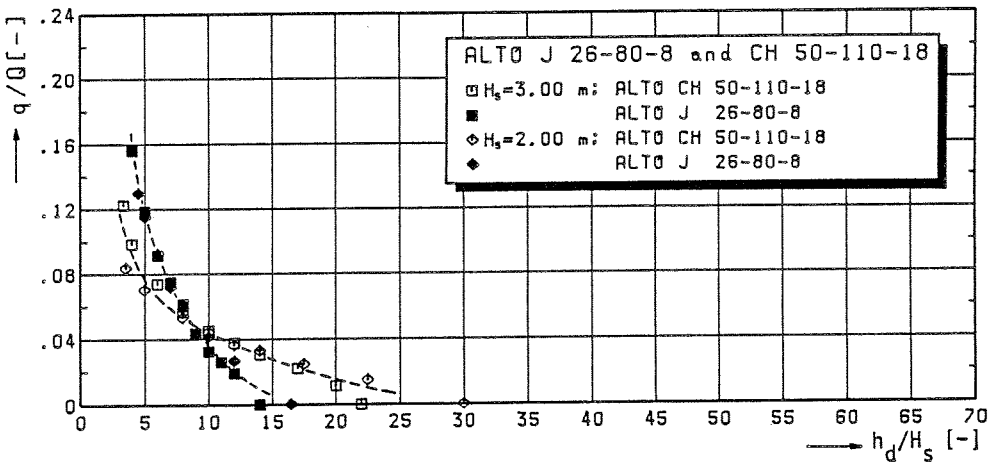

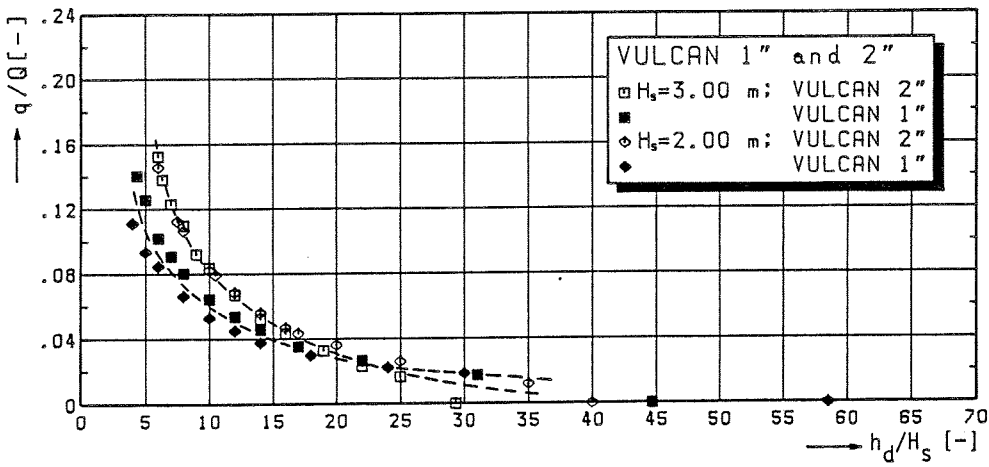

Fig. IV-21 Dimensionless performance characteristics

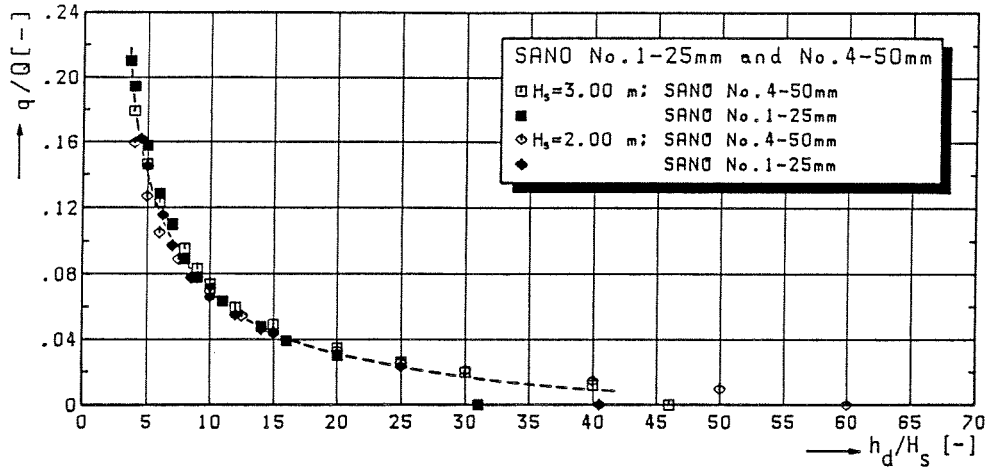

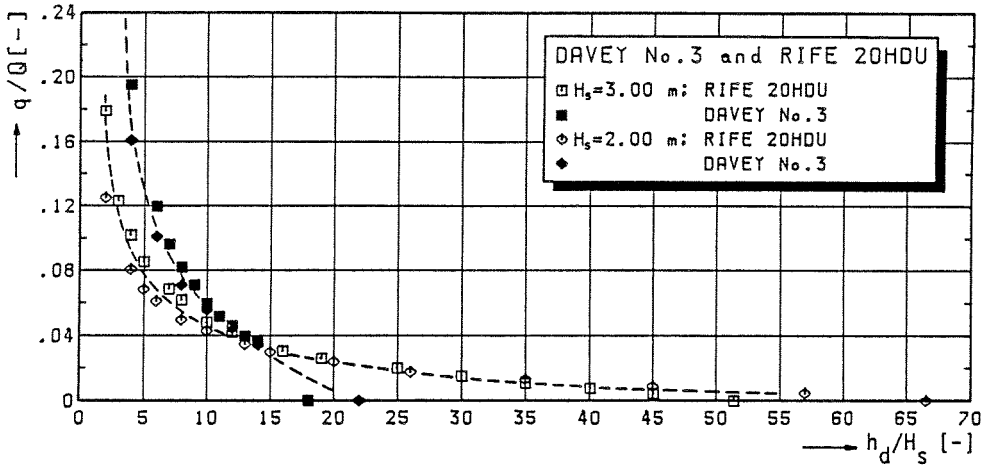

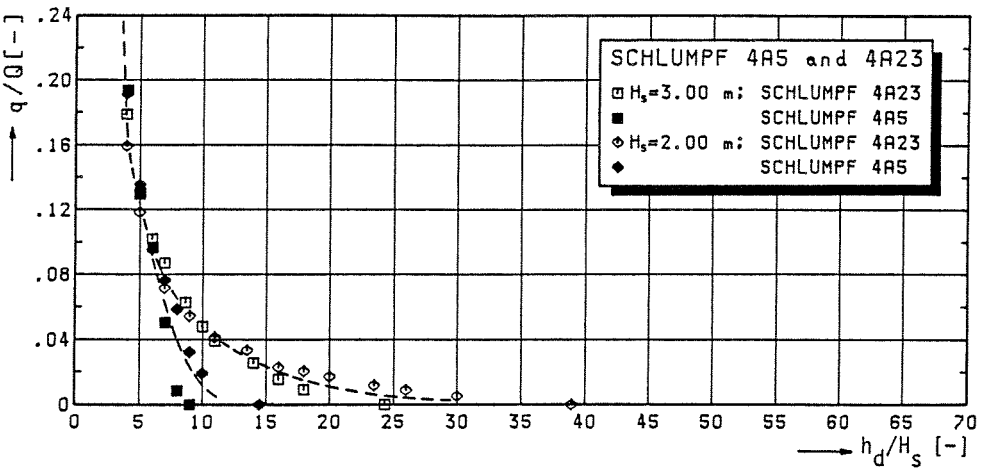

Fig. IV-21 Dimensionless performance characteristics (continuation)

V SUMMARY AND CONCLUSIONS

In this report it is sought to simplify the complex picture of hydraulic ram operation in order to clarify the possibilities and limitations of the ram relative to its site and its adjustments. For that purpose a mathematical model describing the essential features of hydraulic ram operation is developed.
Beforehand it is concluded from observation that the hydraulic ram owes its pumping capacity to two facts. For one thing the action of both valves, the sudden closure of the waste valve in particular; for another the high value of the wavespeed (c) at which pressure waves propagate through liquids in pipelines. The latter implies that both the hydraulic ram and the drive pipe must be made of material having a large value of Young's modulus of elasticity (E), and that the water in the drive pipe should be absolutely free of air (bubbles) to ensure a high value for the bulk modulus (K) of the water. In general: the higher the wavespeed (c) the more water can be pumped to higher levels.

Starting from assumptions based on experimental evidence, the mathematical model described in this report distinguishes three different periods in the pumping cycle of the hydraulic ram: acceleration - retardation - recoil. For each period the relation u(t) for the water in the drive pipe is derived. From these relationships rational, mathematical expressions are obtained for the amount of water wasted per cycle (V_{out}), the quantity of water pumped per cycle (V_d), the total period time (T) of the pumping cycle, the pumping rate (q) and the waste flow (Q).
The following conclusions relating to the performance characteristics of the hydraulic ram can be drawn from the mathematical model:

- given an available source supply the pumping rate (q) is primarily determined by the supply head (H_s) and the delivery head (h_d).
- an increase of the delivery head (h_d) decreases the quantity pumped per cycle (V_d) and by that the pumping rate (q) decreases.
- an increase of the supply head (H_s) increases the pumping frequency and by that the pumping rate (q) increases.
- an increase of u_c (i.e. the velocity of the water in the drive pipe at waste valve closure) normally increases the pumping rate (q) while the pumping frequency decreases, but more water (Q) is needed to operate the ram. However, there is a limitation as to this point: an increase in u_c such that the value of the ratio u_c/u_o approaches unity (where u_o is the maximum attainable velocity of the water in the drive pipe) implies a decrease in

pumping rate (q) while, as before, the waste flow (Q) increases, a condition to be avoided.

- the larger the size (i.e. drive pipe bore) of the ram, the more water (Q) is required to operate the ram and the more water (q) can be delivered to a higher level (h_d).

The foregoing conclusions are found to be in conformity with experimental results obtained from tests carried out on commercially made hydraulic rams. In addition to the conclusions, the effects of combined alterations may be qualitatively apparant from the model as well.

For calculation purposes the mathematical model is modified to some extent, in order to improve the description of the phenomenon governing the motion of the water during the period of retardation. Though limited in number, the agreement between calculated values and experimental results may be called reasonably good. Furthermore, the model compares well with the pressure + time recordings obtained from the experiments.

One of the purposes of the present investigation was to carry out tests on commercially-available hydraulic rams in order to determine their specific performance characteristics. In total twelve hydraulic rams were tested. As to the results no conclusions are drawn here. The reader is referred to the relevant parts in Appendix A, which includes all test results together with the information provided by the manufacturers.

LIST OF SYMBOLS

c : wavespeed
D : drive pipe bore (internal diameter)
d : delivery pipe bore (internal diameter)
E : Young's modulus of elasticity of the drive pipe material
ΔE_{pot} : change in potential energy
e : thickness of the drive pipe wall
f : Darcy-Weisbach friction factor
g : acceleration due to gravity
H_s : supply head
$H_{s,\,min}$: minimum supply head required to accomplish impulse valve closure
ΔH_{fr} : friction head loss
ΔH_{in} : head loss at intake end of drive pipe
ΔH_{out} : head loss at discharge end of drive pipe
ΔH_{vlv} : head loss at impulse valve
h : pressure head
Δh : (sudden) change in pressure head
h_d : delivery head
h_{max} : greatest possible rise in pressure head
K : bulk modulus of elasticity of the water
L_d : length of delivery pipe
L_s : length of drive pipe (measured from supply tank to impulse valve)
N : number of pressure waves observed during the period of retardation
p : pressure
Q : time rate of wasting
Q_{source} : minimum available source supply
q : time rate of pumping
s : length of impulse valve stroke
T : period time = duration of a complete cycle of operation
T_a : duration of the period of acceleration
T_d : duration of the period of retardation
T_r : duration of the period of recoil
t : time
Δt_c : time taken for impulse valve closure
u : velocity of the water in the drive pipe
Δu : (sudden) change in velocity
u_c : velocity in the drive pipe at impulse valve closure
u_i : velocity at downstream end of the drive pipe, observed during the propagation of the i^{th} pressure wave

u_o : asymptotic value of u = maximum attainable velocity of the water in the drive pipe (fully developed, steady flow)

u_r : velocity at downstream end of the drive pipe at the beginning of the period of recoil (reverse flow)

u_l : velocity in the drive pipe at the instant the impulse valve begins to close

V_a : amount of water flowing through the ram during the period of acceleration

V_d : quantity of water delivered per cycle

V_{out} : quantity of water wasted per cycle

V_r : amount of water flowing through the ram during the period of recoil

v : average velocity in the delivery pipe

v_{valve} : velocity of the impulse valve

x : distance along the drive pipe

α : coefficient

β : angle of declination of the drive pipe

η : efficiency - η_{rnk} : Rankine efficiency
η_{aub} : D'Aubuisson efficiency
η_{trd} : Trade expression

Θ : argument of hyperbolic tangent

ξ : sum of head loss coefficients

ξ_d : sum of minor loss factors - delivery pipe

ξ_{fr} : head loss coefficient due to friction

ξ_{in} : head loss coefficient at intake end of drive pipe

ξ_{out} : head loss coefficient at discharge end of drive pipe

ξ_{vlv} : head loss coefficient at impulse valve

π : 3.141592654

ρ : mass density of the water

φ_l : coefficient introducing pipe constraint condition

BIBLIOGRAPHY

[1] Allievi, L.
'The Theory of Waterhammer', American Society of Mechanical Engineers, New York, 1929.

[2] d'Aubuisson, J.F.
'Traité d'Hydraulique à l'Usage des Ingénieurs', Paris, 1840.

[3] Bergeron, L.
'Waterhammer in Hydraulics and Wave Surges in Electricity', John Wiley & Sons, Inc., New York, 1961.

[4a] Calvert, N.G.
'The Hydraulic Ram', The Engineer, p. 597-600, London, 1957.

[4b] Calvert, N.G.
'Drive Pipe of a Hydraulic Ram', The Engineer, p. 1001, London, 1958.

[5] Chaudhry, M.H.
'Applied Hydraulic Transients', Van Nostrand Reinhold Co., New York, 1979.

[6] Eytelwein, J.A.
'Bemerkungen über die Wirkung und vorteilhafte Anwendung des Stoßhebers', Berlin, 1805.

[7] Fox, J.A.
'Hydraulic Analysis of Unsteady Flow in Pipe Networks', Macmillan Press Ltd, London, 1977.

[8] Inversin, A.R.
'Hydraulic Ram for Tropical Climates', VITA-publication, Volunteers in Technical Assistance, Arlington, Virginia (USA), 1980.

[9] Joukowski, N.
'Waterhammer', Proceedings of the American Waterworks Association, Vol. 24, p. 341-424, 1904.

[10] Kindel, E.W.
'A Hydraulic Ram for Village Use', VITA-publication, Volunteers in Technical Assistance, Arlington, Virginia (USA), 1975.

[11] Krol, J.
'The Automatic Hydraulic Ram', Proceedings of the Institution of Mechanical Engineers, Vol. 165, p. 53-65, London, 1951.

[12] Lansford, W.M., Dugan, W.D.
'An Analytical and Experimental Study of the Hydraulic Ram', University of Illinois Engineering Experiment Station, Bulletin Series No. 326, Urbana, Illinois, 1941.

[13] Lister, M.
'The Numerical Solutions of Hyperbolic Partial Differential Equations by the Method of Characteristics', in 'Numerical Methods for Digital Computers', A. Ralston and H.S. Wilf (eds.), John Wiley & Sons, Inc., New York, 1960.

[14] Montgolfier, J.M. de
'Note sur le Bélier Hydraulique (et sur la manière d'en calculer les effets)', Journal des Mines, No. 73, Vol. 13, p. 42-51, Paris, 1802.

[15] Montgolfier, J.M. de
'De l'Utilité du Bélier Hydraulique', Bulletin de la Société d'Encouragement, No. XIX, Vol. IV, p. 170 ff., Paris, 1805.

[16] Parmakian, J.
'Waterhammer Analysis', Dover Publications, Inc., 2nd edition, New York, 1963.

[17] Pickford, J.
'Analysis of Surge', Macmillan and Co. Ltd, London, 1969.

[18] Provoost, G.A.
'The Dynamic Behaviour of Non-return Valves', Delft Hydraulics Laboratory, Publication no. 229, 1980.

[19] Rankine, W.J.
'On the Mathematical Theory of the Hydraulic Ram', The Engineer, Vol. 33, p. 55, 84 and 163, London, 1872.

[20] Renaud, H.
'Le Bélier Hydraulique', Dunod, Paris, 1950.

[21] Schiller, E.J. (ed.)
'Proceedings of a Workshop on Hydraulic Ram Pump (Hydram) Technology - held at Arusha, Tanzania, 1984', International Development Research Centre - Manuscript Report (IDRC-MR 102e), Ottawa, Canada, 1985.

[22] Schwarz, W.
'Druckstoßberechnung unter Berücksichtigung der Radial- und Längsverschiebungen der Rohrwandung', Universität Stuttgart, Institut für Wasserbau, Mitteilungen Heft 43, Stuttgart, 1978.

[23] Silver, M.
'Use of Hydraulic Rams in Nepal - a guide to manufacturing and installation', UNICEF, Kathmandu, Nepal, 1977.

[24] Stevens-Guille, P.D.
'An Innovation in Water Ram Pumps for Domestic and Irrigation Use', Appropriate Technology, Vol. 5, No. 1, London, 1970.

[25] Stevens-Guille, P.D.
'How to Make and Install a Low-cost Water Ram Pump for Domestic and Irrigation Use', Department of Mechanical Engineering, University of Cape Town, 1977.

[26] Watt, S.B.
'A Manual on the Hydraulic Ram for Pumping Water', Intermediate Technology Development Group, Intermediate Technology Publication Ltd, London, 1975 (Revised and reprinted 1978).

[27] Whitehurst, J.
'Account of a Machine for Raising Water', Philosophical Transactions XIII, p. 645-646, London, 1775.

[28] Wylie, E.B., Streeter, V.L.
'Fluid Transients', McGraw-Hill Book Co., New York, 1978.

Appendix A

Appendix A: TEST RESULTS

One of the purposes of the present hydraulic ram investigation was to carry out tests on a selected number of commercially made hydraulic rams in order to determine their specific performance characteristics and to compare these results with the information - if any - provided by the manufacturers. In total 12 hydraulic rams (six different manufactures) were tested.

As described in chapter IV, for each hydraulic ram a series of tests was made with each of three different values of the supply head H.[1] In each series the delivery head h was varied over the entire range of operation of the ram, other factors such as waste valve adjustment kept constant. For each setting of the delivery head the waste flow Q and pumping rate q were measured by weight and time method; the period time T of the pumping cycle was determined with use of an electronic counter and stopwatch. From the measurements compound variables such as head ratio h/H, flow ratio q/Q, Rankine efficiency η, volume of water delivered per cycle V_{up} and volume of water wasted per cycle V_{out} were established. The results thus obtained are presented in tabular form in the next sections, where each section is dealing with one type of hydraulic ram.[2] In addition to the tables best-fitted curves of the most significant performance characteristics were plotted as compiled from the measurements. To enable visual comparison the relevant figures have been completed with the manufacturer's data.[3]

Prior to presenting the results it must be stated that the lowest supply heads applied in the tests (H = 1.00-1.35 m) occasionally turned out to be somewhat on the low side for the imposed test configuration (drive pipe length, waste valve setting, etc.) resulting in a somewhat 'sluggish' action of some of the rams when operated under these conditions. This also appears from the curves depicting flow ratio q/Q versus head ratio h/H included in the sections hereafter (see also chapter III for the effect of supply head and waste valve adjustment on hydraulic ram performance).

Notes:

1) In this appendix the notation differs from the one used so far in that the supply head is denoted by H (instead of H_s) and the delivery head by h (instead of h_d).

2) Except for section A.5, which deals with two different types (brands) of hydraulic ram made by the same manufacturer.

3) General remarks on hydraulic ram performance characteristics as well as on performance figures and tables published by manufacturers are also included in chapter II (section II-2).

A.1 BLAKE HYDRAM

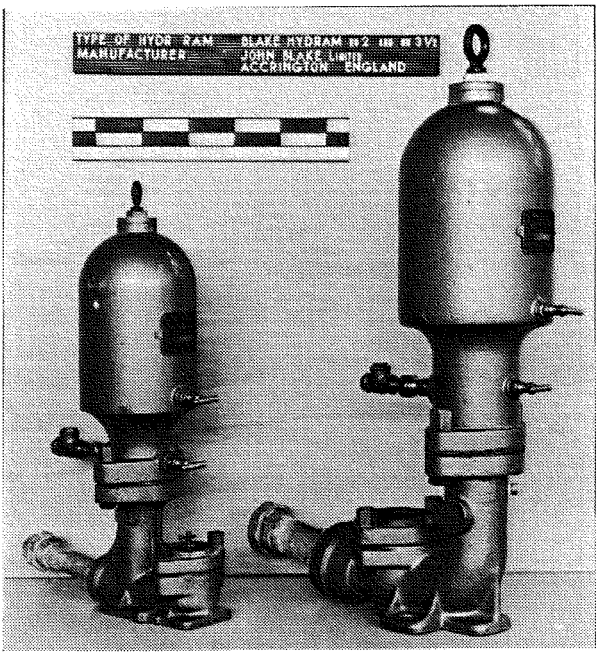

Rams tested (see picture): Blake Hydram No.2 (1 1/2")
Blake Hydram No.3 1/2 (2 1/2")

Manufacturer: John Blake Ltd,
Accrington - England.

Description

The Blake Hydram is a well-established, conventional design of hydraulic ram which has altered little over the years. The ram is made of cast-iron with brass and gunmetal components. Hydram sizes range from size 1 (1 1/4"-32 mm) through to size 10 (8"-200 mm), covering a wide range of source supplies (see Table A.1-1). In the larger sizes, that is from size 5 through to size 10, the Hydram is made in several configurations of waste and delivery valves. The standard waste valve consists of a conical, perforated gunmetal seat fitted with a rubber clack (Fig. A.1-1). The valve setting can be tuned to the available source supply by adjusting the valve stroke, i.e. bringing the clack nearer to or farther

Size of Hydram			1	2	3	3½	4	5	6	7	8	10
Volume of driving water available	Litres per minute	From	7	12	27	45	68	136	180	750	1136	1545
		To	16	25	55	96	137	270	410	364	545	770
	Gallons per minute	From	1.5	2.5	6	10	15	30	40	165	250	340
		To	3.5	5.5	12	21	30	60	90	80	120	170
Maximum height to which Hydram will pump water	Metres		150	150	120	120	120	105	105	105	105	105
	Feet		500	500	400	400	400	350	350	350	350	350
Nominal diameter of Drive Pipe	m.m. bore		32	40	50	65	80	100	125	150	175	200
	ins. bore		1¼	1½	2	2½	3	4	5	6	7	8

Table A.1-1 Hydram input capacity; source: John Blake Ltd.

(a)

Working Fall (Metres)	Vertical height to which water is raised above the Hydram (Metres)											
	5	7.5	10	15	20	30	40	50	60	80	100	125
1.0	144	77	65	33	29	19.5	12.5					
1.5		135	96.5	70	54	36	19	15				
2.0		220	156	105	79	53	33	25	19.5	12.5		
2.5		280	200	125	100	66	40.5	32.5	24	15.5	12	
3.0			260	180	130	87	65	51	40	27	17.5	12
3.5				215	150	100	75	60	46	31.5	20	14
4.0				255	173	115	86	69	53	36	23	16
5.0				310	236	155	118	94	71.5	50	36	23
6.0					282	185	140	112	93.5	64.5	47.5	34.5
7.0						216	163	130	109	82	60	48
8.0							187	149	125	94	69	55
9.0							212	168	140	105	84	62
10.0	LITRES PUMPED IN 24 HOURS						245	187	156	117	93	69
12.0	PER LITRE/MIN OF DRIVE WATER						295	225	187	140	113	83
14.0								265	218	167	132	97
16.0									250	187	150	110
18.0									280	210	169	124
20.0										237	188	140

(b)

Working Fall (Feet)	Vertical height to which water is raised above the Hydram (Feet)											
	20	25	30	40	50	75	100	150	200	250	300	400
3½	113	90	72	52	39	24	17					
4	144	110	80	63	42	30	21	13				
4½	162	130	106	75	57	35	25	15	11			
5	200	162	130	90	69	43	30	19	13			
5½	230	180	145	103	80	48	35	21	15	11		
6		200	165	116	90	55	39	24	17	13		
6½		225	185	130	100	62	44	27	19	15	11	
7		240	200	146	110	69	47	30	21	16	13	
7½			220	162	124	76	54	33	24	18	14	
10				230	185	118	82	51	36	28	22	16
15						188	141	92	66	51	41	28
20							196	130	98	78	63	44
25	GALLONS PUMPED IN 24 HOURS						250	168	126	100	80	58
30	PER GALL/MIN OF DRIVE WATER							200	150	118	98	71
40								270	200	160	134	100
50									250	200	168	126
75											252	188
100												250

Table A.1-2 Hydram output capacity: (a) metric units,
(b) imperial units;
source: John Blake Ltd.

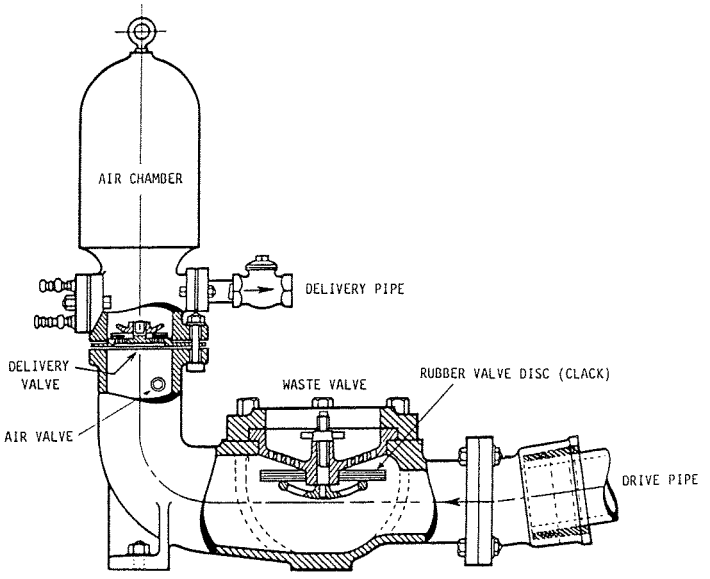

Fig. A.1-1 Cross-sectional diagram of the Hydram; source: John Blake Ltd.

away from the seat. The standard delivery valve consists of a rubber clack covering a flat perforated gunmetal seat. All Hydrams are equipped with an air valve (a small brass plug with a pinhole drilled through it), two brass drain cocks on the air chamber and a back pressure valve to connect the delivery pipe to the ram. A stop-valve and strainer for the drive pipe and a set of spanners are available as optional extras. Tables A.1-1 and A.1-2 show the performance characteristics for the Hydram as provided by the manufacturer. In Table A.1-1 are listed the various sizes of Hydrams together with the volumes of water per minute that each can handle. Table A.1-2a gives the quantity, in litres, of water raised per 24 hours for each litre of driving water used per minute by the ram under the 'chosen' conditions of delivery head (vertical height above ram) and supply head (working fall). The use of the tables has been demonstrated in chapter II.

Test results

The Hydrams were tested at three different values of the supply head: H= 1.35 m, 2.00 m and 3.00 m respectively. The results are presented in the tables and figures hereafter;

Blake Hydram No.2 : Tables A.1-3,4,5 and Figs. A.1-2,3,4,5

Blake Hydram No.3 $^{1}/2$: Tables A.1-6,7,8 and Figs. A.1-6,7,8,9.

The performance data from the manufacturer as pictured in some of the figures are as derived from Table A.1-2a; for example:

supply head H= 2 m and delivery head h= 40 m then

$\frac{q}{Q} = \frac{33}{24*60} = 0.023$ and q = 0.9 l/min for Q = 39 l/min (Hydram No.2),

q = 2.3 l/min for Q =100 l/min (Hydram No.3 1/2).

As can be seen from the figures the test results compare favourably with the manufacturer's data. Furthermore, the curves depicting flow ratio q/Q versus head ratio h/H (Figs. A.1-4 and A.1-8) illustrate that for the higher supply heads the dimensionless ram performances tend to be similar. Some divergence is observed for the lowest supply head, owing to the rather sluggish operation of the rams experienced at this supply head.*) As can be noticed from the test results the amount of driving water used by the rams exceeded the upper limits claimed by the manufacturer (Table A.1-1). Although the waste flow Q may be reduced by shortening the stroke length of the waste valve, it should be remembered from chapter III that this will also limit the range of attainable delivery heads. To conclude, Fig. A.1-10 illustrates dimensionless performance characteristics for both rams together, as compiled from the tests taken at H= 2.00 m and 3.00 m.

Concluding remarks

Both Hydrams operated well under the laboratory conditions. Of all rams tested the Hydrams were found to be the only self-starting ones. A good set of instructions for the installation, regulation and maintenance of the Hydram as well as several additional information sheets are provided by the manufacturer.

*) As already mentioned in chapter IV, it should be noted that H= 1.35 m only differs a little from the minimum supply head required to operate the rams for the given configuration (drive pipe length, waste valve setting, etc.).

Table A.1-3 Testresults Hydram No.2; supply head H = 1.35 m

Type of Hydr.Ram: **BLAKE HYDRAM No.2** Supply Head H= 1.35 m

Manufacturer : JOHN BLAKE Ltd, ACCRINGTON, ENGLAND. Drive Pipe: D= 1 1/2" (40mm) L= 11.90 m

Test No.	Delivery Head h [m]	Head Ratio h/H [-]	Period Time T [s]	Pumping Rate q [l/min]	Supply Flow Rate Q [l/min]	Flow Ratio q/Q [-]	Efficiency $\eta=\frac{q*(h-H)}{Q*H}$ [%]	Filename	Volume of Water Delivered V_{up} [$*10^{-3}$ l/cycle]	Volume of Water Wasted V_{out} [$*10^{-3}$ l/cycle]
2	12	8.89	1.495	2.00	40.90	0.0489	38.6	-	49.8	1019
4	14	10.37	1.502	1.75	40.90	0.0428	40.1	-	43.8	1024
6	16	11.85	1.500	1.60	40.20	0.0398	43.2	-	40.0	1005
8	20	14.81	1.530	1.25	39.85	0.0314	43.3	B2/11,11A	31.9	1016
10	28	20.74	1.580	0.85	38.40	0.0221	43.7	B2/10,10A	22.4	1011
12	35	25.93	1.535	0.68	40.60	0.0167	41.7	-	17.4	1039
14	45	33.33	1.665	0.43	35.60	0.0121	39.1	B2/9	11.9	988
16	50	37.04	1.670	0.39	36.10	0.0108	38.9	-	10.9	1005
18	60	44.44	1.610	0.34	40.00	0.0085	36.9	-	9.1	1073
20	h_{max}=112	82.96	-	0	-	0	0	-	0	-

Type of Hydr.Ram: **BLAKE HYDRAM No. 2**

Supply Head H= 2.00 m

Manufacturer : JOHN BLAKE Ltd, ACCRINGTON, ENGLAND.

Drive Pipe: D= 1 1/2" (40mm) L= 11.90 m

Test No.	Delivery Head h [m]	Head Ratio h/H [-]	Period Time T [s]	Pumping Rate q [l/min]	Supply Flow Rate Q [l/min]	Flow Ratio q/Q [-]	Efficiency $\eta=\frac{q*(h-H)}{Q*H}$ [%]	Filename	Volume of Water Delivered V_{up} [$*10^{-3}$ l/cycle]	Volume of Water Wasted V_{out} [$*10^{-3}$ l/cycle]
30	11	5.5	0.971	4.75	39.70	0.1196	53.8	-	76.9	642
32	12	6	0.968	4.40	40.00	0.1100	55.0	-	71.0	645
34	15	7.5	0.967	3.70	40.10	0.0923	60.0	-	59.6	646
36	18	9	0.972	3.00	40.15	0.0747	59.8	B2/8	48.6	650
38	23	11.5	0.986	2.35	39.75	0.0591	62.1	B2/7,7A	38.6	653
40	28	14	0.960	2.00	41.80	0.0478	62.2	-	32.0	669
42	32	16	0.994	1.65	38.40	0.0430	64.4	B2/6,6A	27.3	636
44	36	18	0.960	1.50	40.10	0.0374	63.6	-	24.0	642
46	44	22	0.972	1.20	39.80	0.0302	63.3	-	19.4	645
48	52	26	1.060	0.81	34.70	0.0233	58.4	B2/5,5A	14.3	613
50	60	30	1.048	0.74	35.75	0.0207	60.0	-	12.9	624
52	70	35	0.992	0.66	39.90	0.0165	56.2	-	10.9	660
54	90	45	1.040	0.43	37.50	0.0115	50.4	-	7.5	650
56	h_{max}=130	65	-	0	-	0	0	-	0	-

Table A.1-4 Testresults Hydram No.2; supply head H = 2.00 m

Type of Hydr.Ram: **BLAKE HYDRAM No. 2** — Supply Head H= 3.00 m

Manufacturer : JOHN BLAKE Ltd, ACCRINGTON, ENGLAND. — Drive Pipe: D= 1 1/2" (40mm), L= 11.90 m

Test No.	Delivery Head h [m]	Head Ratio h/H [-]	Period Time T [s]	Pumping Rate q [l/min]	Supply Flow Rate Q [l/min]	Flow Ratio q/Q [-]	Efficiency $\eta=\frac{q*(h-H)}{Q*H}$ [%]	Filename	Volume of Water Delivered V_{up} [$*10^{-3}$ l/cycle]	Volume of Water Wasted V_{out} [$*10^{-3}$ l/cycle]
60	11	3.67	0.686	7.70	36.90	0.2087	55.6	-	88.0	422
62	12	4	0.686	7.30	37.00	0.1973	59.2	-	83.5	423
64	15	5	0.663	6.20	38.45	0.1612	64.5	-	68.5	425
66	20	6.67	0.667	4.80	38.30	0.1253	71.0	B2/4	53.4	426
68	25	8.33	0.669	3.60	38.30	0.0940	68.9	B2/3,3A	40.1	427
70	30	10	0.645	3.10	40.30	0.0769	69.2	-	33.3	433
72	35	11.67	0.683	2.50	37.25	0.0671	71.6	B2/2,2A	28.5	424
74	42	14	0.640	2.20	41.65	0.0528	68.7	-	23.5	444
76	50	16.67	0.696	1.60	36.80	0.0435	68.1	-	18.6	427
78	57	19	0.737	1.25	33.60	0.0372	67.0	B2/1,1A,1B	15.4	413
80	66	22	0.714	1.15	36.20	0.0318	66.7	-	13.7	431
82	72	24	0.695	1.05	38.40	0.0273	62.9	-	12.2	445
84	90	30	0.697	0.76	38.90	0.0195	56.6	-	8.8	452
86	105	35	0.758	0.50	32.60	0.0153	52.1	-	6.3	412
88	h_{max}=140	46.67	-	0	-	0	0	-	0	-

Table A.1-5 Testresults Hydram No.2; supply head H = 3.00 m

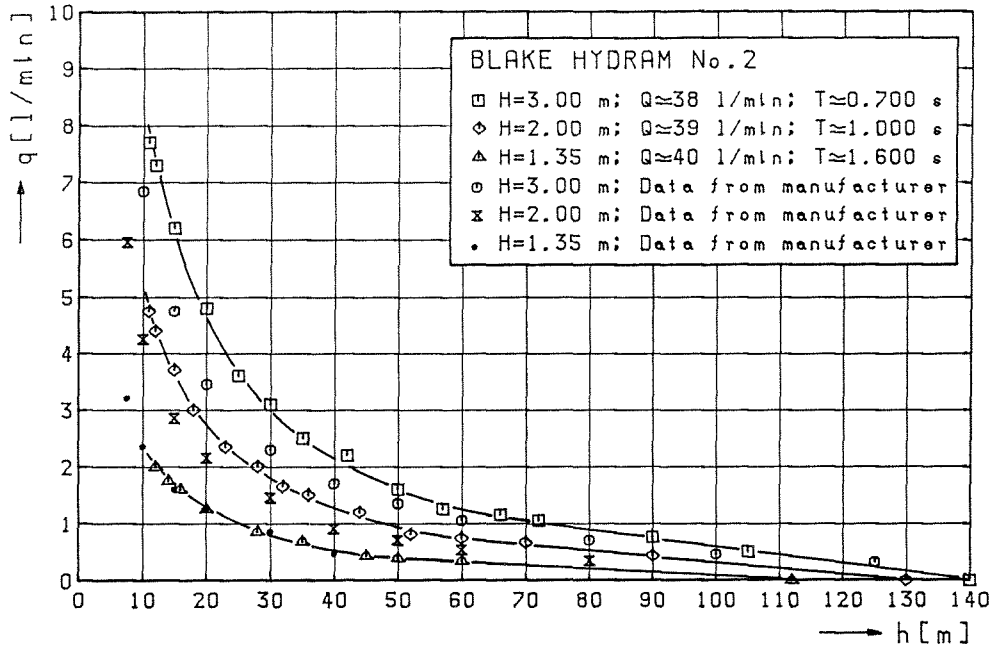

Fig. A.1-2 Pumping rate q versus delivery head h; Hydram No.2

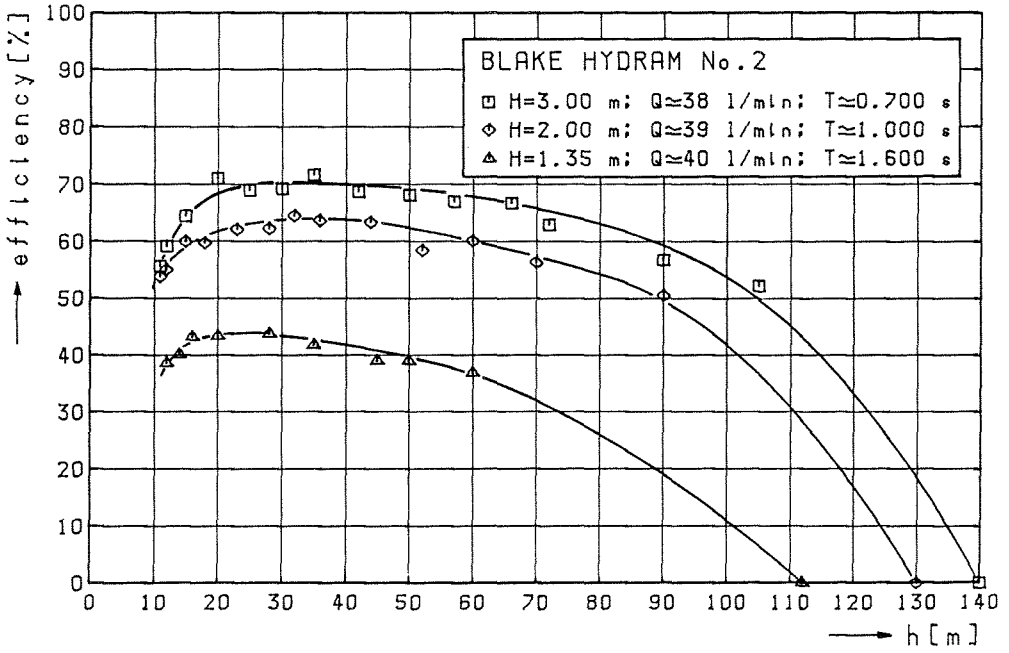

Fig. A.1-3 Rankine efficiency η versus delivery head h; Hydram No.2

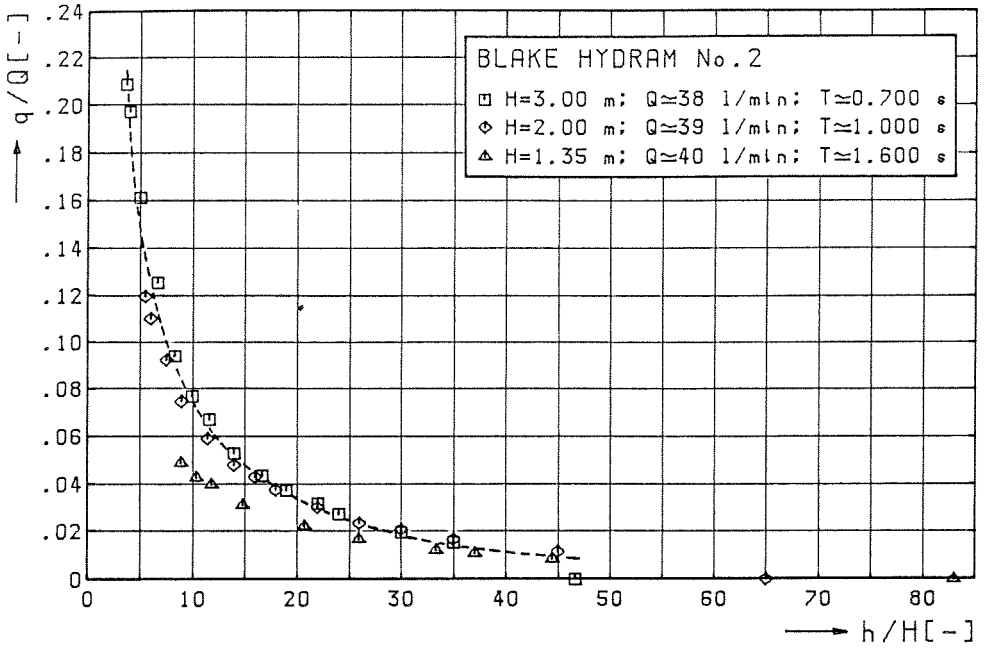

Fig. A.1-4 Flow ratio $^{q}/_{Q}$ versus head ratio $^{h}/_{H}$; Hydram No.2

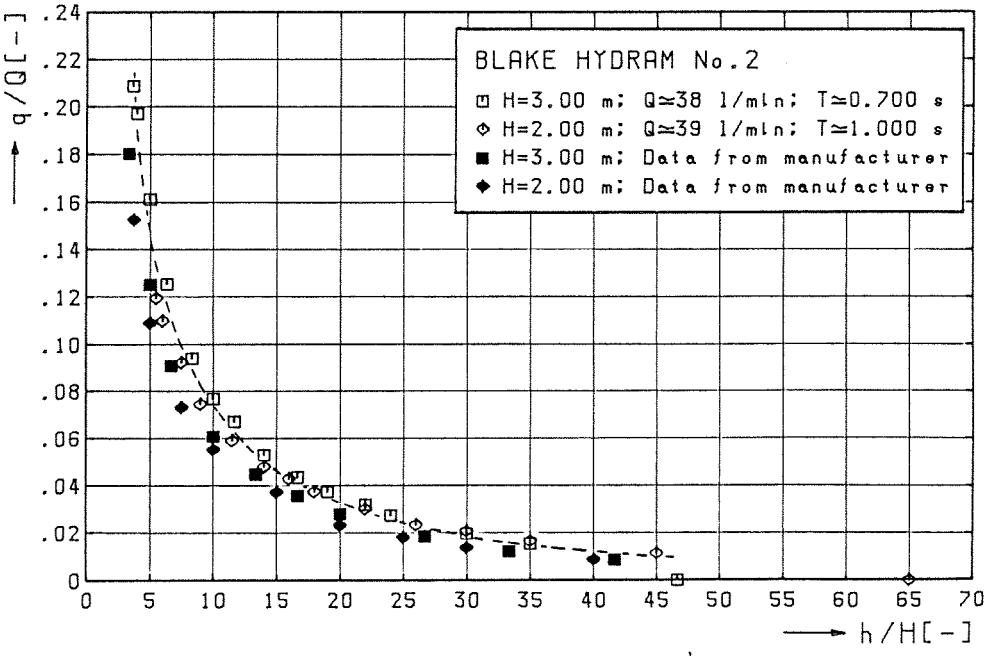

Fig. A.1-5 Flow ratio $^{q}/_{Q}$ versus head ratio $^{h}/_{H}$; Hydram No.2

Type of Hydr.Ram: **BLAKE HYDRAM No.3 1/2** Supply Head H= 1.35 m

Manufacturer : JOHN BLAKE Ltd, ACCRINGTON, ENGLAND. Drive Pipe: D= 2 1/2" (65mm) L= 12.20 m

Test No.	Delivery Head h [m]	Head Ratio h/H [-]	Period Time T [s]	Pumping Rate q [l/min]	Supply Flow Rate Q [l/min]	Flow Ratio q/Q [-]	Efficiency $\eta = \frac{q*(h-H)}{Q*H}$ [%]	Filename	Volume of Water Delivered V_{up} [$*10^{-3}$ l/cycle]	Volume of Water Wasted V_{out} [$*10^{-3}$ l/cycle]
100	8	5.93	1.500	9.75	114.80	0.0849	41.8	-	243.8	2870
102	10	7.41	1.513	8.00	111.90	0.0715	45.8	-	201.7	2822
104	14	10.37	1.500	5.85	114.00	0.0513	48.1	-	146.3	2850
106	18	13.33	1.506	4.50	113.60	0.0396	48.9	-	113.0	2851
108	21.5	15.93	1.539	3.80	111.00	0.0342	51.1	B3/10 B3/10A	97.5	2847
110	25	18.52	1.525	3.20	112.10	0.0285	50.0	-	81.3	2849
112	31	22.96	1.600	2.50	106.50	0.0235	51.6	B3/9 B3/9A	66.7	2840
114	35	25.93	1.550	2.25	110.00	0.0205	51.0	-	58.1	2842
116	42	31.11	1.590	1.75	105.50	0.0166	50.0	-	46.4	2796
118	50	37.04	1.705	1.20	95.60	0.0126	45.2	B3/8 B3/8A	34.1	2717
120	55	40.74	1.725	1.10	94.30	0.0117	46.4	-	31.6	2711
122	65	48.15	1.704	0.90	96.60	0.0093	43.9	-	25.6	2743
124	75	55.56	1.700	0.65	96.50	0.0067	36.7	-	18.4	2734
126	h_{max}=112	82.96	-	0	-	0	0	-	0	-

Table A.1-6 Testresults Hydram No.3 1/2; supply head H = 1.35 m

Table A.1-7 Testresults Hydram No.3 1/2; supply head H = 2.00 m

Type of Hydr.Ram: **BLAKE HYDRAM No.3 1/2**

Supply Head H= 2.00 m

Manufacturer : JOHN BLAKE Ltd, ACCRINGTON, ENGLAND.

Drive Pipe: D= 2 1/2" (65mm) L= 12.20 m

Test No.	Delivery Head h [m]	Head Ratio h/H [-]	Period Time T [s]	Pumping Rate q [l/min]	Supply Flow Rate Q [l/min]	Flow Ratio q/Q [-]	Efficiency $\eta=\frac{q*(h-H)}{Q*H}$ [%]	Filename	Volume of Water Delivered V_{up} [$*10^{-3}$ l/cycle]	Volume of Water Wasted V_{out} [$*10^{-3}$ l/cycle]
130	8	4	0.968	17.15	102.30	0.1676	50.3	-	276.7	1650
132	10	5	0.964	14.50	102.80	0.1411	56.4	-	233.0	1652
134	12	6	0.940	12.70	105.70	0.1202	60.1	-	199.0	1656
136	14	7	0.955	10.70	104.40	0.1025	61.5	-	170.3	1662
138	18	9	0.958	8.25	103.30	0.0799	63.9	-	131.7	1649
140	23	11.5	0.971	6.30	101.80	0.0619	65.0	B3/7 B3/7A	102.0	1647
142	32	16	1.004	4.15	97.20	0.0427	64.0	B3/6 B3/6A	69.4	1626
144	42	21	0.976	3.10	100.20	0.0309	61.9	-	50.4	1630
146	54	27	1.072	2.00	86.40	0.0231	60.2	B3/5 B3/5A	35.7	1544
148	66	33	1.043	1.55	91.60	0.0169	54.2	-	26.9	1592
150	80	40	1.004	1.15	96.40	0.0119	46.5	-	19.2	1613
152	100	50	1.114	0.48	79.60	0.0060	29.5	-	9.0	1478
154	h_{max}=120	60	-	0	-	0	0	-	0	-

Type of Hydr.Ram: **BLAKE HYDRAM No.3 1/2**

Supply Head H= 3.00 m

Manufacturer : JOHN BLAKE Ltd, ACCRINGTON, ENGLAND.

Drive Pipe: D= 2 1/2" (65mm) L= 12.20 m

Test No.	Delivery Head h [m]	Head Ratio h/H [-]	Period Time T [s]	Pumping Rate q [l/min]	Supply Flow Rate Q [l/min]	Flow Ratio q/Q [-]	Efficiency $\eta=\frac{q*(h-H)}{Q*H}$ [%]	Filename	Volume of Water Delivered V_{up} [$*10^{-3}$ l/cycle]	Volume of Water Wasted V_{out} [$*10^{-3}$ l/cycle]
160	12	4	0.671	20.30	97.60	0.2080	62.4	-	227.0	1091
162	15	5	0.664	16.10	97.50	0.1651	66.1	-	178.2	1079
164	18	6	0.657	13.60	99.20	0.1370	68.6	-	148.9	1086
166	21	7	0.646	11.80	101.90	0.1158	69.5	-	127.0	1097
168	24	8	0.667	10.00	97.00	0.1031	72.2	B3/3 B3/3A	111.2	1078
170	27	9	0.633	9.15	102.10	0.0896	71.7	-	96.5	1077
172	30	10	0.664	7.85	97.80	0.0803	72.2	-	86.9	1082
174	33	11	0.686	6.90	94.60	0.0729	72.9	B3/2 B3/2A	78.9	1082
176	36	12	0.652	6.60	100.00	0.0660	72.6	-	71.7	1087
178	45	15	0.672	5.00	99.10	0.0504	70.6	-	56.0	1110
180	54	18	0.735	3.50	85.10	0.0411	69.9	B3/1 B3/1A,1B	42.9	1042
182	60	20	0.727	3.10	86.30	0.0359	68.3	-	37.6	1046
184	75	25	0.644	2.55	101.50	0.0251	60.3	-	27.4	1089
186	90	30	0.697	1.65	91.70	0.0180	52.2	-	19.2	1065
188	105	35	0.761	0.96	76.10	0.0126	42.9	-	12.2	965
190	120	40	0.828	0.38	61.70	0.0062	24.0	-	5.2	851
192	h_{max}=133	44.3	0.880	0	50.30	0	0	B3/0	0	738

Table A.1-8 Testresults Hydram No.3 1/2; supply head H = 3.00 m

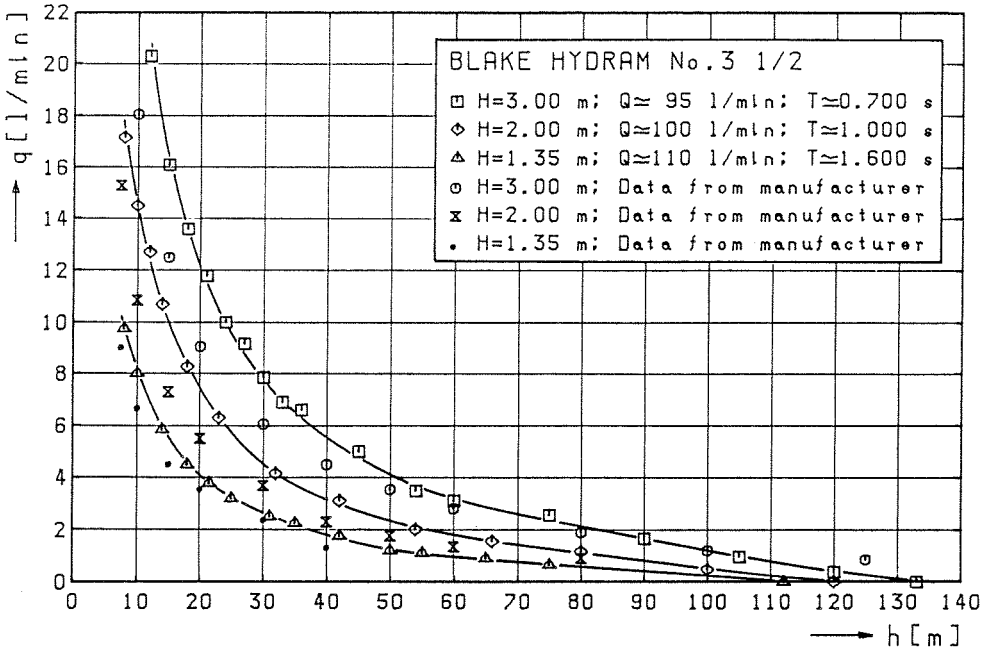

Fig. A.1-6 Pumping rate q versus delivery head h; Hydram No.3 1/2

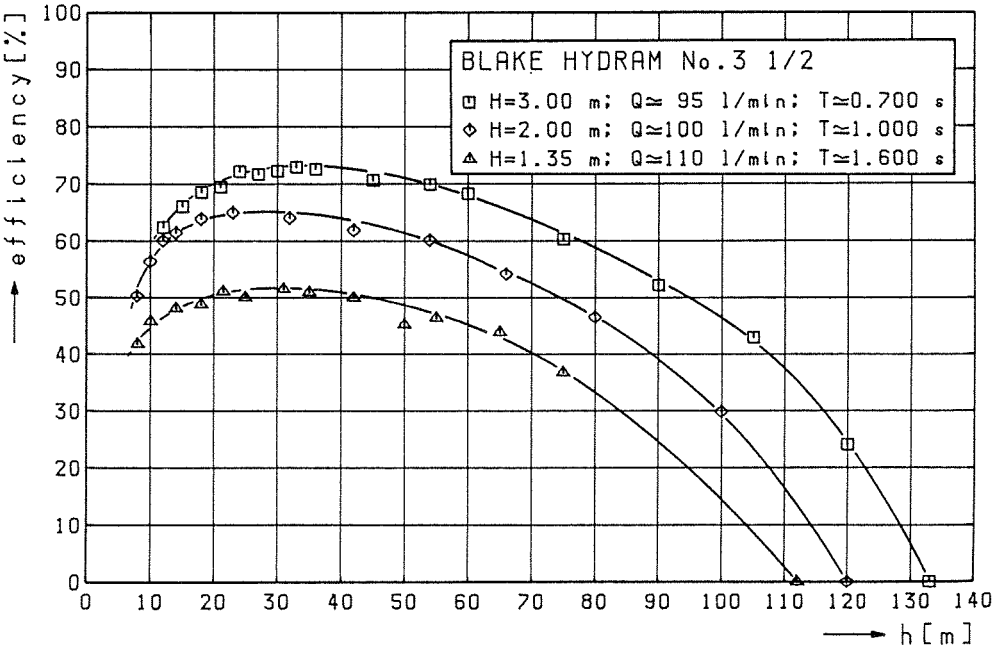

Fig. A.1-7 Rankine efficiency η versus delivery head h; Hydram No.3 1/2

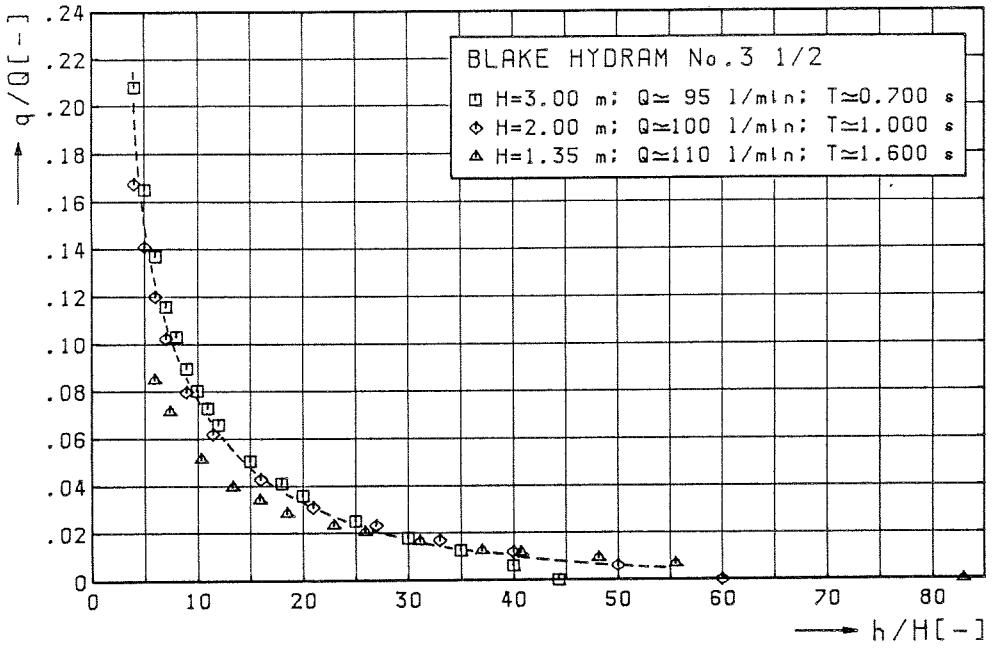

Fig. A.1-8 Flow ratio $^{q}/_{Q}$ versus head ratio $^{h}/_{H}$; Hydram No.3 1/2

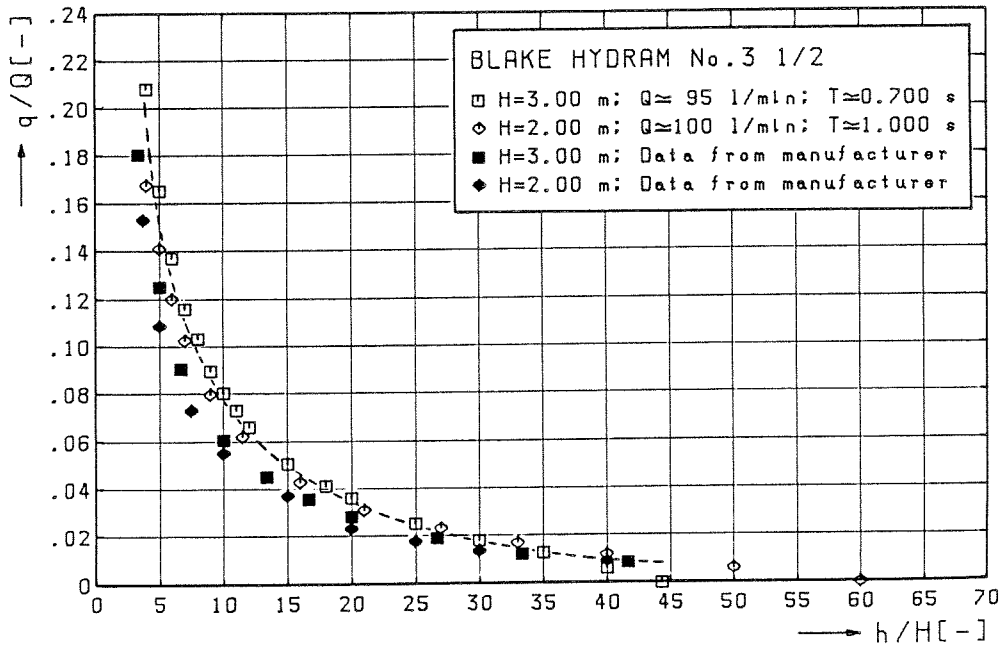

Fig. A.1-9 Flow ratio $^{q}/_{Q}$ versus head ratio $^{h}/_{H}$; Hydram No.3 1/2

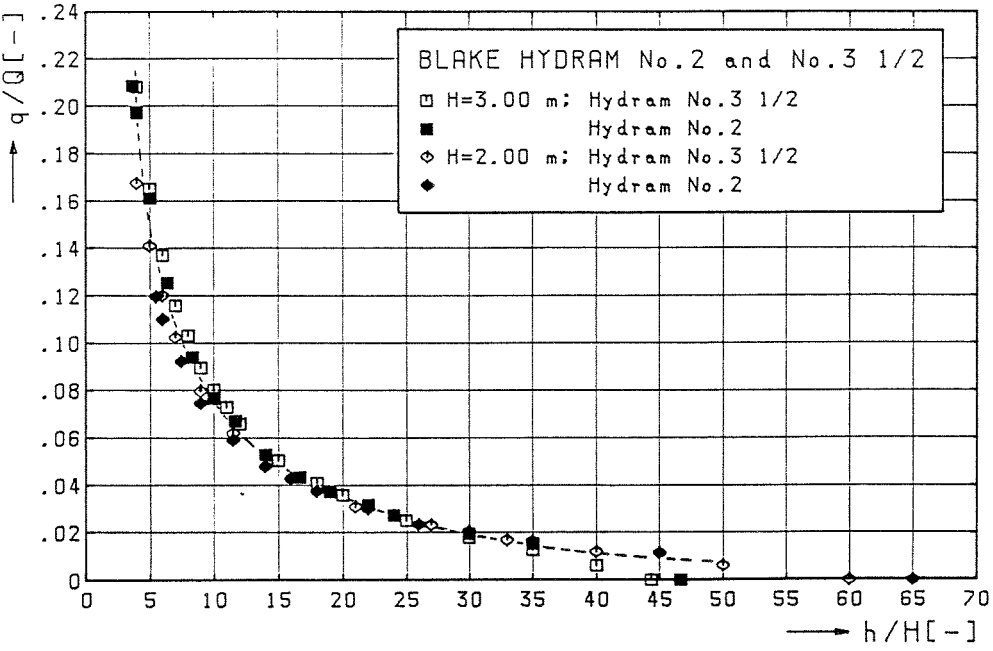

Fig. A.1-10 Dimensionless performance characteristics;
Hydram No.2 and No.3 1/2

A.2 BELIER 'ALTO'

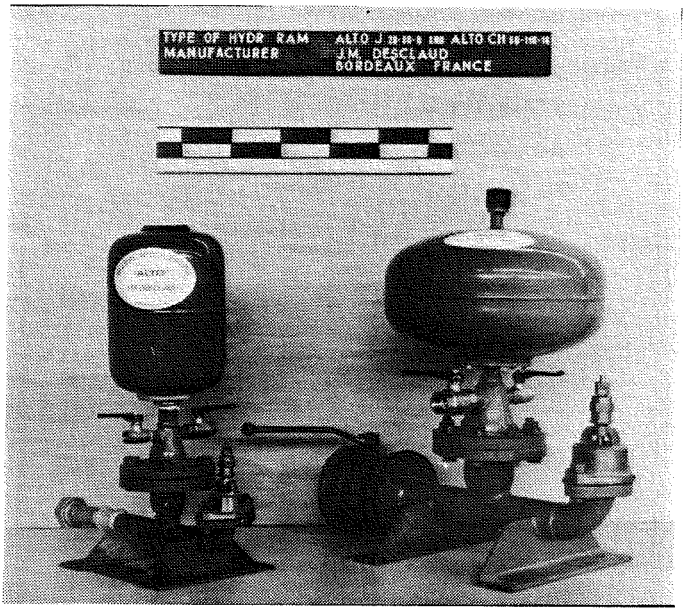

Rams tested (see picture): Alto J 26-80-8 (1")
Alto CH 50-110-18 (2")

Manufacturer: J.M. Desclaud,
Bordeaux - France.

Description

The Alto hydraulic ram is claimed to be a recently renewed and improved pump design. Formerly made of cast-iron the ram is nowadays constructed of steel pipe components. The design uses a gunmetal, weight-loaded waste valve with adjustable valve stroke. The delivery valve is a spring-loaded rubber clack mounted on a brass spindle and covering a grid-shaped brass seat. Instead of an air valve the air chamber of the ram is equipped with an inflatable rubber air compartement to ensure a permanent separation of water and air in the air chamber. The Alto ram is delivered complete with two stainless steel globe-valves on the air chamber, a globe-valve and a strainer for the drive pipe and a pressure gauge.

Performance characteristics for the Alto ram as published by the manufacturer are shown in Table A.2-1. As can be seen from the table two

CARACTERISTIQUES GENERALES DES BELIERS HYDRAULIQUES "ALTO" NOUVELLE SERIE

A RESERVOIR HYDROPNEUMATIQUE PRE-GONFLE A VESSIE INTERCHANGEABLE.

Béliers type J Elévation normale	Béliers type CH Haute élévation	Quantité d'eau absorbée à la source en litres/minute	ø intérieur Batterie	Orifice Refoulement	Rendement suivant rapport $\frac{HR}{HC}$ = 6 à 20
n° 20 - 80 - 8 (70 m.)	même type 70 m.	4 à 8 litres.	20 mm.	15/21	54 % à 12 %
n° 26 - 80 - 8 (70 m.)	même type 70 m.	8 à 15 litres.	26 mm.	15/21	56 % à 16 %
n° 33 - 50 - 16 (40 m.)	n° 33 - 110 - 18 (100 m.)	15 à 25 litres.	33 mm.	20/27	59 % à 20 %
n° 40 - 50 - 16 (40 m.)	n° 40 - 110 - 18 (100 m.)	20 à 40 litres.	40 mm.	20/27	60 % à 24 %
n° 50 - 40 - 19 (30 m.)	n° 50 - 110 - 18 (100 m.)	30 à 60 litres.	50 mm.	26/34	63 % à 30 %
n° 66 - 40 - 24 (30 m.)	n° 66 - 110 - 18 (100 m.)	50 à 90 litres.	66 mm.	26/34	67 % à 40 %
n° 80 - 40 - 24 (30 m.)	n° 80 - 110 - 18 (100 m.)	80 à 160 litres.	80 mm.	33/42	68 % à 45 %
n° 100 - 40 - 2x19 (30 m.)	n° 100 - 110 - 2x18 (100 m.)	150 à 300 litres.	100 mm.	40/49	70 % à 47 %
n° 125 - 40 - 2x24 (30 m.)	n° 125 - 110 - 2x25 (100 m.)	350 à 700 litres.	125 mm.	50/60	72 % à 48 %

Le rendement maximum se situe pour $\frac{HR}{HC}$ = 6 à 8

Pour $\frac{HR}{HC} < 4$, le fonctionnement est impossible; il faut créer une perte de charge au refoulement.

Pour $\frac{HR}{HC} > 20$, le rendement devient très faible pour les petits modèles.

Toutes les indications de ce tableau sont indicatives. Seules, les données spécifiées dans nos études-devis peuvent nous engager.

Formule donnant la quantité d'eau refoulée :

$$q = Q \times \frac{HC}{HR} \times Y$$ dans laquelle :

Y = Rendement < 1. (suivant tableau ci-dessus).
q = Débit refoulé par le Bélier.
Q = Débit absorbé par le Bélier.
HC = Hauteur géométrique de chute en mètres.
HR = Hauteur manométrique de refoulement en mètres.

TRES IMPORTANT - La longueur de la tuyauterie de batterie doit être déterminée par nos soins d'après les conditions d'installation. Les limites supérieures et inférieures sont les suivantes :

$6\ hc < LB < 12\ hc$

Table A.2-1 Performance characteristics Bélier 'Alto'; source: J.M. Descloud.

types of rams are available: type J for 'normal' elevations and type CH suited for 'high' elevations. The standard sizes range from 3/4"-20 mm through to 5"-125 mm drive pipe bore, but larger sizes are available on request. The provided data have been found insufficient to compile reliable performance figures for varying arrangements of supply and delivery heads. Only efficiency limits are given (Table A.2-1):

Alto J 26-80-8 : η_{trd}= 56% - 16% for $^{h}/H$ = 6 - 20

Alto CH 50-110-18: η_{trd}= 63% - 30% for $^{h}/H$ = 6 - 20

where the efficiency is defined as

$$\eta_{trd} = \frac{q * h}{Q * H}$$

Test results

Both Alto rams were tested at three different values of the supply head: H= 1.00 m, 2.00 m and 3.00 m respectively. The results are presented in the tables and figures hereafter;

Alto J 26-80-8 : Tables A.2-2,3,4 and Figs. A.2-1,2,3

Alto CH 50-110-18: Tables A.2-5,6,7 and Figs. A.2-4,5,6.

Dimensionless performance figures ($^{q}/Q$ v. $^{h}/H$) for both rams together are illustrated in Fig. A.2-7.

As stated above only limiting values of the efficiency calculated from the measurements can be compared with the figures specified by the manufacturer:

Alto J: $^{h}/H$ = 6 --> from Fig. A.2-7 it follows that $^{q}/Q \simeq 0.09$

and so

$$\eta_{trd} = \frac{q * h}{Q * H} \simeq 0.54 \ (54\ \%)$$

which compares well with the figure given by the manufacturer.

$^{h}/H$ = 20 --> not attained in the tests.

Alto CH: $^{h}/H$ = 6 --> from Fig. A.2-7 it follows that $^{q}/Q \simeq 0.07$

and so

$$\eta_{trd} = \frac{q * h}{Q * H} \simeq 0.42 \ (42\ \%)$$

which is low as compared with the manufacturer's figure (63 %).

$^{h}/H$ = 20 --> $^{q}/Q \simeq 0.015$ and thus $\eta_{trd} \simeq 0.3$ (30 %) which is as specified by the manufaturer.

Concluding remarks

The Alto rams performed moderately under the laboratory conditions. In particular the range of delivery heads obtained in the tests was found to be somewhat limited, especially for the Alto J ram. This is probably

due to the uncontrolled amount of air sucked in through the waste valve during the suction part of the pumping cycle. Though most of this air will be removed by the flow in the subsequent period of acceleration, some of it may remain trapped in the vertical pipe-section underneath the delivery valve, thereby limiting the effect of the next pressure rise. Eventually this reduces the range of obtainable delivery heads. A good set of instructions (in French) for the installation, tuning and maintenance of the Alto ram is provided by the manufacturer.

Table A.2-2 Testresults Alto J 26-80-8; supply head H = 1.00 m

Type of Hydr.Ram: **ALTO J 26—80—8** Supply Head H= 1.00 m

Manufacturer : J.M. DESCLAUD, BORDEAUX, FRANCE. Drive Pipe: D= 1" (25mm) L= 11.67 m

Test No.	Delivery Head h [m]	Head Ratio h/H [-]	Period Time T [s]	Pumping Rate q [l/min]	Supply Flow Rate Q [l/min]	Flow Ratio q/Q [-]	Efficiency $\eta=\frac{q*(h-H)}{Q*H}$ [%]	Filename	Volume of Water Delivered V_{up} [$*10^{-3}$ l/cycle]	Volume of Water Wasted V_{out} [$*10^{-3}$ l/cycle]
200	6	6	1.305	1.10	13.40	0.0821	41.0	-	23.9	291
202	7	7	1.269	0.85	13.70	0.0620	37.2	-	18.0	290
204	9	9	1.274	0.60	13.65	0.0440	35.2	-	12.7	290
206	11	11	1.264	0.40	13.95	0.0287	28.7	-	8.4	294
208	13	13	1.248	0.30	13.80	0.0217	26.1	AL-J/8,8A	6.2	287
210	h_{max}= 19	19	1.274	0	13.45	0	0	AL-J/7	0	286

Table A.2-3 Testresults Alto J 26-80-8; supply head H = 2.00 m

Type of Hydr.Ram: **ALTO J 26-80-8** Supply Head H= 2.00 m

Manufacturer : J.M. DESCLAUD, BORDEAUX, FRANCE. Drive Pipe: D= 1" (25mm) L= 11.67 m

Test No.	Delivery Head h [m]	Head Ratio h/H [-]	Period Time T [s]	Pumping Rate q [l/min]	Supply Flow Rate Q [l/min]	Flow Ratio q/Q [-]	Efficiency $\eta=\frac{q*(h-H)}{Q*H}$ [%]	Filename	Volume of Water Delivered V_{up} [$*10^{-3}$ l/cycle]	Volume of Water Wasted V_{out} [$*10^{-3}$ l/cycle]
230	9	4.5	0.744	1.75	13.50	0.1296	45.4	-	21.7	167
232	10	5	0.725	1.60	13.90	0.1151	46.0	-	19.3	168
234	12	6	0.713	1.30	14.05	0.0925	46.3	-	15.4	167
236	14	7	0.720	1.00	13.90	0.0719	43.2	-	12.0	167
238	16	8	0.703	0.84	14.20	0.0592	41.4	AL-J/6,6A	9.8	166
240	20	10	0.690	0.60	14.45	0.0415	37.4	-	6.9	166
242	24	12	0.715	0.37	13.80	0.0268	29.5	AL-J/5,5A	4.4	164
244	h_{max}= 33	16.5	0.691	0	14.30	0	0	AL-J/4	0	165

Table A.2-4 Testresults Alto J 26-80-8; supply head H = 3.00 m

Type of Hydr.Ram: **ALTO J 26-80-8** — Supply Head H= 3.00 m

Manufacturer : J.M. DESCLAUD, BORDEAUX, FRANCE. — Drive Pipe: D= 1" (25mm) L= 11.67 m

Test No.	Delivery Head h [m]	Head Ratio h/H [-]	Period Time T [s]	Pumping Rate q [l/min]	Supply Flow Rate Q [l/min]	Flow Ratio q/Q [-]	Efficiency $\eta = \frac{q*(h-H)}{Q*H}$ [%]	Filename	Volume of Water Delivered V_{up} [$*10^{-3}$ l/cycle]	Volume of Water Wasted V_{out} [$*10^{-3}$ l/cycle]
270	12	4	0.561	2.20	14.10	0.1560	46.8	-	20.6	132
272	15	5	0.550	1.70	14.30	0.1189	47.6	-	15.6	131
274	18	6	0.530	1.35	14.75	0.0915	45.8	AL-J/3,3A	11.9	130
276	21	7	0.538	1.10	14.65	0.0751	45.1	-	9.9	131
278	24	8	0.510	0.95	15.40	0.0617	43.2	-	8.1	131
280	27	9	0.539	0.63	14.40	0.0438	35.0	AL-J/2,2A	5.7	129
282	30	10	0.530	0.48	14.75	0.0325	29.3	-	4.2	130
284	33	11	0.510	0.40	15.40	0.0260	26.0	-	3.4	131
286	36	12	0.507	0.30	15.50	0.0194	21.3	-	2.5	131
288	h_{max}= 42	14	0.551	0	13.75	0	0	AL-J/1	0	126

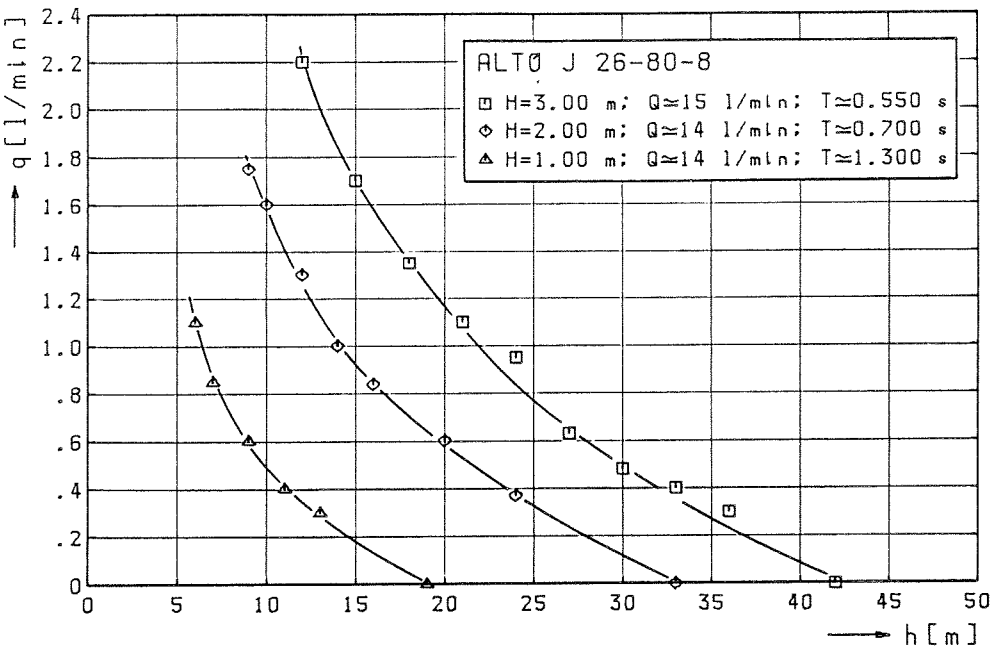

Fig. A.2-1 Pumping rate q versus delivery head h; Alto J 26-80-8

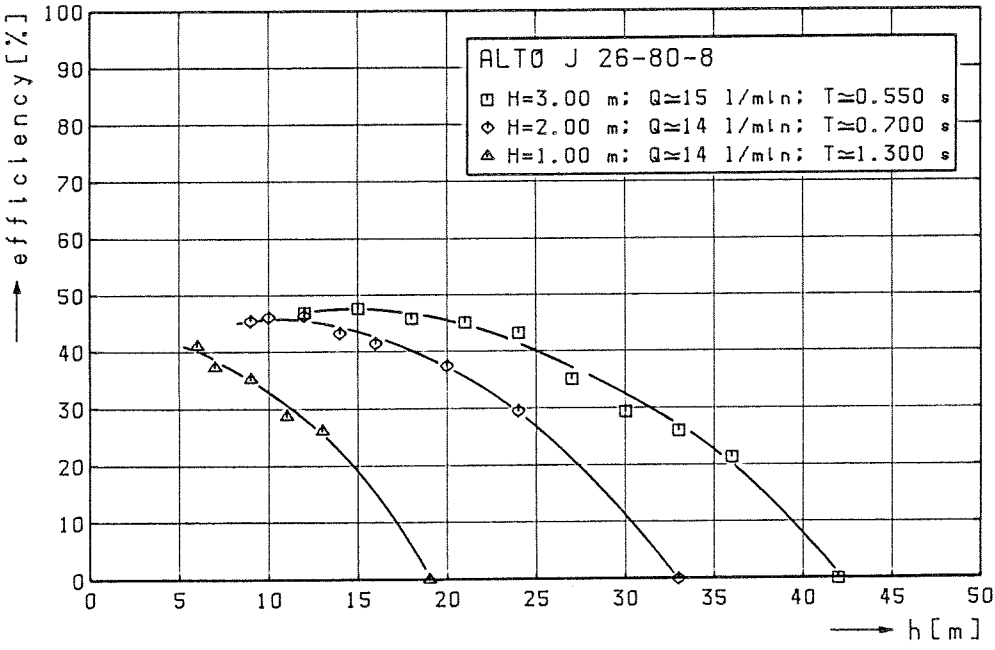

Fig. A.2-2 Rankine efficiency η versus delivery head h; Alto J 26-80-8

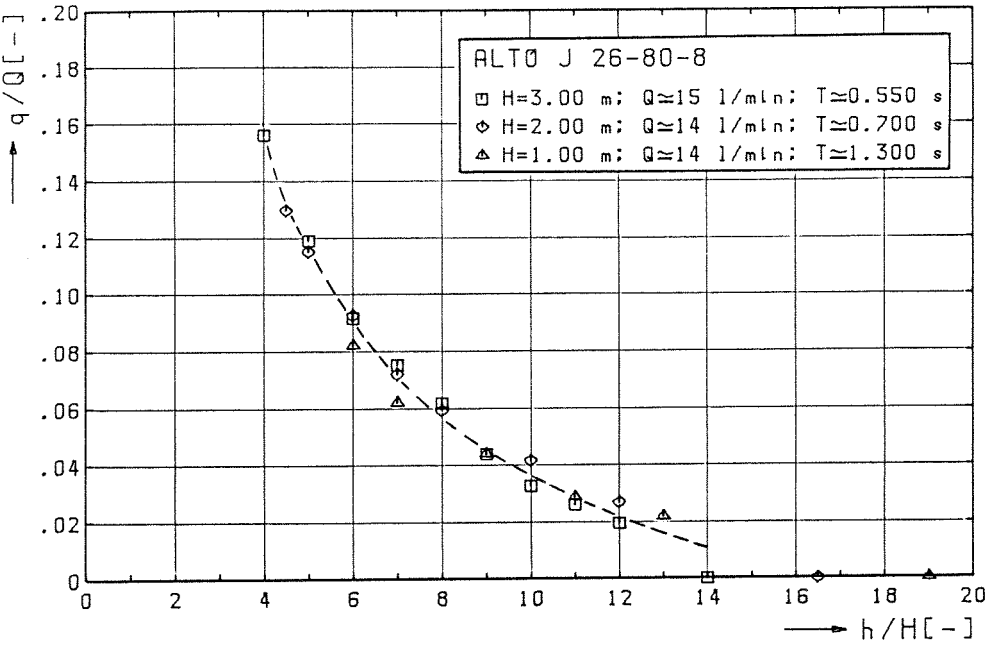

Fig. A.2-3 Flow ratio $^{q}/_{Q}$ versus head ratio $^{h}/_{H}$; Alto J 26-80-8

Table A.2-5 Testresults Alto CH 50-110-18; supply head H = 1.00 m

Type of Hydr.Ram: **ALTO CH 50-110-18** Supply Head H= 1.00 m

Manufacturer : J.M. DESCLAUD, BORDEAUX, FRANCE. Drive Pipe: D= 2" (50mm) L= 12.51 m

Test No.	Delivery Head h [m]	Head Ratio h/H [-]	Period Time T [s]	Pumping Rate q [l/min]	Supply Flow Rate Q [l/min]	Flow Ratio q/Q [-]	Efficiency $\eta = \frac{q*(h-H)}{Q*H}$ [%]	Filename	Volume of Water Delivered V_{up} [$*10^{-3}$ l/cycle]	Volume of Water Wasted V_{out} [$*10^{-3}$ l/cycle]
300	6	6	1.010	1.25	33.60	0.0372	18.6	AL-CH/19	21.0	566
302	10	10	1.003	0.96	34.10	0.0282	25.3	AL-CH/18	16.0	570
304	14	14	1.055	0.67	31.90	0.0210	27.3	AL-CH/17	11.8	561
306	20	20	1.065	0.45	31.40	0.0143	27.2	AL-CH/16	8.0	557
308	28	28	1.067	0.25	32.00	0.0078	21.1	AL-CH/15	4.4	569
310	h_{max}= 40	40	-	0	-	0	0	-	0	-

Table A.2-6 Testresults Alto CH 50-110-18; supply head H = 2.00 m

Type of Hydr.Ram: **ALTO CH 50-110-18** Supply Head H= 2.00 m

Manufacturer : J.M. DESCLAUD, BORDEAUX, FRANCE. Drive Pipe: D= 2" (50mm) L= 12.51 m

Test No.	Delivery Head h [m]	Head Ratio h/H [-]	Period Time T [s]	Pumping Rate q [l/min]	Supply Flow Rate Q [l/min]	Flow Ratio q/Q [-]	Efficiency $\eta = \frac{q*(h-H)}{Q*H}$ [%]	Filename	Volume of Water Delivered V_{up} [$*10^{-3}$ l/cycle]	Volume of Water Wasted V_{out} [$*10^{-3}$ l/cycle]
330	7	3.5	0.588	3.05	36.40	0.0838	20.9	-	29.9	357
332	10	5	0.593	2.55	36.15	0.0705	28.2	AL-CH/14	25.2	357
334	16	8	0.587	1.95	36.40	0.0536	37.5	AL-CH/13	19.1	356
336	20	10	0.608	1.55	34.70	0.0447	40.2	AL-CH/12	15.7	352
338	24	12	0.608	1.30	35.50	0.0366	40.3	AL-CH/11	13.2	360
340	28	14	0.587	1.20	36.25	0.0331	43.0	AL-CH/10	11.7	355
342	35	17.5	0.549	0.95	38.40	0.0247	40.8	-	8.7	351
344	45	22.5	0.608	0.50	33.50	0.0149	32.1	AL-CH/9	5.1	339
346	h_{max}= 60	30	-	0	-	0	0	-	0	-

Table A.2-7 Testresults Alto CH 50-110-18; supply head H = 3.00 m

Type of Hydr.Ram: **ALTO CH 50-110-18** Supply Head H= 3.00 m

Manufacturer : J.M. DESCLAUD, BORDEAUX, FRANCE. Drive Pipe: D= 2" (50mm) L= 12.51 m

Test No.	Delivery Head h [m]	Head Ratio h/H [-]	Period Time T [s]	Pumping Rate q [l/min]	Supply Flow Rate Q [l/min]	Flow Ratio q/Q [-]	Efficiency $\eta=\frac{q*(h-H)}{Q*H}$ [%]	Filename	Volume of Water Delivered V_{up} [$*10^{-3}$ l/cycle]	Volume of Water Wasted V_{out} [$*10^{-3}$ l/cycle]
360	10	3.33	0.407	4.45	36.30	0.1226	28.6	AL-CH/8	30.2	246
362	12	4	0.447	3.90	39.50	0.0987	29.6	AL-CH/7	29.1	294
364	18	6	0.420	3.00	40.50	0.0741	37.0	AL-CH/6	21.0	284
366	24	8	0.452	2.25	39.40	0.0571	40.0	AL-CH/5	17.0	297
368	30	10	0.448	1.80	39.65	0.0454	40.9	AL-CH/4	13.4	296
370	36	12	0.435	1.55	40.90	0.0379	41.7	-	11.2	297
372	42	14	0.392	1.25	40.80	0.0306	39.8	AL-CH/3,3A	8.2	267
374	51	17	0.442	0.88	39.70	0.0222	35.5	AL-CH/2	6.5	292
376	60	20	0.476	0.40	34.80	0.0115	21.8	AL-CH/1	3.2	276
378	h_{max}= 66	22	-	0	-	0	0	-	0	-

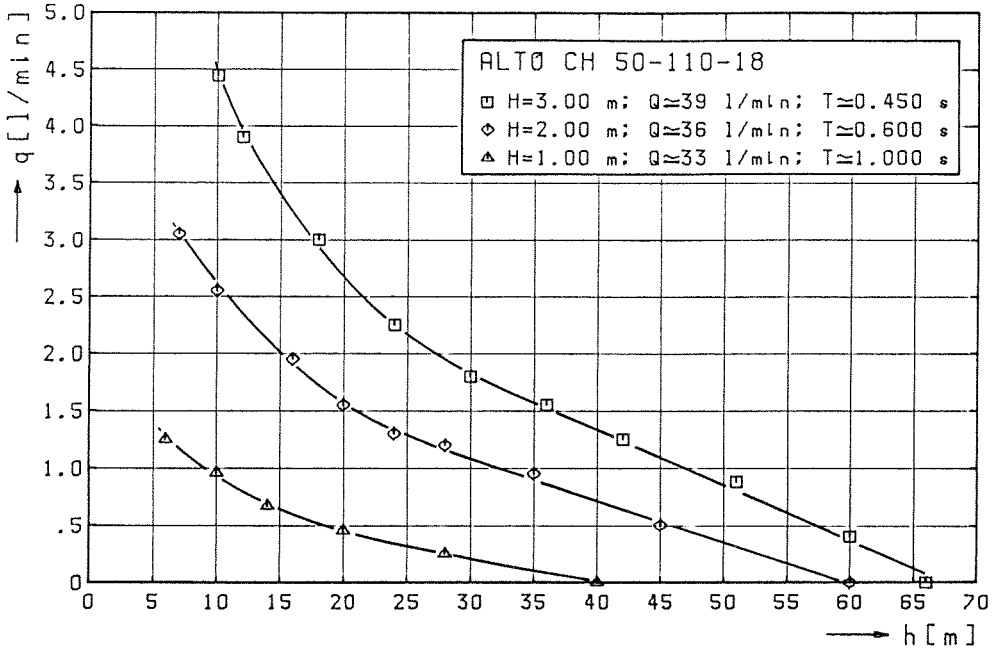

Fig. A.2-4 Pumping rate q versus delivery head h; Alto CH 50-110-18

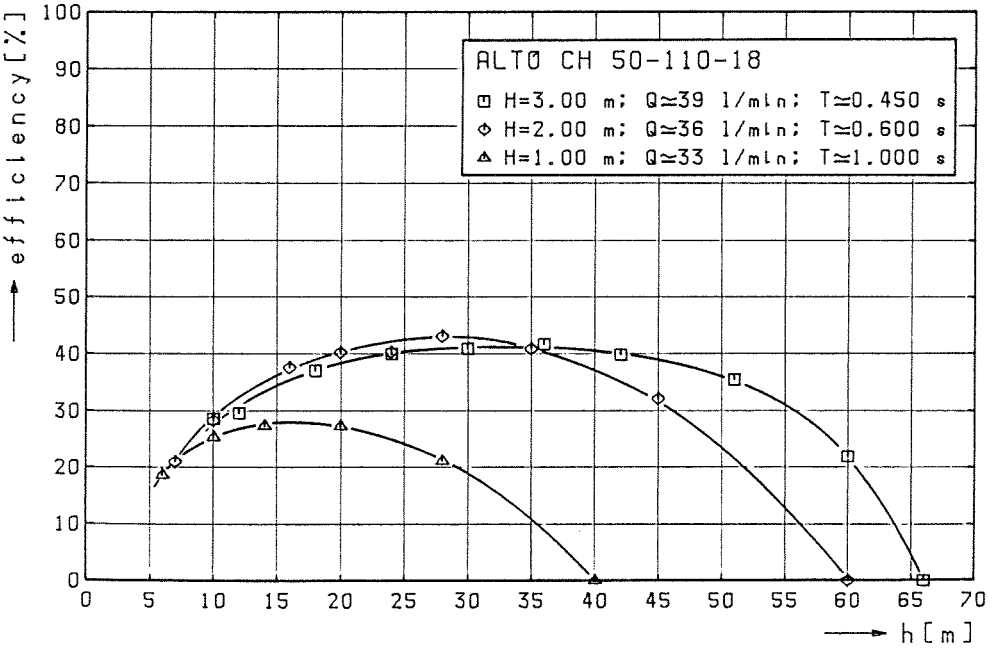

Fig. A.2-5 Rankine efficiency η versus delivery head h; Alto CH 50-110-18

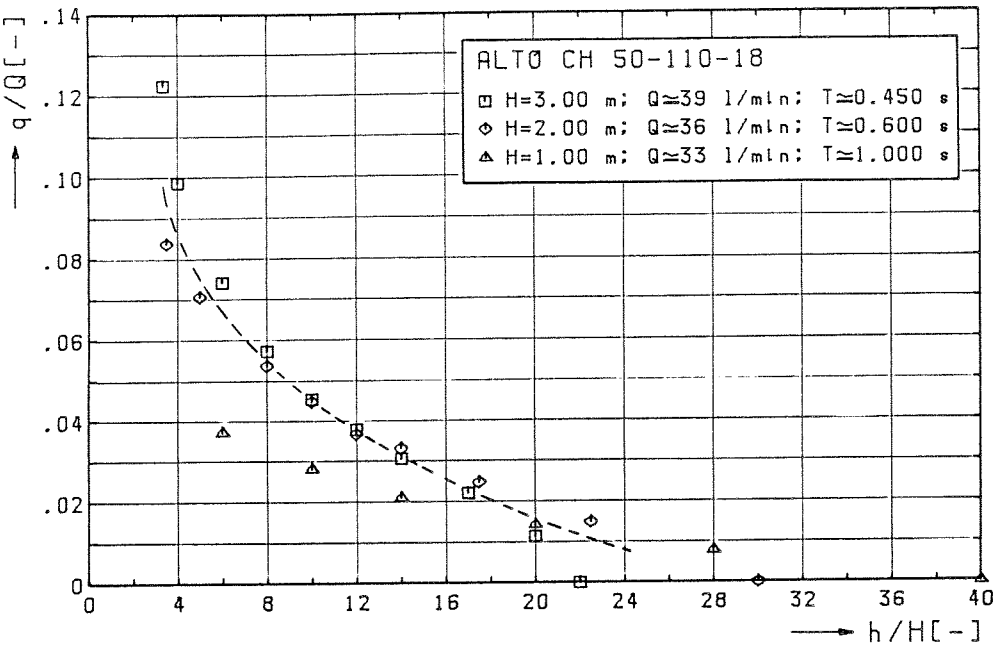

Fig. A.2-6 Flow ratio $^{q}/_{Q}$ versus head ratio $^{h}/_{H}$; Alto CH 50-110-18

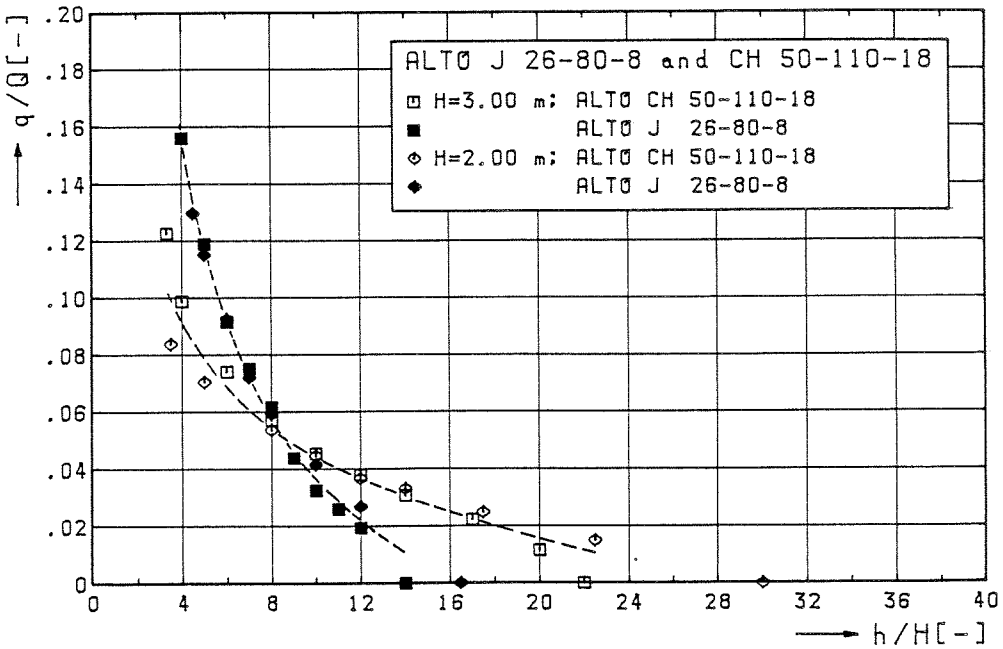

Fig. A.2-7 Dimensionless performace characteristics;
Alto J 26-80-8 and CH 50-110-18

A.3 VULCAN

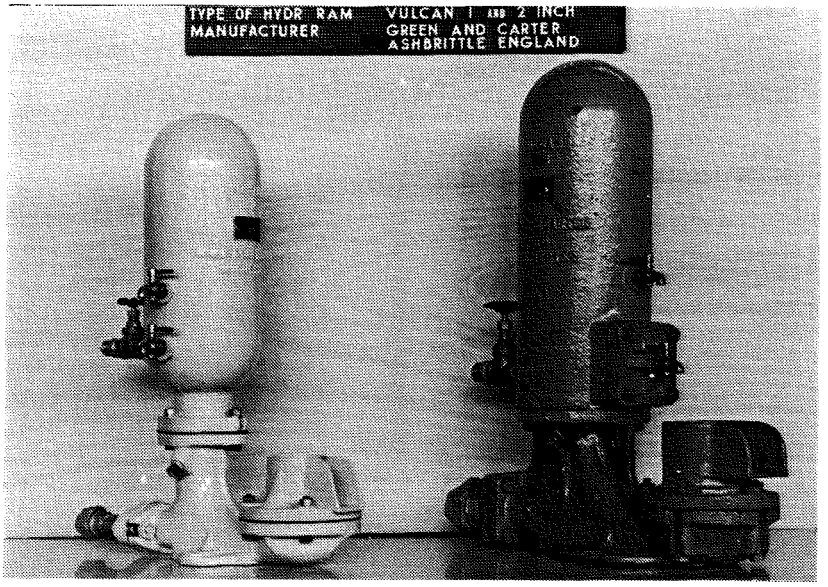

Rams tested (see picture): VULCAN 1"
VULCAN 2"

Manufacturer: Green & Carter,
Ashbrittle - England.

Description

The Vulcan ram is like the Blake Hydram a well-established standard design which has been available for a long time. The ram is made of cast-iron with brass and gunmetal components. The standard waste valve and delivery valve consist of a rubber disc (clack) covering a grid-shaped gunmetal seat (see Fig. A.3-1). The valve setting of the waste valve can be tuned to the available source supply by adjusting the valve stroke. Alternative types of waste valve (made of NC or metal) are available at additional charges. Vulcan sizes range from 1" (25 mm) through to 10" (250 mm) drive pipe bore, suitable for source supplies up to approximately 1800 l/min (see Table A.3-1).

The Vulcan rams are equipped with a brass air valve and two brass drain cocks on the air chamber. Stop-valves for drive pipe and delivery pipe are optional extras.

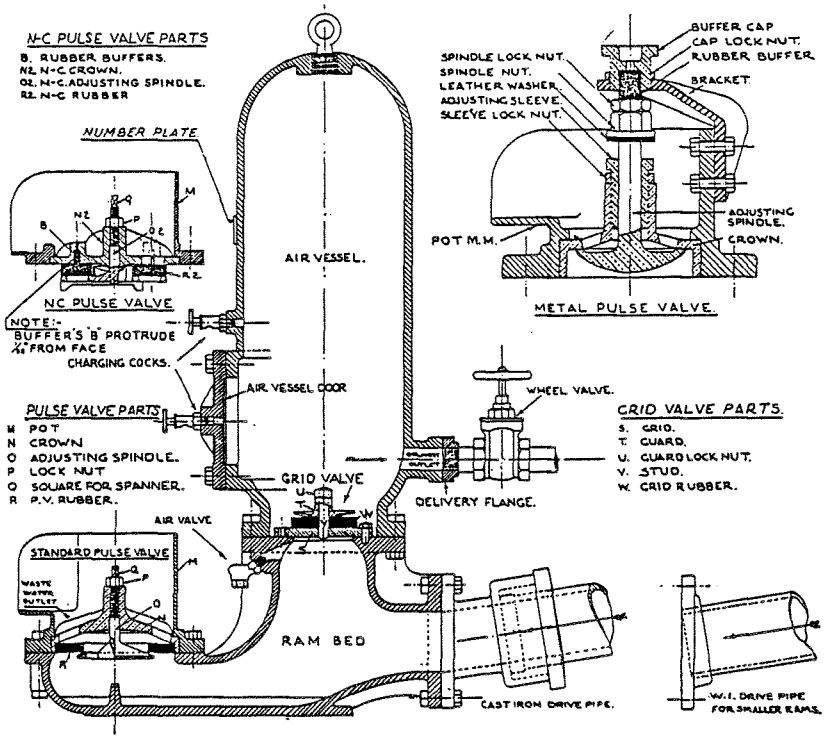

Fig. A.3-1 Cross-sectional diagram of the Vulcan ram; source: Green & Carter.

LIST OF SIMPLE TYPE VULCAN RAMS

Size of Hydraulic Ram and diameter of Drive Pipe	Quantity supplied by Spring or Stream per minute	Diameter of Delivery Pipe (minimum)	Quantity of Water per 24 hours Ram may be expected to raise under suitable conditions	Code Word
In.	Litres	In.	Litres	
1-1¼	4,5 to 18	¾	454 to 2724	**Dobberen**
1½	9 ,, 27	¾	1816 ,, 4540	**Dobbering**
2	23 ,, 46	1	2724 ,, 9080	**Docent**
2½	36 ,, 114	1	3405 ,, 13620	**Docile**
3	55 ,, 114	1	4540 ,, 22700	**Dochter**
4	91 ,, 182	1¼	9080 ,, 45400	**Doddering**
5	136 ,, 272	1½	18160 ,, 81720	**Doedelzak**
6	227 ,, 454	2	27240 ,, 136200	**Doeken**
8	454 ,, 908	2½	68100 ,, 272400	**Doedlec**
9	908 ,, 1362	3	136200 ,, 408600	**Doeleinde**
10	1362 ,, 1816	4	295100 ,, 544800	**Doebelter**

Table A.3-1 Performance characteristics for the Vulcan ram; source: Green & Carter.

According to the manufacturer the pumping rate q of the Vulcan ram may be estimated using the formula

$$q = \frac{Q * H}{h} * 0.67 \qquad \text{for} \quad 3 < {}^{h}/_{H} < 30 \text{ to } 40$$

(see also chapter II). Results thus obtained for various arrangements of supply and delivery heads are published by the manufacturer in a tabular form, which is not reproduced here. For the rams tested, claimed performance figures were calculated in the above manner and plotted in Figs. A.3-2, A.3-5, A.3-6 and A.3-9.

Test results

The Vulcan rams were tested at three different values of the supply head: H= 1.00 m, 2.00 m and 3.00 m respectively. The results are presented in the tables and figures hereafter;

Vulcan 1": Tables A.3-2,3,4 and Figs. A.3-2,3,4,5

Vulcan 2": Tables A.3-5,6,7 and Figs. A.3-6,7,8,9.

In addition to the individual results, Fig. A.3-10 shows that the assumed similarity in dimensionless performance characteristics for both rams as implied by the manufacturer's calculation rule, has not been ascertained in the tests.

Concluding remarks

The Vulcan rams operated reasonably well in the laboratory tests, although the performances of the 1"-ram stayed somewhat behind the figures claimed by the manufacturer. As compared to the condition used in the laboratory, the 2"-ram may very well be operated at a larger valve stroke resulting in more water to be used by the ram and more water to be delivered to even higher heads. Instructions for installing, regulating and maintaining the Vulcan rams are available in several languages.

Table A.3-2 Testresults Vulcan 1"; supply head H = 1.00 m

Type of Hydr.Ram: **VULCAN 1"**

Supply Head H= 1.00m

Manufacturer : GREEN & CARTER Ltd, ASHBRITTLE, ENGLAND.

Drive Pipe: D= 1" (25mm) L= 11.60 m

Test No.	Delivery Head h [m]	Head Ratio h/H [-]	Period Time T [s]	Pumping Rate q [l/min]	Supply Flow Rate Q [l/min]	Flow Ratio q/Q [-]	Efficiency $\eta=\frac{q*(h-H)}{Q*H}$ [%]	Filename	Volume of Water Delivered V_{up} [$*10^{-3}$ l/cycle]	Volume of Water Wasted V_{out} [$*10^{-3}$ l/cycle]
400	4	4	1.553	1.00	14.35	0.0697	20.9	-	25.9	371
402	5	5	1.534	0.87	14.70	0.0592	23.7	-	22.2	376
404	7	7	1.523	0.70	15.15	0.0462	27.7	-	17.8	385
406	9.5	9.5	1.535	0.54	15.25	0.0354	30.1	V1/10	13.8	390
408	12	12	1.533	0.45	15.30	0.0294	32.4	V1/9	11.5	391
410	18	18	1.570	0.31	15.10	0.0205	34.9	V1/8,8A	8.1	395
412	26	26	1.583	0.22	14.85	0.0148	37.0	V1/7	5.8	392
414	h_{max}= 75	75	-	0	-	0	0	-	0	-

Type of Hydr.Ram: **VULCAN 1"** Supply Head H= 2.00 m

Manufacturer : GREEN & CARTER Ltd, ASHBRITTLE, ENGLAND. Drive Pipe: D= 1" (25mm) L= 11.60 m

Test No.	Delivery Head h [m]	Head Ratio h/H [-]	Period Time T [s]	Pumping Rate q [l/min]	Supply Flow Rate Q [l/min]	Flow Ratio q/Q [-]	Efficiency $\eta = \frac{q*(h-H)}{Q*H}$ [%]	Filename	Volume of Water Delivered V_{up} [$*10^{-3}$ l/cycle]	Volume of Water Wasted V_{out} [$*10^{-3}$ l/cycle]
430	8	4	0.923	1.90	17.10	0.1111	33.3	-	29.2	263
432	10	5	0.914	1.60	17.10	0.0936	37.4	-	24.4	260
434	12	6	0.911	1.45	17.10	0.0848	42.4	-	22.0	260
436	16	8	0.904	1.15	17.30	0.0665	46.5	-	17.3	261
438	20	10	0.924	0.92	17.40	0.0529	47.6	V1/6,6A	14.2	268
440	24	12	0.918	0.79	17.55	0.0450	49.5	-	12.1	269
442	28	14	0.965	0.64	17.00	0.0376	48.9	V1/5,5A	10.3	273
444	36	18	0.963	0.52	17.40	0.0299	50.8	-	8.3	279
446	48	24	1.025	0.33	14.85	0.0222	51.1	V1/4,4A	5.6	254
448	60	30	1.026	0.27	14.70	0.0184	53.3	-	4.6	251
450	h_{max}=117	58.5	-	0	-	0	0	-	0	-

Table A.3-3 Testresults Vulcan 1"; supply head H = 2.00 m

Table A.3-4 Testresults Vulcan 1", supply head H = 3.00 m

Type of Hydr.Ram: **VULCAN 1"** Supply Head H= 3.00 m

Manufacturer : GREEN & CARTER Ltd, ASHBRITTLE, ENGLAND. Drive Pipe: D= 1" (25mm) L= 11.60 m

Test No.	Delivery Head h [m]	Head Ratio h/H [-]	Period Time T [s]	Pumping Rate q [l/min]	Supply Flow Rate Q [l/min]	Flow Ratio q/Q [-]	Efficiency $\eta=\frac{q*(h-H)}{Q*H}$ [%]	Filename	Volume of Water Delivered V_{up} [$*10^{-3}$ l/cycle]	Volume of Water Wasted V_{out} [$*10^{-3}$ l/cycle]
470	13	4.33	0.626	2.25	16.00	0.1406	46.9	-	23.5	167
472	15	5	0.619	2.05	16.30	0.1258	50.3	-	21.1	168
474	18	6	0.612	1.70	16.65	0.1021	51.1	-	17.3	170
476	21	7	0.621	1.50	16.50	0.0909	54.6	V1/3,3A	15.5	171
478	24	8	0.623	1.35	16.80	0.0804	56.2	-	14.0	174
480	30	10	0.643	1.05	16.30	0.0644	58.0	V1/2,2A	11.3	175
482	36	12	0.644	0.87	16.20	0.0537	59.1	-	9.3	174
484	42	14	0.660	0.73	16.00	0.0456	59.3	-	8.0	176
486	51	17	0.702	0.50	14.20	0.0352	56.3	V1/1,1A	5.9	166
488	66	22	0.710	0.37	13.95	0.0265	55.7	-	4.4	165
490	93	31	0.775	0.24	13.90	0.0173	51.8	-	3.0	180
492	h_{max}=134	44.67	-	0	-	0	0	-	0	-

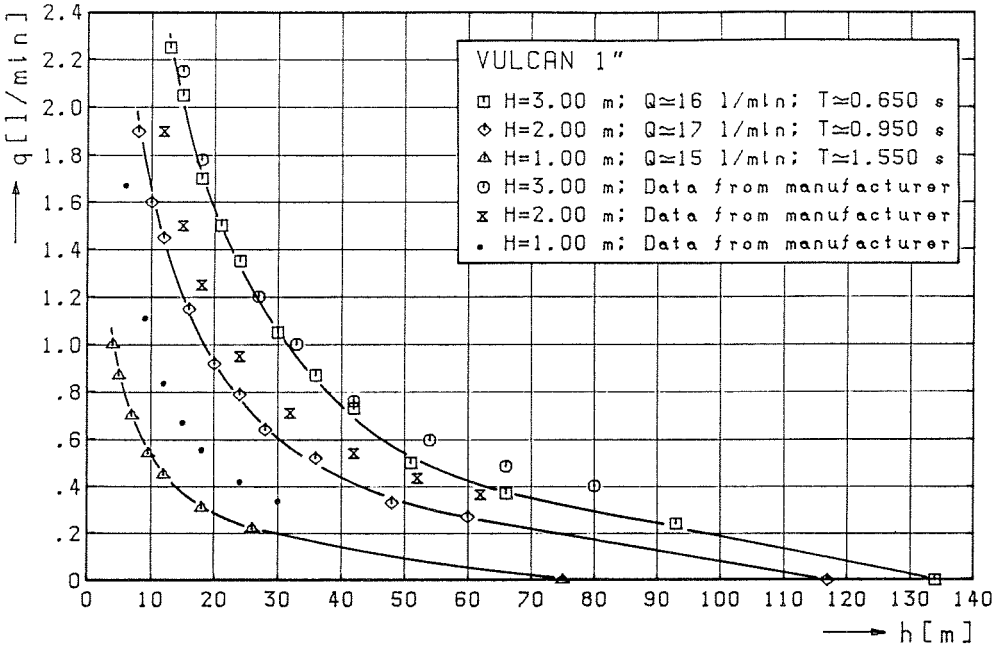

Fig. A.3-2 Pumping rate q versus delivery head h; Vulcan 1"

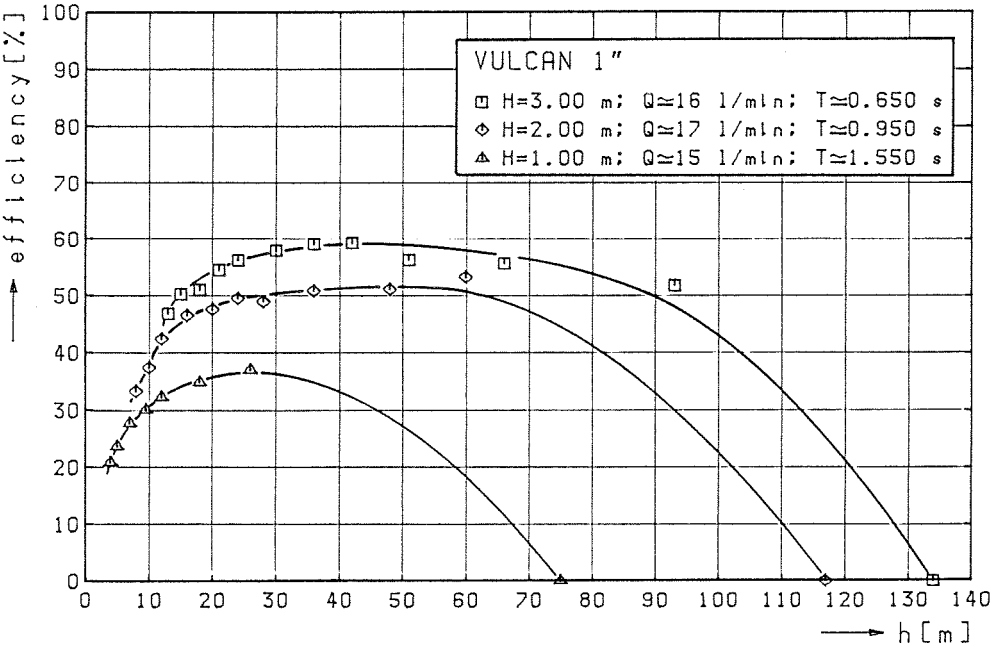

Fig. A.3-3 Rankine efficiency η versus delivery head h; Vulcan 1"

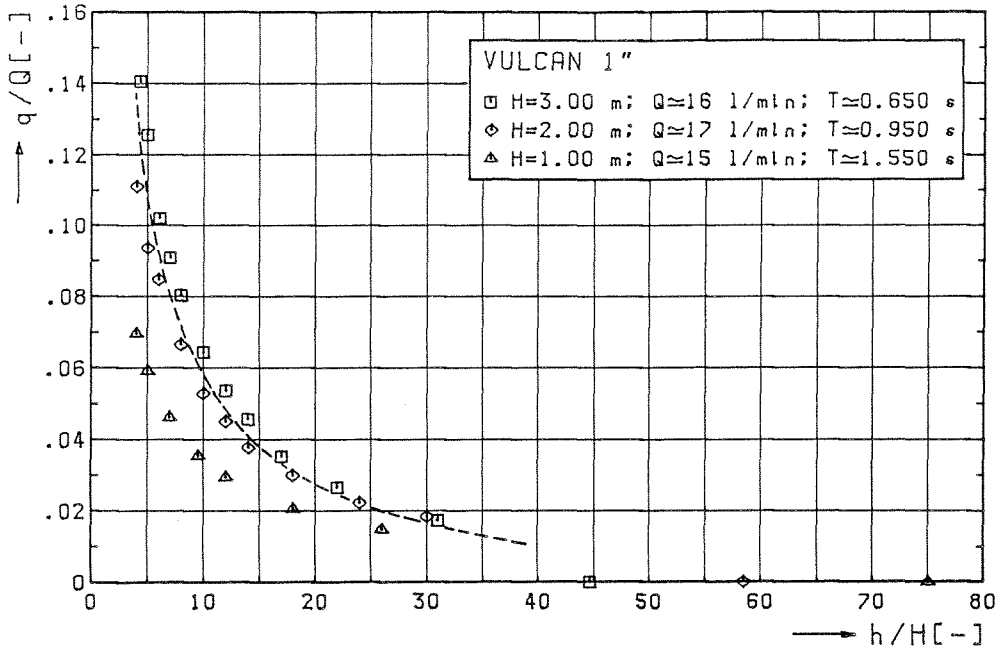

Fig. A.3-4 Flow ratio $^{q}/_{Q}$ versus head ratio $^{h}/_{H}$; Vulcan 1"

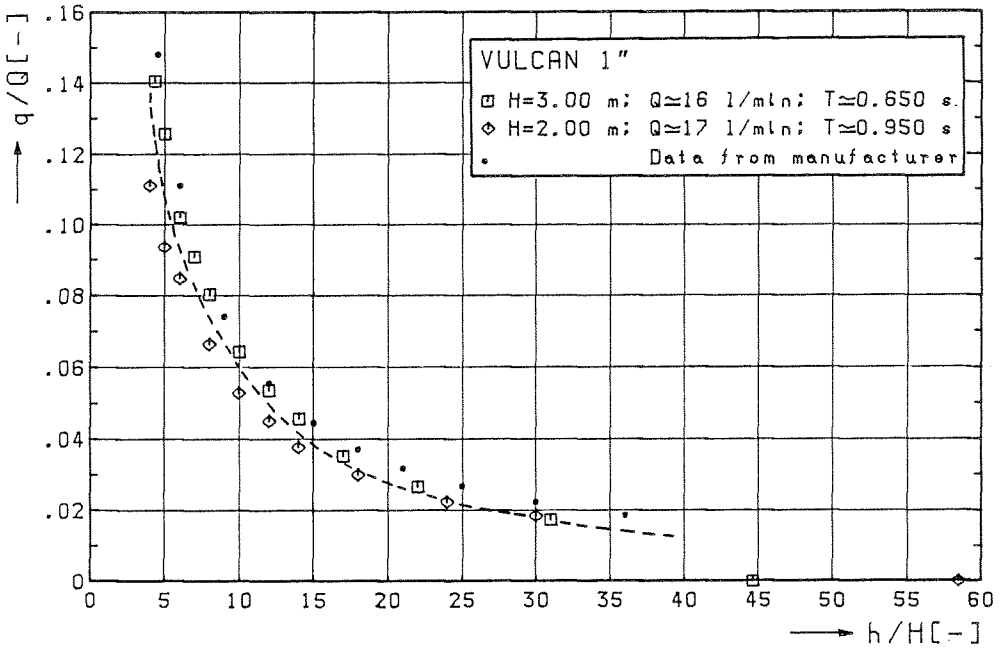

Fig. A.3-5 Flow ratio $^{q}/_{Q}$ versus head ratio $^{h}/_{H}$; Vulcan 1"

Type of Hydr.Ram: **VULCAN 2"** Supply Head H= 1.00 m

Manufacturer : GREEN & CARTER Ltd, ASHBRITTLE, ENGLAND. Drive Pipe: D= 2" (50mm) L= 12.15 m

Test No.	Delivery Head h [m]	Head Ratio h/H [-]	Period Time T [s]	Pumping Rate q [l/min]	Supply Flow Rate Q [l/min]	Flow Ratio q/Q [-]	Efficiency $\eta=\frac{q*(h-H)}{Q*H}$ [%]	Filename	Volume of Water Delivered V_{up} [$*10^{-3}$ l/cycle]	Volume of Water Wasted V_{out} [$*10^{-3}$ l/cycle]
500	6	6	1.128	4.25	36.10	0.1177	58.9	-	79.9	679
502	7	7	1.123	3.75	36.60	0.1025	61.5	V2/15	70.2	685
504	8	8	1.117	3.25	37.00	0.0878	61.5	V2/14,14A	60.5	689
506	10	10	1.115	2.67	37.35	0.0715	64.3	V2/13,13A	49.6	694
508	13	13	1.119	2.10	37.00	0.0568	68.1	V2/12,12A	39.2	690
510	15	15	1.102	1.90	37.60	0.0505	70.7	-	34.9	691
512	18	18	1.159	1.40	35.50	0.0394	67.0	V2/11	27.0	686
514	21	21	1.131	1.25	36.35	0.0344	68.8	V2/11A,11B -	23.6	685
516	25	25	1.130	1.05	36.40	0.0288	69.2	-	19.8	686
518	30	30	1.235	0.80	31.40	0.0255	73.9	V2/10,10A	16.5	646
520	35	35	1.212	0.62	32.75	0.0189	64.4	-	12.5	662
522	40	40	1.192	0.53	33.20	0.0160	62.2	-	10.5	660
524	50	50	1.241	0.34	31.45	0.0108	53.0	-	7.0	650
526	h_{max}= 68	68	-	0	-	0	0	-	0	-

Table A.3-5 Testresults Vulcan 2"; supply head H = 1.00 m

Type of Hydr.Ram: **VULCAN 2"**

Manufacturer : GREEN & CARTER Ltd, ASHBRITTLE, ENGLAND.

Supply Head H= 2.00 m

Drive Pipe: D= 2" (50mm)
L= 12.15 m

Test No.	Delivery Head h [m]	Head Ratio h/H [-]	Period Time T [s]	Pumping Rate q [l/min]	Supply Flow Rate Q [l/min]	Flow Ratio q/Q [-]	Efficiency $\eta=\frac{q*(h-H)}{Q*H}$ [%]	Filename	Volume of Water Delivered V_{up} [$*10^{-3}$ l/cycle]	Volume of Water Wasted V_{out} [$*10^{-3}$ l/cycle]
530	12	6	0.590	5.05	34.60	0.1460	73.0	V2/5,5A	49.7	340
532	15	7.5	0.603	3.95	35.10	0.1125	73.1	V2/6,6A	39.7	353
534	16	8	0.586	3.85	36.10	0.1066	74.6	-	37.6	353
536	20	10	0.609	2.85	34.60	0.0824	74.1	-	28.9	351
538	21	10.5	0.611	2.70	34.00	0.0794	75.4	V2/7,7A	27.5	346
540	24	12	0.586	2.50	36.40	0.0687	75.5	-	24.4	356
542	28	14	0.595	2.00	35.75	0.0559	72.7	-	19.8	355
544	32	16	0.636	1.50	32.10	0.0467	70.1	-	15.9	340
546	34	17	0.645	1.35	31.20	0.0433	69.2	V2/8,8A	14.5	335
548	40	20	0.626	1.20	33.20	0.0361	68.7	-	12.5	346
550	50	25	0.626	0.85	32.90	0.0258	62.0	V2/9,9A	8.9	343
552	60	30	0.670	0.53	28.90	0.0183	53.2	-	5.9	323
554	70	35	0.729	0.28	23.50	0.0119	40.5	-	3.4	286
556	h_{max}= 80	40	-	0	-	0	0	-	0	-

Table A.3-6 Testresults Vulcan 2"; supply head H = 2.00 m

Type of Hydr.Ram: **VULCAN 2"**

Manufacturer : GREEN & CARTER Ltd, ASHBRITTLE, ENGLAND.

Supply Head H= 3.00m

Drive Pipe: D= 2" (50mm)
L= 12.15 m

Test No.	Delivery Head h [m]	Head Ratio h/H [-]	Period Time T [s]	Pumping Rate q [l/min]	Supply Flow Rate Q [l/min]	Flow Ratio q/Q [-]	Efficiency $\eta=\frac{q*(h-H)}{Q*H}$ [%]	Filename	Volume of Water Delivered V_{up} [$*10^{-3}$ l/cycle]	Volume of Water Wasted V_{out} [$*10^{-3}$ l/cycle]
560	18	6	0.422	5.40	35.40	0.1525	76.3	V2/0,0A	38.0	249
562	19	6.33	0.410	5.05	36.55	0.1382	73.7	-	34.5	250
564	21	7	0.425	4.44	36.05	0.1232	73.9	-	31.5	255
566	24	8	0.428	3.90	35.50	0.1099	76.9	V2/1,1A	27.8	253
568	27	9	0.413	3.45	37.45	0.0921	73.7	-	23.7	258
570	30	10	0.420	3.05	36.40	0.0838	75.4	V2/2,2A,2B	21.3	255
572	36	12	0.455	2.20	32.75	0.0672	73.9	-	16.7	248
574	42	14	0.445	1.78	34.00	0.0524	68.1	-	13.2	252
576	48	16	0.440	1.50	34.55	0.0434	65.1	V2/3	11.0	253
578	57	19	0.453	1.07	32.80	0.0326	58.7	-	8.1	248
580	66	22	0.481	0.66	28.80	0.0229	48.1	-	5.3	231
582	75	25	0.522	0.38	23.20	0.0164	39.3	V2/4,4A	3.3	202
584	h_{max}= 88	29.33	-	0	-	0	0	-	0	-

Table A.3-7 Testresults Vulcan 2"; supply head H = 3.00 m

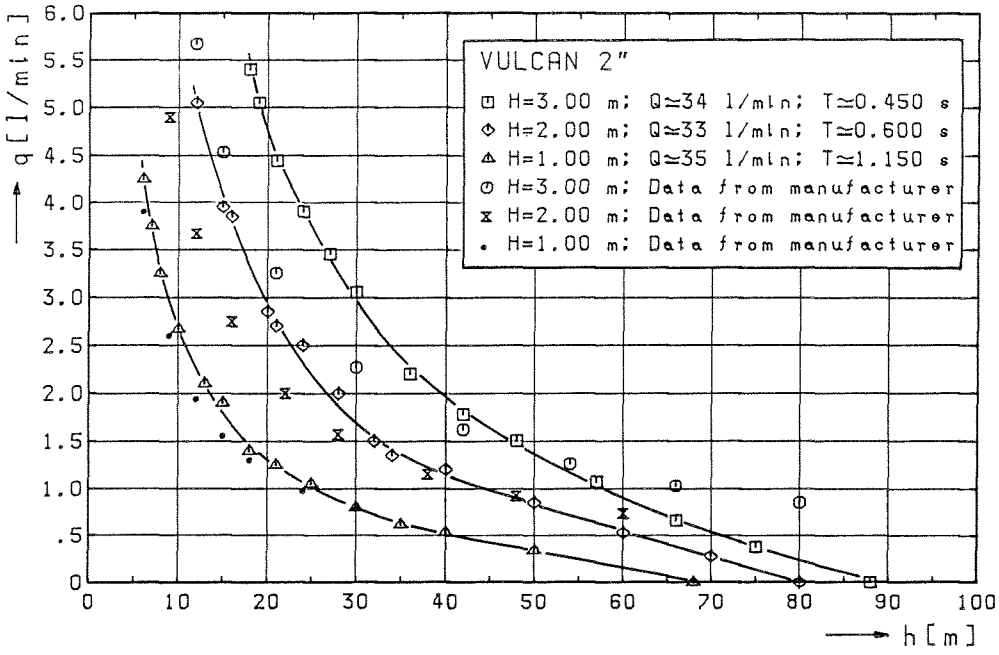

Fig. A.3-6 Pumping rate q versus delivery head h; Vulcan 2"

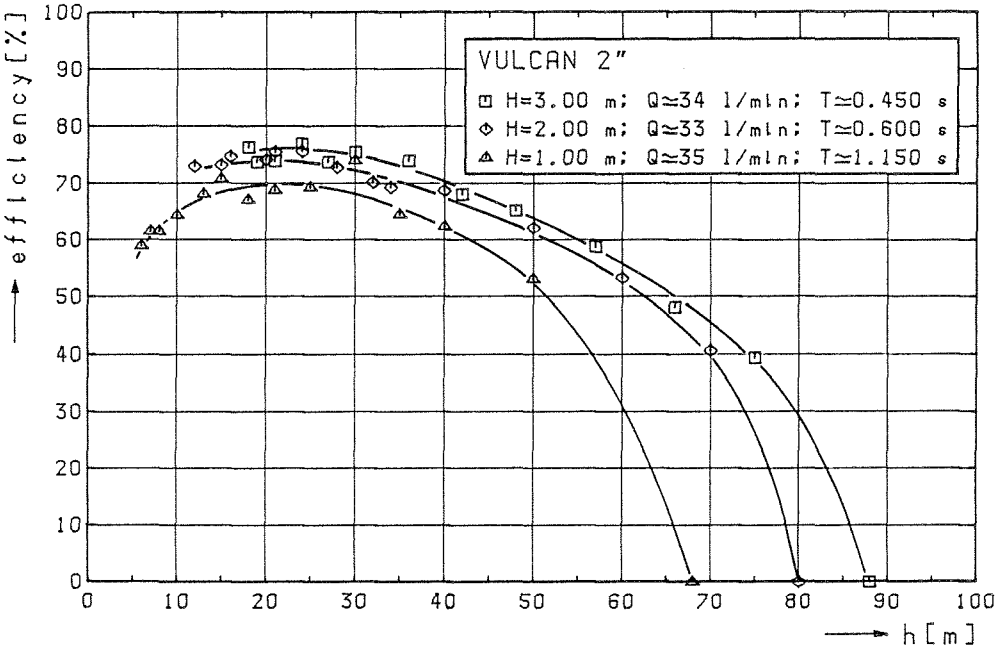

Fig. A.3-7 Rankine efficiency η versus delivery head h; Vulcan 2"

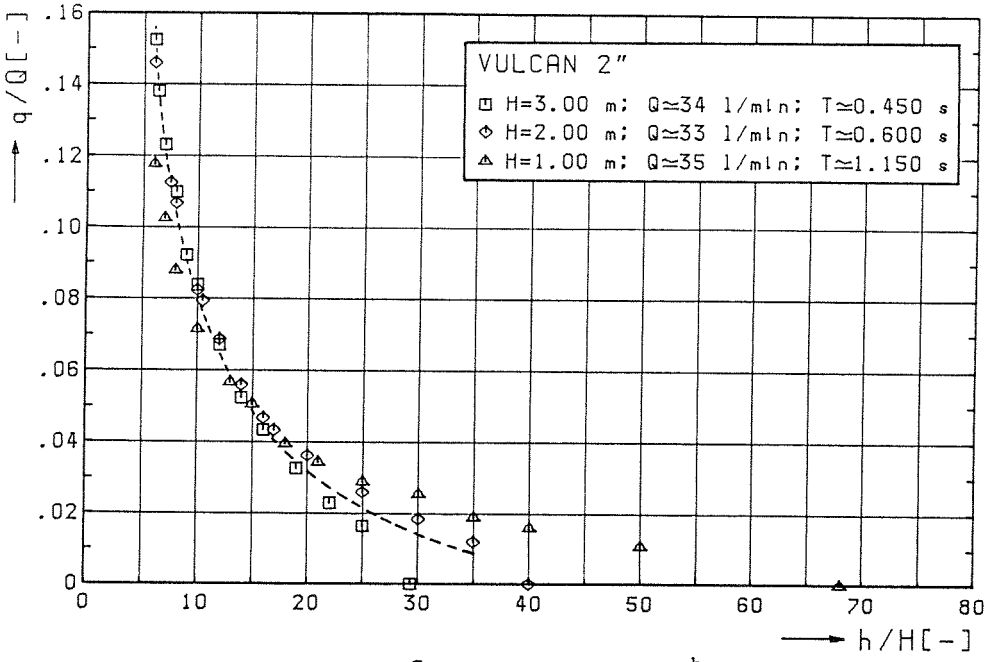

Fig. A.3-8 Flow ratio $^{q}/_{Q}$ versus head ratio $^{h}/_{H}$; Vulcan 2"

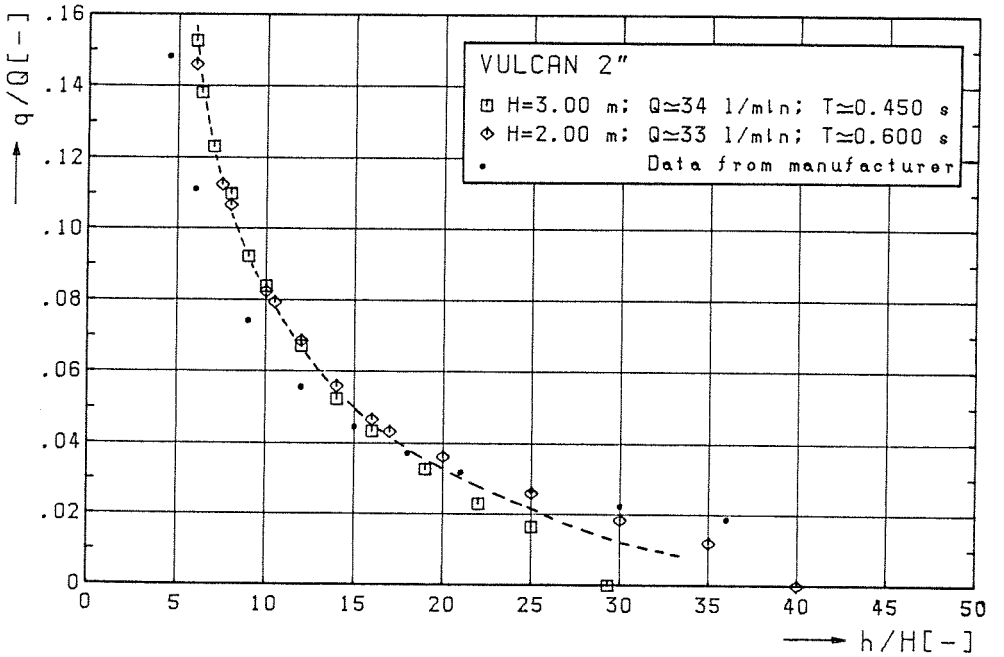

Fig. A.3-9 Flow ratio $^{q}/_{Q}$ versus head ratio $^{h}/_{H}$; Vulcan 2"

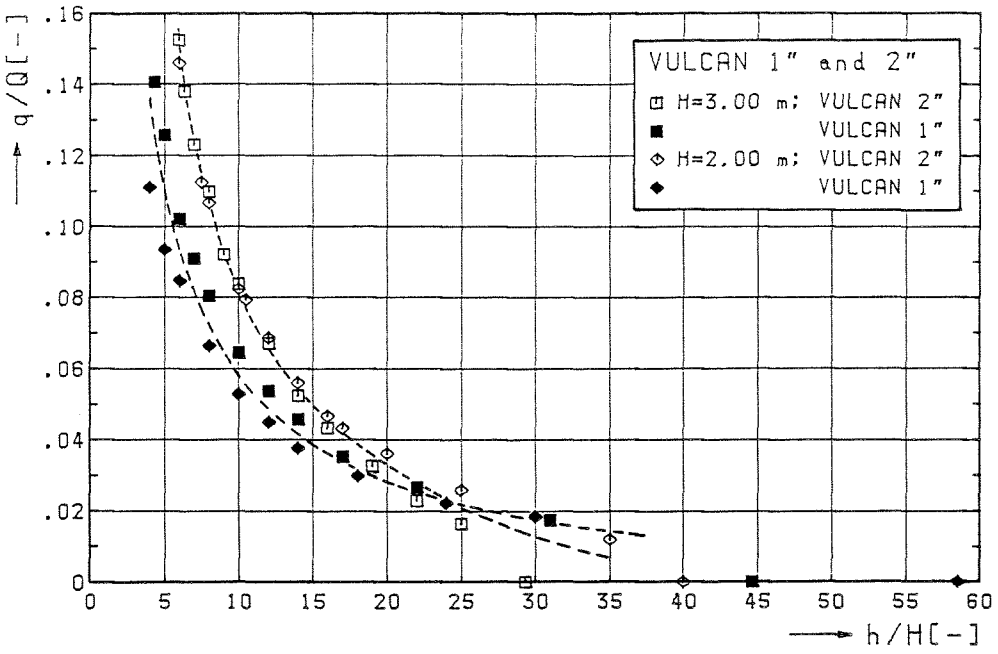

Fig. A.3-10 Dimensionless performance characteristics; Vulcan 1" and 2"

A.4 SANO

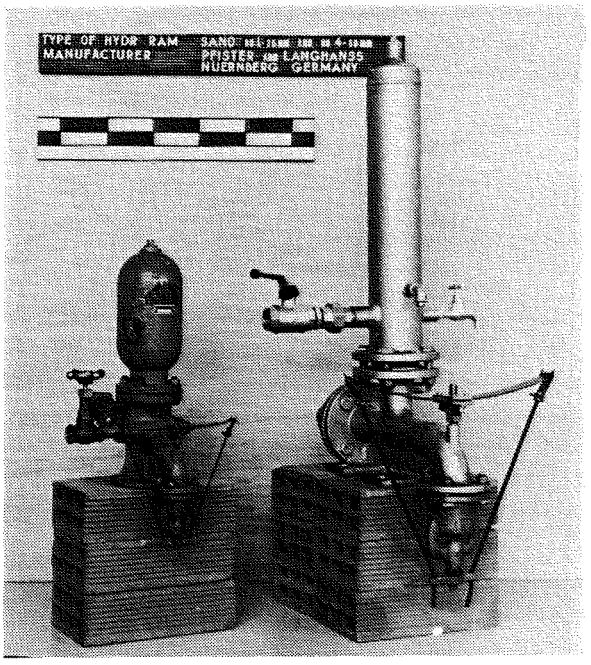

Rams tested (see picture): SANO No.1 - 25 mm (1") old construction
SANO No.4 - 50 mm (2") new construction

Manufacturer: Pfister + Langhanss,
Nuernberg - Germany.

Description

The SANO ram is an unconventional 'standard' pump design, formerly made of cast-iron but nowadays constructed of steel pipe components finished with a fire-zinc coating (Fig. A.4-1). Both waste valve and delivery valve are spring-activated and substantially made of gunmetal. SANO-sizes range from size No.0 (3/4"-20 mm) through to size No.9 (6"-150 mm) covering supply flows from 3 l/min up to 700 l/min; see Table A.4-1. Within the limits mentioned in the table, the rams can be adjusted to the available source supply by increasing/decreasing the spring-load on the waste valve. The SANO ram is equipped with an air valve and a drip valve and drain cock on the air chamber. The rams are delivered complete with two stop-valves, one for the drive pipe and one for the delivery

GRÖSSE SIZE		№	0	1	2	3	4	5	6	7	8	9
DURCHMESSER DN		mm	20	25	32	40	50	65	80	100	125	150
DIAMETER ø		"	3/4	1	1 1/4	1 1/2	2	2 1/2	3	4	5	6
TREIBWASSER-DURCHFLUSS DRIVING WATER		l/min	3 ⋮ 6	6 ⋮ 16	12 ⋮ 30	18 ⋮ 45	30 ⋮ 65	50 ⋮ 110	80 ⋮ 180	120 ⋮ 250	180 ⋮ 400	280 ⋮ 700
ABMESSUNGEN DIMENSIONS	a	"	3/8	1/2	1/2	3/4	1	1	1 1/2	2	2	2 1/2
	b	mm	400	480	500	750	850	1000	1250	1450	1500	1600
	c	mm	200	250	250	250	250	300	350	400	450	480
	d	mm	-	-	35	40	45	50	60	70	80	80
	e	mm	120	150	380	440	500	550	640	680	780	880
	f	mm	-	-	200	250	270	300	350	400	450	480
	g	mm	-	-	350	400	500	500	600	700	800	900
	h	mm	-	-	280	350	400	480	600	650	750	800
SCHIFFSRAUM SHIPPING SPACE		m^3	0,03	0,04	0,04	0,06	0,08	0,15	0,25	0,35	0,40	0,50
GESAMTGEWICHT TOTAL WEIGHT		kg	6	8	14	20	35	70	100	165	210	290

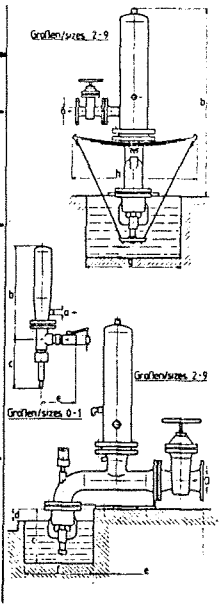

Table A.4-1 SANO ram sizes and specifications; source: Pfister + Langhanss.

WIDDER-GRÖSSE RAM-SIZE № / HÖHEN-VERHÄLTNIS HEIGHT-RELATION H : h	0	1	2	3	4	5	6	7	8	9
DN	20	25	32	40	50	65	80	100	125	150
1 : 2 +)	0,330	0,340	0,350	0,370	0,380	0,390	0,400	0,410	0,420	0,430
1 : 4	0,170	0,175	0,182	0,189	0,196	0,200	0,204	0,208	0,212	0,217
1 : 6	0,116	0,119	0,123	0,127	0,131	0,135	0,139	0,143	0,147	0,149
1 : 8	0,086	0,089	0,091	0,094	0,098	0,101	0,103	0,106	0,108	0,111
1 : 10	0,065	0,067	0,069	0,072	0,075	0,077	0,079	0,080	0,082	0,085
1 : 12	0,050	0,051	0,053	0,055	0,058	0,060	0,062	0,063	0,064	0,066
1 : 14	0,038	0,040	0,042	0,044	0,046	0,048	0,050	0,051	0,052	0,053
1 : 16		0,031	0,033	0,036	0,038	0,040	0,041	0,042	0,043	0,044
1 : 18			0,028	0,030	0,032	0,033	0,034	0,035	0,036	0,037
1 : 20				0,025	0,026	0,028	0,029	0,030	0,031	0,032

+) nur mit Spezial-Stoßventil

+) only with special ram valve

Table A.4-2 Performance characteristics for the SANO ram; source: Pfister + Langhanss.

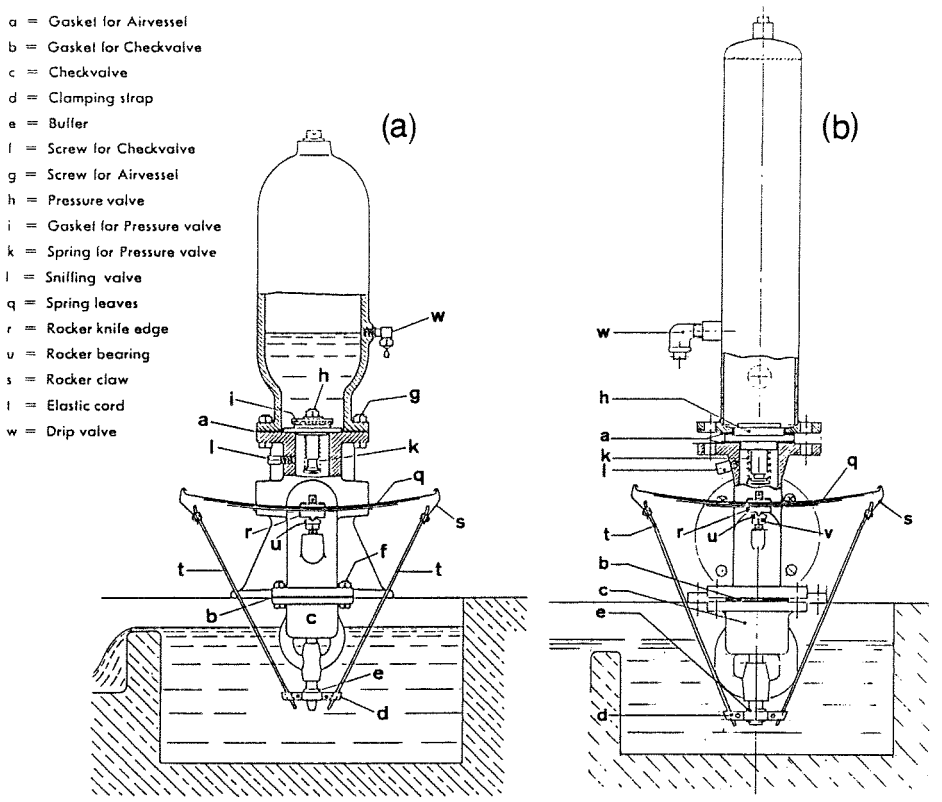

Fig. A.4-1 Sectional diagram of the SANO ram: (a) old construction, (b) new construction; source: Pfister + Langhanss.

main. When installing the ram, provisions are to be made to ensure that the waste valve is constantly immersed as pictured in Fig. A.4-1. This has to be done to prevent an uncontrolled amount of air to be sucked in through the waste valve during the suction part of the pumping cycle; it also has the minor advantage that the ram discharges its waste water with no splashing of water in the immediate vicinity of the ram.

SANO ram performance figures as claimed by the manufacturer are presented in Table A.4-2. The table lists flow ratios $^{q}/_{Q}$ for various head ratios $^{H}/_{h}$, where each column of the table applies to the specified ram size.

Test results

The SANO rams were tested at three different values of the supply head: H= 1.00 m, 2.00 m and 3.00 m respectively. The results are presented in

the tables and figures hereafter;

SANO No.1-25mm (old constr.): Tables A.4-3,4,5 and Figs. A.4-2,3,4,5

SANO No.4-50mm (new constr.): Tables A.4-6,7,8 and Figs. A.4-6,7,8,9.

Dimensionless performance characteristics ($^{q}/_{Q}$ versus $^{h}/_{H}$) for both rams together are illustrated in Fig. A.4-10.

Concluding remarks

The operation of both SANO rams turned out satisfactory. As can be seen from the figures the test results compare well with the manufacturer's data, except for the results obtained for H = 1.00 m. It should however be noted that, as mentioned before, the test configuration was not found to be optimum for the rams operating under a supply head as low as 1.00 m. Furthermore the manufacturer recommends its rams to be operated at a supply head of at least 1.50 m. Instructions (in German and English) for installing, tuning and maintaining the SANO ram are provided by the manufacturer.

Table A.4-3 Testresults SANO No.1-25 mm; supply head H = 1.00 m

Type of Hydr.Ram: **SANO NO.1 — 25mm** Supply Head H= 1.00 m

Manufacturer : PFISTER + LANGHANSS, NUERNBERG, GERMANY. Drive Pipe: D= 1" (25mm) L= 11.55 m

Test No.	Delivery Head h [m]	Head Ratio h/H [-]	Period Time T [s]	Pumping Rate q [l/min]	Supply Flow Rate Q [l/min]	Flow Ratio q/Q [-]	Efficiency $\eta = \frac{q*(h-H)}{Q*H}$ [%]	Filename	Volume of Water Delivered V_{up} [$*10^{-3}$ l/cycle]	Volume of Water Wasted V_{out} [$*10^{-3}$ l/cycle]
600	4	4	1.107	1.05	9.05	0.1160	34.8	-	19.4	167
602	5	5	1.078	0.86	9.30	0.0925	37.0	-	15.5	167
604	6	6	1.070	0.74	9.50	0.0779	39.0	-	13.2	169
606	8	8	1.065	0.56	9.50	0.0589	41.3	S1/11	9.9	169
608	10	10	1.060	0.45	9.45	0.0476	42.9	S1/10,10A	7.9	167
610	12	12	1.030	0.39	9.95	0.0392	43.1	-	6.7	171
612	14	14	1.075	0.31	9.15	0.0339	44.0	S1/9,9A	5.6	164
614	18	18	1.030	0.26	10.00	0.0260	44.2	-	4.5	172
616	23	23	1.105	0.18	8.95	0.0201	44.2	S1/8	3.3	165
618	h_{max}= 67	67	-	0	-	0	0	-	0	-

Type of Hydr.Ram: **SANO NO.1 — 25mm**

Supply Head H= 2.00 m

Manufacturer : PFISTER + LANGHANSS, NUERNBERG, GERMANY.

Drive Pipe: D= 1" (25mm) L= 11.55 m

Test No.	Delivery Head h [m]	Head Ratio h/H [-]	Period Time T [s]	Pumping Rate q [l/min]	Supply Flow Rate Q [l/min]	Flow Ratio q/Q [-]	Efficiency $\eta = \frac{q*(h-H)}{Q*H}$ [%]	Filename	Volume of Water Delivered V_{up} [$*10^{-3}$ l/cycle]	Volume of Water Wasted V_{out} [$*10^{-3}$ l/cycle]
630	9	4.5	0.577	1.50	9.25	0.1622	56.8	-	14.4	89
632	10	5	0.556	1.35	9.30	0.1452	58.1	-	12.5	86
634	12.5	6.25	0.544	1.10	9.50	0.1158	60.8	S1/7,7A	10.0	86
636	14	7	0.557	0.95	9.75	0.0974	58.5	-	8.8	91
638	17	8.5	0.547	0.78	10.00	0.0780	58.5	S1/6,6A	7.1	91
640	20	10	0.557	0.64	9.70	0.0660	59.4	-	5.9	90
642	24	12	0.524	0.57	10.35	0.0551	60.6	-	5.0	90
644	28	14	0.568	0.42	9.20	0.0462	60.1	S1/5*,5A*	4.0	87
646	30	15	0.591	0.37	8.50	0.0435	60.9	S1/5,5A	3.6	84
648	40	20	0.551	0.30	9.60	0.0313	59.4	-	2.8	88
650	50	25	0.538	0.23	9.90	0.0232	55.8	-	2.1	89
652	h_{max}= 81	40.5	-	0	-	0	0	-	0	-

Table A.4-4 Testresults SANO No.1-25 mm; supply head H = 2.00 m

Type of Hydr.Ram: **SANO NO.1 — 25mm** Supply Head H= 3.00 m

Manufacturer : PFISTER + LANGHANSS, NUERNBERG, GERMANY. Drive Pipe: D= 1" (25mm) L= 11.55 m

Test No.	Delivery Head h [m]	Head Ratio h/H [-]	Period Time T [s]	Pumping Rate q [l/min]	Supply Flow Rate Q [l/min]	Flow Ratio q/Q [-]	Efficiency $\eta=\frac{q*(h-H)}{Q*H}$ [%]	Filename	Volume of Water Delivered V_{up} [$*10^{-3}$ l/cycle]	Volume of Water Wasted V_{out} [$*10^{-3}$ l/cycle]
660	11	3.67	0.419	2.05	9.75	0.2103	56.1	-	14.3	68
662	12	4	0.426	1.85	9.50	0.1947	58.4	-	13.1	67
664	15	5	0.419	1.50	9.50	0.1579	63.2	S1/4,4A	10.5	66
666	18	6	0.390	1.30	10.10	0.1287	64.4	-	8.5	66
668	21	7	0.420	1.05	9.50	0.1105	66.3	S1/3,3A	7.3	67
670	24	8	0.405	0.93	10.40	0.0894	62.5	-	6.3	70
672	27	9	0.384	0.86	11.00	0.0782	62.6	-	5.5	70
674	30	10	0.409	0.70	9.85	0.0711	64.0	S1/2*,2A*	4.8	67
676	33	11	0.432	0.57	8.95	0.0637	63.7	S1/2,2A	4.1	64
678	42	14	0.424	0.46	9.60	0.0480	62.3	-	3.3	68
680	48	16	0.397	0.42	10.75	0.0391	58.6	-	2.8	71
682	60	20	0.403	0.30	10.00	0.0300	57.0	S1/1	2.0	67
684	h_{max}= 93	31	-	0	-	0	0	-	0	-

Table A.4-5 Testresults SANO No.1-25 mm; supply head H = 3.00 m

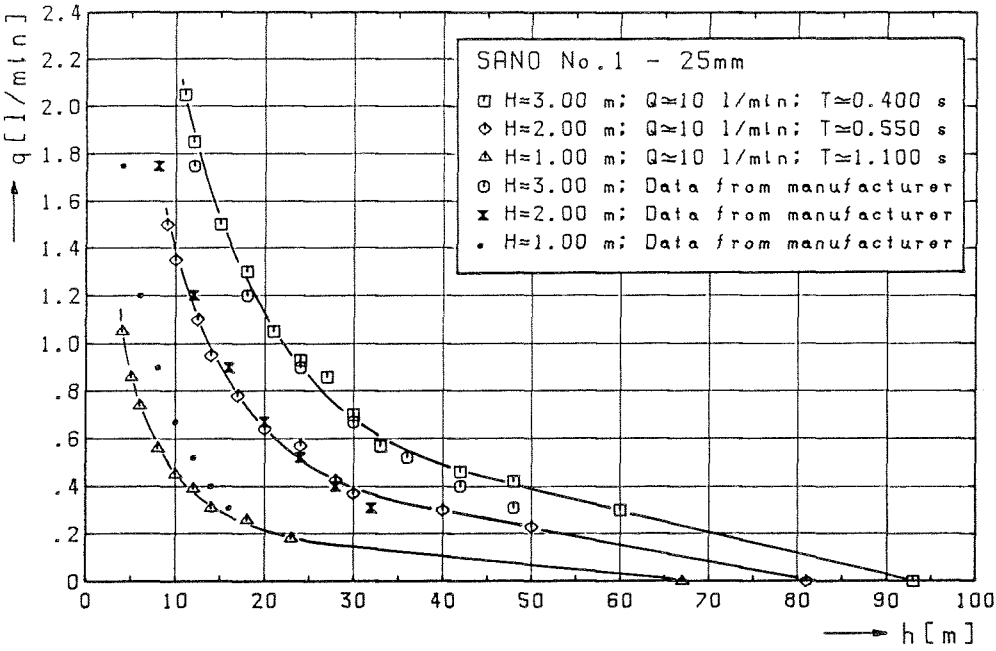

Fig. A.4-2 Pumping rate q versus delivery head h; SANO No.1-25 mm

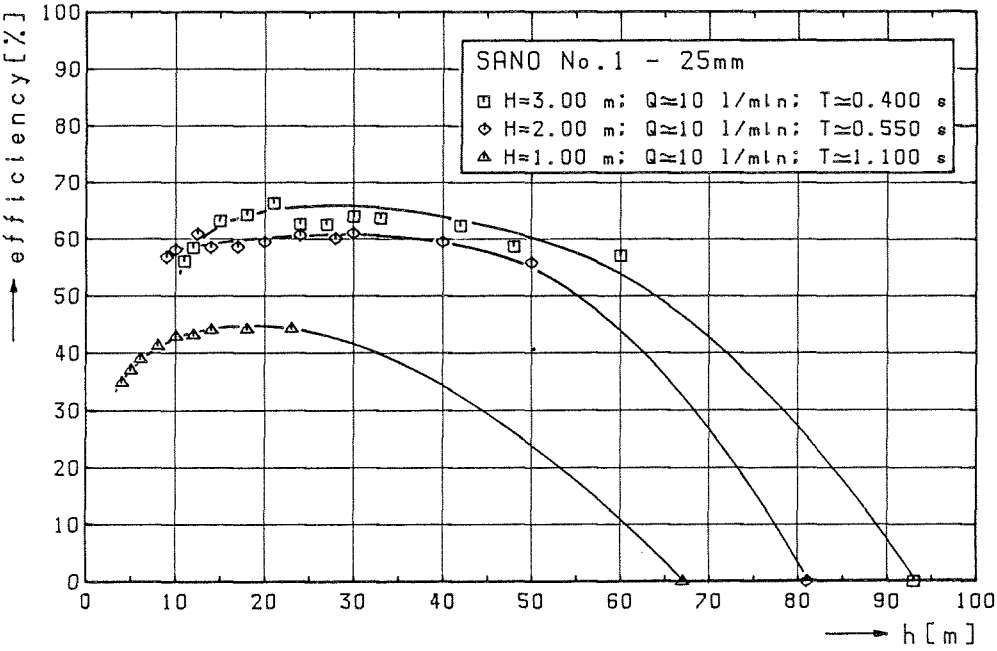

Fig. A.4-3 Rankine efficiency η versus delivery head h; SANO No.1-25 mm

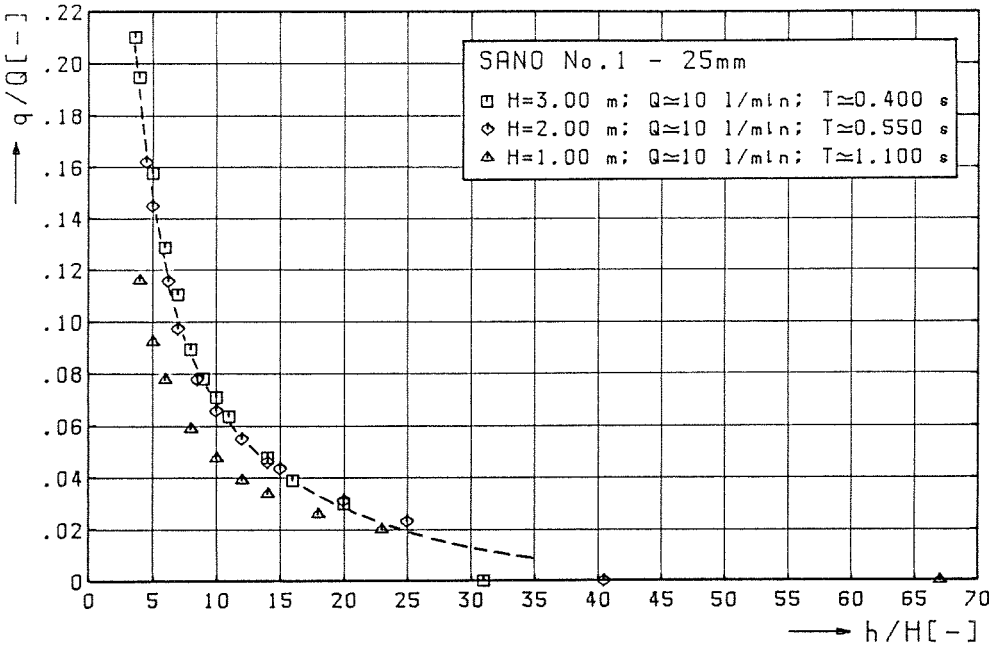

Fig. A.4-4 Flow ratio $^{q}/_{Q}$ versus head ratio $^{h}/_{H}$; SANO No.1-25 mm

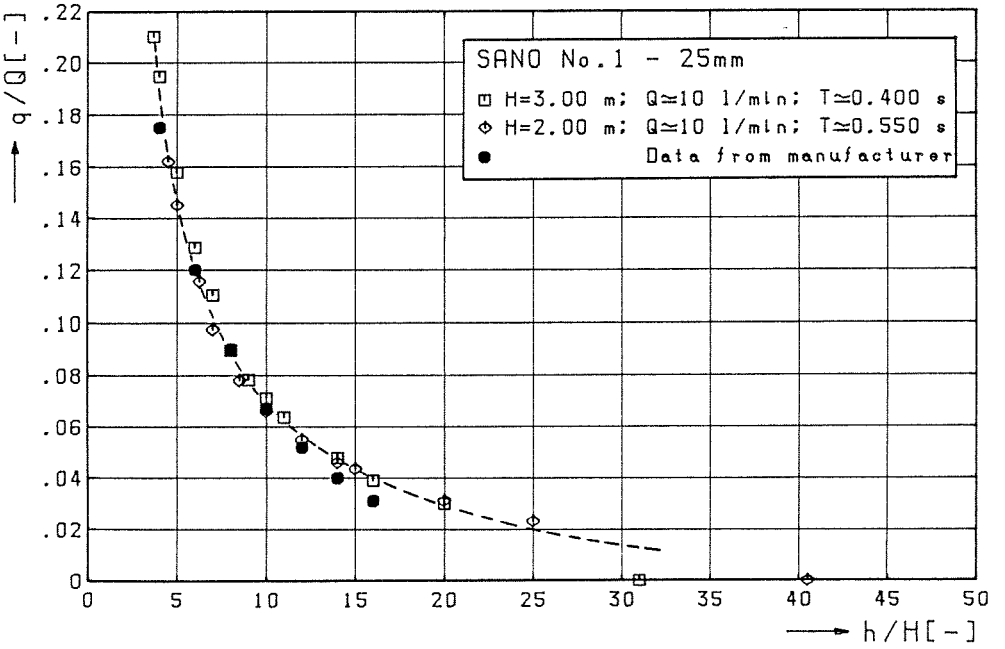

Fig. A.4-5 Flow ratio $^{q}/_{Q}$ versus head ratio $^{h}/_{H}$; SANO No.1-25 mm

Table A.4-6 Testresults SANO No.4-50 mm; supply head H = 1.00 m

Type of Hydr.Ram: **SANO No.4 — 50mm** Supply Head H= 1.00 m

Manufacturer : PFISTER + LANGHANSS, NUERNBERG, GERMANY.

Drive Pipe: D= 2" (50mm) L= 12.20 m

Test No.	Delivery Head h [m]	Head Ratio h/H [-]	Period Time T [s]	Pumping Rate q [l/min]	Supply Flow Rate Q [l/min]	Flow Ratio q/Q [-]	Efficiency $\eta=\frac{q*(h-H)}{Q*H}$ [%]	Filename	Volume of Water Delivered V_{up} [$*10^{-3}$ l/cycle]	Volume of Water Wasted V_{out} [$*10^{-3}$ l/cycle]
700	4	4	1.834	4.70	59.10	0.0795	23.9	-	143.7	1806
702	6	6	1.812	3.60	60.10	0.0599	30.0	-	108.7	1815
704	8	8	1.810	3.00	61.50	0.0488	34.1	-	90.5	1855
706	10	10	1.845	2.35	62.40	0.0377	33.9	-	72.3	1919
708	12	12	1.765	2.10	62.50	0.0336	37.0	S4/3 S4/3A	61.8	1839
710	15	15	1.890	1.65	62.50	0.0264	37.0	-	52.0	1969
712	18	18	1.890	1.45	65.50	0.0221	37.6	S4/2 S4/2A	45.7	2063
714	20	20	1.920	1.25	61.50	0.0203	38.6	-	40.0	1968
716	25	25	1.860	1.00	60.00	0.0167	40.0	-	31.0	1860
718	30	30	1.940	0.80	64.40	0.0124	36.0	-	25.9	2082
720	35	35	2.070	0.60	58.25	0.0103	35.0	S4/1 S4/1A	20.7	2010
722	40	40	2.050	0.47	56.10	0.0084	32.7	-	16.1	1917
724	50	50	1.960	0.40	59.65	0.0067	32.9	-	13.1	1949
726	h_{max}=102	102	2.400	0	44.00	0	0	-	0	1760

Table A.4-7 Testresults SANO No.4-50 mm; supply head H = 2.00 m

Type of Hydr.Ram: **SANO No.4 – 50mm** Supply Head H= 2.00 m

Manufacturer : PFISTER + LANGHANSS, NUERNBERG, GERMANY. Drive Pipe: D= 2" (50mm) L= 12.20 m

Test No.	Delivery Head h [m]	Head Ratio h/H [-]	Period Time T [s]	Pumping Rate q [l/min]	Supply Flow Rate Q [l/min]	Flow Ratio q/Q [-]	Efficiency $\eta=\frac{q*(h-H)}{Q*H}$ [%]	Filename	Volume of Water Delivered V_{up} [$*10^{-3}$ l/cycle]	Volume of Water Wasted V_{out} [$*10^{-3}$ l/cycle]
730	8	4	0.917	8.40	52.65	0.1595	47.9	-	128.4	805
732	10	5	0.901	7.00	55.10	0.1270	50.8	-	105.1	827
734	12	6	0.889	5.90	56.10	0.1052	52.6	S4/8	87.4	831
736	15	7.5	0.874	5.00	55.95	0.0894	58.1	-	72.8	815
738	18	9	0.900	4.30	55.10	0.0780	62.4	S4/7	64.5	826
740	20	10	0.887	3.90	56.00	0.0696	62.7	-	57.7	828
742	25	12.5	0.907	2.95	54.20	0.0544	62.6	S4/6 S4/6A	44.6	819
744	30	15	0.876	2.50	56.40	0.0443	62.1	-	36.5	823
746	40	20	0.926	1.75	52.70	0.0332	63.1	S4/5 S4/5A,5B	27.0	813
748	50	25	0.955	1.30	50.60	0.0257	61.7	-	20.7	805
750	60	30	0.903	1.15	54.70	0.0210	61.0	-	17.3	823
752	80	40	0.927	0.77	52.40	0.0147	57.3	-	11.9	810
754	100	50	1.054	0.40	40.95	0.0098	47.9	S4/4 S4/4A	7.0	719
756	h_{max}=120	60	1.300	0	-	0	0	-	0	-

Type of Hydr.Ram: **SANO No.4 – 50mm** Supply Head H= 3.00 m

Manufacturer : PFISTER + LANGHANSS, NUERNBERG, GERMANY.

Drive Pipe: D= 2" (50mm) L= 12.20 m

Test No.	Delivery Head h [m]	Head Ratio h/H [-]	Period Time T [s]	Pumping Rate q [l/min]	Supply Flow Rate Q [l/min]	Flow Ratio q/Q [-]	Efficiency $\eta=\frac{q*(h-H)}{Q*H}$ [%]	Filename	Volume of Water Delivered V_{up} [$*10^{-3}$ l/cycle]	Volume of Water Wasted V_{out} [$*10^{-3}$ l/cycle]
760	12	4	0.656	10.25	57.10	0.1795	53.8	–	112.1	624
762	15	5	0.645	8.55	58.40	0.1464	58.6	–	91.9	628
764	18	6	0.622	7.45	60.30	0.1235	61.8	–	77.2	625
766	21	7	0.641	6.40	58.30	0.1098	65.9	S4/12	68.4	623
768	24	8	0.618	5.75	60.15	0.0956	66.9	–	59.2	620
770	27	9	0.633	4.90	58.70	0.0835	66.8	S4/11 S4/11A	51.7	619
772	30	10	0.648	4.20	56.70	0.0741	66.7	–	45.4	612
774	36	12	0.608	3.70	61.90	0.0598	65.8	–	37.5	627
776	45	15	0.653	2.80	56.80	0.0493	69.0	S4/10 S4/10A,10B	30.5	618
778	60	20	0.663	1.95	56.10	0.0348	66.0	–	21.5	620
780	75	25	0.613	1.60	61.45	0.0260	62.5	–	16.3	628
782	90	30	0.665	1.10	54.95	0.0200	58.1	–	12.2	609
784	120	40	0.798	0.45	37.10	0.0121	47.3	S4/9 S4/9A	6.0	493
786	h_{max}=138	46	–	0	–	0	0	–	0	–

Table A.4-8 Testresults SANO No.4-50 mm; supply head H = 3.00 m

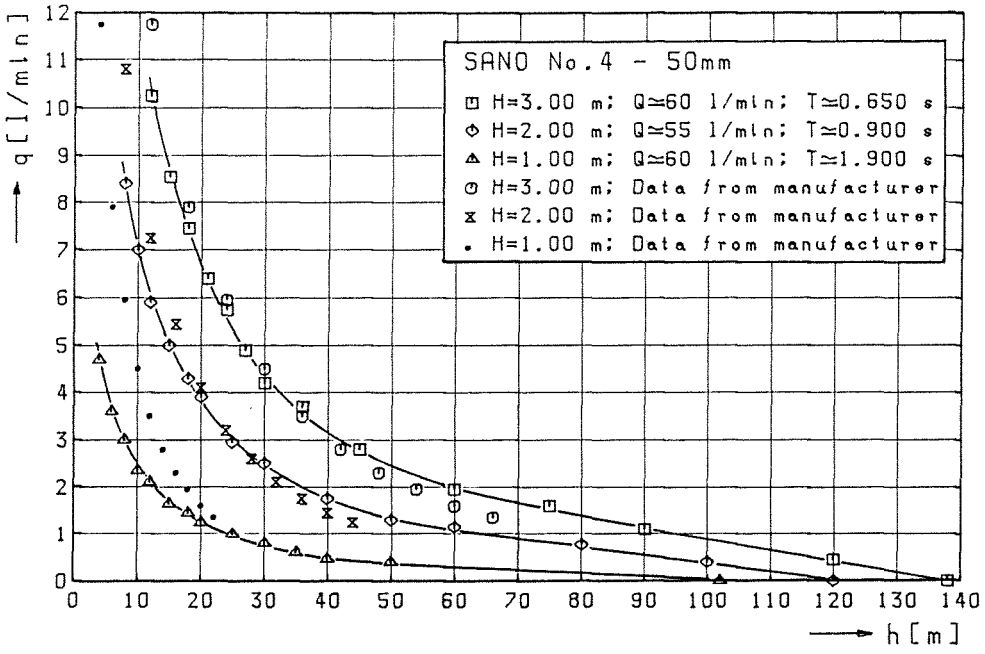

Fig. A.4-6 Pumping rate q versus delivery head h; SANO No.4-50 mm

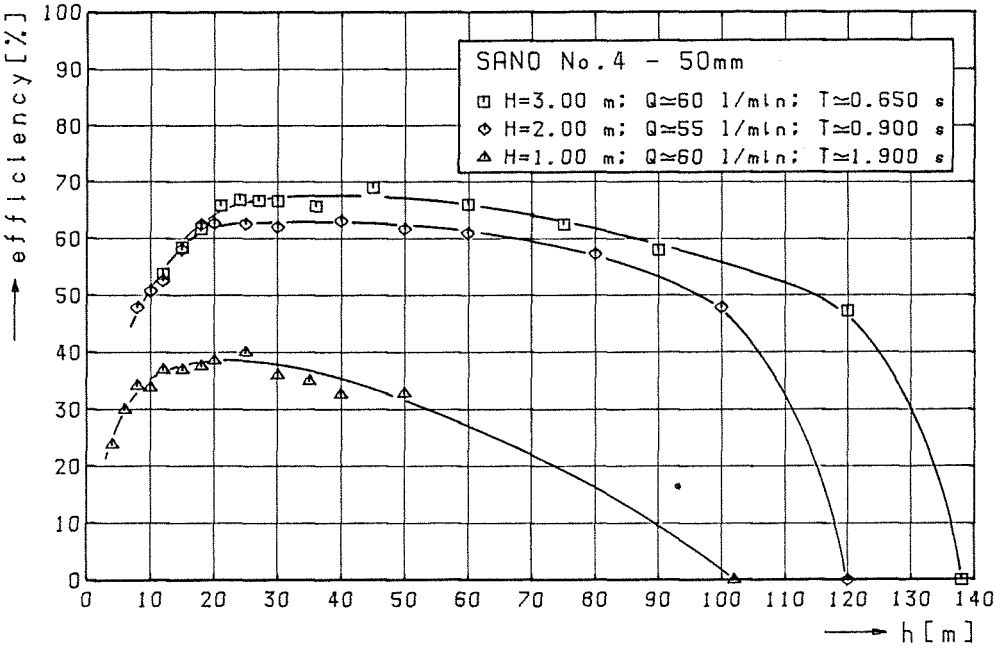

Fig. A.4-7 Rankine efficiency η versus delivery head h; SANO No.4-50 mm

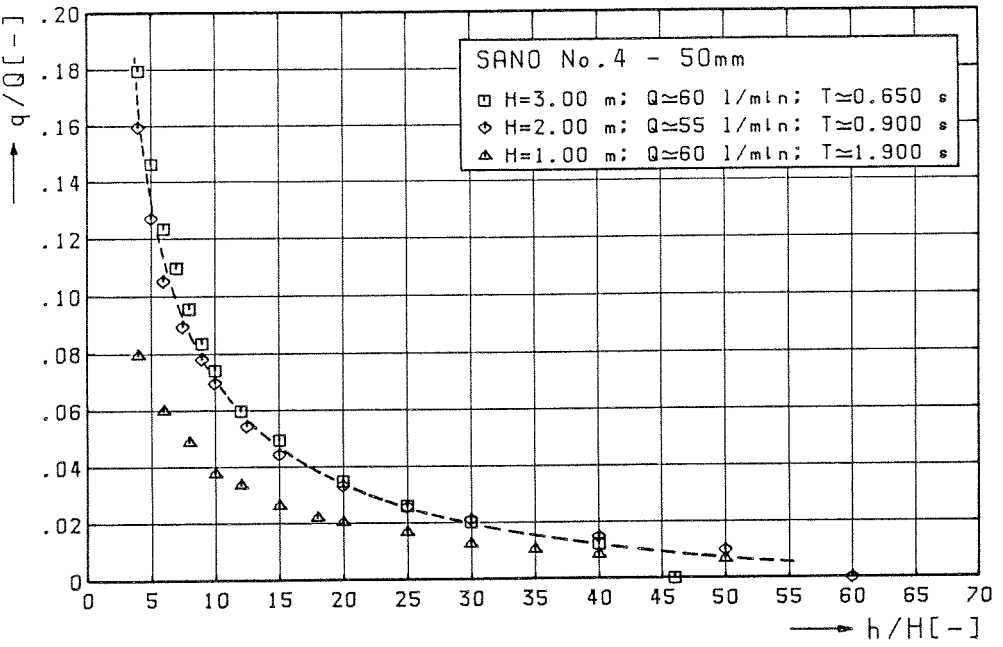

Fig. A.4-8 Flow ratio $^{q}/_{Q}$ versus head ratio $^{h}/_{H}$; SANO No.4-50 mm

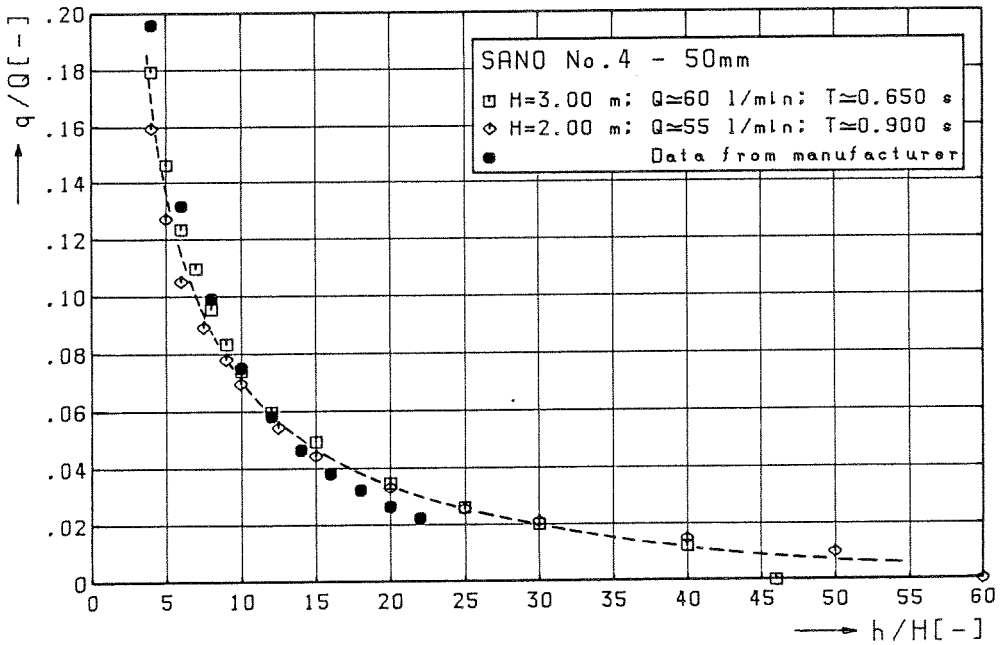

Fig. A.4-9 Flow ratio $^{q}/_{Q}$ versus head ratio $^{h}/_{H}$; SANO No.4-50 mm

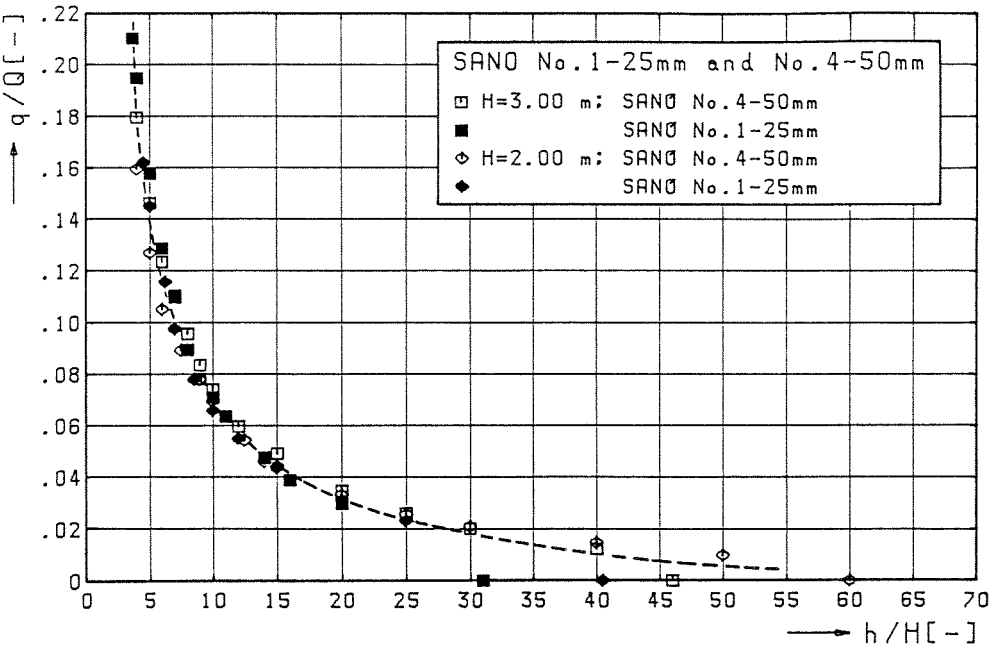

Fig. A.4-10 Dimensionless performance characteristics;
SANO No.1-25 mm and No.4-50 mm

A.5 DAVEY / RIFE

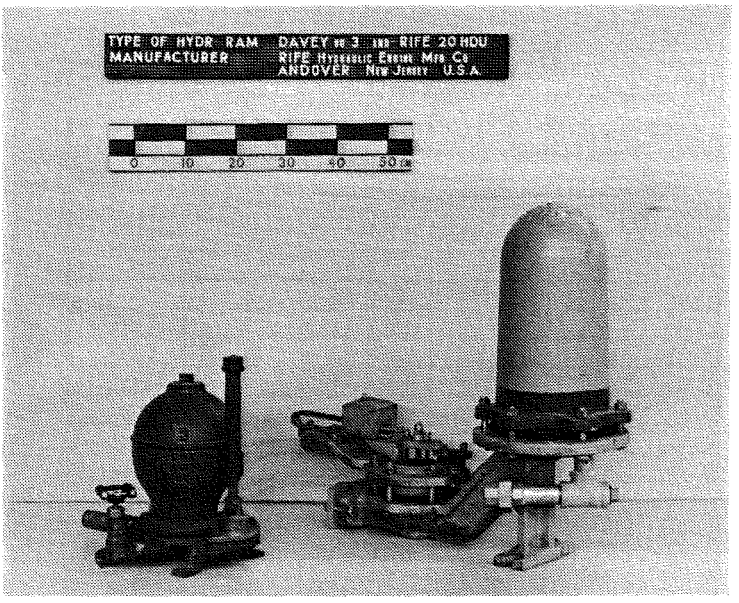

Rams tested (see picture): Davey No.3 (1")
Rife 20HDU (2")

Manufacturer: Rife Hydraulic Engine Manufacturing Co.,
Norristown - U.S.A.

Description

The Rife ram is a fairly standard design made of cast-iron with galvanized and plated steel parts. The ram is available in three so-called high-base models (see Table A.5-1 and Fig. A.5-1):

- BU series, suited for supply flows from approx. 7.5 l/min up to 75 l/min and delivery heads up to 50 m,
- SU series, suited for supply flows from approx. 10 l/min up to 1325 l/min and delivery heads up to 75 m,
- HDU series, suited for supply flows from approx. 10 l/min up to 1500 l/min and delivery heads up to 150 m.

It should be noticed that the intake capacities mentioned in Table A.5-1 are given in gallons per minute (1 US gallon = 3.785 litres).

RAM MODEL #	INTAKE DRIVE PIPE	DISCHARGE DELIVERY PIPE SIZE	INTAKE CAP GPM USED MIN. MAX.	MIN,VERT FALL REQ (IN fett)	SHIP & WT IN Lb. APPROX.
RIFE "NEW MODEL" SERIES BU RAMS (4-BOLTS DESIGN) Maximum vertical fall 15 ft. Maximum vertical lift 150 ft.					
10BU	1¼"	3/4"	2 - 7	3	120
15BU	1½"	3/4"	5 - 13	3	120
20BU	2"	1"	8 - 20	3	120
RIFE "EVERLASTING" STANDARD RAMS A more rugged development of the previous series "A" (6-Bolts Design) Maximum vertical fall 25 ft. Maximum vertical lift 250 ft.					
10SU	1¼"	3/4"	3 - 10	3	125
15SU	1½"	3/4"	5 - 14	3	125
20SU	2"	1"	10 - 22	4	125
20SUL	2"	1"	12 - 30	4	270
25SU	2½"	1"	15 - 45	4	270
30SU	3"	1¼"	20 - 70	4	270
40SU	4"	2"	35 - 125	4	565
60SU	6"	3"	75 - 350	4	1325
RIFE "UNIVERSAL" HEAVY DUTY RAMS (6-BOLTS DESIGN) Maximum vertical fall 50 ft. Maximum vertical lift 500 ft.					
10HDU	1¼"	3/4"	3 - 10	3	170
15HDU	1½"	3/4"	5 - 15	3	170
20HDU	2"	1"	10 - 25	4	170
20HDUL	2"	1"	12 - 33	4	310
25HDU	2½"	1"	15 - 45	4	310
30HDU	3"	1¼"	25 - 75	4	310
40HDU	4"	2"	35 - 150	5	565
60HDU	6"	3"	75 - 400	5	1325

Table A.5-1 Rife ram models and specifications; source: Rife Hydr.Eng.Mfg.Co.

Vertical Lift in Feet Including Delivery Pipe Friction

Vertical Fall in Feet	8	16	25	50	75	100	125	150	200	250	300	400	500	
4	22.5%	12.5%	8.0%	3.6%	1.6%									4
8		22.5%	16.0%	9.6%	6.4%	4.8%	3.5%	2.7%	2.0%					8
12			21.5%	13.2%	9.6%	7.2%	5.7%	4.8%	3.3%	2.4%	2.0%			12
16				16.0%	11.7%	9.6%	7.7%	6.4%	4.8%	3.8%	2.9%	2.0%		16
20				18.0%	14.7%	12.0%	9.6%	8.0%	6.0%	4.8%	4.0%	2.5%	2.0%	20
25				22.5%	16.7%	13.8%	12.0%	10.0%	7.5%	6.0%	5.0%	3.8%	2.5%	25
30					18.0%	15.0%	13.2%	12.0%	9.0%	7.2%	6.0%	4.5%	3.3%	30
35					21.0%	17.5%	15.2%	14.0%	10.5%	8.4%	7.0%	5.3%	4.2%	35
40						18.0%	16.0%	14.7%	12.0%	9.6%	8.0%	6.0%	4.8%	40
50						22.5%	18.0%	16.7%	13.8%	12.0%	10.0%	7.5%	6.0%	50
	8	16	25	50	75	100	125	150	200	250	300	400	500	

Table A.5-2 Performance chart for the Rife ram; source: Rife Hydr.Eng.Mfg.Co.

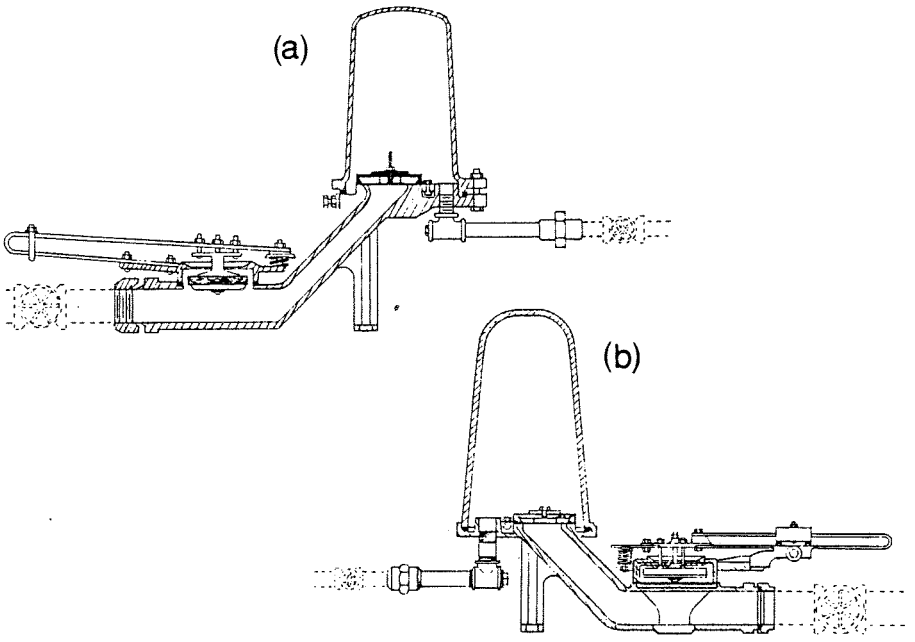

Fig. A.5-1 Sectional diagram of the Rife ram: (a) BU series, (b) SU and HDU series; source: Rife Hydr.Eng.Mfg.Co.

In the BU series the design uses a spring-mounted rubber waste valve (Fig. A.5-1a); the 'standard' (SU) and 'heavy duty' (HDU) rams are equipped with a weight-loaded rubber waste valve mounted on a rocker-arm (Fig. A.5-1b). For all designs the delivery valve consists of a rubber disc covering a gridiron seat. The rams can be tuned to the available source supply by adjusting the waste valve stroke and by increasing/decreasing the spring or weight load on the valve. All rams are equipped with an adjustable air valve; each unit includes a special steel strainer for the intake end of the drive pipe. Stop-valves for drive pipe and delivery pipe are optional extras.

In its manual of information the manufacturer publishes a performance chart for the Rife rams (Table A.5-2), which lists the ratio $^{q}/_{Q}$ (percentages) under various conditions of supply head H (vertical fall) and delivery head h (vertical lift).

The Rife Company also manufacturers a less efficient and less expensive ram in a low-base configuration under the trade name 'Davey', suited for supply flows from approx. 3 l/min up to 50 l/min (see Table A.5-3). The

SIZE OF RAM No.	QUANITY OF WATER FURNISHED PER MIN. BY SPRING OR BROOK TO WHICH RAM IS ADAPTED	SIZE OF PIPE DRIVE DISCHARGE	
2	3 Quarts to 2 Gallons	3/4"	½"
3	1½" Gallons to 4 Gallons	1"	½"
4	3 Gallons to 7 Gallons	1¼"	3/4"
5	6 Gallons to 14 Gallons	2"	1"

Table A.5-3 Davey ram specifications;
source: Rife Hydr.Eng.Mfg.Co.

Davey ram uses a weight-loaded gunmetal waste valve and a weight-loaded leather washer as delivery valve. No performance figures were provided by the manufacturer for these rams.

Test results

The Rife ram was tested at three different values of the supply head: H= 1.25 m, 2.00 m and 3.00 m; the Davey ram at H= 1.00 m, 2.00 m and 3.00 m respectively. The results are presented in the tables and figures hereafter;

Davey No.3: Tables A.5-4,5,6 and Figs. A.5-2,3,4

Rife 20HDU: Tables A.5-7,8,9 and Figs. A.5-5,6,7,8.

The manufacturer's data for the Rife ram as pictured in the Figs. A.5-5 and A.5-8 are derived from Table A.5-2 by interpolation. Although no similarity in dimensionless performance figures is to be expected (both rams are of a complete different nature) combined characteristics ($^{q}/_{Q}$ versus $^{h}/_{H}$) are illustrated in Fig. A.5-9.

Concluding remarks

The performances of the Rife ram under laboratory conditions were found to be somewhat disappointing, the heavy waste valve construction causing a relative slow action of the ram. Likely the results may improve to some extent when operating the ram at higher supply heads. In addition, the waste valve assembly proved to be rather complex with many bolts and nuts which may work loose. Among other things the manual of information supplied with the Rife ram includes a good set of instructions for the installation, adjustment and maintanance of the ram. Though claimed to be less efficient the Davey ram performed well within its limits, as can be seen from the relevant figures.

Table A.5-4 Testresults Davey No.3; supply head H = 1.00 m

Type of Hydr.Ram: **DAVEY No.3**

Manufacturer : RIFE Hydraulic Engine Mfg.Co., NORRISTOWN - U.S.A.

Supply Head H= 1.00 m

Drive Pipe: D= 1" (25mm)
L= 11.60 m

Test No.	Delivery Head h [m]	Head Ratio h/H [-]	Period Time T [s]	Pumping Rate q [l/min]	Supply Flow Rate Q [l/min]	Flow Ratio q/Q [-]	Efficiency $\eta=\frac{q*(h-H)}{Q*H}$ [%]	Filename	Volume of Water Delivered V_{up} [$*10^{-3}$ l/cycle]	Volume of Water Wasted V_{out} [$*10^{-3}$ l/cycle]
800	2	2	2.225	2.67	11.30	0.2363	23.6	-	99.0	419
802	3	3	2.010	1.91	12.55	0.1522	30.4	-	64.0	420
804	4	4	1.941	1.45	13.15	0.1103	33.1	-	46.9	425
806	6	6	1.822	0.95	13.65	0.0696	34.8	-	28.8	415
808	8	8	1.791	0.70	13.65	0.0513	35.9	-	20.9	407
810	10	10	1.797	0.53	14.00	0.0379	34.1	-	15.9	419
812	12	12	1.845	0.44	14.00	0.0314	34.6	-	13.5	431
814	14	14	1.793	0.36	13.25	0.0272	35.3	-	10.7	396
816	h_{max}= 28	28	-	0	-	0	0	-	0	-

Table A.5-5 Testresults Davey No.3; supply head H = 2.00 m

Type of Hydr.Ram: **DAVEY No.3** Supply Head H= 2.00 m

Manufacturer : RIFE Hydraulic Engine Mfg.Co., NORRISTOWN - U.S.A.

Drive Pipe: D= 1" (25mm) L= 11.60 m

Test No.	Delivery Head h [m]	Head Ratio h/H [-]	Period Time T [s]	Pumping Rate q [l/min]	Supply Flow Rate Q [l/min]	Flow Ratio q/Q [-]	Efficiency $\eta=\frac{q*(h-H)}{Q*H}$ [%]	Filename	Volume of Water Delivered V_{up} [$*10^{-3}$ l/cycle]	Volume of Water Wasted V_{out} [$*10^{-3}$ l/cycle]
820	4	2	1.203	3.77	11.20	0.3366	33.7	-	75.6	225
822	8	4	1.031	2.10	13.05	0.1609	48.3	-	36.1	224
824	12	6	0.986	1.35	13.35	0.1011	50.6	-	22.2	219
826	16	8	0.973	0.97	13.65	0.0711	49.7	-	15.7	221
828	20	10	0.989	0.73	13.15	0.0555	50.0	-	12.0	217
830	24	12	1.041	0.54	12.00	0.0450	49.5	-	9.4	208
832	28	14	1.043	0.41	11.90	0.0345	44.8	-	7.1	207
834	h_{max}= 44	22	-	0	-					

Type of Hydr.Ram: **DAVEY No. 3** Supply Head H= 3.00 m

Manufacturer : RIFE Hydraulic Engine Mfg.Co., NORRISTOWN - U.S.A.

Drive Pipe: D= 1" (25mm) L= 11.60 m

Test No.	Delivery Head h [m]	Head Ratio h/H [-]	Period Time T [s]	Pumping Rate q [l/min]	Supply Flow Rate Q [l/min]	Flow Ratio q/Q [-]	Efficiency $\eta=\frac{q*(h-H)}{Q*H}$ [%]	Filename	Volume of Water Delivered V_{up} [$*10^{-3}$ l/cycle]	Volume of Water Wasted V_{out} [$*10^{-3}$ l/cycle]
840	6	2	0.939	4.80	10.75	0.4465	44.6	-	75.1	168
842	12	4	0.743	2.60	13.30	0.1955	58.6	-	32.2	165
844	18	6	0.712	1.64	13.70	0.1197	59.8	-	19.5	163
846	21	7	0.724	1.33	13.80	0.0964	57.8	-	16.0	167
848	24	8	0.713	1.11	13.55	0.0819	57.3	-	13.2	161
850	27	9	0.748	0.91	12.80	0.0711	56.9	D1	11.3	160
852	30	10	0.767	0.72	12.05	0.0598	53.8	-	9.2	154
854	33	11	0.760	0.63	12.20	0.0516	51.6	-	8.0	155
856	36	12	0.757	0.54	11.75	0.0460	50.6	-	6.8	148
858	39	13	0.785	0.44	11.10	0.0396	47.6	-	5.8	145
860	42	14	0.798	0.38	10.50	0.0362	47.0	-	5.1	140
862	h_{max}= 54	18	-	0	-	0	0	-	0	-

Table A.5-6 Testresults Davey No.3; supply head H = 3.00 m

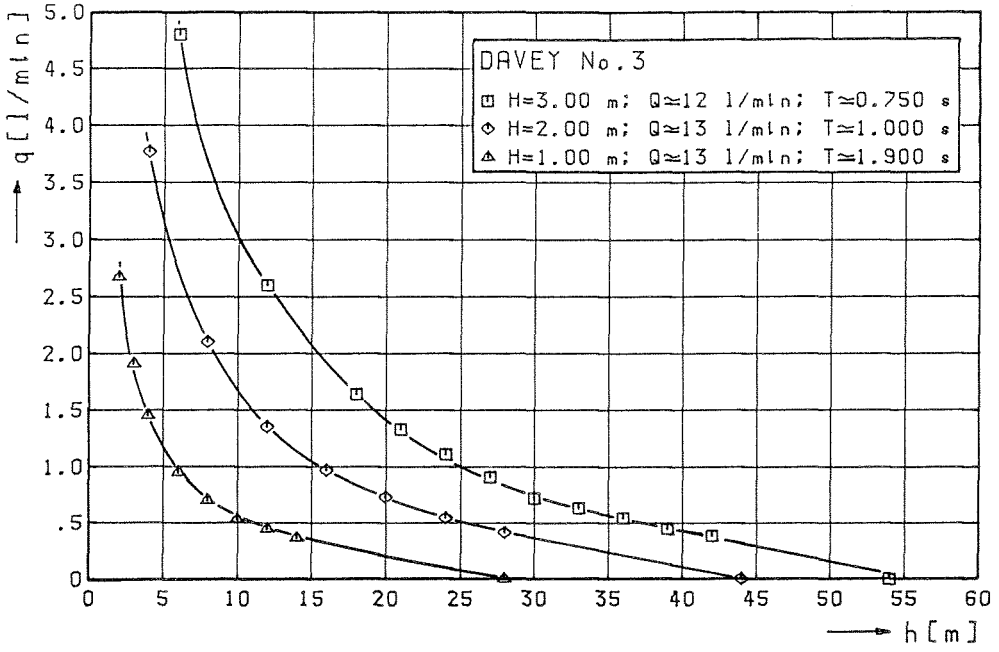

Fig. A.5-2 Pumping rate q versus delivery head h; Davey No.3

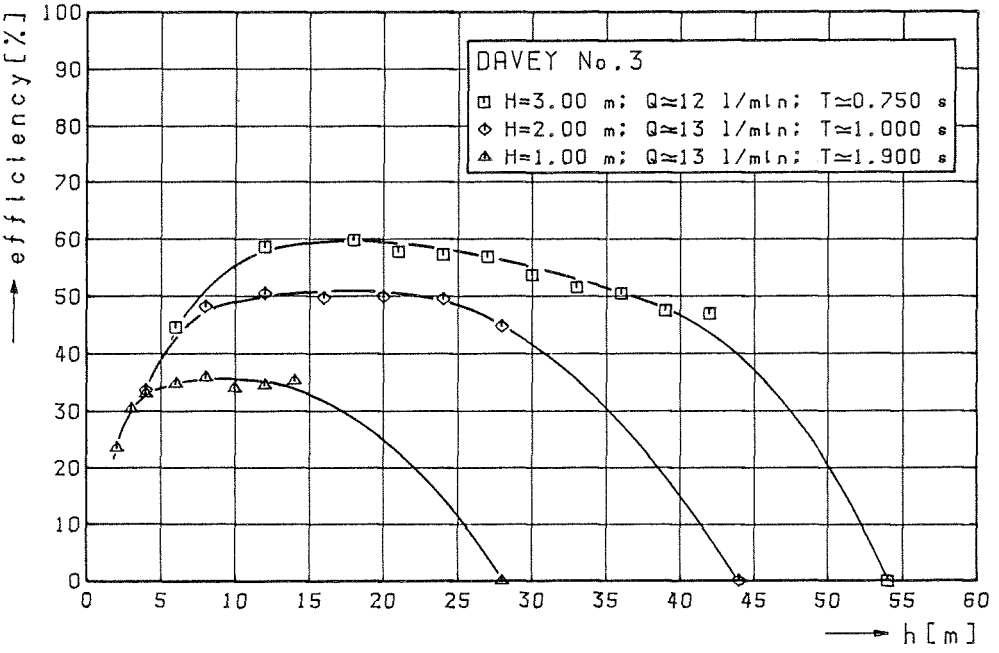

Fig. A.5-3 Rankine efficiency η versus delivery head h; Davey No.3

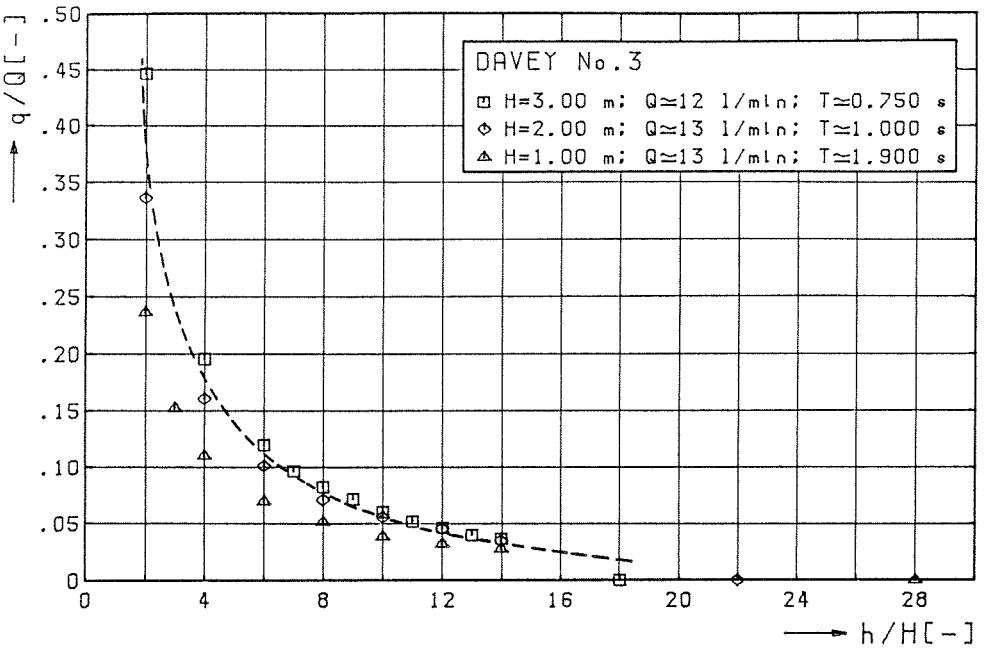

Fig. A.5-4 Flow ratio $^{q}/_{Q}$ versus head ratio $^{h}/_{H}$; Davey No.3

Type of Hydr.Ram: **RIFE 20HDU** — Supply Head H= 1.25 m

Manufacturer : RIFE Hydraulic Engine Mfg.Co., NORRISTOWN - U.S.A. — Drive Pipe: D= 2" (50mm), L= 12.10 m

Test No.	Delivery Head h [m]	Head Ratio h/H [-]	Period Time T [s]	Pumping Rate q [l/min]	Supply Flow Rate Q [l/min]	Flow Ratio q/Q [-]	Efficiency $\eta=\frac{q*(h-H)}{Q*H}$ [%]	Filename	Volume of Water Delivered V_{up} [$*10^{-3}$ l/cycle]	Volume of Water Wasted V_{out} [$*10^{-3}$ l/cycle]
900	4	3.2	2.545	3.90	84.50	0.0462	10.2	-	165.4	3584
902	8	6.4	2.477	2.65	87.25	0.0304	16.4	-	109.4	3602
904	12	9.6	2.482	2.00	87.50	0.0229	19.7	RF20/26	82.7	3620
906	16	12.8	2.485	1.75	88.15	0.0199	23.4	RF20/25	72.5	3651
908	20	16.0	2.455	1.50	89.20	0.0168	25.2	-	61.4	3650
910	24	19.2	2.500	1.25	86.75	0.0144	26.2	RF20/24	52.1	3615
912	30	24.0	2.474	1.05	86.80	0.0121	27.8	-	43.3	3579
914	45	36.0	2.600	0.65	81.50	0.0080	27.9	RF20/23, 23A, 23B	28.2	3532
916	70	56.0	2.560	0.40	85.20	0.0047	25.8	-	17.1	3635
918	90	72.0	2.575	0.27	81.15	0.0033	23.6	RF20/22	11.6	3483
920	h_{max}=112	89.6	-	0	-	0	0	-	0	-

Table A.5-7 Testresults Rife 20HDU; supply head H = 1.25 m

Type of Hydr.Ram: **RIFE 20HDU** — Supply Head H= 2.00 m

Manufacturer : RIFE Hydraulic Engine Mfg.Co., NORRISTOWN - U.S.A. — Drive Pipe: D= 2" (50mm), L= 12.10 m

Test No.	Delivery Head h [m]	Head Ratio h/H [-]	Period Time T [s]	Pumping Rate q [l/min]	Supply Flow Rate Q [l/min]	Flow Ratio q/Q [-]	Efficiency $\eta = \frac{q*(h-H)}{Q*H}$ [%]	Filename	Volume of Water Delivered V_{up} [$*10^{-3}$ l/cycle]	Volume of Water Wasted V_{out} [$*10^{-3}$ l/cycle]
930	4	2	1.400	8.90	71.15	0.1251	12.5	-	207.7	1660
932	8	4	1.305	6.20	76.70	0.0808	24.2	-	134.9	1668
934	10	5	1.290	5.40	79.00	0.0684	27.3	RF20/21	116.1	1699
936	12	6	1.274	4.85	79.30	0.0612	30.6	RF20/20	103.0	1684
938	16	8	1.259	4.00	80.50	0.0497	34.8	RF20/19	83.9	1689
940	20	10	1.285	3.40	79.20	0.0429	38.6	RF20/18	72.8	1696
942	26	13	1.260	2.75	79.75	0.0345	41.4	RF20/17	57.8	1675
944	30	15	1.280	2.30	77.25	0.0298	41.7	RF20/16	49.1	1648
946	40	20	1.250	1.90	79.20	0.0240	45.6	RF20/15	39.6	1650
948	52	26	1.350	1.25	70.80	0.0177	44.1	RF20/14, 14A, 14B	28.1	1593
950	70	35	1.320	0.98	74.00	0.0132	45.0	-	21.6	1628
952	90	45	1.300	0.68	76.25	0.0089	39.2	-	14.7	1652
954	114	57	1.425	0.30	62.90	0.0048	26.7	RF20/13	7.1	1494
956	h_{max}=133	66.5	-	0	-	0	0	-	0	-

Table A.5-8 Testresults Rife 20HDU; supply head H = 2.00 m

Type of Hydr.Ram: **RIFE 20HDU** — Supply Head H= 3.00 m

Manufacturer : RIFE Hydraulic Engine Mfg.Co., NORRISTOWN - U.S.A. — Drive Pipe: D= 2" (50mm), L= 12.10 m

Test No.	Delivery Head h [m]	Head Ratio h/H [-]	Period Time T [s]	Pumping Rate q [l/min]	Supply Flow Rate Q [l/min]	Flow Ratio q/Q [-]	Efficiency $\eta=\frac{q*(h-H)}{Q*H}$ [%]	Filename	Volume of Water Delivered V_{up} [$*10^{-3}$ l/cycle]	Volume of Water Wasted V_{out} [$*10^{-3}$ l/cycle]
960	6	2	0.965	12.90	72.00	0.1792	17.9	-	207.5	1158
962	9	3	0.882	9.70	78.70	0.1233	24.6	-	142.6	1157
964	12	4	0.865	8.25	80.80	0.1021	30.6	RF20/12	118.9	1165
966	15	5	0.853	7.00	81.85	0.0855	34.2	RF20/11	99.5	1164
968	21	7	0.847	5.70	83.10	0.0686	41.2	RF20/10	80.5	1173
970	24	8	0.828	5.20	84.20	0.0618	43.2	RF20/9	71.8	1162
972	30	10	0.858	3.90	81.10	0.0481	43.3	RF20/8 RF20/8A,8B	55.8	1160
974	36	12	0.835	3.50	83.25	0.0420	46.2	RF20/7	48.7	1159
976	48	16	0.866	2.40	78.70	0.0305	45.7	RF20/6	34.6	1136
978	57	19	0.890	1.95	74.90	0.0260	46.9	RF20/5,5A	28.9	1111
980	75	25	0.858	1.60	80.00	0.0200	48.0	RF20/4	22.9	1144
982	90	30	0.840	1.25	82.40	0.0152	44.0	RF20/3,3A	17.5	1154
984	105	35	0.888	0.82	75.30	0.0109	37.0	RF20/2	12.1	1114
986	120	40	0.947	0.51	66.50	0.0077	29.9	-	8.0	1050
988	135	45	0.999	0.25	55.75	0.0045	19.7	RF20/1	4.2	928
990	h_{max}=154	51.33	-	0	-	0	0	-	0	-

Table A.5-9 Testresults Rife 20HDU; supply head H = 3.00 m

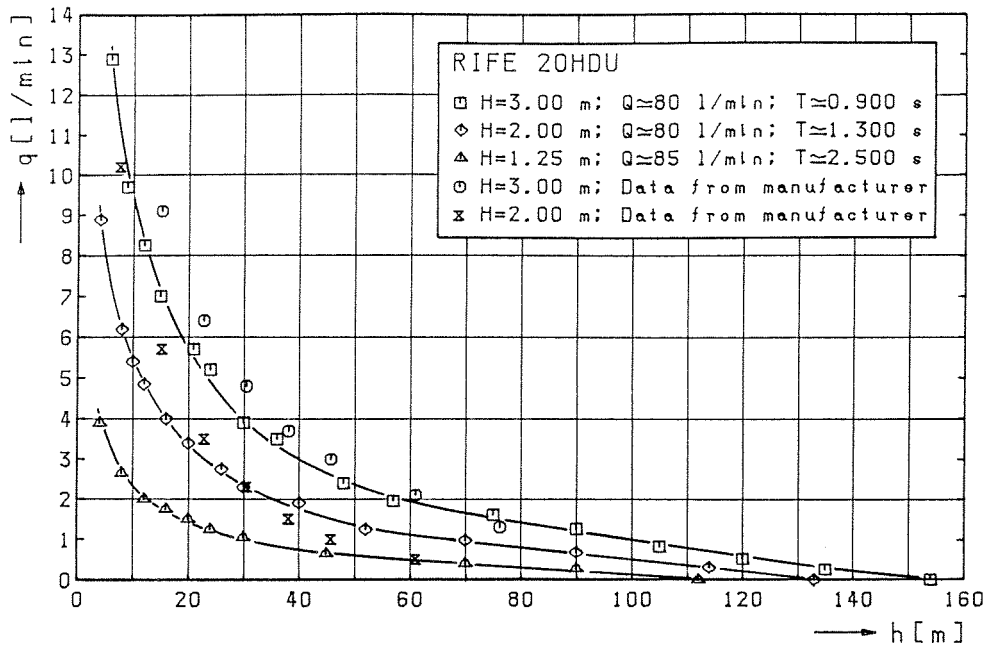

Fig. A.5-5 Pumping rate q versus delivery head h; Rife 20HDU

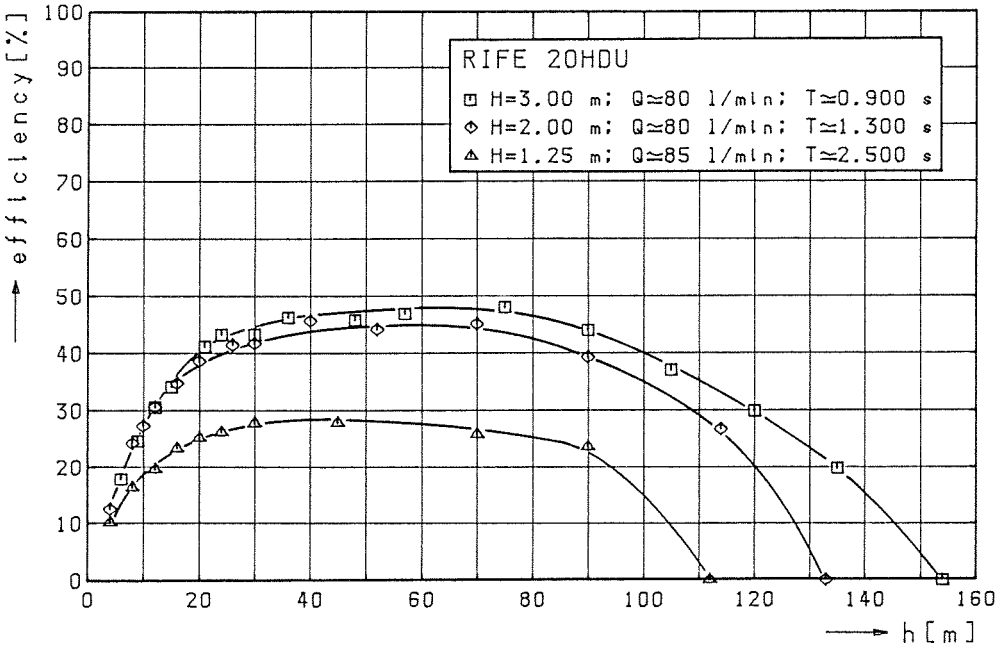

Fig. A.5-6 Rankine efficiency η versus delivery head h; Rife 20HDU

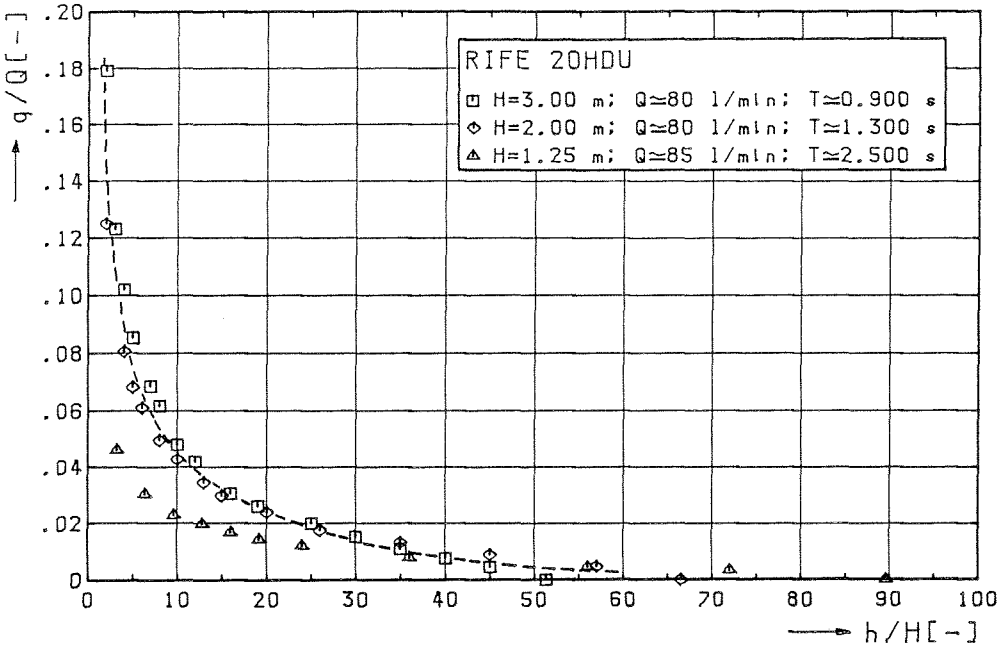

Fig. A.5-7 Flow ratio $^{q}/_{Q}$ versus head ratio $^{h}/_{H}$; Rife 20HDU

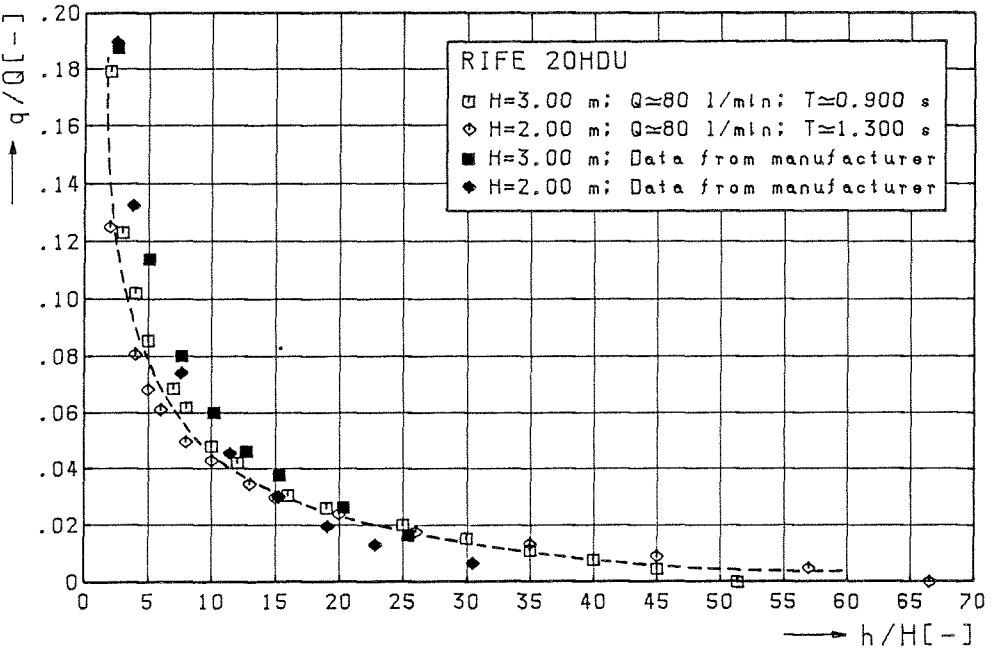

Fig. A.5-8 Flow ratio $^{q}/_{Q}$ versus head ratio $^{h}/_{H}$; Rife 20HDU

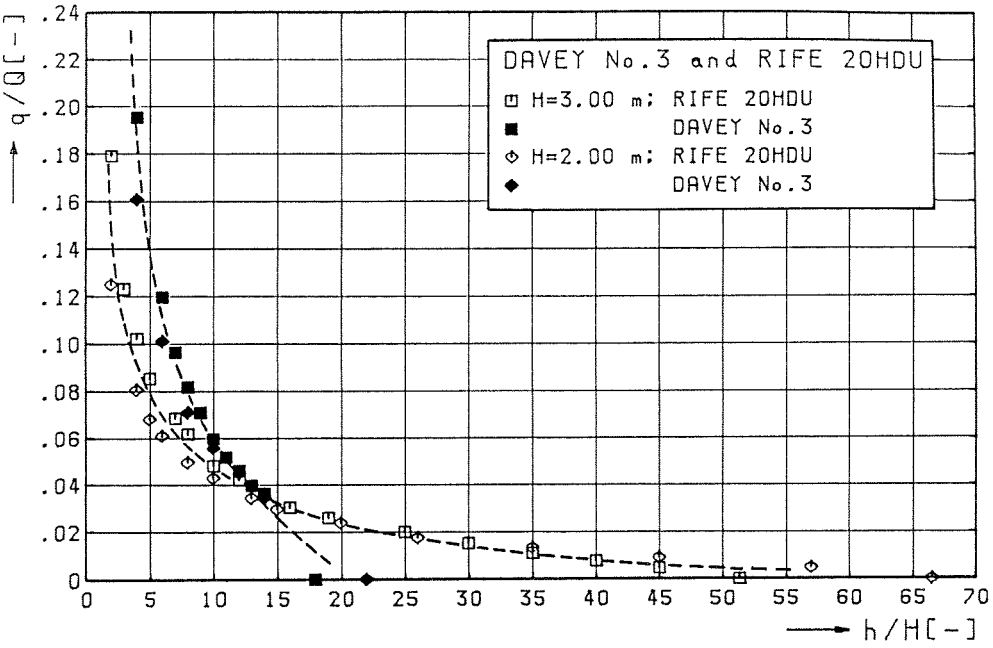

Fig. A.5-9 Dimensionless performance characteristics; Davey No.3 and Rife 20HDU

A.6 SCHLUMPF

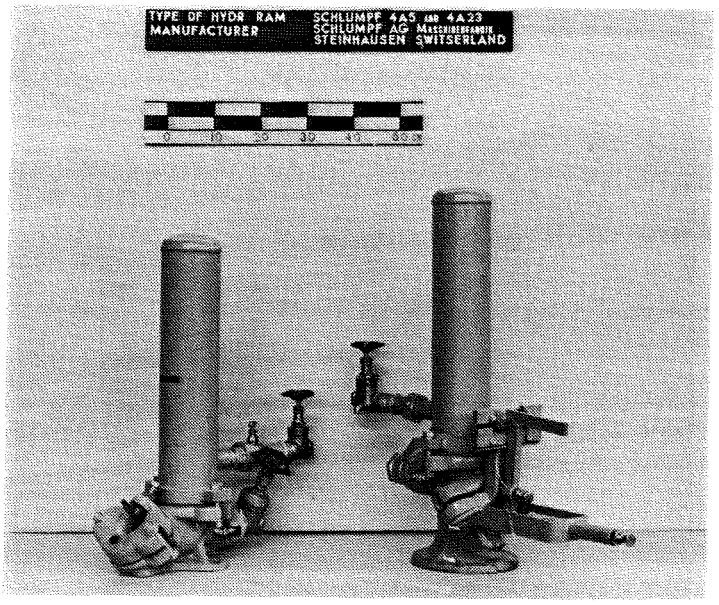

Rams tested (see picture): Schlumpf 4A5 (1 1/2")
Schlumpf 4A23 (1 1/2")

Manufacturer: Schlumpf AG Maschinenfabrik,
Steinhausen - Switzerland.

Description

The Schlumpf hydraulic ram is a design available in two models: model A5 and model A23. The rams are partly made of cast-iron and partly of steel, with minor gunmetal and galvanized iron components. Standard sizes of the model A5 range from size 1 (3/4"-20 mm) through to size 6 (2 1/2"-65 mm) covering source supplies from 3 l/min up to 150 l/min (see Table A.6-1). Sizes of the model A23 continue up to size 8 (4"-100 mm) suitable for supply flows up to 400 l/min. Larger sizes are available on request. The Schlumpf A23 is equipped with an adjustable spring-loaded rubber waste valve mounted on a rocker with adjustable stroke length. The less efficient model A5 uses a weight-loaded rubber waste valve with adjustable valve stroke. For both models the delivery

Typ	A 5	A 23	A 5	A 23	A 5	A 23	A 5	A 23	A 5	A 23	A 5	A 23	A 23	A 23
Grösse	1		2		3		4		5		6		7	8
Triebleitung	¾ "		1 "		1¼ "		1½ "		2 "		2½ "		3 "	4 "
Förderleitung	½ "		½ "		¾ "		1 "		1 "		1¼ "		1½ "	2 "
lit./min.	3—10		6—20		15—35		30—60		50—100		80—150		100—200	150—400
Länge des Widders cm	38	55	40	52	50	76	50	78	70	102	72	102	127	127
Breite des Widders cm	21		21		23		29		32		32		50	
Höhe des Widders cm	59	66	59	66	64	72	64	72	90	108	92	108	125	
Gewicht netto kg	14	18	14	18	30	36	31	37	67	110	95	112	275	
Gewicht brutto kg	18	22	18	22	47	53	47	54	83	143	120	145	360	

Table A.6-1 Schlumpf ram sizes and specifications; source: Schlumpf AG

valve is a simple, weight-loaded rubber washer covering a gunmetal seat. All rams are fitted with a drain cock on the air chamber outlet. At additional charges the Schlumpf rams are delivered complete with a stop-valve and strainer for the drive pipe and a stop-valve for the delivery pipe.

According to the manufacturer the pumping rate q of the Schlumpf rams can be calculated using the formula

$$q = \frac{Q * H}{h} * \eta$$ where $\eta = 0.7$ (70%) for the model A23,

$\eta = 0.6$ (60%) for the model A5,

with the annotation that for extreme high head ratios $^{h}/_{H}$ the efficiency factor η must be reduced; however 'when' and 'by how much' has not been specified in the information leaflet.

Test results

Both Schlumpf rams were operated at three different values of the supply head: H= 1.00 m, 2.00 m and 3.00 m respectively. The results are presented in the tables and figures hereafter;

Schlumpf 4A5 : Tables A.6-2,3,4 and Figs. A.6-1,2,3

Schlumpf 4A23: Tables A.6-5,6,7 and Figs. A.6-4,5,6.

The performance data from the manufacturer as pictured in Figs. A.6-3 and A.6-6 are calculated using the fore-mentioned formula. Except for very low head ratios the test results stay behind the figures claimed by

the manufacturer. It should however be noted that for the various delivery heads as simulated in the tests the manufacturer recommends, in general, larger supply heads to be used than those applied in the laboratory. If so, this is likely to improve the pumping rate to some extent. Dimensionless performance characteristics for both rams together are illustrated in Fig. A.6-7.

Concluding remarks

The Schlumpf rams performed moderately under the laboratory conditions. In particular at 'higher' delivery heads an irregular operation of the rams was observed, due to the uncontrolled amount of air sucked in through the waste valve during the suction part of the pumping cycle. Part of this air may remain trapped under the delivery valve, thereby limiting the effect of the pressure rise in the next pumping cycle. Eventually this reduces the range of obtainable delivery heads, which is particularly evident from the results obtained for the Schlumpf 4A5.
The delivery valve of the Schlumpf rams, formerly made out of leather, is nowadays replaced by a rather thin rubber washer, which in the long run is unlikely to withstand the air chamber pressures experienced at high delivery heads. In fact, after the relative short time the rams operated in the laboratory the valve rubber of the Schlumpf 4A23 was already slightly damaged due to the punching effect of the metal valve weight on one side and the valve seat on the other (see sketch below).

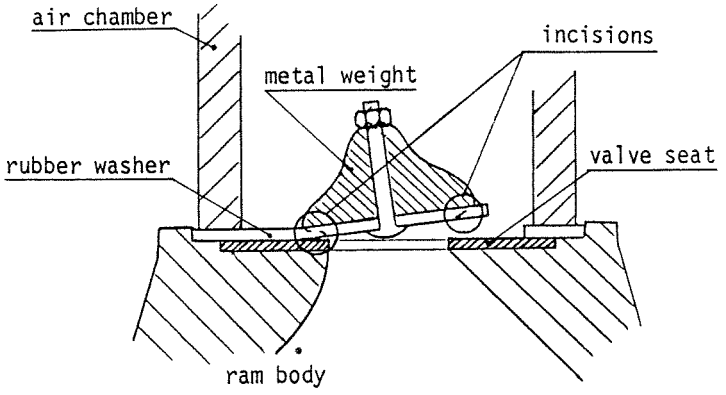

Type of Hydr.Ram: **SCHLUMPF 4A5** Supply Head H= 1.00 m

Manufacturer : SCHLUMPF AG MASCHINENFABRIK, STEINHAUSEN, SWITZERLAND. Drive Pipe: D= 1 1/2" (40mm) L= 11.75 m

Test No.	Delivery Head h [m]	Head Ratio h/H [-]	Period Time T [s]	Pumping Rate q [l/min]	Supply Flow Rate Q [l/min]	Flow Ratio q/Q [-]	Efficiency $\eta = \frac{q*(h-H)}{Q*H}$ [%]	Filename	Volume of Water Delivered V_{up} [$*10^{-3}$ l/cycle]	Volume of Water Wasted V_{out} [$*10^{-3}$ l/cycle]
1000	4	4	1.580	3.85	24.45	0.1575	47.2	-	101.4	644
1002	6	6	1.497	2.40	25.85	0.0928	46.4	SCHL-5/7	59.9	645
1004	8	8	1.496	1.45	26.35	0.0550	38.5	-	36.2	657
1006	10	10	1.512	0.87	26.35	0.0330	29.7	SCHL-5/6	21.9	664
1008	13	13	1.545	0.40	25.10	0.0159	19.1	-	10.3	646
1010	h_{max}= 32	32	-	0	-					

Table A.6-2 Testresults Schlumpf 4A5; supply head H = 1.00 m

Table A.6-3 Testresults Schlumpf 4A5; supply head H = 2.00 m

Type of Hydr.Ram: **SCHLUMPF 4A5**

Manufacturer : SCHLUMPF AG MASCHINENFABRIK, STEINHAUSEN, SWITZERLAND.

Supply Head H= 2.00 m

Drive Pipe: D= 1 1/2" (40mm)
L= 11.75 m

Test No.	Delivery Head h [m]	Head Ratio h/H [-]	Period Time T [s]	Pumping Rate q [l/min]	Supply Flow Rate Q [l/min]	Flow Ratio q/Q [-]	Efficiency $\eta=\frac{q*(h-H)}{Q*H}$ [%]	Filename	Volume of Water Delivered V_{up} [$*10^{-3}$ l/cycle]	Volume of Water Wasted V_{out} [$*10^{-3}$ l/cycle]
1030	6	3	1.493	9.30	31.80	0.2925	58.5	-	231.4	791
1032	8	4	1.361	6.80	35.50	0.1915	57.5	-	154.2	805
1034	10	5	1.320	5.00	36.80	0.1359	54.3	-	110.0	810
1036	12	6	1.351	3.35	35.10	0.0954	47.7	-	75.4	790
1038	14	7	1.387	2.45	32.00	0.0766	45.9	SCHL-5/5	56.6	740
1040	16	8	1.417	1.85	31.60	0.0585	41.0	-	43.7	746
1042	18	9	1.468	0.92	28.60	0.0322	25.7	SCHL-5/4	22.5	700
1044	20	10	1.504	0.50	26.00	0.0192	17.3	-	12.5	652
1046	h_{max}= 29	14.5	-	0	-					

Table A.6-4 Testresults Schlumpf 4A5; supply head H = 3.00 m

Type of Hydr.Ram: **SCHLUMPF 4A5** — Supply Head H= 3.00 m

Manufacturer : SCHLUMPF AG MASCHINENFABRIK, STEINHAUSEN, SWITZERLAND. — Drive Pipe: D= 1 1/2" (40mm) L= 11.75 m

Test No.	Delivery Head h [m]	Head Ratio h/H [-]	Period Time T [s]	Pumping Rate q [l/min]	Supply Flow Rate Q [l/min]	Flow Ratio q/Q [-]	Efficiency $\eta = \frac{q*(h-H)}{Q*H}$ [%]	Filename	Volume of Water Delivered V_{up} [$*10^{-3}$ l/cycle]	Volume of Water Wasted V_{out} [$*10^{-3}$ l/cycle]
1060	9	3	0.964	10.30	33.60	0.3065	61.3	-	165.5	540
1062	12	4	0.919	6.95	35.80	0.1941	58.2	-	106.4	548
1064	15	5	0.950	4.30	32.90	0.1307	52.3	SCHL-5/3	68.1	521
1068	18	6	0.974	2.90	30.00	0.0967	48.3	SCHL-5/2 SCHL-5/2A	47.1	487
1068	21	7	1.027	1.25	24.80	0.0504	30.2	SCHL-5/1	21.4	424
1070	24	8	1.068	0.18	20.80	0.0087	6.1	-	3.2	370
1072	h_{max}= 27	9	-	0	-					

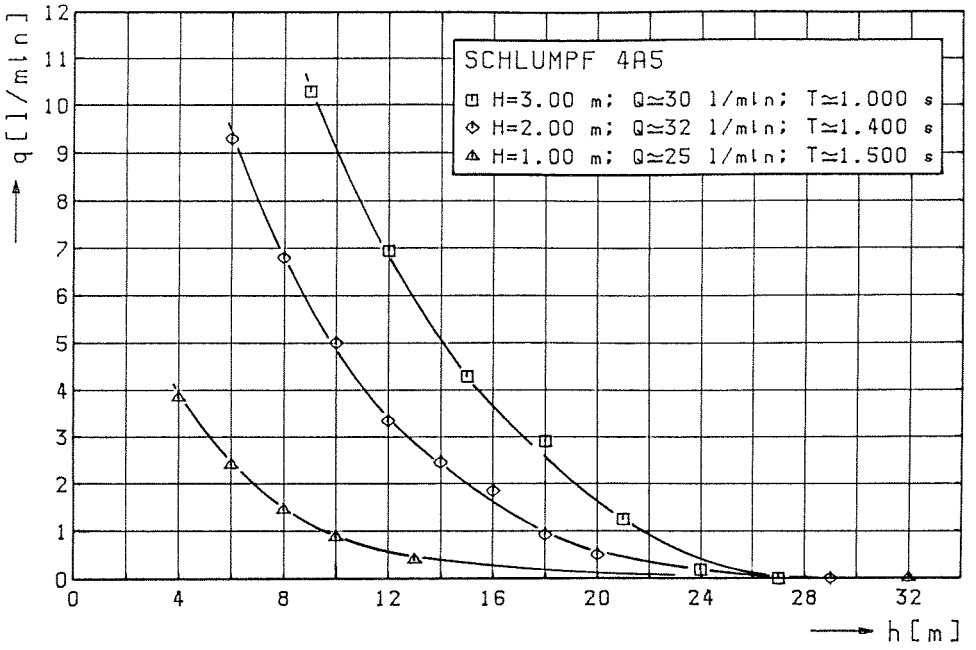

Fig. A.6-1 Pumping rate q versus delivery head h; Schlumpf 4A5

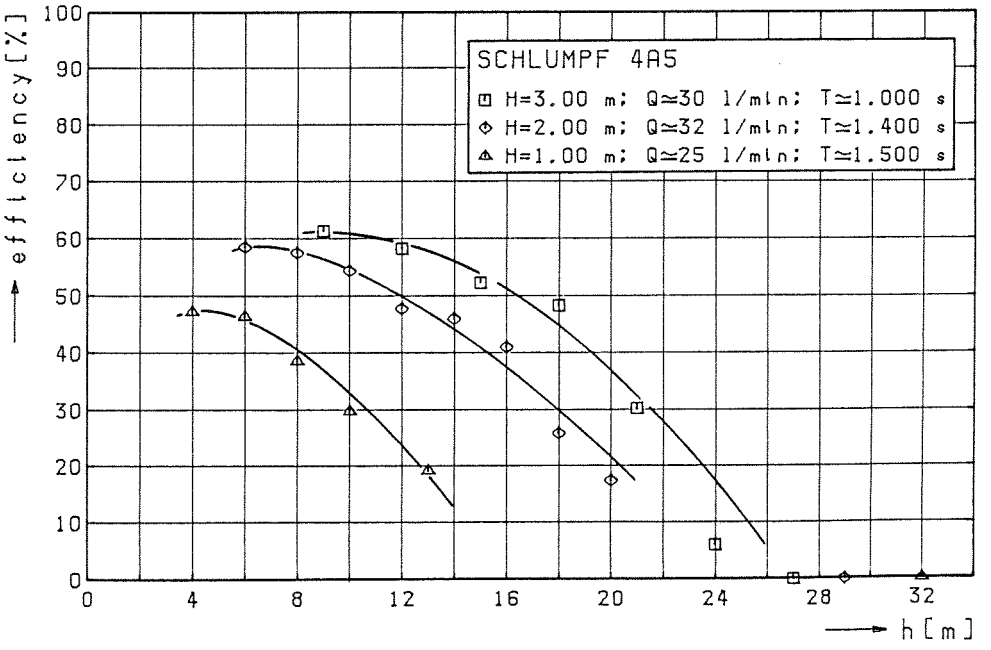

Fig. A.6-2 Rankine efficiency η versus delivery head h; Schlumpf 4A5

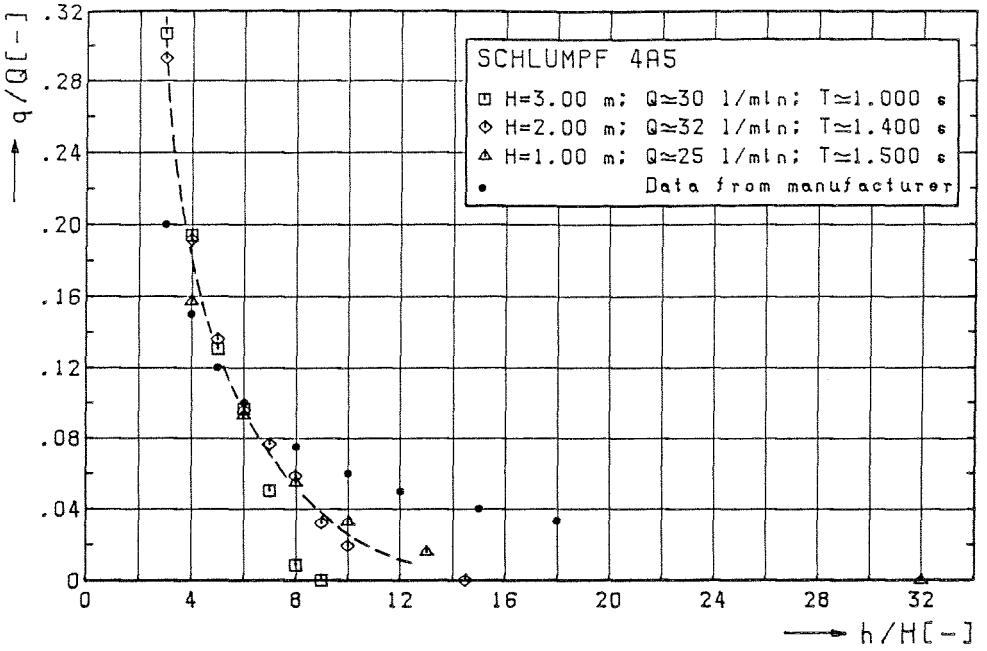

Fig. A.6-3 Flow ratio $^{q}/_{Q}$ versus head ratio $^{h}/_{H}$; Schlumpf 4A5

Table A.6-5 Testresults Schlumpf 4A23; supply head H = 1.00 m

Type of Hydr.Ram: **SCHLUMPF 4A23** — Supply Head H= 1.00 m

Manufacturer : SCHLUMPF AG MASCHINENFABRIK, STEINHAUSEN, SWITZERLAND. — Drive Pipe: D= 1 1/2" (40mm), L= 11.70 m

Test No.	Delivery Head h [m]	Head Ratio h/H [-]	Period Time T [s]	Pumping Rate q [l/min]	Supply Flow Rate Q [l/min]	Flow Ratio q/Q [-]	Efficiency $\eta = \frac{q*(h-H)}{Q*H}$ [%]	Filename	Volume of Water Delivered V_{up} [$*10^{-3}$ l/cycle]	Volume of Water Wasted V_{out} [$*10^{-3}$ l/cycle]
1100	4	4	2.010	3.70	23.75	0.1558	46.7	-	124.0	796
1102	6	6	1.870	2.55	26.00	0.0981	49.0	-	79.5	810
1104	8	8	1.800	1.75	27.50	0.0636	44.5	-	52.5	825
1106	10	10	1.780	1.50	27.95	0.0537	48.3	SCHL-23/14	44.5	829
1108	12	12	1.766	1.05	27.80	0.0378	41.5	SCHL-23/13 13A	30.9	818
1110	15	15	1.790	0.80	27.25	0.0294	41.1	-	23.9	813
1112	18	18	1.815	0.60	26.50	0.0226	38.5	SCHL-23/12 ,, 12A	18.2	802
1114	21	21	1.847	0.40	25.00	0.0160	32.0	-	12.3	770
1116	27	27	1.880	0.24	23.75	0.0101	26.3	-	7.5	744
1118	h_{max}= 40	40	1.972	0	19.10	-	-	SCHL-23/11	-	628

Type of Hydr.Ram: **SCHLUMPF 4A23**

Supply Head H= 2.00 m

Manufacturer : SCHLUMPF AG MASCHINENFABRIK, STEINHAUSEN, SWITZERLAND.

Drive Pipe: D= 1 1/2" (40mm) L= 11.70 m

Test No.	Delivery Head h [m]	Head Ratio h/H [-]	Period Time T [s]	Pumping Rate q [l/min]	Supply Flow Rate Q [l/min]	Flow Ratio q/Q [-]	Efficiency $\eta = \frac{q*(h-H)}{Q*H}$ [%]	Filename	Volume of Water Delivered V_{up} [$*10^{-3}$ l/cycle]	Volume of Water Wasted V_{out} [$*10^{-3}$ l/cycle]
1130	8	4	1.583	7.65	47.90	0.1597	47.9	-	201.8	1264
1132	10	5	1.520	5.85	49.30	0.1187	47.5	-	148.2	1249
1134	14	7	1.495	3.60	50.25	0.0716	43.0	-	89.7	1252
1136	18	9	1.492	2.65	48.70	0.0544	43.5	-	65.9	1211
1138	22	11	1.500	2.05	49.50	0.0414	41.4	SCHL-23/10	51.3	1238
1140	27	13.5	1.506	1.60	47.80	0.0335	41.8	SCHL-23/9, 9A	40.2	1200
1142	32	16	1.542	1.05	45.60	0.0230	34.5	SCHL-23/8, 8A	27.0	1172
1144	36	18	1.524	0.93	45.15	0.0206	35.0	-	23.6	1147
1146	40	20	1.538	0.77	44.50	0.0173	32.9	-	19.7	1141
1148	47	23.5	1.607	0.49	41.10	0.0119	26.8	SCHL-23/7, 7A	13.1	1101
1150	52	26	1.620	0.35	38.50	0.0091	22.7	-	9.5	1040
1152	60	30	1.636	0.20	37.90	0.0053	15.3	-	5.5	1033
1154	h_{max}= 78	39	1.685	0	33.80	0	0	SCHL-23/6, 6A	0	949

Table A.6-6 Testresults Schlumpf 4A23; supply head H = 2.00 m

Type of Hydr.Ram: **SCHLUMPF 4A23** Supply Head H= 3.00 m

Manufacturer : SCHLUMPF AG MASCHINENFABRIK, STEINHAUSEN, SWITZERLAND. Drive Pipe: D= 1 1/2" (40mm) L= 11.70 m

Test No.	Delivery Head h [m]	Head Ratio h/H [-]	Period Time T [s]	Pumping Rate q [l/min]	Supply Flow Rate Q [l/min]	Flow Ratio q/Q [-]	Efficiency $\eta = \frac{q*(h-H)}{Q*H}$ [%]	Filename	Volume of Water Delivered V_{up} [$*10^{-3}$ l/cycle]	Volume of Water Wasted V_{out} [$*10^{-3}$ l/cycle]
1160	9	3	1.170	11.70	38.05	0.3075	61.5	-	228.2	742
1162	12	4	1.060	7.60	42.45	0.1790	53.7	-	134.3	750
1164	15	5	1.037	5.50	42.45	0.1296	51.8	-	95.1	734
1166	18	6	1.043	4.30	42.20	0.1019	51.0	-	74.7	734
1168	21	7	1.045	3.60	41.35	0.0871	52.2	-	62.7	720
1170	26	8.67	1.055	2.55	40.70	0.0627	48.0	SCHL-23/5, 5A	44.8	716
1172	30	10	1.070	1.80	37.60	0.0479	43.1	SCHL-23/4, 4A	32.1	671
1174	33	11	1.070	1.50	38.30	0.0392	39.2	-	26.8	683
1176	42	14	1.108	0.85	33.10	0.0257	33.4	SCHL-23/3, 3A	15.7	611
1178	48	16	1.119	0.48	30.80	0.0156	23.4	-	9.0	574
1180	54	18	1.146	0.26	27.85	0.0093	15.6	SCHL-23/2	5.0	532
1182	h_{max}= 73	24.33	1.142	0	27.45	0	0	SCHL-23/1	0	522

Table A.6-7 Testresults Schlumpf 4A23; supply head H = 3.00 m

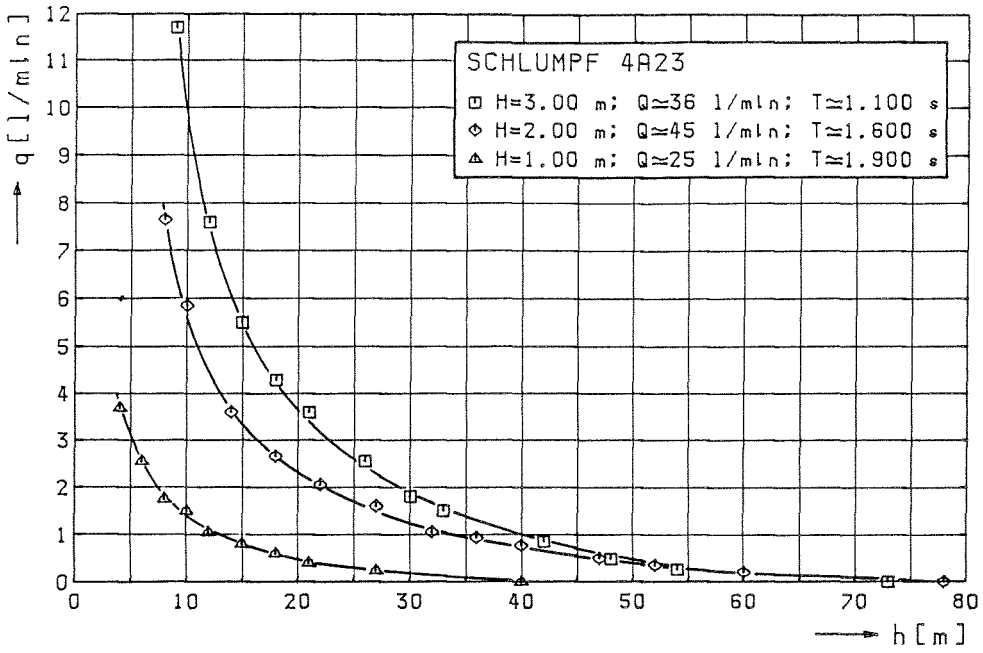

Fig. A.6-4 Pumping rate q versus delivery head h; Schlumpf 4A23

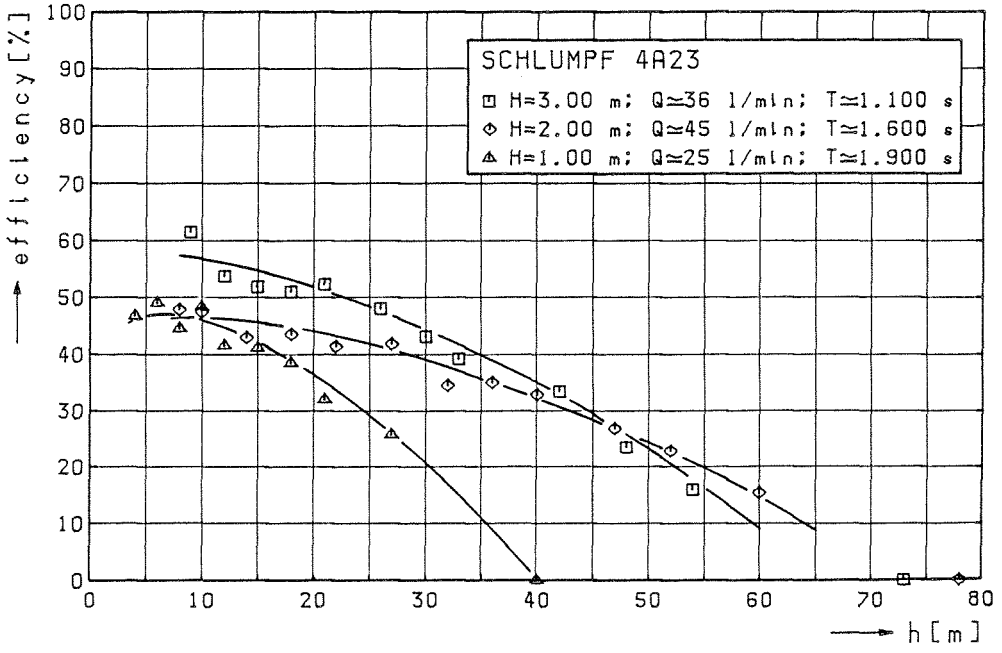

Fig. A.6-5 Rankine efficiency η versus delivery head h; Schlumpf 4A23

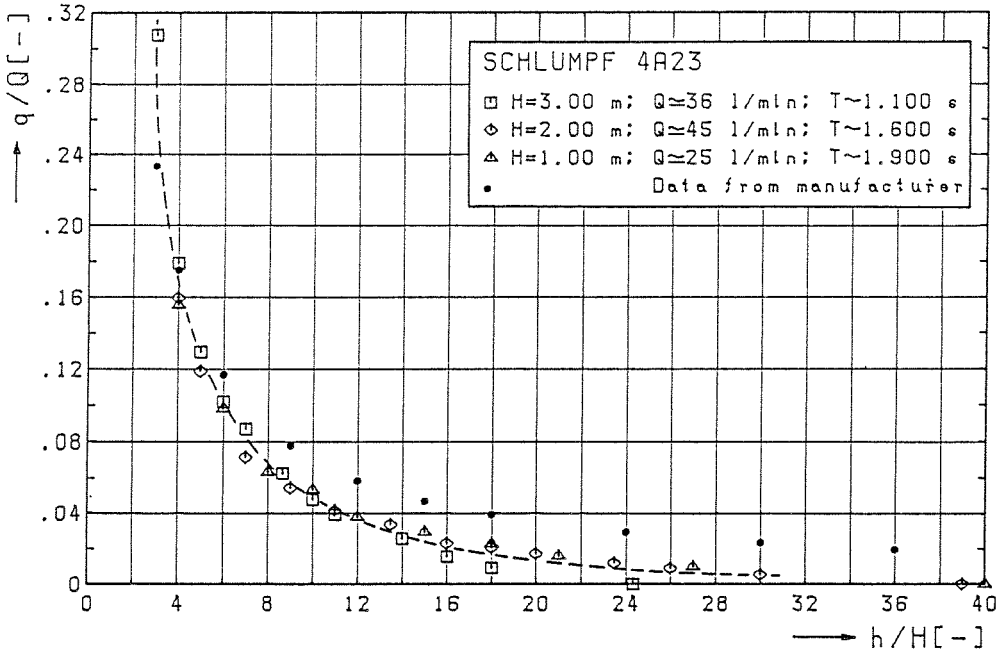

Fig. A.6-6 Flow ratio $^{q}/_{Q}$ versus head ratio $^{h}/_{H}$; Schlumpf 4A23

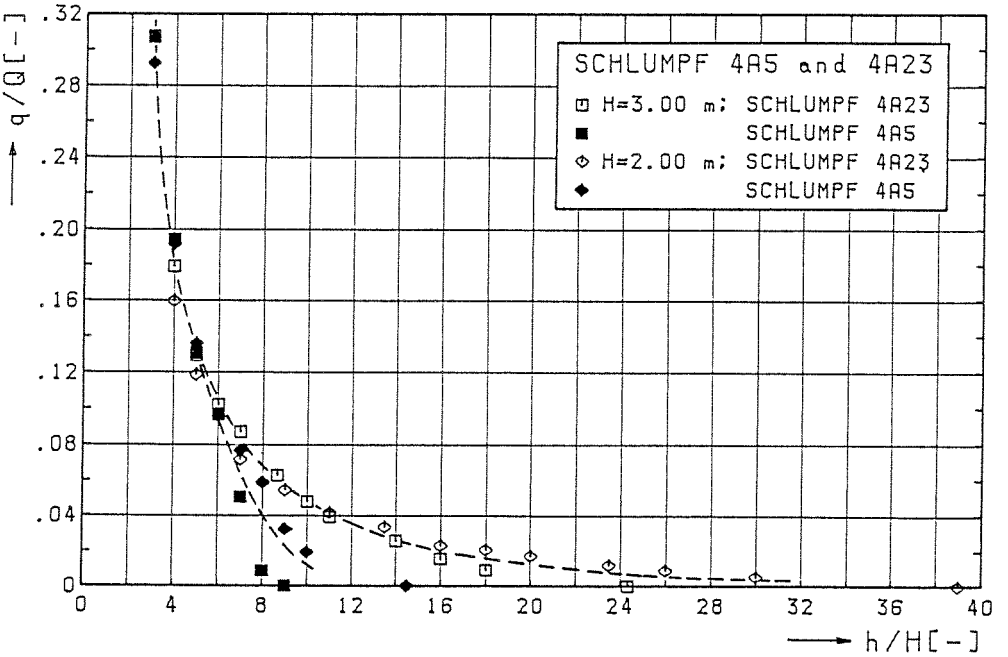

Fig. A.6-7 Dimensionless performance characteristics; Schlumpf 4A5 and 4A23

Appendix B

Appendix B: UNSTEADY FLOW IN A PIPELINE

B-1 Introduction

B-1.1 Classification of flow

Pipe flow in general, deals with the flow of fluids (liquids and gasses) through closed conduits. Since the diameter of a pipe normally is very small compared to the length of the pipe, the flow is considered to be one-dimensional.

In unsteady flow the conditions at a point may change with time. Any variation of flow in a pipeline causes a change in pressure. The magnitude of these pressure fluctuations depends on the time rate and magnitude of the velocity changes, as well as on the compressibility of the fluid and the elasticity of the pipe wall material.

B-1.2 Pressure waves

Sudden alteration of the flow rate can give rise to large pressure surges which move at an acoustic speed up and down the pipe causing it to 'knock'. The phenomenon is called waterhammer whether actual 'hammering' or knocking occurs or not.

Even if the velocity head is negligible, the abrupt closure of a valve somewhere in a pipe through which a fluid is passing results in an immediate rise of pressure upstream of the valve (Fig.B-1). Downstream of the valve the pressure falls by the same amount (in liquids however, the pressure drop is limited by the vapour pressure of the liquid; see hereafter).

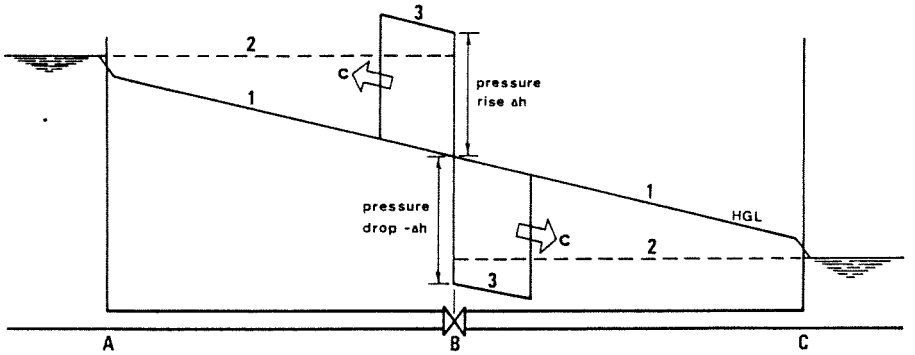

Fig.B-1 1.initial steady state with valve open
2.final steady state with valve closed
3.transient state: rapidly-moving pressure waves

Conversely (re-)opening of the valve results in an immediate drop of pressure upstream of the valve and a rise of pressure downstream of the valve.
Expressions for the change in pressure Δh and wavespeed c can be obtained by applying the equations of momentum and continuity, as shown below.

Transient flow equations. Consider the case of instantaneous stoppage of flow at a downstream valve. Friction and minor losses are neglected as they are very small in comparison with waterhammer pressures.

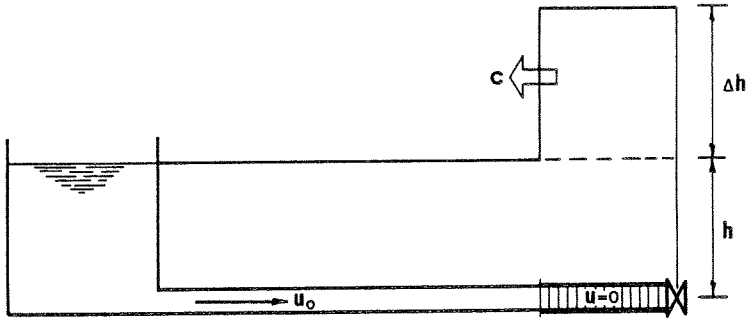

Fig.B-2 Sudden closure of a downstream valve

The instant the valve is closed, the fluid immediately adjacent to it is brought from u_o to rest by the impulse of the higher pressure developed at the face of the valve (see Fig.B-2). As soon as the first layer is brought to rest, the same action is applied to the next layer of fluid. In this way a pulse wave of high pressure is travelling upstream at some sonic wavespeed c and at a sufficient pressure to apply just the impulse to the fluid to bring it to rest.

The momentum equation is applied to a control volume containing a section of the pipe (Fig.B-3). A change in valve setting results in a velocity change Δu accompanied by a head change Δh. The wave front of pressure changes is moving within the control volume with an absolute speed of $(c - u_o)$. The momentum equation states that the impulse of the resultant force on the control volume equals the increase of internal momentum with time plus the net efflux of momentum from the control volume. In formula: $\vec{K}\,dt = d(m\vec{u})$.

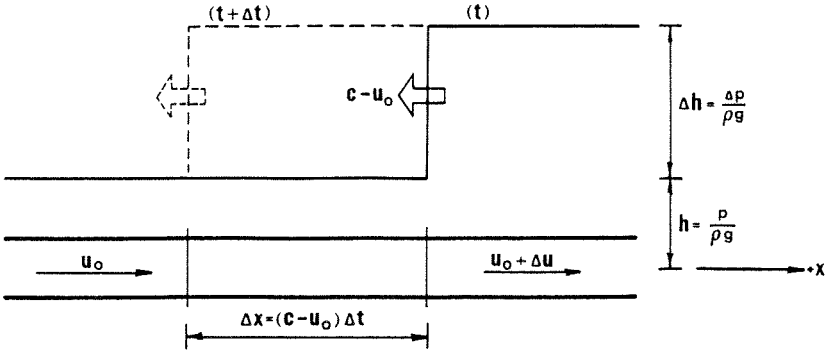

Fig.B-3 Control volume

For the +x direction:

impulse of the resultant x-component of force:

$$-\rho g \Delta h A * \Delta t$$

increase of x-momentum within the control volume during Δt :

$$[mu]_{t+\Delta t} - [mu]_t =$$

$$\rho A \Delta x * (u_0 + \Delta u) - \rho A \Delta x * u_0 = \rho A \Delta x * \Delta u$$

net efflux of x-momentum = flux of x-momentum 'out' during Δt - flux of x-momentum 'in' during Δt :

$$\rho A (u_0 + \Delta u) * (u_0 + \Delta u) \Delta t - \rho A u_0 * u_0 \Delta t =$$

$$\rho A (u_0 + \Delta u)^2 \Delta t - \rho A (u_0)^2 \Delta t =$$

$$\rho A [2 u_0 \Delta u + (\Delta u)^2] \Delta t$$

Hence

$$-\rho g \Delta h A \Delta t = \rho A \Delta x * \Delta u + \rho A [2 u_0 \Delta u + (\Delta u)^2] \Delta t \qquad \text{(B.1a)}$$

or with $\Delta x = (c - u_0) \Delta t$

$$-\rho g \Delta h A \Delta t = \rho A (c - u_0) \Delta t \Delta u + \rho A [2 u_0 \Delta u + (\Delta u)^2] \Delta t \qquad \text{(B.1b)}$$

where ρ = mass density of the fluid [kgm^{-3}]
g = acceleration due to gravity [ms^{-2}]
A = cross-sectional area of the pipe [m^2]
u_0 = initial velocity of the fluid [ms^{-1}]

Δu = increase of velocity during time Δt [ms^{-1}]
c = wavespeed [ms^{-1}]
Δh = increase of pressure head during Δt [m]

By neglecting the small quantity containing $(\Delta u)^2$, the equation reduces to

$$-g\,\Delta h = (c + u_o)\,\Delta u$$

or

$$\Delta h = -\frac{c}{g}\,\Delta u\left[1 + \frac{u_o}{c}\right] \qquad (B.2a)$$

For liquids in metal pipes $u_o/c \ll 1$, so that Eq.(B.2a) simplifies to

$$\Delta h = -\frac{c}{g}\,\Delta u \qquad (B.2b)$$

Eqs.(B.2a) and (B.2b) hold for any valve movement in the absence of reflections, that is, so long as the pressure wave has not reached the upstream end of the pipe and returned as a reflected wave. Therefore the time taken for valve closure (i.e. reduction of the area of the valve opening) such that the maximum pressure head change at the valve is that given by Eqs.(B.2) should be less than $2L/c$, with L the pipe length.

A similar derivation shows that, if the velocity is changed by an upstream valve (which is for instance the case for pipe section BC of Fig. B-1), then $\Delta h = +\frac{c}{g}\Delta u$.
So, in general

$$\Delta h = \pm\frac{c}{g}\,\Delta u \qquad (B.3)$$

describes the change in flow related to a change in head, where the minus sign must be used for changes at the downstream end of the pipe section (wave front moving in upstream direction) and the plus sign for changes at the upstream end (wave front moving in downstream direction). For instance, if the flow at the valve (Fig.B-1) is completely stopped $\Delta u = -u_o$ and the pressure head upstream of the valve is changed by

$$\Delta h = -\frac{c}{g} * (-u_o) = +\frac{c}{g}u_o$$

i.e. a pressure rise or positive pressure wave, while downstream of the valve

$$\Delta h = +\frac{c}{g} * (-u_o) = -\frac{c}{g}u_o$$

i.e. a pressure drop or negative pressure wave.
Eq.(B.3) is the basic equation of waterhammer, also known as Joukowski's Law[9] or the Allievi Expression[1]. The equation holds for any valve movement in the absence of reflections.

The magnitude of the wavespeed c may be determined by applying the equation of continuity to the pipe (Fig.B-4).

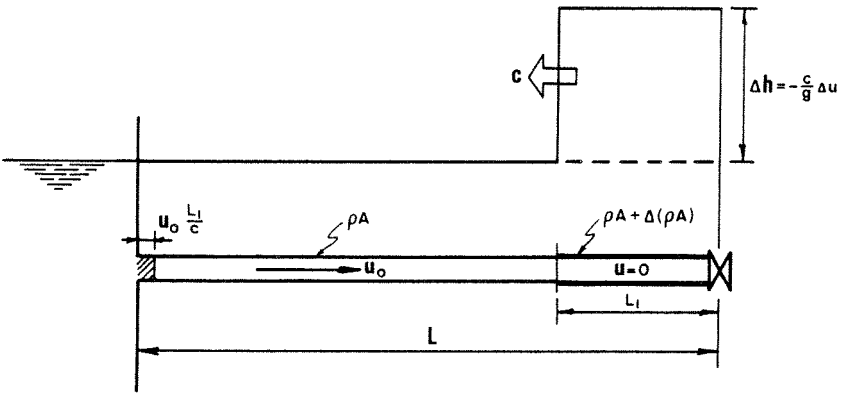

Fig.B-4 Continuity relations in a pipe

As before, if the outlet valve is suddenly shut a pressure wave moves upstream from the valve with velocity c. Due to the high pressure the fluid behind the wave front is compressed and the pipe wall is expanded circumferentially; depending on how it is supported the pipe may also stretch in length. At the same time fluid still enters the pipe from the upstream end with the original velocity u_o and continues to do so L/c seconds, i.e., the time required for the wave front to reach the upstream end of the pipe. Thus, the mass entering the pipe after valve closure is given by $\rho A u_o L/c$. This extra mass is accommodated within the pipe by filling the extra volume due to the pipe extensions ΔA and ΔL, and by the increase of mass density $\Delta\rho$ due to the compression of the fluid.
So,

$$\rho A u_o * \frac{L}{c} = \rho L \Delta A + \rho A \Delta L + L A \Delta \rho \qquad (B.4)$$

Since the pipe has stretched ΔL during time L/c, the velocity of the

fluid at the valve has been changed by

$$\Delta u = \frac{\Delta L}{L/c} - u_o$$

By use of this expression in eliminating u_o, Eq.(B.4) simplifies to

$$-\frac{\Delta u}{c} = \frac{\Delta A}{A} + \frac{\Delta \rho}{\rho}$$

Using Eq.(B.2b) to eliminate Δu yields

$$c^2 = \frac{g \Delta h}{\Delta A/A + \Delta \rho/\rho} \qquad (B.5)$$

Notes: 1. If the pipe is supported so that it cannot extend in length, then $\Delta L = 0$ and the same Eq.(B.5) is obtained, with or without expansion joints.

2. In applying the momentum equation (Eqs.B-1) the small change of momentum due to $\Delta \rho$ and ΔA is negligible compared to the change of momentum due to Δu. However, when considering continuity relations, $\Delta \rho$ and ΔA may no longer be neglected since they are the only factors involved with the change of mass.

Since $\Delta h = \Delta p/\rho g$, Eq.(B.5) may be written as

$$c^2 = \frac{\Delta p/\rho}{\Delta A/A + \Delta \rho/\rho} \qquad (B.6)$$

The coefficient of compressibility or bulk modulus of elasticity K of a fluid is defined by

$$K = -\frac{\Delta p}{\Delta V/V} \qquad (B.7a)$$

with $\Delta V/V$ the fractional volume change.
From conservation of mass, $\Delta(\rho V) = 0$, it follows that

$$\Delta \rho * V + \rho \Delta V = 0 \quad \text{or} \quad \frac{\Delta V}{V} = -\frac{\Delta \rho}{\rho}$$

Hence, Eq.(B.7a) may also be written as

$$K = \frac{\Delta p}{\Delta \rho / \rho} \tag{B.7b}$$

After use of Eq.(B.7b), Eq.(B.6) may be rearranged to yield

$$c^2 = \frac{1}{\rho\left[\frac{\Delta A}{A\,\Delta p} + \frac{1}{K}\right]} \tag{B.8}$$

The term $\frac{\Delta A}{A\,\Delta p}$ will be evaluated for a thin-walled pipeline with circular cross-section. A pipe wall may be considered thin if the ratio $D/e \geq 20$ to 25, where e is the thickness of the pipe wall and D the internal diameter of the pipe (see Fig.B-5b).

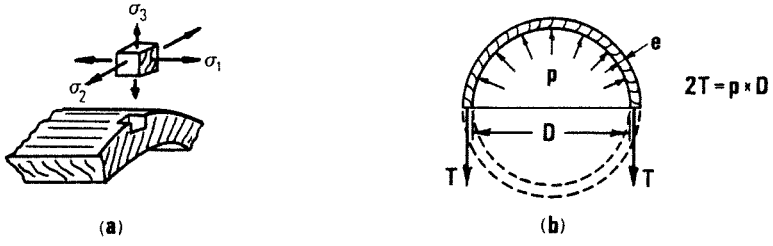

Fig.B-5 Forces and stresses on the pipe wall

For thin-walled pipes the radial stress σ_3 (Fig.B-5a) is small compared to σ_1 and σ_2 and therefore hereafter neglected.
The change in area, ΔA, is the result of the increment of circumferential strain ε_2 :

$$\Delta \varepsilon_2 = \frac{\Delta P}{P}$$

in which P is the perimeter of the cross-section ($P = \pi D$).

So, $\Delta \varepsilon_2 = \frac{\Delta(\pi D)}{\pi D} = \frac{\Delta D}{D}$ or $\Delta D = D\,\Delta \varepsilon_2$ (B.9)

From $A = \frac{1}{4}\pi D^2$ it follows that $\Delta A = \frac{1}{2}\pi D\,\Delta D$

and $\frac{\Delta A}{A} = \frac{2\,\Delta D}{D}$ (B.10)

Combining Eqs.(B.9) and (B.10) yields:

$$\frac{\Delta A}{A} = 2\,\Delta\varepsilon_2 \tag{B.11}$$

Stress and strain are related by Young's modulus of elasticity E; in the two-dimensional case ($\sigma_3 \approx 0$):

-longitudinal strain $\quad \varepsilon_1 = \frac{1}{E}\left(\sigma_1 - \nu\sigma_2\right)$ (B.12a)

and thus $\quad \Delta\varepsilon_1 = \frac{1}{E}\left(\Delta\sigma_1 - \nu\Delta\sigma_2\right)$ (B.12b)

-circumferential strain $\quad \varepsilon_2 = \frac{1}{E}\left(\sigma_2 - \nu\sigma_1\right)$ (B.13a)

and thus $\quad \Delta\varepsilon_2 = \frac{1}{E}\left(\Delta\sigma_2 - \nu\Delta\sigma_1\right)$ (B.13b)

in which

σ_1	= longitudinal stress	[Nm^{-2}]
σ_2	= circumferential stress	[Nm^{-2}]
ν	= Poisson's ratio	[-]
E	= Young's modulus	[Nm^{-2}]

The circumferential tension σ_2 is related to pressure by

$$\sigma_2 = \frac{T}{e} = \frac{pD}{2e} \tag{B.14}$$

in which T is the circumferential tensile force per unit length of pipe (see Fig.B-5b).

The increase in σ_2 due to the waterhammer pressure Δp may now be written as

$$\Delta\sigma_2 = \frac{\Delta p * D}{2e} \tag{B.15}$$

where D is considered constant for this finite differentiation since it changes only a little as compared to p in transient flow.

In order to yield expressions for the longitudinal stress σ_1, three support situations for the pipeline are examened:

(a) pipe anchored at its upstream end only

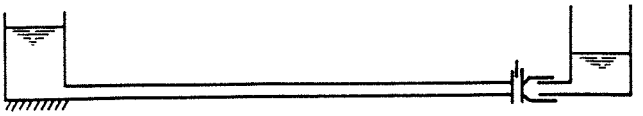

(b) pipe anchored throughout against longitudinal movement

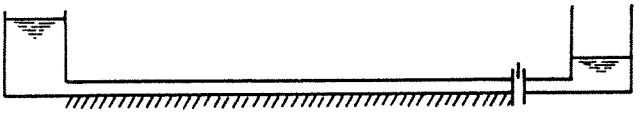

(c) pipe anchored with expansion joints throughout

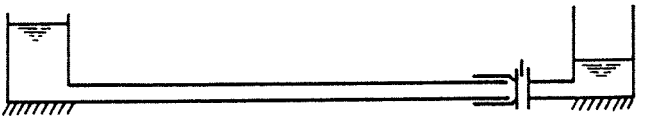

Case a: The axial stress in the pipe wall is equal to the force on the closed valve, $p * \frac{1}{4}\pi D^2$, divided by the area of the pipe wall, $\pi D e$, or

$$\sigma_1 = \frac{\frac{1}{4}\pi p D^2}{\pi D e} = \frac{pD}{4e} \qquad \text{and} \qquad \Delta\sigma_1 = \frac{\Delta p * D}{4e} \tag{B.16}$$

Then with the use of Eqs.(B.11), (B.13b), (B.15) and (B.16)

$$\frac{\Delta A}{A \Delta p} = \frac{2\Delta\varepsilon_2}{\Delta p} = \frac{2}{\Delta p} * \frac{1}{E}\left[\frac{\Delta p * D}{2e} - \nu \frac{\Delta p * D}{4e}\right] = \frac{D}{Ee}\left(1 - \nu/2\right) \tag{B.17}$$

Case b: For a pipe anchored throughout $\varepsilon_1 = 0$ and thus, with Eqs.(B.12) in mind, it can be noted that $\sigma_1 = \nu\sigma_2$ or $\Delta\sigma_1 = \nu\Delta\sigma_2$. So,

$$\frac{\Delta A}{A \Delta p} = \frac{2}{\Delta p} * \frac{1}{E}\left[\Delta\sigma_2 - \nu^2 \Delta\sigma_2\right] = \frac{D}{Ee}\left(1 - \nu^2\right) \tag{B.18}$$

Case c: For expansion joints throughout $\sigma_1 = 0$, and

$$\frac{\Delta A}{A \Delta p} = \frac{2}{\Delta p} * \frac{1}{E}\,\Delta\sigma_2 = \frac{D}{Ee} \tag{B.19}$$

Hence, for liquids in pipelines with circular cross-section, the wave-speed c can be written as

$$c = \frac{1}{\sqrt{\frac{\rho}{K} + \frac{\rho D}{E e}\varphi_i}} \qquad (B.20)$$

where

ρ = mass density of the liquid [kgm^{-3}]

K = bulk modulus of the liquid [Nm^{-2}]

D = inside diameter of the pipe [m]

e = thickness of the pipe wall [m]

E = Young's modulus of the pipe wall material [Nm^{-2}]

φ_i = dimensionless parameter that describes the effect of pipe constraint condition; for thin-walled pipes, φ_i takes on the values:

$$\text{(a) } \varphi_a = 1 - \nu/2 \qquad (B.21a)$$

$$\text{(b) } \varphi_b = 1 - \nu^2 \qquad (B.21b)$$

$$\text{(c) } \varphi_c = 1 \qquad (B.21c)$$

ν = Poisson's ratio of the pipe wall material [-]

c = wavespeed [ms^{-1}]

For thick-walled pipes, i.e., when the ratio D/e is less than approximately 20, the stresses in the pipe wall are no longer uniformly distributed throughout the wall. In this condition the following coefficients φ_i should be used.([22],[28])

$$\text{case (a): } \varphi_a = \frac{2e}{D}(1+\nu) + \frac{D}{D+e}(1-\nu/2) \qquad (B.22a)$$

$$\text{case (b): } \varphi_b = \frac{2e}{D}(1+\nu) + \frac{D}{D+e}(1-\nu^2) \qquad (B.22b)$$

$$\text{case (c): } \varphi_c = \frac{2e}{D}(1+\nu) + \frac{D}{D+e} \qquad (B.22c)$$

From Eqs.(B.22) it can be noted that as the thickness e and thus the ratio e/D becomes small, i.e.

$$e/D \to 0 \qquad \text{and} \qquad \frac{D}{D+e} = \frac{1}{1+e/D} \to 1$$

each coefficient approaches the corresponding φ_i for the thin-walled pipeline (Eqs.B-21).

Example:

steel pipe: $E = 210*10^9$ Nm^{-2} water(20°C): $\rho = 998$ kgm^{-3}

$\nu = 0.3$ $K = 2.2*10^9$ Nm^{-2}

$D = 50*10^{-3}$ m

1. $e = 2*10^{-3}$ m and $D/e = 25$ --> thin-walled pipeline
   (a) $\psi_a = 0.85$ and wavespeed $c = 1343$ ms^{-1}
   (b) $\psi_l = 0.91$ $c = 1334$ ms^{-1}
   (c) $\psi_c = 1.00$ $c = 1322$ ms^{-1}

2. $e = 5*10^{-3}$ m and $D/e = 10$ --> thick-walled pipeline
   (a) $\psi_a = 1.03$ and wavespeed $c = 1410$ ms^{-1}
   (b) $\psi_l = 1.09$ $c = 1407$ ms^{-1}
   (c) $\psi_c = 1.17$ $c = 1401$ ms^{-1}

For the thick-walled, steel pipe the type of constraint has little effect on the wavespeed. This may also be observed from Fig.B-6, showing wavespeeds for varying ratio D/e, for three different pipe wall materials.

Thus for water at ordinary temperatures the maximum wavespeed ($D/Ee \approx 0$ and $c \approx \sqrt{K/\rho}$) is approximately 1450 m/s. Wavespeeds for large steel pipelines conveying water, may be as low as 1000 m/s, whereas wavespeeds in small pipes may be 1300 to 1400 m/s.
With the wavespeed determined by Eq.(B.20), Eq.(B.2b) yields the change in head given a change in velocity, vice versa. For example with c = 1300 m/s a reduction in velocity of 1 m/s creates an immediate head rise

$$\Delta h = -\frac{c}{g}\Delta u = -\frac{1300}{10} * (-1) = 130 \text{ m}$$

or a pressure rise

$$\Delta p = \rho g \Delta h = 1000 * 10 * 130 = 1.3 * 10^6 \text{ N/m}^2 = 1.3 \text{ MPa}.$$

The maximum pressure in a pipe caused by the combination of steady state pressure and waterhammer pressure is limited by the strength of the pipe. When waterhammer causes a drop in pressure (e.g. downstream of a rapidly closing valve) the total pressure may fall as low as the vapour pressure of the liquid. At this pressure vapour cavaties are formed in

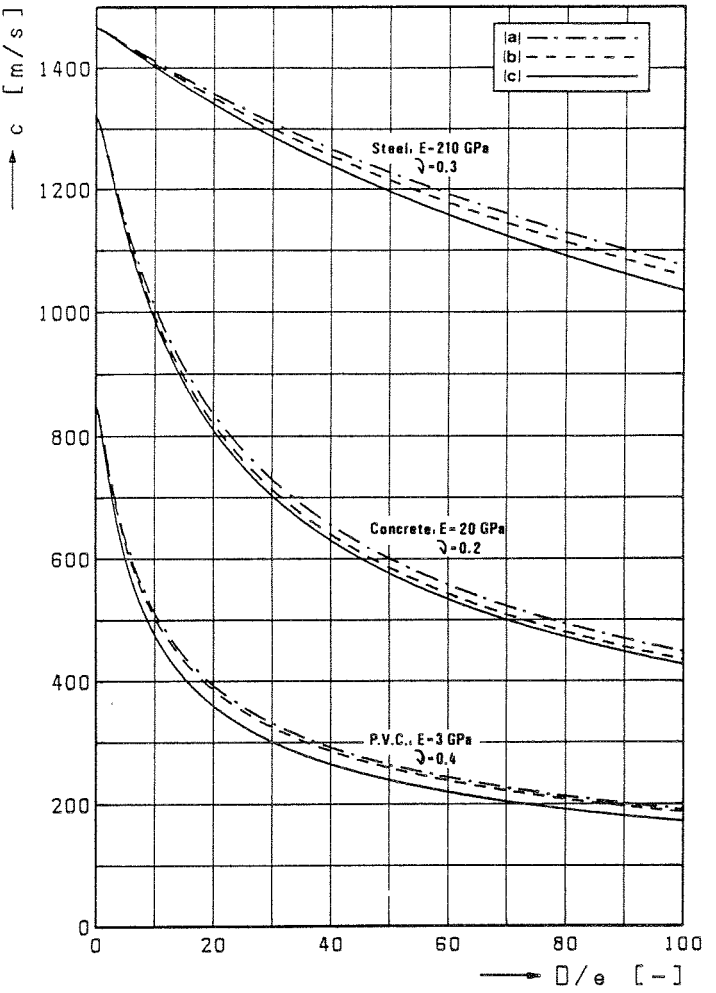

Fig.B-6 Wavespeeds c for pipelines with circular cross-section, transporting fresh water; source: [22]

the liquid, thus creating a liquid-gas mixture. The vapour pressure head of fresh water at normal temperatures is approximately 0.3 m, while atmospheric pressure is equivalent to 10.3 m water head. Therefore the maximum negative head for water is about -10 m measured relative to atmospheric conditions.

Effect of gas in liquids. Even small amounts of free gas dispersed throughout a liquid (or dissolved gas which has come out of solution due to the above-mentioned cavitation) greatly reduce the velocity of

propagation of pressure waves in a pipeline.

An expression for the wavespeed in a liquid-gas mixture may be derived by considering a pipeline containing a liquid with gas bubbles uniformly distributed throughout. The total volume V of the mixture can be expressed by

$$V = V_{Liq} + V_g$$

Thus the volume change due to an instantaneous change in pressure Δp can be written as

$$\Delta V = \Delta V_{Liq} + \Delta V_g$$

The bulk moduli of elasticity of the individual components are defined by

$$K_{Liq} = -\frac{\Delta p}{\Delta V_{Liq} / V_{Liq}}$$

and

$$K_g = -\frac{\Delta p}{\Delta V_g / V_g}$$

Combining these expressions with the bulk modulus of the mixture

$$K = -\frac{\Delta p}{\Delta V / V} = -\frac{\Delta p}{\left[\Delta V_{Liq} + \Delta V_g\right] / \left[V_{Liq} + V_g\right]}$$

yields

$$K = \frac{K_{Liq}}{1 + \frac{V_g}{V}\left[\frac{K_{Liq}}{K_g} - 1\right]} \qquad \text{(B.23)}$$

The mixture density can be written in terms of the liquid and gas densities

$$\rho = \rho_{Liq}\frac{V_{Liq}}{V} + \rho_g\frac{V_g}{V} \qquad \text{(B.24)}$$

Now by substituting Eq.(B.23) and Eq.(B.24) into Eq.(B.20) an expression for the wavespeed can be obtained. Fig.B-7 illustrates the effect of air bubbles in a pipeline containing water. It can be noted from the figure

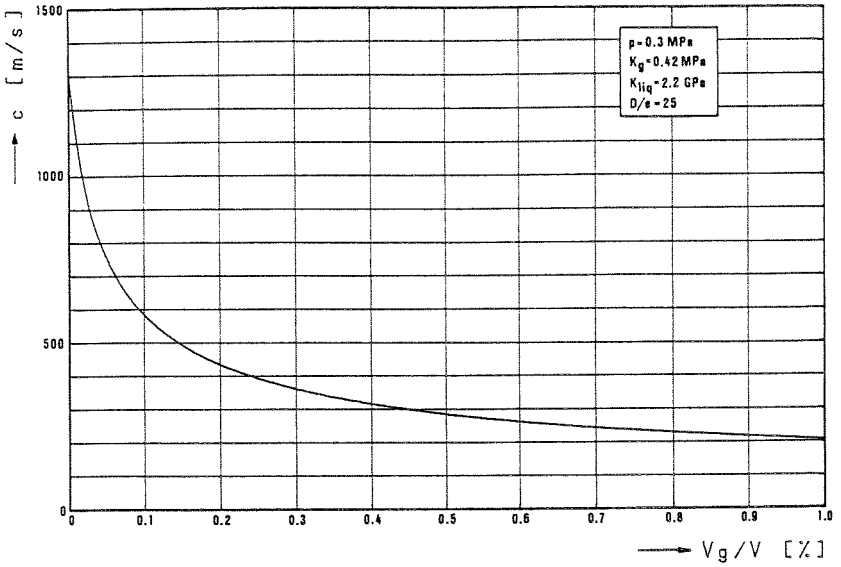

Fig.B-7 Wavespeed c for varying air content

that even a very small air content significantly reduces the wavespeed in the pipeline.

Wave propagation and reflections in a single pipeline. Fig.B-8 shows the sequence of events for one complete cycle, or period, that results from an instantaneous closure of a downstream valve. If friction and minor losses are neglected, then the initial steady-state pressure head along the entire pipeline is h_o. The fluid is flowing with velocity $u = +u_o$ in the downstream ($+x$) direction.

The sequence of events following the valve closure at time $t = 0$ can be divided into four parts:

part 1: $0 < t \leq L/a$ (Figs.B-8a and b)

At the moment of valve closure the flow velocity at the valve is instantly reduced from $u = u_o$ to $u = 0$. Hence the velocity is changed by $\Delta u = -u_o$, which causes a pressure wave of magnitude $\Delta h = -(a/g)\Delta u = +(a/g)u_o$ (i.e. a pressure head rise). The front of this shock wave moves upstream, bringing the fluid to rest as it passes, compressing the fluid thus increasing its density, and expanding the pipe. When the wave reaches the

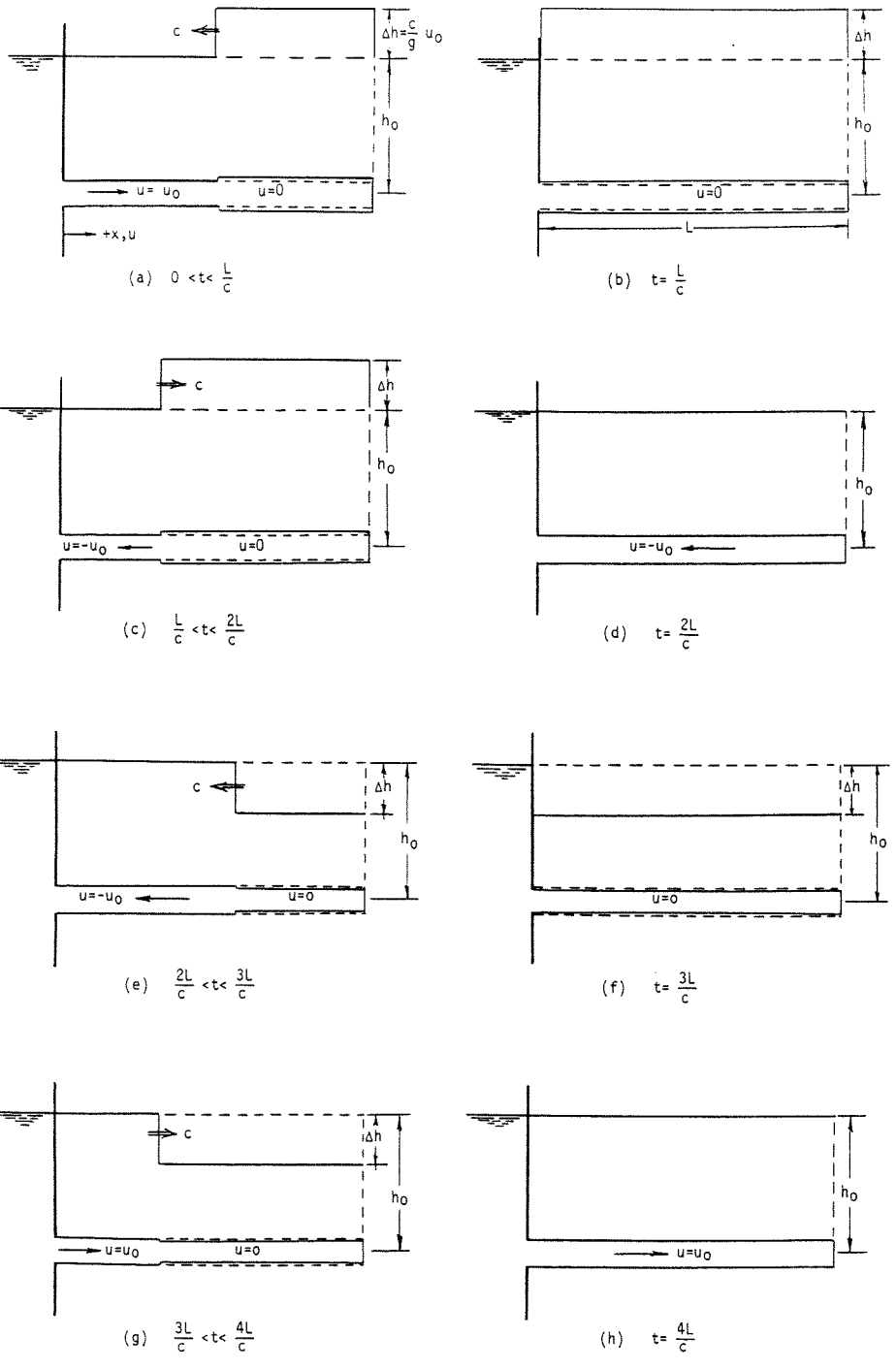

Fig.B-8 Wave propagation and reflections in a single pipeline

upstream end of the pipe (at time $t = L/c$), all the fluid is under the extra head Δh, the flow velocity along the entire pipeline is reduced to zero ($u = 0$) and all the kinetic energy originally in the moving fluid has been converted into elastic energy ('stored' in compression of the fluid and expansion of the pipe wall).

part 2: $L/c < t \leq 2L/c$ (Figs.B-8c and d)

Since the reservoir level remains unchanged ($h = h_o$ = constant) there is an unbalanced situation at the upstream end of the pipe as the pressure wave ($h = h_o + \frac{c}{g} * u_o$) reaches there. The pressure head at the upstream end of the pipe can only remain equal to the reservoir level if the fluid at the upstream end instantly starts to flow backward from the pipeline into the reservoir in such a way that the pressure head in the pipe falls from $h = h_o + \frac{c}{g} u_o$ to $h = h_o$.

Thus the pressure head must change by $\Delta h = -\frac{c}{g} u_o$. According to Eq.(B.3) $\Delta h = +\frac{c}{g} \Delta u$ at the upstream end of a pipe, from which it follows that $\Delta u = -u_o$ and the velocity in the pipe is changed from $u = 0$ to $u = -u_o$. In other words: on the arrival of the positive pressure wave ($\Delta h = +\frac{c}{g} u_o$) at the reservoir an equal but negative wave ($\Delta h = -\frac{c}{g} u_o$) travels away from the reservoir towards the valve. Behind the wave front, i.e. on the upstream side, the pressure returns to its original steady-state value ($h = h_o$), the fluid decompresses and the pipe resumes its original diameter, while the fluid is flowing with $u = -u_o$ in the backward direction.

At time $t = 2L/c$ the wave arrives at the valve, the pressure head in the entire pipeline is $h = h_o$ and the fluid velocity $u = -u_o$ everywhere.

part 3: $2L/c < t \leq 3L/c$ (Figs.B-8e and f)

Since the valve is completely closed, no fluid is available to maintain the negative flow at the valve and a low pressure develops such that the fluid velocity is instantly changed from $u = -u_o$ to $u = 0$. Thus $\Delta u = +u_o$ and the pressure head is reduced by $\Delta h = -\frac{c}{g} \Delta u = -\frac{c}{g} u_o$. This negative pressure wave travels upstream at speed c, brings the fluid to rest again,

causes the fluid to expand because of the lower pressure and allows the pipe wall to contract.

At time $t = 3L/c$ the wave front arrives at the upstream end of the pipe, the pressure head in the entire pipeline is $h = h_o - \frac{c}{g} u_o$ and all the fluid is at rest ($u = 0$).

part 4: $3L/c < t \leq 4L/c$ (Figs.B-8g and h)

At the instant the negative wave reaches the reservoir ($t = 3L/c$) an unstable situation is created again at the upstream end of the pipe. Now the pressure is higher on the reservoir side and fluid instantly starts to flow from the reservoir into the pipeline with velocity $u = u_o$, restoring the pressure head in the pipe from $h = h_o - \frac{c}{g} u_o$ to $h = h_o$. In other words, a positive pressure wave ($\Delta h = + \frac{c}{g} u_o$) propogates downstream at speed c, returning pipe and fluid to the original steady state conditions.

At time $t = 4L/c$ the wave reaches the valve and conditions everywhere in the pipe are exactly the same as at the instant of valve closure.

As the valve is still closed the preceding sequence of events starts again at $t = 4L/c$. Fig.B-9 shows the variation of the pressure near the valve with time. Since the system is assumed to be frictionless the complete cycle continues to repeat every $4L/c$ seconds.

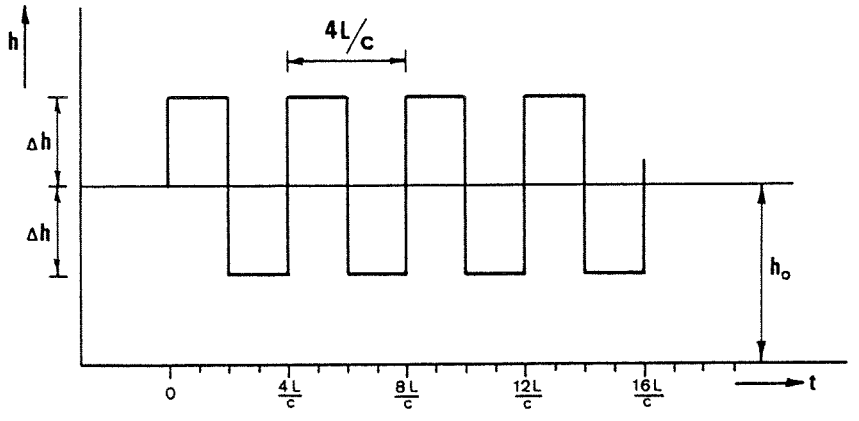

Fig.B-9 Pressure variations at valve; friction losses neglected

In real systems however the oscillation gradually dies out due to friction and imperfect elasticity of fluid and pipe wall and the fluid eventually comes permanently to rest (Fig.B-10).

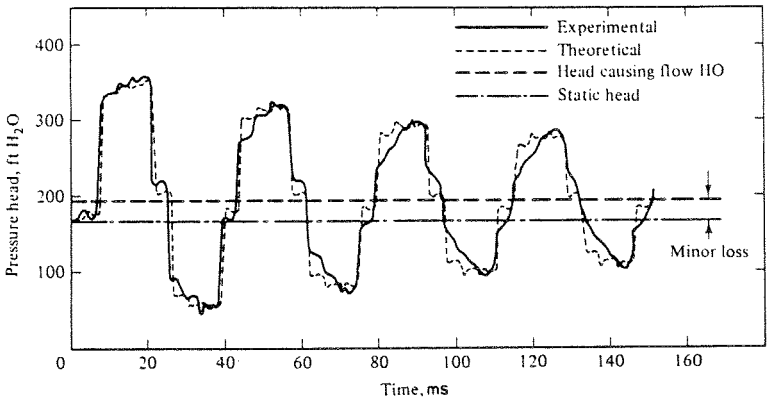

Fig.B-10 Pressure variation near valve, friction included; source: [28]

B-1.3 Rigid water-column theory

If the fluid is a completely incompressible liquid and if it is flowing in a completely rigid pipe, there will be no 'waterhammer'. But there will still be a change of pressure on altering the flowrate, due to the inertia of the flowing liquid. The assumption of complete incompressibility and rigidity may be made when the valve movement, which causes the change of flow, is slow as compared with the period of the pipe:

$$T_c \gg \frac{2L}{c} \qquad (B.25)$$

where $\frac{2L}{c}$ is the period of the pipe, i.e. the time it takes for a pressure wave to move up and down the pipe

and T_c is a time 'characteristic' for the change in boundary condition, in this case the time taken for valve closure.

In other words, the incompressible theory gives a true account of the pressure variations only when the wave caused by the valve movement returns to the valve to find conditions there substantially the same as when it left the valve (see Fig.B-11).

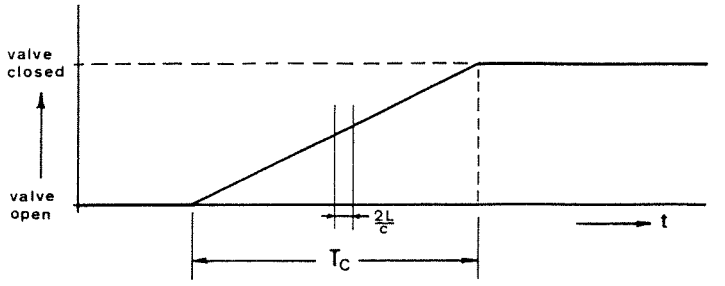

Fig.B-11 Slow valve closure

Now, consider the flow of water through a rigid pipe between two reservoirs. When the valve is closed smooth and slowly the water approaching the valve finds its path gradually impeded by the valve; it is unable to move with its original velocity, and since the water is incompressible the whole of the column upstream of the valve is retarded, thus changing the pressure (Fig.B-12). Consequently downstream of the valve less water is available to maintain the flow and the whole of the column downstream of the valve is retarded likewise.

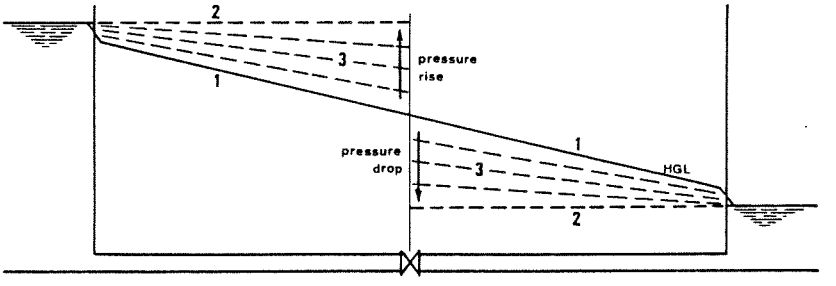

Fig.B-12 1.initial steady state with valve open; 2.final steady state with valve closed; 3.intermediate state: change of pressure throughout the pipeline

Put in other words: the valve closure results in an increasing head loss due to resistance acting at the valve; this extra loss leaves less head available to overcome friction and the flow is reduced correspondingly. If the valve movement may no longer be considered smooth and slowly the assumption of incompressibility and rigidity is no longer correct and the elasticity of fluid and pipe wall should be taken into account as previously discussed (section B-1.2).

B-2 Basic Differential Equations of Unsteady Pipe Flow

Unsteady flow through closed conduits is described by an equation of motion and an equation of continuity. The derivation of these equations is presented for liquid flow through a cylindrical pipe with circular cross-section. The equations are in terms of centerline pressure $p(x,t)$ and average velocity $u(x,t)$. Afterwards they will be converted to a form using the piezometric head $h(x,t)$.

B-2.1 Equation of continuity

In Fig.B-13 is shown a section of pipe, having cross-sectional area A, through which a liquid of density ρ is flowing with velocity $u(x,t)$. Distance x, measured along the centerline of the pipe, and velocity u are considered positive in the downstream direction. The pipe is inclined with the horizontal at an angle β, positive when the elevation of the pipe decreases in the $+x$ direction.

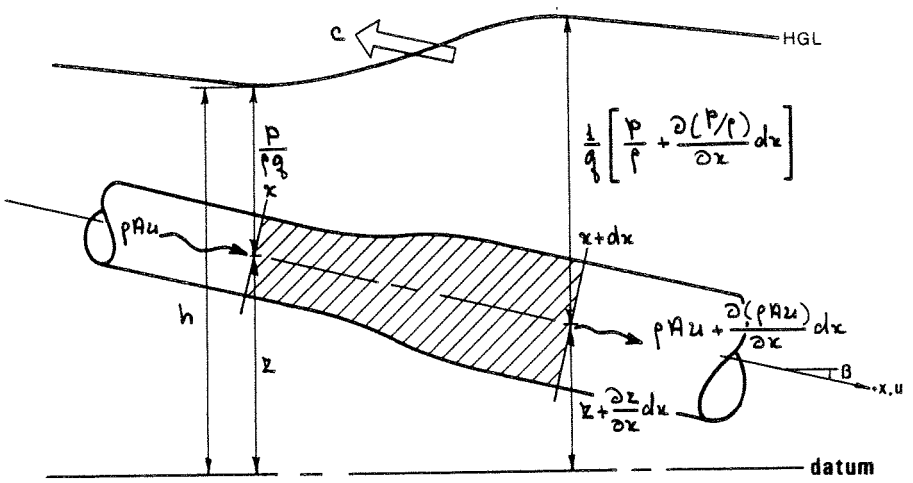

Fig.B-13 Control volume for developing continuity equation (distension of pipe exaggerated)

The equation of continuity is developed by applying 'conservation of mass' to a control volume containing a section of pipe, having length dx. If pressure and velocity at distance x are p and u, then their corresponding values at $x+dx$ are $p+\frac{\partial p}{\partial x}dx$ and $u+\frac{\partial u}{\partial x}dx$, respectively.

Furthermore A and ρ may vary with x and t since they are functions of $p(x,t)$.

The law of conservation of mass states that the time rate of increase of mass within the control volume is equal to the time rate of net mass inflow into the contol volume. With reference to Fig.B-13:

- Increase of mass within the control volume in time dt :

$$\frac{\partial(\rho A dx)}{\partial t} dt = \frac{\partial(\rho A)}{\partial t} dx\, dt$$

Mass entering the contol volume at $x=x$ during time dt :

$$\rho A u * dt$$

Mass leaving the control volume at $x=x+dx$ during dt :

$$\left[\rho A u + \frac{\partial(\rho A u)}{\partial x} dx\right] dt$$

- Net inflow of mass during time dt :

$$\rho A u * dt - \left[\rho A u + \frac{\partial(\rho A u)}{\partial x} dx\right] dt = -\frac{\partial(\rho A u)}{\partial x} dx\, dt$$

Hence

$$\frac{\partial(\rho A)}{\partial t} dx\, dt = -\frac{\partial(\rho A u)}{\partial x} dx\, dt$$

or

$$\frac{\partial(\rho A)}{\partial t} + \frac{\partial(\rho A u)}{\partial x} = 0 \qquad (B.26)$$

which can be written as

$$\frac{\partial(\rho A)}{\partial t} + u \frac{\partial(\rho A)}{\partial x} + \rho A \frac{\partial u}{\partial x} = 0 \qquad (B.27)$$

By use of the total derivative (differentiation with respect to the motion of the liquid)

$$\frac{d..}{dt} = \frac{\partial..}{\partial t} + u \frac{\partial..}{\partial x}$$

Eq.(B.27) takes the form

$$\frac{d(\rho A)}{dt} + \rho A \frac{\partial u}{\partial x} = 0$$

Hence

$$A\frac{dp}{dt} + \rho\frac{dA}{dt} + \rho A\frac{\partial u}{\partial x} = 0$$

or after dividing by ρA

$$\frac{1}{\rho}\frac{dp}{dt} + \frac{1}{A}\frac{dA}{dt} + \frac{\partial u}{\partial x} = 0 \qquad (B.28)$$

From the definition of bulk modulus of elasticity of a liquid, Eq.(B.7b) it follows that

$$\frac{1}{\rho}\frac{dp}{dt} = \frac{1}{K}\frac{dp}{dt} \qquad (B.29)$$

For a cylindrical pipe of circular cross-section it follows from Eqs. (B.17), (B.18) and (B.19) that

$$\frac{1}{A}\frac{dA}{dt} = \frac{D}{Ee}\varphi_i * \frac{dp}{dt} \qquad (B.30)$$

where φ_i introduces the effect of Poisson's ratio for various pipe support conditions. φ_i takes on values according to Eqs.(B.21) for thin-walled pipes and Eqs.(B-22) for thick-walled pipes.

Substitution of Eqs.(B.29) and (B.30) into Eq.(B.28) yields

$$\frac{1}{K}\frac{dp}{dt} + \frac{D}{Ee}\varphi_i * \frac{dp}{dt} + \frac{\partial u}{\partial x} = 0$$

or

$$\frac{dp}{dt}\left[\frac{\rho}{K} + \frac{\rho D}{Ee}\varphi_i\right] + \rho\frac{\partial u}{\partial x} = 0 \qquad (B.31)$$

Introducing wavespeed c (Eq.(B.20))

$$\left[\frac{\rho}{K} + \frac{\rho D}{Ee}\varphi_i\right] = \frac{1}{c^2}$$

and again using the expression for the total derivative, Eq.(B.31) may be written as

$$\frac{1}{c^2}\left[\frac{\partial p}{\partial t} + u\frac{\partial p}{\partial x}\right] + \rho\frac{\partial u}{\partial x} = 0$$

or

$$\frac{1}{c^2}\frac{\partial p}{\partial t} + \frac{u}{c^2}\frac{\partial p}{\partial x} + \rho\frac{\partial u}{\partial x} = 0 \qquad (B.32)$$

Eq.(B-32) is the equation of continuity for unsteady flow of liquids through a cylindrical pipe of circular cross-section. The pressure $p(x,t)$ may be replaced by the piezometric head $h(x,t)$. With reference to Fig. B-13

$$h = z + \frac{p}{\rho g} \qquad (B.33)$$

where z is the elevation of the centerline of the pipe above an arbitrary datum.

Partial differentiation of Eq.(B.33) yields

$$\frac{\partial h}{\partial x} = \frac{\partial z}{\partial x} + \frac{1}{\rho g}\frac{\partial p}{\partial x} - \frac{p}{\rho^2 g}\frac{\partial \rho}{\partial x} \qquad (B.34a)$$

and

$$\frac{\partial h}{\partial t} = \frac{\partial z}{\partial t} + \frac{1}{\rho g}\frac{\partial p}{\partial t} - \frac{p}{\rho^2 g}\frac{\partial \rho}{\partial t} \qquad (B.34b)$$

Since the angle of inclination β is considered positive when the elevation of the pipe decreases in the $+x$ direction (see Fig.B-13)

$$\frac{\partial z}{\partial x} = -\sin\beta \qquad (B.35a)$$

Furthermore it is assumed that the pipe has no transverse motion, thus

$$\frac{\partial z}{\partial t} = 0 \qquad (B.35b)$$

With reference to Eq.(B.7b)

$$\frac{d\rho}{dp} = \frac{\rho}{K} \qquad (B.36)$$

where ρ is a function of $p(x,t)$. So, from differential calculus

$$\frac{\partial \rho}{\partial x} = \frac{d\rho}{dp} * \frac{\partial p}{\partial x} = \frac{\rho}{K}\frac{\partial p}{\partial x} \qquad (B.37a)$$

and

$$\frac{\partial \rho}{\partial t} = \frac{d\rho}{dp} * \frac{\partial p}{\partial t} = \frac{\rho}{K}\frac{\partial p}{\partial t} \qquad (B.37b)$$

Now, with use of Eqs.(B.35) and Eqs.(B.37), Eqs.(B.34) may be rearranged to yield

$$\frac{\partial h}{\partial x} = \frac{1}{\rho g}\left[1 - \frac{p}{K}\right]\frac{\partial p}{\partial x} - \sin\beta \qquad \text{(B.38a)}$$

and

$$\frac{\partial h}{\partial t} = \frac{1}{\rho g}\left[1 - \frac{p}{K}\right]\frac{\partial p}{\partial t} \qquad \text{(B.38b)}$$

As the coefficient of compressibility K for liquids is extremely large in comparison with any practical value of p, even in transient flow, $p/K << 1$ so that Eqs.(B.38) reduce to

$$\frac{\partial h}{\partial x} = \frac{1}{\rho g}\frac{\partial p}{\partial x} - \sin\beta \qquad \text{(B.39a)}$$

and

$$\frac{\partial h}{\partial t} = \frac{1}{\rho g}\frac{\partial p}{\partial t} \qquad \text{(B.39b)}$$

Eqs.(B.39) may also be written as

$$\frac{\partial p}{\partial x} = \rho g \frac{\partial h}{\partial x} + \rho g \sin\beta \qquad \text{(B.40a)}$$

and

$$\frac{\partial p}{\partial t} = \rho g \frac{\partial h}{\partial t} \qquad \text{(B.40b)}$$

After substitution of Eqs.(B.40) into Eq.(B.32) and after division by ρg, the equation of continuity in terms of $u(x,t)$ and $h(x,t)$ takes the form

$$\frac{1}{c^2}\frac{\partial h}{\partial t} + \frac{u}{c^2}\frac{\partial h}{\partial x} + \frac{u}{c^2}\sin\beta + \frac{1}{g}\frac{\partial u}{\partial x} = 0 \qquad \text{(B.41)}$$

B-2.2 Equation of motion

The equation of motion is developed by applying the momentum equation to a control volume containing a section of pipe, having length dx (see Fig.B-14). The momentum equation for the x-direction states that

$$\begin{bmatrix}\text{time rate of increase}\\ \text{of } x\text{-momentum within}\\ \text{the control volume}\end{bmatrix} = \begin{bmatrix}\text{net influx of}\\ x\text{-momentum into}\\ \text{the contr. vol.}\end{bmatrix} + \begin{bmatrix}\text{sum of } x\text{-components}\\ \text{of forces acting on}\\ \text{the control volume}\end{bmatrix}$$

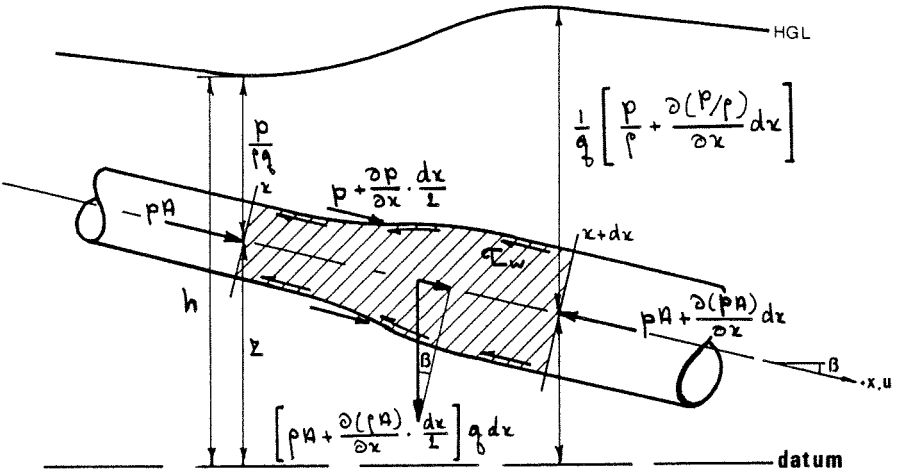

Fig.B-14 Control volume for developing equation of motion (distension of pipe exaggerated)

Since 'influx into the contol volume' = – 'efflux from the control volume' this may also be written as

$$\begin{bmatrix}\text{time rate of increase}\\ \text{of } x\text{-momentum within}\\ \text{the control volume}\end{bmatrix} + \begin{bmatrix}\text{net efflux of}\\ x\text{-momentum from}\\ \text{the control volume}\end{bmatrix} = \left(\Sigma F_x\right) \qquad (B.42)$$

With reference to Fig.B.14

- increase of internal momentum per unit time:

$$\frac{\partial(mu)}{\partial t} = \frac{\partial(\rho A dx * u)}{\partial t} = \frac{\partial(\rho A u)}{\partial t} dx \qquad (B.43)$$

Flux of momentum 'in' at $x = x$ per unit time:

$$\rho A u * (+u) = \rho A u^2$$

Flux of momentum 'out' at $x = x + dx$ per unit time:

$$\rho A u^2 + \frac{\partial(\rho A u^2)}{\partial x} dx$$

- net efflux of momentum from the control volume per unit time:

$$\left[\rho A u^2 + \frac{\partial(\rho A u^2)}{\partial x} dx\right] - \rho A u^2 = + \frac{\partial(\rho A u^2)}{\partial x} dx \qquad (B.44)$$

Now, with use of Eqs.(B.43) and (B.44), Eq.(B.42) may be written as

$$\frac{\partial(\rho A u)}{\partial t} dx + \frac{\partial(\rho A u^2)}{\partial x} dx = \Sigma F_x \qquad (B.45)$$

or

$$u \frac{\partial(\rho A)}{\partial t} dx + \rho A \frac{\partial u}{\partial t} dx + u \frac{\partial(\rho A u)}{\partial x} dx + \rho A u \frac{\partial u}{\partial x} dx = \Sigma F_x$$

which may be rearranged to yield

$$u \left[\frac{\partial(\rho A)}{\partial t} + \frac{\partial(\rho A u)}{\partial x} \right] dx + \rho A \left[\frac{\partial u}{\partial t} + u \frac{\partial u}{\partial x} \right] dx = \Sigma F_x \qquad (B.46)$$

From conservation of mass, Eq.(B.26), it follows that

$$\frac{\partial(\rho A)}{\partial t} + \frac{\partial(\rho A u)}{\partial x} = 0$$

so that Eq.(B.46) simplifies to

$$\rho A \left[\frac{\partial u}{\partial t} + u \frac{\partial u}{\partial x} \right] dx = \Sigma F_x \qquad (B.47)$$

Forces acting in the x- direction on the control volume (see Fig.B-14):

- resultant pressure force acting on the transverse faces of the control volume:

$$+pA - \left[pA + \frac{\partial(pA)}{\partial x} dx \right] = -\frac{\partial(pA)}{\partial x} dx$$

$$= -\left[p \frac{\partial A}{\partial x} + A \frac{\partial p}{\partial x} \right] dx$$

- longitudinal component of the reaction of the mean pressure force from the pipe wall upon the liquid:

$$+ \left[p + \frac{\partial p}{\partial x} \frac{dx}{2} \right] \frac{\partial A}{\partial x} dx$$

- frictional force opposing the flow:

$$-\tau_w P dx \qquad (P = \text{wetted perimeter})$$

- x-component of gravity:

$$+ \left[\rho A + \frac{\partial(\rho A)}{\partial x} \cdot \frac{dx}{2} \right] g dx \sin\beta$$

Hence

$$\Sigma F_x = -p\frac{\partial A}{\partial x}dx - A\frac{\partial p}{\partial x}dx + p\frac{\partial A}{\partial x}dx + \frac{\partial p}{\partial x}\frac{\partial A}{\partial x}\frac{(dx)^2}{2} - \tau_w P dx + \\ + \rho g A dx \sin\beta + \frac{\partial(\rho A)}{\partial x}\frac{(dx)^2}{2} g \sin\beta$$

By dropping out the small quantities containing $(dx)^2$

$$\Sigma F_x = -A\frac{\partial p}{\partial x}dx - \tau_w P dx + \rho g A dx \sin\beta \qquad (B.48)$$

The equation of motion, Eq.(B.47), may now be written as

$$\rho A\left[\frac{\partial u}{\partial t} + u\frac{\partial u}{\partial x}\right]dx = -A\frac{\partial p}{\partial x}dx - \tau_w P dx + \rho g A dx \sin\beta$$

or after dividing by $\rho A dx$

$$\frac{\partial u}{\partial t} + u\frac{\partial u}{\partial x} = -\frac{1}{\rho}\frac{\partial p}{\partial x} - \frac{\tau_w}{\rho R} + g\sin\beta \qquad (B.49)$$

where $R = A/P$ is the hydraulic radius of the pipe.

- For a pipe of circular cross-section

$$R = \frac{A}{P} = \frac{\frac{1}{4}\pi D^2}{\pi D} = \frac{D}{4} \qquad (B.50)$$

- If the shear stress τ_w is considered to be the same in transient flow as in steady flow, then

$$\tau_w = \frac{1}{8}\rho f u|u| \qquad (B.51)$$

where f is the Darcy-Weisbach friction factor. The absolute value sign on the velocity term ensures that the shear stress always opposes the direction of the flow.

Now by use of Eqs.(B.50) and (B.51), Eq.(B.49) takes the form

$$\frac{\partial u}{\partial t} + u\frac{\partial u}{\partial x} + \frac{1}{\rho}\frac{\partial p}{\partial x} + f\frac{u|u|}{2D} - g\sin\beta = 0 \qquad (B.52)$$

Eq.(B.52) is the equation of motion for unsteady flow through a prismatic pipe of circular cross-section. The equation may be converted to a form using the piezometric head $h(x,t)$. From Eq.(B-39a) it follows that

$$\frac{1}{\rho}\frac{\partial p}{\partial x} - g\sin\beta = g\frac{\partial h}{\partial x}$$

so that after substitution of this expression into Eq.(B.52) the equation of motion in terms of $u(x,t)$ and $h(x,t)$ is written as

$$\frac{\partial u}{\partial t} + u\frac{\partial u}{\partial x} + g\frac{\partial h}{\partial x} + f\frac{u|u|}{2D} = 0 \qquad (B.53)$$

B-3 Methods of Solution

As shown in the previous section, unsteady flow of liquids through a cylindrical pipe of circular cross-section is governed by

the equation of continuity

$$\frac{1}{c^2}\frac{\partial h}{\partial t} + \frac{u}{c^2}\frac{\partial h}{\partial x} + \frac{u}{c^2}\sin\beta + \frac{1}{g}\frac{\partial u}{\partial x} = 0 \qquad (B.41)$$

where

$$\frac{1}{c^2} = \left[\frac{\rho}{K} + \frac{\rho D}{Ee}\varphi_1\right] \qquad (B.20)$$

and

the equation of motion

$$\frac{\partial u}{\partial t} + u\frac{\partial u}{\partial x} + g\frac{\partial h}{\partial x} + f\frac{u|u|}{2D} = 0 \qquad (B.53)$$

in which

h	= piezometric head	[m]
u	= cross-sectional average of the liquid velocity	[ms^{-1}]
x	= distance along the pipe	[m]
t	= time	[s]
g	= acceleration due to gravity	[ms^{-2}]
β	= angle of declination	[-]
c	= wavespeed	[ms^{-1}]
ρ	= mass density of the liquid	[kgm^{-3}]
K	= bulk modulus of elasticity of the liquid	[Nm^{-2}]
D	= internal diameter of the pipe	[m]
e	= thickness of the pipe wall	[m]
E	= Young's modulus of the pipe wall material	[Nm^{-2}]
φ_1	= coeff. introducing pipe constraint condition	[-]
f	= Darcy-Weisbach friction factor	[-]

The continuity and momentum equation form a pair of quasi-linear hyperbolic partial differential equations in terms of two dependant variables, velocity u and pressure head h, and two independant variables, distance along the pipe x and time t. A closed-form analytical solution of these equations is not available. However, graphical techniques as well as various numerical methods for solving the equations have been developed; see e.g. Refs.[5,7,16,17,28].
In the next section the essentials of the 'method of characteristics' will be presented. The appendix on 'Unsteady Pipe Flow' is then concluded with a method of solution valid only in those cases for which the 'rigid water-column theory' applies.

B-3.1 Method of characteristics

By use of the method of characteristics the partial differential equations (B.41) and (B.50) are transformed into particular total differential equations. These ordinary differential equations may be used as a starting point for either graphical or numerical handling. In particular the graphical method of solution is of great value in visualizing unsteady flow.

Characteristic equations.

There are a variety of ways of obtaining the characteristic forms of the unsteady flow equations. The method given here is a modification of the general approach proposed by Lister[13]. To facilitate the derivation the equations of motion and continuity are rewritten as

$$F_1 = g\frac{\partial h}{\partial x} + \frac{\partial u}{\partial t} + u\frac{\partial u}{\partial x} + f\frac{u|u|}{2D} = 0 \qquad (B.54)$$

and

$$F_2 = \frac{\partial h}{\partial t} + u\frac{\partial h}{\partial x} + \frac{c^2}{g}\frac{\partial u}{\partial x} + u\sin\beta = 0 \qquad (B.55)$$

These equations are combined linearly using a, so far, unknown multiplier λ.

$$F = F_1 + \lambda F_2 = g\frac{\partial h}{\partial x} + \frac{\partial u}{\partial t} + u\frac{\partial u}{\partial x} + f\frac{u|u|}{2D} + \lambda\left[\frac{\partial h}{\partial t} + u\frac{\partial h}{\partial x} + \frac{c^2}{g}\frac{\partial u}{\partial x} + u\sin\beta\right] = 0$$

which may be rearranged to yield

$$\lambda\left[\frac{\partial h}{\partial t} + u\frac{\partial h}{\partial x} + \frac{g}{\lambda}\frac{\partial h}{\partial x}\right] + \left[\frac{\partial u}{\partial t} + u\frac{\partial u}{\partial x} + \frac{c^2}{g}\lambda\frac{\partial u}{\partial x}\right] + \lambda u\sin\beta + f\frac{u|u|}{2D} = 0$$

or

$$\lambda\left[\frac{\partial h}{\partial t}+\left(u+\frac{g}{\lambda}\right)\frac{\partial h}{\partial x}\right]+\left[\frac{\partial u}{\partial t}+\left(u+\frac{c^2}{g}\lambda\right)\frac{\partial u}{\partial x}\right]+\lambda u\sin\beta+f\frac{u|u|}{2D}=0 \qquad (B.56)$$

Since both variables h and u are functions of x and t, it follows from differential calculus that

$$\frac{dh}{dt}=\frac{\partial h}{\partial t}+\frac{dx}{dt}\frac{\partial h}{\partial x} \qquad (B.57a)$$

and

$$\frac{du}{dt}=\frac{\partial u}{\partial t}+\frac{dx}{dt}\frac{\partial u}{\partial x} \qquad (B.57b)$$

Now, by examination of Eq.(B.56) with Eqs.(B.57) in mind, it can be noted that if

$$\frac{dx}{dt}=u+\frac{g}{\lambda}=u+\frac{c^2}{g}\lambda \qquad (B.58)$$

Eq.(B.56) becomes the ordinary differential equation

$$\lambda\frac{dh}{dt}+\frac{du}{dt}+\lambda u\sin\beta+f\frac{u|u|}{2D}=0 \qquad (B.59)$$

The solution of the right-hand part of Eq.(B.58) yields

$$\frac{g}{\lambda}=\frac{c^2}{g}\lambda \qquad \text{or} \qquad \lambda^2=\frac{g^2}{c^2}$$

So, the multiplier λ takes the values

$$\lambda=\pm\frac{g}{c} \qquad (B.60)$$

By substituting these values of λ back into Eq.(B.58), the particular manner in which x and t are related is given by

$$\frac{dx}{dt}=u\pm c \qquad (B.61)$$

while substitution for λ in Eq.(B.59) gives

$$\pm\frac{g}{c}\frac{dh}{dt}+\frac{du}{dt}\pm\frac{g}{c}u\sin\beta+f\frac{u|u|}{2D}=0 \qquad (B.62)$$

When the plus (minus) sign is used in Eq.(B.61), the plus (minus) sign must be used in Eq.(B.62). That is to say:

$$+\frac{g}{c}\frac{dh}{dt} + \frac{du}{dt} + \frac{g}{c} u \sin\beta + f\frac{u|u|}{2D} = 0 \qquad \text{(B.63a)}$$

if

$$\frac{dx}{dt} = u + c \qquad \text{(B.64a)}$$

$\Big\}\ C^+$

and

$$-\frac{g}{c}\frac{dh}{dt} + \frac{du}{dt} - \frac{g}{c} u \sin\beta + f\frac{u|u|}{2D} = 0 \qquad \text{(B.63b)}$$

if

$$\frac{dx}{dt} = u - c \qquad \text{(B.64b)}$$

$\Big\}\ C^-$

Thus by imposing the relations given by Eqs.(B.64) the original partial differential Eqs.(B.41) and (B.53) have been converted into two total differential equations, Eqs.(B.63a) and (B.63b), each with the restriction that it is valid only when the respective Eqs.(B.64a) and (B.64b) are satisfied.

For liquid flow through metal pipes $u \ll c$, so that in Eqs.(B.64) u is negligible as compared with c, while in Eqs.(B.63) the term $\frac{g}{c} u \sin\beta$ is small and therefore usually omitted. The characteristic equations may then be written as

$$+\frac{g}{c}\frac{dh}{dt} + \frac{du}{dt} + f\frac{u|u|}{2D} = 0 \qquad \text{(B.65a)}$$

if

$$\frac{dx}{dt} = +c \qquad \text{(B.66a)}$$

$\Big\}\ C^+$

and

$$-\frac{g}{c}\frac{dh}{dt} + \frac{du}{dt} + f\frac{u|u|}{2D} = 0 \qquad \text{(B.65b)}$$

if

$$\frac{dx}{dt} = -c \qquad \text{(B.66b)}$$

$\Big\}\ C^-$

Inasmuch as c generally is constant for a given pipe, Eq.(B.66a) represents a straight line in the x,t-plane, having slope $+\frac{1}{c}$. Similarly Eq.(B.66b) plots as a straight line, having slope $-\frac{1}{c}$ (Fig.B-15). These lines on the x,t-plane are the characteristic lines along which the compatibility equations (B.65a) and (B.65b) apply, each one being valid only on the appropriate characteristic line.

Mathematically, a characteristic line divides the x,t-plane into two regions which may be dominated by two different kinds of solution, i.e.

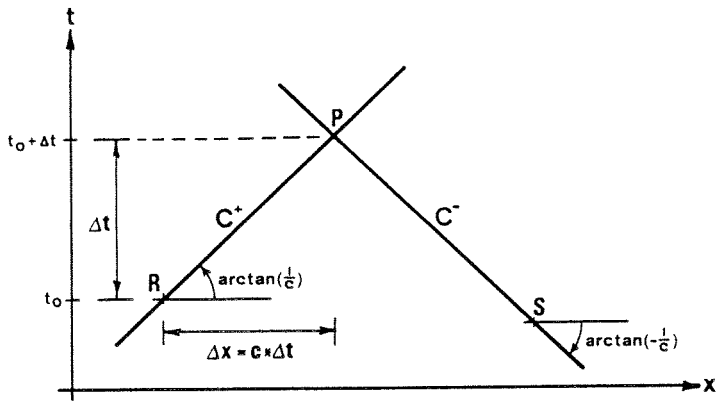

Fig.B-15 Characteristic lines in the x,t-plane

the solution may be discontinuous along this line. Physically, characteristic lines represent the path traversed by a disturbance. For example, consider a pipeline as shown in Fig.B-16. Through any point in the x,t-plane two lines can be drawn, the forward characteristic C^+ having slope $\frac{dt}{dx} = +\frac{1}{c}$, e.g. RPW, and the backward characteristic C^- having slope $\frac{dt}{dx} = -\frac{1}{c}$, e.g. SPV. A disturbance initiated at time t_p and at location x_p along the pipe, will travel as a wave downstream at velocity $+c$ and upstream at velocity $-c$. If the movement of these waves is plotted on the x,t-plane, it will be represented by PW and PV respectively. Any point lying within the area VPW will at some time $t>t_p$ experience the effect of the disturbance, so this area is called the zone of influence of P.

On the other hand, if disturbances originate from points lying at time $t<t_p$, then events occurring at P can only be affected by events occurring at points lying within area RPS. For example, the forward characteristic from X intersects the backward characteristic from Y at Z, so that events at P, located within the zone of influence of Z, are affected by events occurring at X~Y. Any events originating from points lying outside area RPS cannot affect events in P in any way. The area RPS is called the domain of dependency of P.

If conditions (x, t, u, h) are known at point R and S, then conditions at point P can be calculated, e.g. by using a first-order finite difference approximation of the differential equations (B.65) and (B.66):

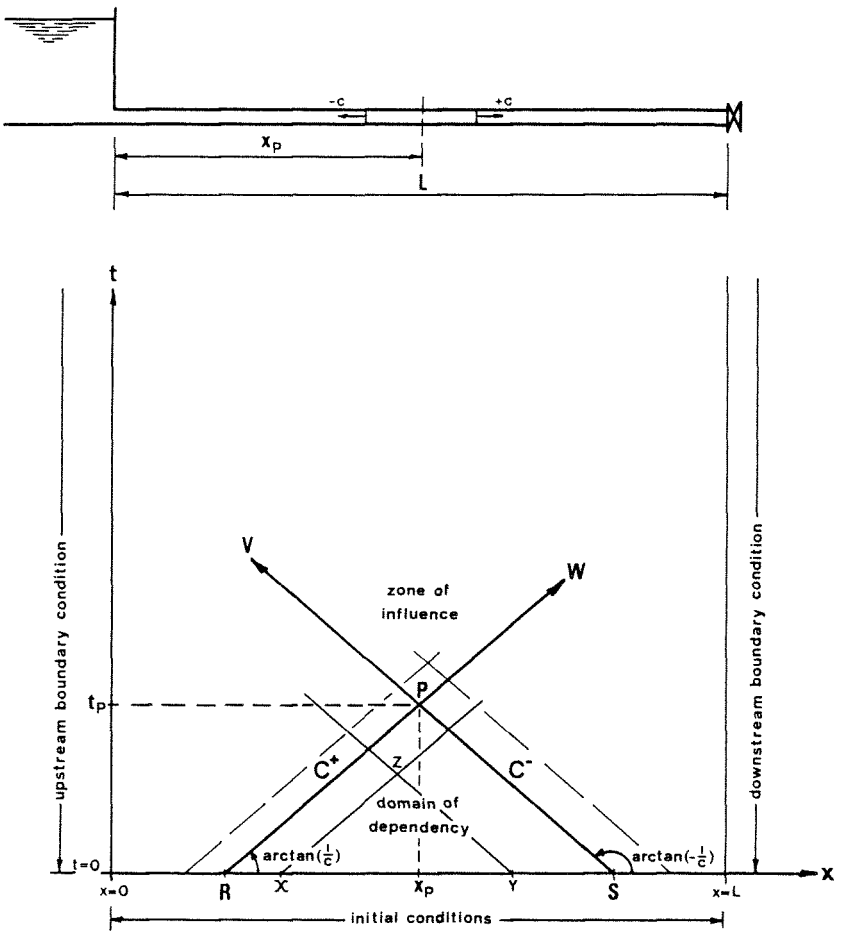

Fig.B-16 x,t-plane for a single pipeline

$$C^+ \begin{cases} +\frac{g}{c}(h_p - h_R) + u_p - u_R + f\frac{u_R|u_R|}{2D}(t_p - t_R) = 0 & \text{(B.67a)} \\ x_p - x_R = c\,(t_p - t_R) & \text{(B.68a)} \end{cases}$$

$$C^- \begin{cases} -\frac{g}{c}(h_p - h_S) + u_p - u_S + f\frac{u_S|u_S|}{2D}(t_p - t_S) = 0 & \text{(B.67b)} \\ x_p - x_S = -c\,(t_p - t_S) & \text{(B.68b)} \end{cases}$$

These four equations suffice to find the four unknowns x_p, t_p, u_p and h_p. The equations may for instance be used to accomplish an orderly computer

solution. For that purpose a grid of characteristics is established in the x,t-plane (Fig.B-17). The pipeline under consideration is divided into N equal sections, each $\Delta x = L/N$ in length. By using a time-step size $\Delta t = \Delta x/c$, Eq.(B.68a) is satisfied by a positively sloped diagonal of the grid and Eq.(B.68b) by a negatively sloped diagonal.

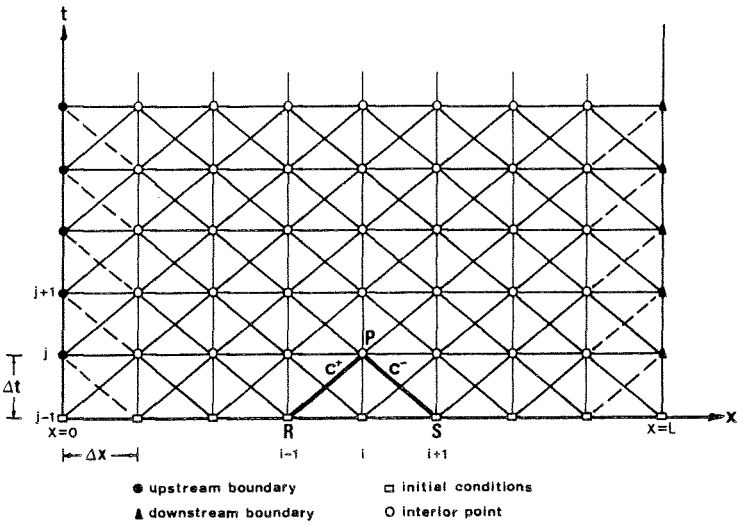

Fig.B-17 Characteristic grid in the x,t-plane

Furthermore, if conditions at P ($x = i\Delta x, t = j\Delta t$) are marked as $h_{i,j}$ and $u_{i,j}$ then Eqs.(B.67) can be generalised as

$$+\frac{g}{c}\left(h_{i,j} - h_{i-1,j-1}\right) + u_{i,j} - u_{i-1,j-1} + f\,\frac{u_{i-1,j-1}\,|u_{i-1,j-1}|}{2D}\,\Delta t = 0$$

and

$$-\frac{g}{c}\left(h_{i,j} - h_{i+1,j-1}\right) + u_{i,j} - u_{i+1,j-1} + f\,\frac{u_{i+1,j-1}\,|u_{i+1,j-1}|}{2D}\,\Delta t = 0$$

which is a convenient notation for computer solutions.
It is beyond the scope of this appendix to present a full treatment of the numerical procedures available to solve the characteristic equations Detailed information on the subject may be found in Refs.[5,7,13,28].

In unsteady flow problems conditions at time $t = 0$ are usually defined by the initial steady-state conditions, while unsteadiness is initiated

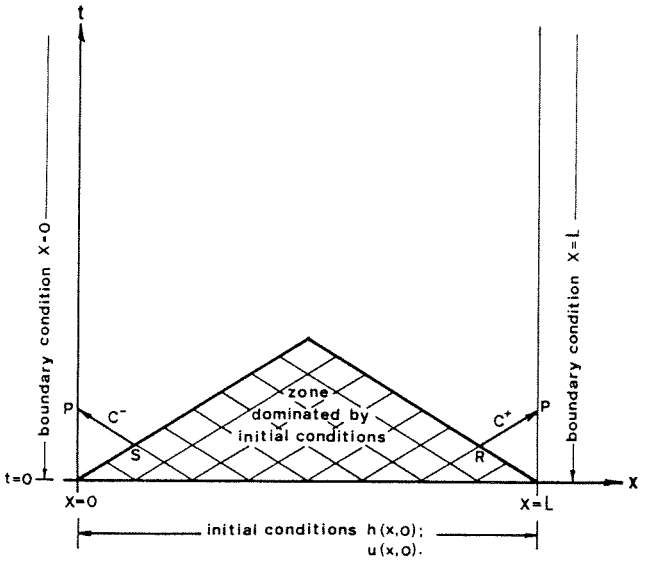

Fig.B-18 Initial situation in the x,t-plane

from the boundaries as a result of a change in boundary conditions (changes in valve setting, starting or stopping of pumps, etc.).

Fig.B-18 illustrates the region on the x,t-plane which is influenced by the initial conditions only. A close look at the figure also shows that at either end of the pipeline only one of the compatibility equations is available. For the upstream end ($x=0$), Eq.(B.67b) holds along the C^- characteristic and for the downstream boundary ($x=L$), Eq.(B.67a) applies along the C^+ characteristic. So, in order to proceed the solution an auxiliary equation is needed at both ends that introduces the appropriate boundary condition, i.e. that specifies $h(t)$ or $u(t)$ or some relation between them.

For example:

- Constant-head reservoir at the upstream end ($x=0$).

  If, for simplicity, the entrance losses as well as the velocity head are neglected, then

  $$h_p = h_{res} \qquad (B.69)$$

  in which h_{res} = height of the reservoir water surface above the datum-line.

  Now, with use of Eq.(B.69), u_p can be calculated directly from Eq. (B.67b).

- Dead end at the downstream end of the pipe ($x=L$).
  At the dead (closed) end $u_p=0$ and h_p can be obtained directly from Eq.(B.67a).

With knowledge of the behaviour of the boundaries as imposed upon the pipeline, the computations can be proceeded step-by-step by simultaneous solving of the compatibility Eqs.(B.67) for the interior points and simultaneous solving of the compatibility Eq.(B.67a) or (B.67b) and the appropriate auxiliary equation for the boundaries, until the transient-state conditions for the desired time duration are determined.

Graphical solution.

In account of presenting a specific application of 'graphical water-hammer', the method is briefly introduced. For a full treatment of the graphical techniques available to solve unsteady flow problems the reader is referred to the appropriate literature, e.g. Refs.[3,7,16,17].

As shown in the previous section, for liquid flow through metal pipes the characteristic equations can be written as

$$\pm \frac{g}{c}\frac{dh}{dt} + \frac{du}{dt} + f\frac{u|u|}{2D} = 0 \qquad \text{Eq.(B.65)}$$

if $$\frac{dx}{dt} = \pm c \qquad \text{Eq.(B.66)}$$

To facilitate the graphical solution friction head losses, which are actually distributed along the length of the pipe, are considered to be concentrated at selected points of the pipe: e.g. half the entire friction head loss ($=\frac{1}{2} * \frac{fL}{D}\frac{u|u|}{2g}$) at the upstream end of the pipe, the other half at the downstream end of the pipe. In this way friction head loss can be taken into account by lumping it with the boundary conditions at either end of the pipe. The characteristic equations then reduce to

$$\pm \frac{g}{c}\frac{dh}{dt} + \frac{du}{dt} = 0 \qquad \text{if} \quad \frac{dx}{dt} = \pm c$$

or

$$\left.\begin{aligned} &\frac{dh}{du} = -\frac{c}{g} \\ &\text{if } \frac{dx}{dt} = +c \end{aligned}\right\} \qquad \text{and} \qquad \left.\begin{aligned} &\frac{dh}{du} = +\frac{c}{g} \\ &\text{if } \frac{dx}{dt} = -c \end{aligned}\right\} \qquad \begin{matrix}\text{(B.70a \& b)} \\ \\ \text{(B.71a \& b)}\end{matrix}$$

As before, since c normally is constant for a given pipe, equations (B.71) plot as straight lines on the x,t-plane, called the characteristic lines along which the compatibility equations (B.70) apply, each one being valid only on the corresponding characteristic line. The compatibility equations themselves represent straight lines on the u,h-plane, having slopes $\frac{dh}{du} = -\frac{c}{g}$ and $\frac{dh}{du} = +\frac{c}{g}$ respectively. These lines relate u and h at one location and time to u and h at another point of the pipe, distance Δx from the first point and at time $\Delta x/c$ later. For example, Fig.B-19 illustrates characteristic lines on the x,t-plane together with the corresponding characteristic relations on the u,h-plane. If conditions (x, t, u, h) are known at two different locations along the pipe, they may be represented by point 1 (x_1, t_1) and point 2 (x_2, t_2) on the x,t-plane and by point ① (u_1, h_1) and point ② (u_2, h_2) on the u,h-plane respectively. Conditions (u, h) at point 3 (x_3, t_3), being the intersection point of the forward chracteristic ($\frac{dx}{dt} = +c$) from point 1 and the backward characteristic ($\frac{dx}{dt} = -c$) from point 2 , are now obtained on the u,h-plane by determining the intersection point ③ of the characteristic relation $\frac{dh}{du} = -\frac{c}{g}$ from point ① and the characteristic relation $\frac{dh}{du} = +\frac{c}{g}$ from point ②.

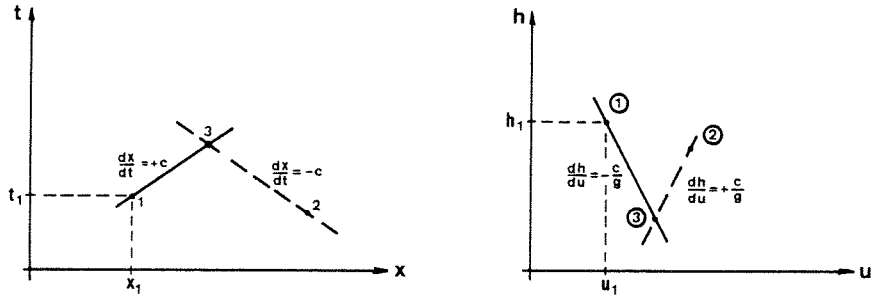

Fig.B-19 Characteristic lines on the x,t-plane and characteristic relations on the u,h-plane

In this way conditions (u, h) at any point of the x,t-plane can be obtained step-by-step, provided that the necessary initial conditions and boundary conditions are known (see also previous section). Again, to accomplish an orderly solution a grid of characteristics may be established in the x,t-plane by dividing the pipeline into N equal sections, each $\Delta x = L/N$ in length and by using a time-step size $\Delta t = \Delta x/c$. Furthermore, it may be found convenient to turn the x,t-plane upside

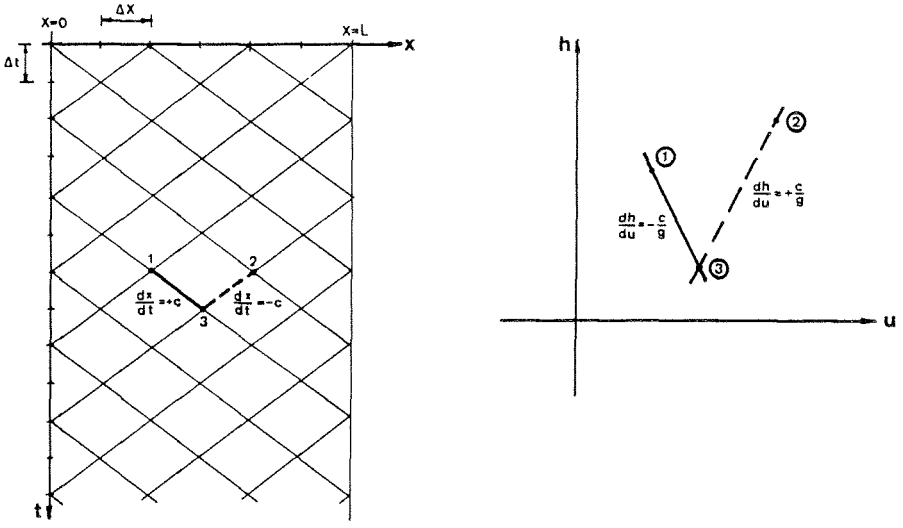

Fig.B-20 Characteristic lines on the x,t-plane and characteristic relations on the u,h-plane

down, so that corresponding lines in the x,t-plane and u,h-plane incline in the same direction (Fig.B-20).

Once that the solution is completed for the desired time duration, the results portrayed in both the x,t-diagram and the u,h-diagram may be used to derive $h(x_o,t)$ and $u(x_o,t)$ for any location $x=x_o$ on the pipe as well as $h(x,t_o)$ and $u(x,t_o)$ at any point of time $t=t_o$ of the time duration covered by the solution. This is done by following the respective paths ($x=x_o$ or $t=t_o$) on the x,t-plane and adding the corresponding information obtained from the u,h-diagram to it.

The foregoing graphical technique may for instance be used to analyse hydraulic ram operation. With reference to chapter III the main events in hydraulic ram operation are summarized as follows:

- the impulse valve closes instantaneously at the moment the velocity of the water at the downstream end of the drive pipe $u \geq u_c$
- the delivery valve opens instantaneously at the moment the pressure head at the downstream end of the drive pipe $h > h_d$
- the delivery valve closes instantaneously when $h < h_d$ and $u \leq o$ at the downstream end of the drive pipe
- the impulse valve (re-)opens at the moment $h < o$ at the downstream end of the drive pipe.

If friction head losses are assumed to be concentrated at both ends of the drive pipe, then the following initial conditions and boundary conditions apply.

Inital conditions

$t=0$: $h=H_s$, $u=0$ — for $0 \le x \le L_s$, i.e. along the entire drive pipe

Boundary conditions

$x=0$ (supply reservoir):

$h=H_s-\zeta_1 \frac{u|u|}{2g}$ — at any point of time t , i.e. for the complete duration of the hydraulic ram cycle. $(\zeta_1=\zeta_{in}+\frac{1}{2}\zeta_{fr}+1)$

$x=L_s$ (hydraulic ram):

$u=0$ — while both valves are closed

$h=\zeta_2 \frac{u|u|}{2g}$ — for $u \le u_c$ with the impulse valve in open position. $(\zeta_2=\zeta_{out}+\zeta_{valve}+\frac{1}{2}\zeta_{fr}-1)$

$h=h_d+\zeta_3 \frac{u|u|}{2g}$ — with the delivery valve in open position ($\zeta_3=\zeta'_{out}+\zeta'_{valve}+\frac{1}{2}\zeta_{fr}-1$; where ζ'_{out} and ζ'_{valve} refer to the delivery valve)

Note: the last equation may usually be approximated by $h \approx h_d$ since head losses normally are small as compared with the delivery head

The results of the graphical analysis of hydraulic ram operation are illustrated in Fig.B-21 and Fig.B-22. The presentation is rather qualitative than quantitative. Because of the limited space available only the most significant parts of the x,t-diagram are shown. The numerals on the x,t-plane indicate that at any point within the respective triangles conditions (u,h) are as pictured by the corresponding numerals in the u,h-diagram. Finally, from the results conveyed in the x,t-diagram and the u,h-diagram the relation $u(L_s,t)$, i.e. the relation between velocity and time at the downstream end of the drive pipe, can be derived.

It may be clear that the solution obtained in Fig.B-22 refers to a delivery head h_d which is somewhat lower than the one applying to Fig.B-21. In particular, Fig.B-21 relates to the so-called 'Case A' of section III-3 (i.e. the impulse valve reopens immediately after delivery valve closure), whereas Fig.B-22 is an example of 'Case B' (impulse valve reopens $^{2L_s}/_{c}$ second after delivery valve closure).

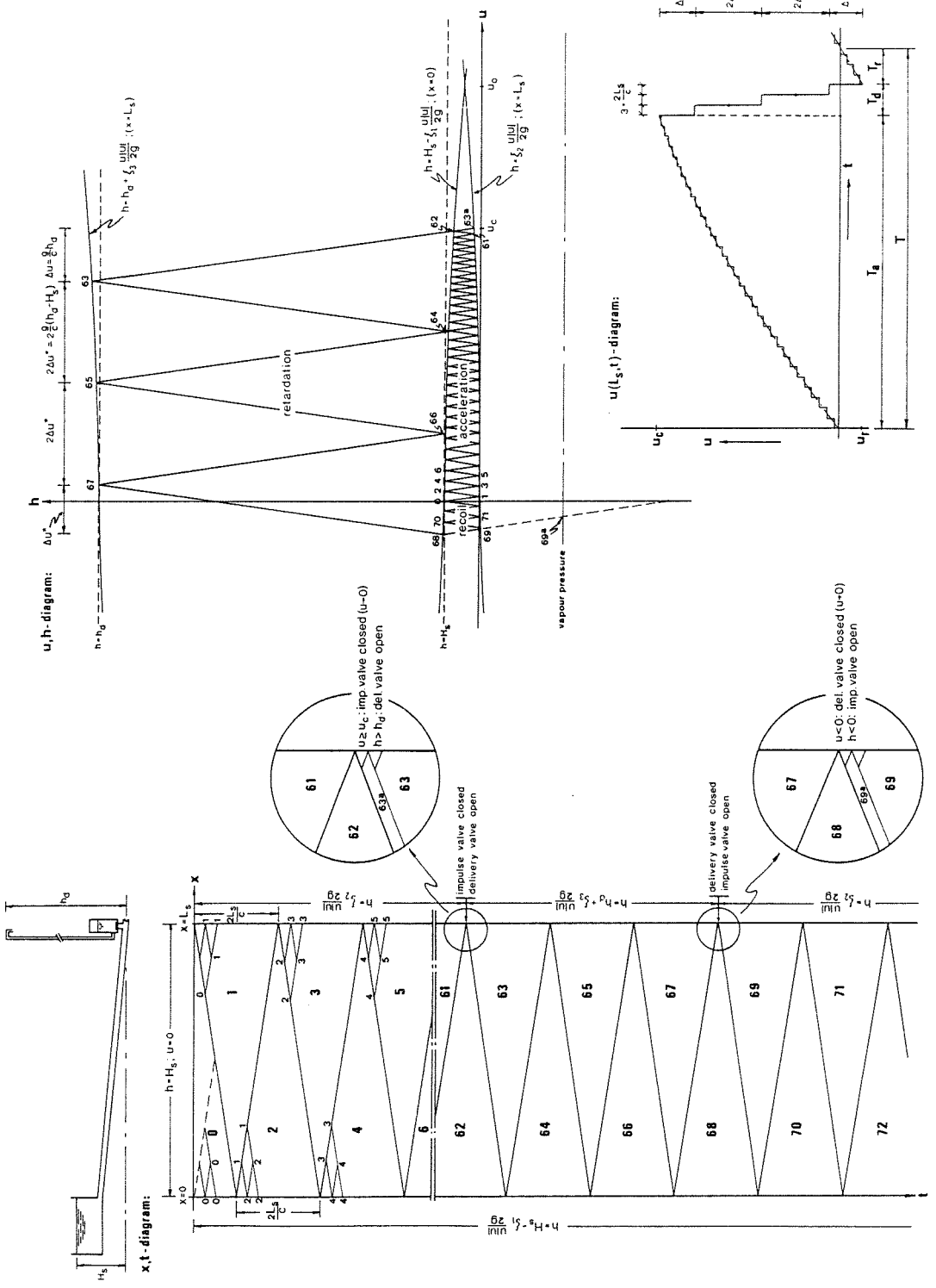

Fig.B-21 Graphical analysis of hydraulic ram operation - Case A

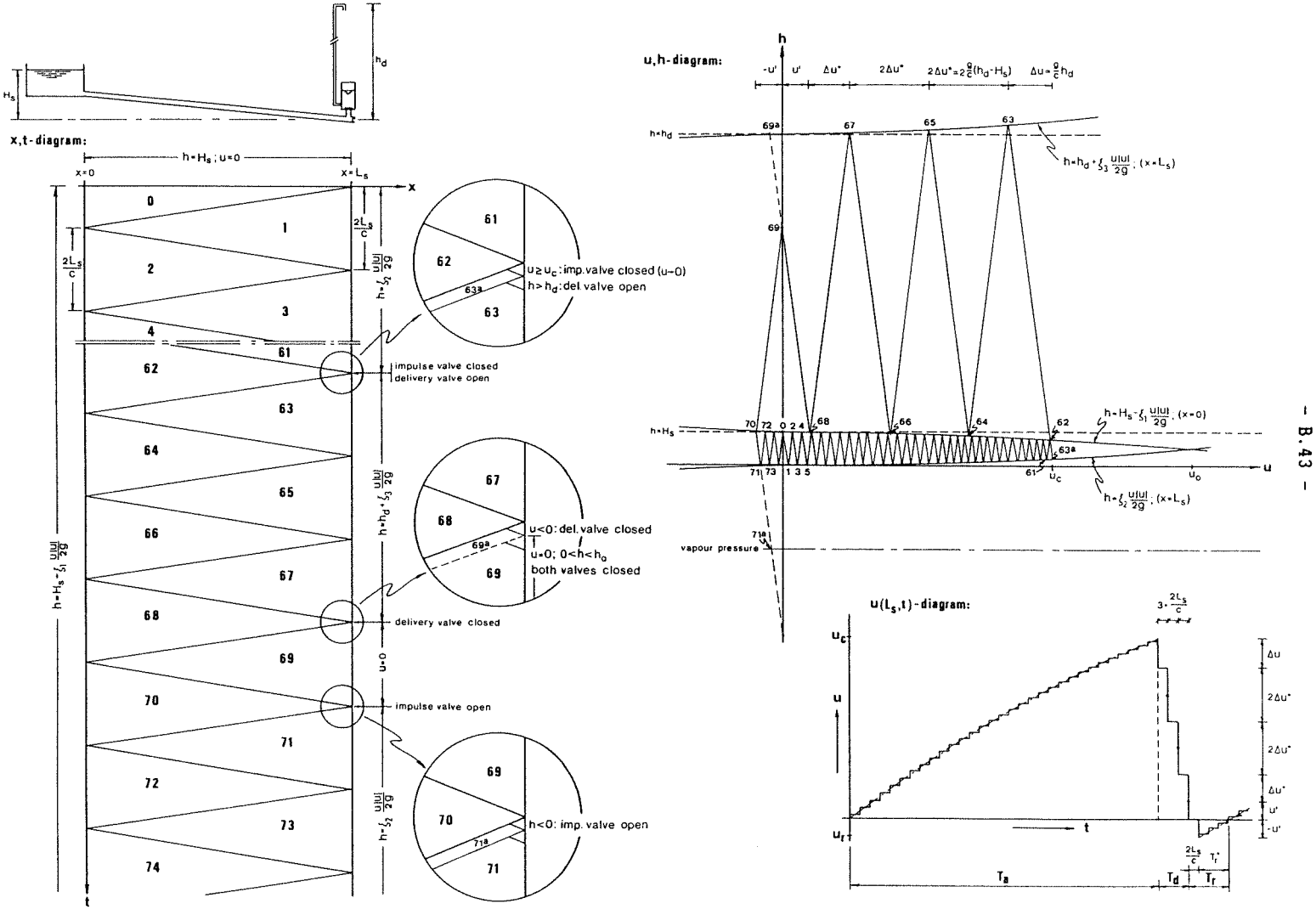

Fig. B-22 Graphical analysis of hydraulic ram operation - Case B

B-3.2 Rigid water-column theory

As already mentioned in section B-1.3 the rigid water-column theory is based on the assumption of a completely incompressible liquid ('$K \to \infty$') flowing in a completely rigid pipe ('$E \to \infty$'), which implies that the wavespeed c is assumed to be infinitely large

$$c \to \infty \tag{B.72}$$

In practice this means that the rigid water-column theory applies to those cases in which the time scale of velocity changes is large as compared with the time scale of pressure wave propagation; see Eq.(B.25) With use of Eq.(B.72) the continuity Eq.(B.41) reduces to

$$\frac{\partial u}{\partial x} = 0 \tag{B.73}$$

and the equation of motion, Eq.(B.53), then simplifies to

$$\frac{\partial u}{\partial t} + g\frac{\partial h}{\partial x} + f\frac{u|u|}{2D} = 0$$

or

$$\frac{\partial h}{\partial x} = -\frac{1}{g}\frac{\partial u}{\partial t} - \frac{f}{D}\frac{u|u|}{2g} \tag{B.74}$$

From Eq.(B.73) it follows that $\frac{\partial u}{\partial t} \equiv \frac{du}{dt}$ and that both u and $\frac{du}{dt}$ are constant throughout the pipelength; i.e. the entire water-column in the pipeline accelerates at the same value throughout its length, which fits the mental picture of a 'rigid' water-column.
Hence, the right-hand side of Eq.(B.74) is no longer a function of x and the equation can be integrated with respect to x to give

$$\int_{x=0}^{L} \frac{\partial h}{\partial x}\,dx = -\int_{x=0}^{L} \frac{1}{g}\frac{du}{dt}\,dx - \int_{x=0}^{L} \frac{f}{D}\frac{u|u|}{2g}\,dx$$

or

$$h(L,t) - h(0,t) = -\frac{L}{g}\frac{du}{dt} - \frac{fL}{D}\frac{u|u|}{2g} \tag{B.75}$$

where $h(L,t)$ and $h(0,t)$ are the boundary conditions at the downstream end and the upstream end of the pipe respectively. When these conditions are known -for example as functions of u- and with known intial condition, Eq.(B.75) can be integrated with respect to t to yield an expression $u(t)$. For example, in the case of a flow accelerating under a head H in a single pipeline with free discharge at the downstream end, this leads to the well-known 'hyperbolic tangent law':

$$u = u_o \tanh \frac{u_o \zeta}{2L} t \qquad (B.76)$$

where

$$u_o = \sqrt{\frac{2gH}{\zeta}} \qquad (B.77)$$

with ζ = sum of head loss coefficients.

This is elaborated in detail in section III-2 of this report.

Appendix C

Appendix C: HYDRAULIC RAM MANUFACTURERS

Hydraulic ram:	Manufacturer:
Ariete de Alta Cabeza 'Gaviotas'	Centro Las Gaviotas Paseo Bolivar no.20-90 Bogota - Columbia
Auto-Lift Pump	Godbole & Sons New Ramdaspeth Kachipura Nagpur-1, India
Bélier 'ALTO'	J.M. Desclaud 57, Rue Bertrand - de - Goth 33800 Bordeaux - France
Billabong	John Danks & Son Pty Ltd Doody Street, Alexandria Sydney - Australia
Blake Hydram	John Blake Ltd P.O.Box 43, Accrington Lancashire BB5 5LP, UK
Bomba Hydraulicas Rochfer	Industrias Mecanicas Rochfer Ltda Avenida Jose de Silva 3765 Jardin Moria Rosa, Caixa Postal 194 São Paulo, CEP 14400 - Brazil
Briau Bélier Hydr.	Briau S.A. B.P. 0903 37009 Tours Cedex - France
BZH-Ram	Aktiebolaget Bruzaholms Bruk 570 34 Bruzaholm - Sweden
CeCoCo Hydro-Hi-Lift Pump	CeCoCo Chuo Boeki Goshi Kaisha P.O.Box 8, Ibaraki City Osaka 567 - Japan

Chandra Hydr.Ram	Singh Metal Casting Works 110-D Nirala Nagar Lucknow - India
Fleming Hydro-Pump	C.W. Pipe, Inc. P.O.Box 698, Amherst Virginia 24521 - USA
Jandu's Hydr.Ram	Jandu Plumbers Ltd P.O.Box 409, Uhuru Road Arusha - Tanzania
Premier Hydr.Ram	Premier Irrigation Equipment Ltd 17/1C Alipore Road Calcutta 700 027 - India
Rife Ram	Rife Hydraulic Engine Manufacturing Co. 316 W.Poplar Street, P.O.Box 790 Norristown, PA 19401 - USA
SANO	Pfister + Langhanss Sandstrass 2-8 Postfach 3555, 8500 Nürnberg 1 Fed. Rep. of Germany
Schlumpf Hydr.Widder	Schlumpf AG Maschinenfabrik CH-6312 Steinhausen Kanton Zug - Switzerland
Vulcan	Green & Carter Ltd (Rams) Ashbrittle - nr Wellington Somerset TA21 0LQ, UK
WAMA Hydr.Widder	WAMA Maschinenbau Max Wagner Bergstrass 8, 8018 Grafing Fed. Rep. of Germany